REGULATION OF P97 SEGREGASE RECRUITMENT TO CHROMATIN DURING DNA REPLICATION

by

Zeynep Tarcan

A thesis submitted to the University of Birmingham for the degree of DOCTOR OF PHILOSOPHY

Institute of Cancer and Genomic Sciences

School of Cancer Sciences

College of Medical and Dental Sciences

University of Birmingham

July 2021

ACKNOWLEDGEMENT

Primarily, I would like to express my deep and sincere gratitude to my great supervisor Dr. Aga Gambus for giving me the opportunity of the joining her lab. I consider myself as a very lucky individual for letting me be part of this incredible group. Your guidance always at every stage of my research project and for your insightful comments and suggestions helped me to do the research and write my thesis. It was a great privilege and honor to do research under your guidance. Your dynamism, vision, sincerity, motivation and motherhood always inspired me. I would also like to thank you, your friendship and empathy. You were always with me when I was in dark periods. I cannot express enough thanks to you for your continued support for my personal life.

I would like to express my thanks to everyone that worked or is currently working in our group. You all have supported me and had to put up with my stresses and moans for the past three years of study! Special thanks to Becky, Divya, Abi, Shaun and Paolo whose support allowed my studies to go the extra mile. Massive thanks to Becky! Without your support and kind discussions, I would not have been able to complete this research. When I need any help in my life, your kind words always warm my heart. You made me feel so at home that I forgot I was not. Thank you for being a close friend and a caring, generous study partner. My appreciation also goes out to Divya! Thank you for always stepping in to help when I need you the most. I will miss our deep conversation, most probably everything… How grateful I am for a friend like you, Abi. Your art studies, nice chatting and your kind support always will be in my memory. Thank you for helping me through that difficult Ph.D. time. If I ever need a shoulder to cry on, I have three for you. Furthermore, I want to thank Shaun for always helping me even in the evening and weekend. You really make my life easier.

Finally, yet importantly, I would like to thank my family and friends for their encouragement and support all through my studies. For my kids, Beyza and Akif, sorry for being even grumpier than normal whilst I wrote this thesis! Thank you for your patience and big hugs during my tough times. We can now turn our attention to our favourite part of day which is when we play together. I love hearing you laugh! You are my biggest motivation factor to start and finish Ph.D. And for my dear husband Hasan, thank you so much for being there for me, for all the little things you do to make my life easier. You have been amazing. We deserve this degree together: me, you and our children. I am lucky to be with someone who is always by my side. It was a great comport and relief to know you are always taking care of our family. Your encouragement when the times go rough was precious. My mum and dad, I

have been fortunate to have you as parents. Thank you, dad! I feel honoured to have such an amazing and supportive father like you. I had never forgotten your contribution to my life. Love you both.

Hicbir sey icin gec kalmadin,

Sadece henuz dogru zaman gelmedi.

Herkesin zamani farklidir...

(kucukilhamkutusu.com)

Dedication

To my mum and dad,

For raising me that anything was possible

To my husband,

For make me believe everything is possible

To my children Beyza and Akif,

For the reason to make everything possible

and

Mostly to myself…

ABSTRACT

Every step of chromosomal replication must be executed in an error free manner to protect genome stability. Ubiquitylation is a fundamental regulatory post-translational protein modification that controls intracellular signalling events including regulation of DNA replication. p97 segregase works through binding proteins that are marked by ubiquitin and extracting them from membranes, cellular surfaces or protein complexes that they are interacting with.

Little is known about how p97 with its cofactors regulates unperturbed DNA replication. Our group has shown over the last few years that p97 segregase plays a key role in unloading of the replicative helicase from chromatin at termination of DNA replication. To prime it for unloading during S-phase, the terminated helicase is first ubiquitylated by $Cul2^{Lrr1}$ ubiquitin ligase.

Using the well-established cell-free system of *Xenopus leavis* egg extract, which is ideal for studying DNA replication at the biochemical level, we have now analysed the mode of p97 recruitment to chromatin during S-phase. Our data suggest that the p97 core complex is primarily brought to S-phase chromatin not through direct binding to its substrate: the polyubiquitylated proteins, but by its cofactor Ubxn7, which in turn binds to active (neddylated) Cul2 ubiquitin ligase. Immunodepletion of Ubxn7 from the egg extract leads to a delay in unloading of terminated helicase despite an accumulation of active $Cul2^{Lrr1}$ ligase. In conclusion, we have identified Ubxn7 as a p97 cofactor playing a role specifically during S-phase unloading of terminated helicase by interacting with $Cul2^{Lrr1}$ ubiquitin ligase and p97. Ubxn7 also interplays with Faf1 for recruitment of p97 to polyubiquitylated CMG helicase in S phase and mitosis. Furthermore, I also identified a number of posttranslational modifications of p97 in S phase and mitosis, which may regulate p97 interactions with cofactors in higher-order complex assemblies and allow for chain type specificity of p97 recognition. Finally, I also identified that RPA could be a potential substrate of p97 in the S phase and mitosis, whilst p97 might be itself a possible substrate of ATR kinase in mitosis.

Table of Contents

List of Figures

List of Tables

ABBREVIATIONS

AAA^{+}– ATPase Associated with diverse cellular Activities

APC2 – Anaphase-promoting complex-2

APP-BP1 – Amyloid protein-binding protein 1.

ARID – AT rich interaction domain

Aspc1 – Alveolar soft part sarcoma chromosomal region candidate gene 1 protein

ATG8 – Autophagy-related protein 8

ATG12 – Autophagy-related protein 8

ATM – Ataxia-Telangiectasia mutated protein

ATR – Ataxia-Telangiectasia and Rad3 protein

ATP – Adenosine triphosphate

Baz1-b – Bromodomain adjacent to zinc finger domain 1-b

BRCA1 – Breast and ovarian cancer susceptibility protein 1

BSA – Bovine Serum Albumins

CAD – Chromatin Associated Degradation

CAND1 – Cullin associated and neddylation dissociated 1

CDC6 – Cell division cycle protein 6

CDK – Cyclin dependent kinase

Cdt1 – Chromatin licensing and DNA replication factor 1

CENPE – Centrosome-associated protein E

Chk1 – Checkpoint kinase 1

CHROMASS – Chromatin mass spectrometry

CMG – Cdc45/Mcm2-7/GINS complex CRL – Cullin/RING ubiquitin ligase

CSN - Signalosome 205

Ctf – Chromosome transmission fidelity protein

Cttn – Src Substrate Cortactin

DCN1 – Cullin neddylation protein 1

DDB1 – DNA damage binding protein 1

DDB2 DNA damage binding protein 2

DDR – DNA damage response

DDK – Dbf4 dependent kinase

DMF - Dimethylformamide

DNA – Deoxyribonucleic acid

DNA-PK – DNA dependent protein kinase

DNMT1 – DNA (cytosine 5) methyl transferase 1

dNTP - Deoxyribonucleotide

DSB – Double strand break

dsDNA – Double stranded DNA

DUB – Deubiquitylating enzyme

E6AP – Ubiquitin-protein ligase E3A, UBE3A

ELYS – AT-Hook Containing Transcription Factor 1, AHCTF1

ER – Endoplasmic reticulum

ERAD – Endoplasmic reticulum associated protein degradation 2

FACT – Facilitates chromatin transcription complex

Faf1 – FAS associated factor 1

Faf2 – Fas Associated Factor Family Member 2

FANC – Fanconi anemia complementation group protein

FEN1 – Flap endonuclease 1

Flna – Flamin A

GINS – Go, Ichi, Nii, andSan

H – Histone

H2b1.1 – Histone H2B type 1-A

HECT – Homologous to the E6AP carboxyl terminus

Hf1oo – H1.8 Linker Histone

Hif1α – Hypoxia inducible factor 1 alpha

IgG – Immunoglobulin G

IP – Immunoprecipitation

IPTG – Isopropyl-β-D-1-thiogalactopyranoside

ISG15 – Interferon-stimulated gene 15

K - Lysine

LRR1 – Leucine rich repeat protein 1

MAD – Mitochondrion-associated degradation

MCM – Mcm2-7 complex

MPN – Mpr1, Pad1 N-terminal domain

MS – Mass spectrometry

NEDD8 – Neural precursor cell expressed, developmentally down-regulated protein 8

NEM – N-ethylmaleimide

NF-κB – nuclear factor kappa-light-chain-enhancer of activated B cells

Npl4 – Nuclear protein localization protein 4

NUP – Nuclear pore components

OD – Optical density

ORC – Origin recognition complex

PAGE – Polyacrylamide gel electrophoresis

PBS – Phosphate buffered saline

PCNA – Proliferating cell nuclear antigen

PIP box – PCNA interacting protein box

Plx1 – Polo-like kinase

PMSF – Phenylmethylsulfonyl fluoride

Pre-RC – Pre-replication complex

PUB – PNGase/UBA or UBX containing protein

PUL – PLAP, Ufd3 and Lub1p

RanBP2 – RAN binding protein 2

RBR – Ring between ring domain Rbx – Ring box

RFC – Replication factor C

RING – Really interesting new gene

RNA – Ribonucleic acid

RNAi – RNA interference

RPA – Replication protein A

SALL4 – Sal like protein 4

SAKS1 – SAPK substrate protein 1

SCF – Skp1-cullin-F-box complex

SDS – Dodecyl sulfate sodium

SEM – Standard error of the mean

SENP – SUMO specific protease

siRNA – Small interference RNA

SMARCL1 – SWI/SNF related matrix associated actin dependent regulator of chromatin subfamily A like protein 1

Smarca5 – SWI/SNF Related, Matrix Associated, Actin Dependent Regulator Of Chromatin, Subfamily A, Member 5

Smc – Structural Maintenance of Chromosomes Protein

SPT16 – FACT complex subunit SPT16

SPRTN – SprT-Like N-Terminal Domain

SSB – Single strand break

ssDNA – Single stranded DNA

SUMO – Small ubiquitin like modifier

TopBP1 – DNA topoisomerase 2 binding protein 1

TPX2 – Microtubule Nucleation Factor

Traip – TRAF interacting protein

Trafd1 – TRAF-type zinc finger domain-containing protein 1

UBA – Ubiquitin Associated domain

UBA3 – Ubiquitin-like protein-activating enzyme 3

UBE2F – Ubiquitin Conjugating Enzyme E2 F

UBE2M – Ubiquitin Conjugating Enzyme E2 M

Ubi – Ubiquitin

Ubi-NOK – Ubiquitin no lysine

UBL – Ubiquitin like modifier

UBX – Ubiquitin regulatory X domain

UBXD1 – UBX domain containing protein 1

UBXD7 – UBX Domain Protein 7

UBXL – UBX like domain

UCH-L3 – Ubiquitin carboxyl-terminal hydrolase isozyme L3

Ufd1 – Ubiquitin fusion degradation protein 1

UFM1 – Ubiquitin-fold modifier 1

Uhrf1 – Ubiquitin like with PHD and RING finger domain containing protein 1

UIM – Ubiquitin interacting motifs

URM1 – Ubiquitin-related modifier-1

USP21 – Ubiquitin Specific Peptidase 21

USP9X – Ubiquitin Specific Peptidase 9 X-Linked

UV – Ultra violet

VBM – VCP binding motif

VCP – Valosin containing protein

VHL – Von Hippel-Lindau tumour suppressor

VIM – VCP interacting motif

XMAP215 – The member pf microtubule-associated proteins (MAPs)

XPC – Xeroderma pigmentosum complementation group C

WRN – Werner helicase

WSTF – Williams-Beuren syndrome transcription factor, BAZ1B

wt – Wild type

WWP2 – WW Domain Containing E3 Ubiquitin Protein Ligase 2

1 INTRODUCTION

1.1. The Ubiquitin Proteasome system (UPS)

Ubiquitylation is a fundamental, regulatory post-translational protein modification that controls intracellular signalling events. The ubiquitin proteasome system includes ubiquitin, the proteasome and a variety of enzymes that manage the process of substrate ubiquitylation. Through this system, ubiquitylated substrates are degraded by the proteasome and free ubiquitin is released and recycled.

1.1.1. The Structure of Ubiquitin

Ubiquitin is a highly abundant protein that consists of 76 amino acids with an approximate molecular weight of 8.6 kDa. It is conserved from yeast to human. The structure of ubiquitin is compact with a six-residue C terminal tail (Komander, Clague et al. 2009). Ubiquitin is attached to the substrate through C-terminal GG at the distal end of the ubiquitin (Figure 1.1) (Komander, Clague et al. 2009). Ubiquitin core residues are not flexible except for the b1-b2 loop including Leu8 (Komander and Rape 2012). This particular region shows flexibility and has a critical role for recognition by ubiquitin binding proteins (Komander and Rape 2012) (Callis 2014). Ubiquitin is recognised *via* its hydrophobic surfaces. The area containing Ile44, Leu8 and Val70 is called the Ile44 hydrophobic patch (Komander and Rape 2012) (Callis 2014) and most ubiquitin binding domains and proteasome attach to ubiquitin through this Ile44 patch. However, HECT E3 ubiquitin ligases, deubiquitylating enzymes (DUBs) and some UBD ubiquitin binding domains bind ubiquitin through another Ile36 patch. Moreover, the Ile36 patch has the ability to generate binding of ubiquitin molecules to each other. Besides these patches and the C-terminus, the N-terminal region and the seven lysine residues are the most important properties of ubiquitin, which enable ubiquitin chain assembly.

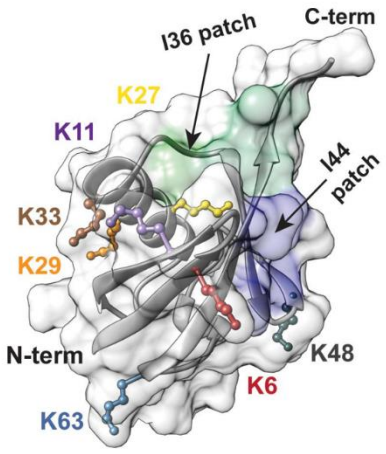

Figure 1. 1 Ubiquitin structure The structural properties of ubiquitin, showing the C terminus (C term), the seven lysine residues of the ubiquitin structure. The bubbles are showing the amino groups participating in ubiquitin chain formation. The I36 (highlighted in green) and I44 (highlighted in blue) hydrophobic patches centered in the N terminus. Taken from Deol et al, 2019 (Deol, Lorenz et al. 2019).

Process of ubiquitylation

The process of ubiquitylation involves three main steps which are activation, conjugation, and ligation. These steps are mediated by an enzymatic cascade including E1 ubiquitin-activating enzymes, E2 ubiquitin-conjugating enzymes and E3 ubiquitin ligases.

The first enzyme, E1, catalyses the activation of ubiquitin in an ATP-dependent manner, which means that the C-terminal carboxyl group of ubiquitin is adenylated and then the E1 activating enzyme becomes linked with ubiquitin through a thioester bond. After ubiquitin is activated, the E1 enzyme transfers it to a cysteine residue in the E2 conjugating enzyme (Callis 2014).

At this stage, either E2 can transfer ubiquitin to its substrate or an E3 ligase catalyses the transfer of the ubiquitin from the E2 to the substrate protein (Figure 1.2.) (Hershko, Ciechanover et al. 2000, Callis 2014). A bond is created between a lysine of the substrate protein and the C-terminal glycine of the active ubiquitin (Pickart and Eddins 2004). For this reaction, the E3 associates directly with the E2. Depending on the type of E3, E2 can either directly transfer the ubiquitin to the substrate or transfer requires catalysis by the E3. E3 ligases have either a HECT domain, which transiently catalyses ubiquitin transfer, or a RING domain that facilitates transfer of the ubiquitin from the E2 enzyme to the target protein (de Bie and Ciechanover 2011) (Berndsen and Wolberger 2014).

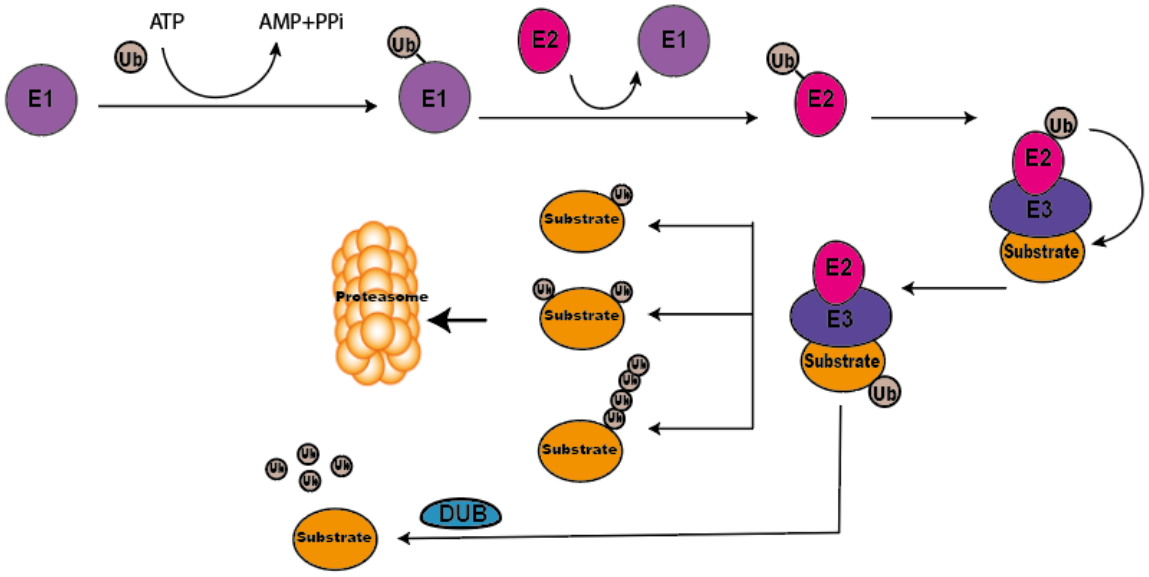

Figure 1. 2 The process of ubiquitylation. Ubiquitin is activated by an E1 enzyme, conjugated by an E2 enzyme and either transferred by an E3 ligase or E2 enzyme. The ubiquitylated substrate is either degraded by the proteasome or deubiquitylated by deubiquitylating enzymes (DUBs) . The ubiquitylated substrate has also other roles role in DNA repair, lysosomal degradation, cell localisation, kinase modification or Endoplasmic reticulum Associated degradation (ERAD) (Komander and Rape 2012, Skaar, Pagan et al. 2014).

So far, there are two known E1 enzymes, ~40 E2 enzymes and more than 600 E3 ligases encoded by the human genome (Maculins, Carter et al. 2016). The process of ubiquitylation is reversible through the action of approximately 100 deubiquitylating enzymes (DUBs), which are ubiquitin specialised proteases. DUBs have a variety of ubiquitin binding domains, and can therefore recognise many different ubiquitin chains and substrates (Komander, Clague et al. 2009). With the activities of DUBs, ubiquitin can be recycled for different cellular processes (Callis 2014). The other important role of DUBs is to prevent inappropriate degradation of proteins and to inhibit certain protein-protein interactions (Hussain, Zhang et al. 2009).

1.1.2. Forms of Protein Ubiquitylation

Once a single ubiquitin has been attached to a single lysine residue of a target protein, the protein is said to be monoubiquitylated (Figure 1.3.a). Monoubiquitylation can occur at several lysines throughout a protein, in which case it is defined as multi-monoubiquitylation (Figure 1.3.b).

Monoubiquitylation regulates various processes such as endocytosis, meiosis and chromatin remodelling. It can change protein activity and localization (Passmore and Barford 2004, Dikic, Wakatsuki et al. 2009, Meyer and Rape 2014). Monoubiquitylation has also a critical importance in regulating the DNA damage response and the DNA polymerase sliding clamp PCNA (Sigismund, Polo et al. 2004, Ulrich 2012). Moreover, polymeric ubiquitin chains can form on the substrate proteins. In this case, the lysine residues on the ubiquitin molecules are themselves ubiquitylated. These polymeric chains can consist of either 2-10 ubiquitin molecules as a short chain, or more than ten molecules as a long chain. This can occur on the same residue on each ubiquitin to form a homogenous ubiquitin chain such as K48, K63 linked ubiquitin chain (Figure 1.3.c) or the first methionine (linear chain) (Figure 1.3.d). Alternatively, different lysine residues within ubiquitin can be modified during chain elongation resulting in mixed or branched ubiquitin chains (Figures 1.3.e and 1.3.f) (Komander and Rape 2012). These are called heterogeneous ubiquitin chains and chains like these are used in NF-κB signalling and protein trafficking (Komander and Rape 2012).

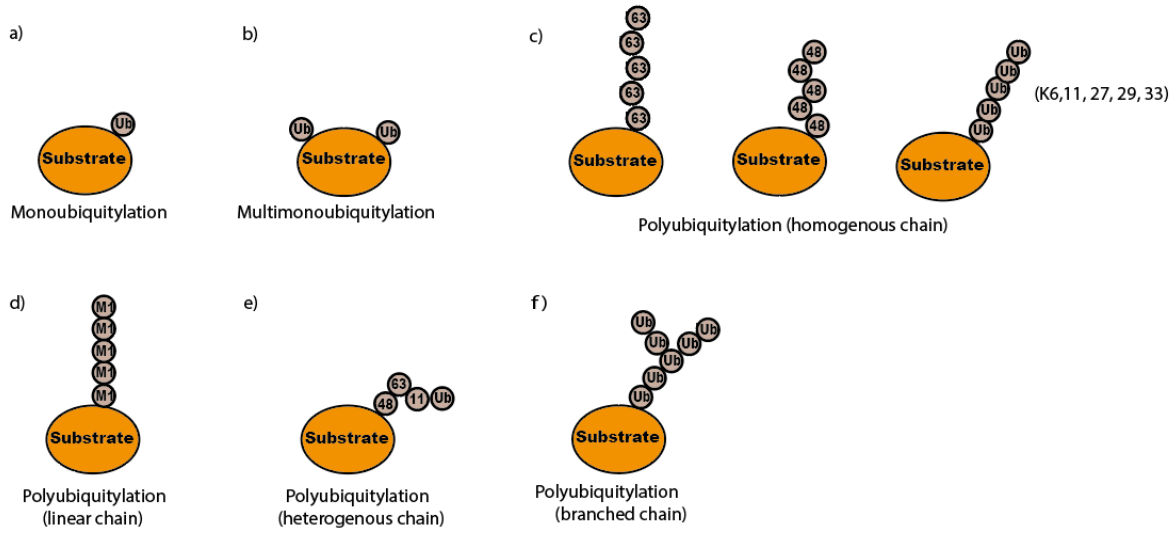

Figure 1. 3 The different forms of ubiquitin chain. Ubiquitin modifications can be classified into two main types: (a) monoubiquitylation and (c, d, e, f) polyubiquitylation. b) Multimonoubiquitylation can take place on more than one lysine residue on the same protein. Polyubiquitylation can be divided into homogenous ubiquitylation (each ubiquitin chain contains one type of ubiquitin linkage) (c, d) or heterogeneous ubiquitylation (containing more than one type of ubiquitin linkage) (e, f) (Komander and Rape 2012).

Cells can detect all different ubiquitin chains through proteins with different types of ubiquitin binding domains and the forms of ubiquitin chains determine the fate of the modified proteins. Either they are targeted for degradation by the proteasome or they function to initiate signalling pathways (Figure 1.4.).

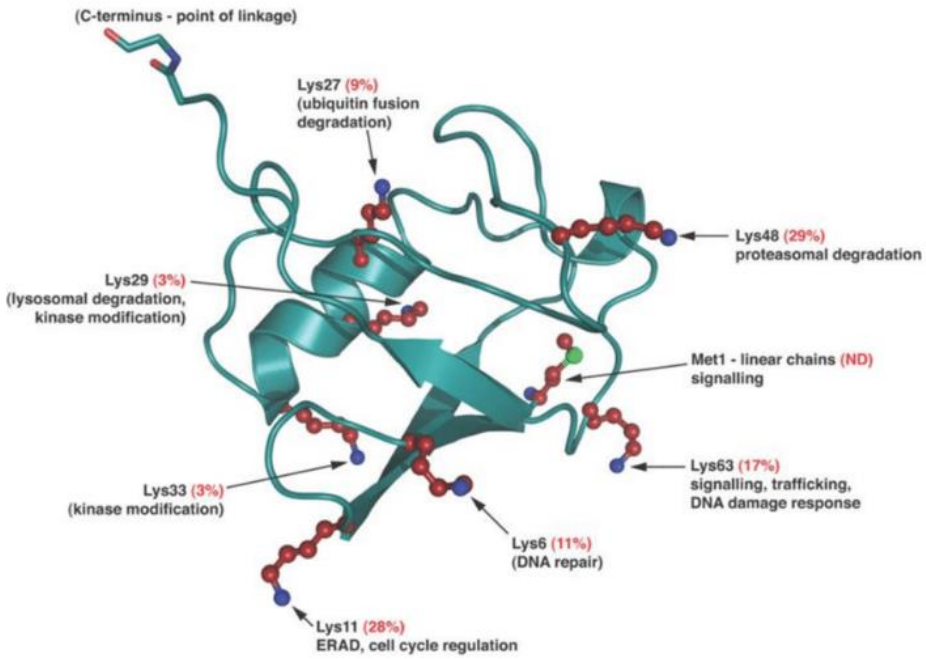

Figure 1. 4 Functions of different types of ubiquitin chains. In brackets I show abundance of the particular type of chain and the most known function of this type of chain. Blue balls indicate the amino group within the ubiquitin structure. Taken from Komander et al, 2009

Ubiquitin has seven lysine residues that are lysine6 (K6), lysine11 (K11), lysine27 (K27), lysine29 (K29), lysine33 (K33), lysine48 (K48) and lysine63 (K63). Although ubiquitin chains, formed using all seven residues, have been identified in a variety of cellular processes (Dittmar and Winklhofer 2019).

Mass spectrometry based proteomics defined ubiquitylation sites and distinguished a various of ubiquitin chain linkages. Xu et al has analysed all ubiquitin content of yeast with quantative proteomics study and detected percentages of ubiquitin chains (Xu, Duong et al. 2009). K48 and K11 linkages are the most abundant ubiquitin chain types in the cells, while K29 and K33 linked chains are rare types in the cells. Polyubiquitin chains consisting of K48 and K11 linkages regulate proteasomal degradation, while others control protein-protein interactions (Komander 2009). The ubiquitins in the linear chains attach to each other through N-terminal methionine. It is spatially close to K63-linked chain, therefore its structure is similar to K63 linkages.

The proteasome, which is a 2.5 MDa protease, has a variety of forms. 26S proteasome is the major proteasome, which consists of the 19S regulatory region and the 20S core region, which is the acting protease (Tanaka 2009). The coefficient sedimentation of these two regions combined is 26S, defined

by density-gradient centrifugation analysis, therefore it called 26S proteasome (Tanaka 2009). Protein homeostasis is a biological process in the cells that controls protein quality by degrading, trafficking and folding of proteins (Webster, Smith et al. 2017, Hoppe and Cohen 2020). Protein homeostasis is a crucial process to maintain cell growth and viability. Degradation of proteins such as misfolded, unfolded or damaged proteins by proteasome using ATP hydrolysis is a critical process that maintains protein homeostasis in all eukaryotic cells (Evans 2005, Lata, Mishra et al. 2018). Most of the ubiquitylated proteins are targeted by proteasome, while some proteins are also degraded by proteasome through ubiquitin independent pathways such as p53, p73 and BIMEL that have unstructured regions (Asher, Tsvetkov et al. 2005, Wiggins, Tsvetkov et al. 2011)

Proteins polyubiquitylated with K48-linked ubiquitin chains initially bind to a variety of ubiquitin receptors within the 19S regulatory region of the proteasome, and then they are translocated into an internal gap within the 20S particle to be hydrolysed. A protein marked with a K48-linked ubiquitin chain is degraded within minutes in the cell (Finley 2009). DUBs and ubiquitin receptors form a part of the proteasome. Many reports suggest that proteins which are to be degraded are generally ubiquitylated with chains containing K48 linkages, but modification by K11-linked chains and with other chain types (excluding K63) also can lead to proteasomal degradation of the substrate (Komander, Clague et al. 2009, Matsumoto, Wickliffe et al. 2010, Wickliffe, Williamson et al. 2011).

1.1.3. Ubiquitin Binding Domains

Ubiquitin binding domains are specific domains within proteins that can recognise different forms of ubiquitin and ubiquitin chains and decipher the ubiquitin signal (Rahighi and Dikic 2012). They non-covalently bind to the ubiquitin protein (Dikic, Wakatsuki et al. 2009, Rahighi and Dikic 2012). Twenty different ubiquitin binding domains (UBD) have been identified in ubiquitin binding proteins (Dikic, Wakatsuki et al. 2009). Ubiquitin and UBD interactions are critical for many cellular processes in the cell such as protein stability or the DNA damage response. Ubiquitin binding domains differ according to the ubiquitylated protein to which they bind and the ubiquitin modifications involved (Dikic, Wakatsuki et al. 2009, Rahighi and Dikic 2012). Although the biggest group of ubiquitin binding domains such as Ubiquitin Interacting Motifs (UIM) and Ubiquitin Associated domains (UBA) use an α-helix to bind the hydrophobic Ile44 patch of ubiquitin, different ubiquitin binding domains are able to bind different surfaces of ubiquitin (Hurley, Lee et al. 2006).

The UIM domain has been found to recognise ubiquitylation of the proteins degraded by the proteasome or proteins related with protein transport (Hofmann and Falquet 2001, Polo, Sigismund

et al. 2002). UIM has low affinity for monoubiquitylated proteins (Fisher, Wang et al. 2003). Some ubiquitin binding domains have linkage selectivity, for example UBAs are classified into different groups: the first group has more affinity for K48-linked ubiquitin chains, while the second group is more selective to K63-linked ubiquitin chains. This is most probably due to conformational differences of polyubiquitin chains (Hurley, Lee et al. 2006).

1.1.4. Other Types of Ubiquitin like Proteins

Following identification of ubiquitin, some other ubiquitin-like molecules (UBLs) were discovered that also have roles in posttranslational modifications and which target substrates in a similar enzymatic way (Welchman, Gordon et al. 2005, Herrmann, Lerman et al. 2007, van der Veen and Ploegh 2012, Cappadocia and Lima 2018). UBLs include SUMOs, NEDD8, ATG8, ATG12, URM1, UFM1, FAT10, and ISG15 protein families. They play roles in different cellular processes such as nuclear transport, autophagy, protein trafficking and DNA repair (Welchman, Gordon et al. 2005, van der Veen and Ploegh 2012, Cappadocia and Lima 2018, Da Costa and Schmidt 2020). The conjugation of UBLs to their substrates is also reversed by specific proteases alike DUBs or sometimes DUBs themselves (Reyes-Turcu, Ventii et al. 2009). For example, deubiquitylating enzymes USP21 and UCH-L3 proteolytically target both ubiquitin and Nedd8, or USP18 cleaves off another UBL: ISG15 (Nijman, Luna-Vargas et al. 2005).

1.1.4.1. NEDD8 targets Cullin type ubiquitin ligases

NEDD8 (neural precursor cell-expressed, developmentally downregulated 8) has the most sequence identity to ubiquitin among the other ubiquitin like proteins, with 58% identity (Figure 1.5.) (van der Veen and Ploegh 2012). The covalent attachment of NEDD8 to a lysine residue of a target protein is called neddylation and it is reversible (Xirodimas 2008). Similarly to ubiquitylation, NEDD8 is activated by a NEDD8 E1 Activating Enzyme (NAE), which is a heterodimeric complex of App-Bp1 and Uba3, conjugated by a NEDD8 E2 Enzyme Ubc12 (alternative name is Ube2M) or Ube2F and ligated by a substrate specific NEDD8 E3 ligase Dcn1 (Kurz, Chou et al. 2008, van der Veen and Ploegh 2012, Zhou, Jiang et al. 2019).

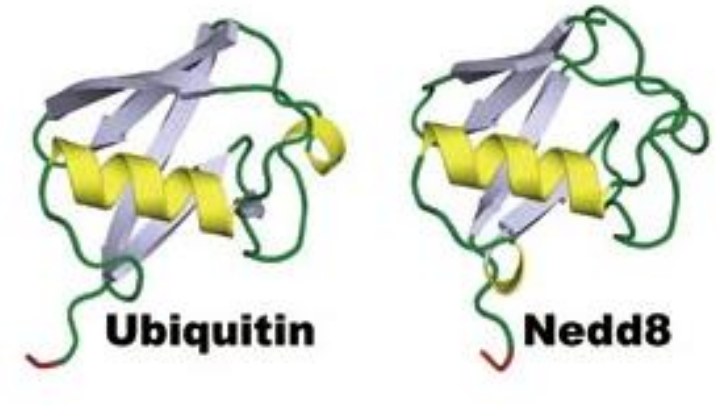

Figure 1. 5 The crystal structure of NEDD8 protein. NEDD8 is a ubiquitin like protein. Red represents the C-terminal tail. Taken from Ronau et al, 2016 (Ronau, Beckmann et al. 2016).

The most well-known substrates for NEDD8 modification are the Cullin family members (Cul1, -2, -3, -4A, -4B, -5, -7 and PARC). Cullins serve as molecular scaffolding subunits of Cullin-Ring Ubiquitin ligases (CRLs) (Welchman, Gordon et al. 2005, Herrmann, Lerman et al. 2007, van der Veen and Ploegh 2012). NEDD8 covalently conjugates with a conserved lysine residue on Cullin and this neddylation leads to enhanced ubiquitylation activity of Cullin *via* a conformational change (van der Veen and Ploegh 2012).

The de-neddylation of Cullins (NEDD8 removal) is carried out by CSN5 (zinc-dependent metalloenzyme), a member of the eight-subunit COP9 signalosome (CSN). Neddylation of Cullins is also inhibited by CAND1 (Cullin associated and neddylation-disassociated) (Liu, Furukawa et al. 2002, Zheng, Yang et al. 2002). The regulation of Cullins activity by Nedd8 is described in more detail in section 1.1.6.3.1.

1.1.5. Different types of ubiquitin ligases

Ubiquitin ligases (also called E3 ubiquitin ligases) regulate many different cellular processes such as trafficking, cell division and cell signalling *via* regulating protein ubiquitylation and degradation. At the final step of ubiquitylation, E3 ubiquitin ligase helps to transfer ubiquitin protein from the E2 conjugating enzyme to the specific substrate (Zheng and Shabek 2017, Horn-Ghetko, Krist et al. 2021). More than 600 E3 ubiquitin ligases has been found in the human genome (Li, Bengtson et al. 2008,

Zheng and Shabek 2017). Ubiquitin ligases are divided into three classes based on their catalytic subunits: HECT (homologous to E6AP C terminus), RBR (RING-between-RING) and RING (really interesting new gene) (George, Hoffiz et al. 2018, Kung, Ramachandran et al. 2019).

1.1.5.1. HECT (homologous to E6AP C terminus) E3 ubiquitin ligases

Unlike RING E3 ligases, ubiquitin is first transferred to the catalytic cysteine on the HECT E3 ligase to form a thioester bond with ubiquitin and then ubiquitin is transferred to the target protein (George, Hoffiz et al. 2018, Kung, Ramachandran et al. 2019, Qian, Zhang et al. 2020, Wang, Argiles-Castillo et al. 2020). There are two lobes in the HECT domain; the C terminal end contains the catalytic cysteine residue and the N terminal end binds the E2 conjugating enzyme (Qian, Zhang et al. 2020, Wang, Argiles-Castillo et al. 2020).

While ubiquitin is conjugated and transferred to the substrate through the HECT domain located in the C terminal end of the E3 ligase, the variable N terminal domain provides substrate binding recognition (Qian, Zhang et al. 2020, Wang, Argiles-Castillo et al. 2020). The two lobes bind each other by a flexible hinge that provides ubiquitin transfer activity *via* rotation of the lobe (Huang, Kinnucan et al. 1999). Based on the protein-protein interaction domains, 28 human HECT E3 ligases have been divided into three main classes: (1) the neuronal precursor cell-expressed developmentally downregulated 4 (NEDD4; nine members); (2) the HECT and RLD domain-containing (HERC; six members) and (3) 'other HECTs' (13 members) (Rotin and Kumar 2009).

1.1.5.2. RBR E3s (RING-between RING)

RBR E3s, which present 14 in humans, have three motifs including RING1 and RING2. The third domain is the IBR domain (in-between-RING domain) that separates these two RING domains. They catalyse ubiquitin conjugation in a similar way to HECT E3 ubiquitin ligases. Ubiquitylation of a substrate occurs in multiple steps: first the RING 1 domain identifies E2-ubiquitin conjugation, then the ubiquitin is attached to the catalytic cysteine in the RING2 domain and finally the target protein is ubiquitylated. The ubiquitylation cascade here combines the characteristics of HECT E3 and RING E3 ligases (Walden and Rittinger 2018, Kung, Ramachandran et al. 2019) .

1.1.5.3. RING (Really Interesting New Gene)-type E3 ligases

RING E3 ubiquitin ligases are the largest subfamily of E3 ligases with 600 family members in human. They comprise a zinc-binding domain called RING (Really Interesting New Gene) or without zinc domain called the U-box. They both use the same mechanism to facilitate the transfer of the E2-conjugated ubiquitin to the target protein, acting as a scaffold (Metzger, Pruneda et al. 2014, Dickson, Cole et al. 2016, Garcia-Barcena, Osinalde et al. 2020).

RING type domains have a variety of established structures. Whereas some RING domains can function as monomers, others function as heterodimers or homodimers (Deshaies and Joazeiro 2009, Kung, Ramachandran et al. 2019). Although some RING domain-containing proteins do not have ubiquitin ligase activity e.g. in Bard1, heterodimerization with a RING domain-containing protein, like BRCA1, makes them functional (Kung, Ramachandran et al. 2019).

Some RING E3 ligases have multiple subunits that recognise substrates. They are divided into two subgroups: CRLs (Cullin type RING ligases) and APC/C (anaphase-promoting complex/cyclosome) (Deshaies and Joazeiro 2009, Bulatov and Ciulli 2015, Kung, Ramachandran et al. 2019). CRLs are also categorised by the Cullin type they contain (Bulatov and Ciulli 2015).

1.1.5.3.1. Cullin type ubiquitin ligases

CRLs are the largest family of E3 ligases with more than 200 members (Sarikas, Hartmann et al. 2011). CRLs consist of a Cullin as a scaffold protein (CUL1, CUL2, CUL3, CUL4A/4B, CUL5 or CUL7), a RING box protein (RBX1 or RBX2) at the C terminus of the Cullin and an adaptor protein with a substrate receptor at the N terminus (Figure 1.6.). RING box proteins interact with E2 conjugating enzymes; the adaptor proteins are specific for each Cullin type and the substrate receptors have substrate specificity (Metzger, Pruneda et al. 2014, Bulatov and Ciulli 2015, Fouad, Wells et al. 2019, Kung, Ramachandran et al. 2019). For example, while Cul1 E3 ligase assembles with the SCF complex (Skp1 as an adaptor protein and an F-box protein as a substrate recruiting factor) (Metzger, Pruneda et al. 2014), both Cul2 and Cul5 assemble with Elongins B and C as an adaptor. However, though they both use the same adaptor, Cul2 and Cul5 interact with different substrate due to having different substrate receptors that recognize specific substrates (Kamura, Maenaka et al. 2004). CRLs are able to ubiquitylate many different target proteins in humans with more than 200 different Cullin substrate receptors (Kung, Ramachandran et al. 2019).

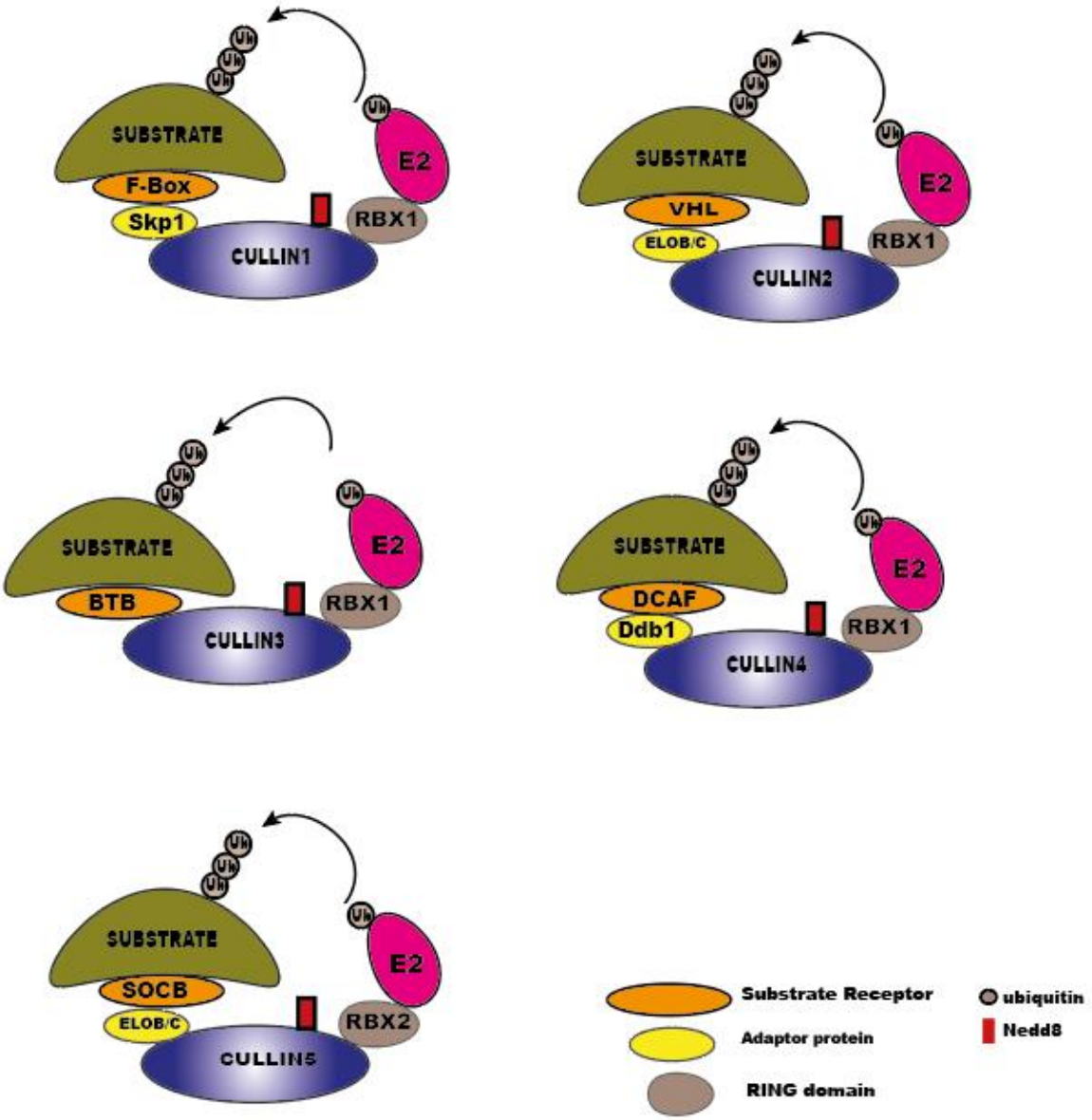

Figure 1. 6. Model of the Cullin RING E3 ligases (CRLs). All Cullin type E3 ligases (Cullin 1, 2, 3, 4 and 5) consist of adaptor protein, substrate receptor, Cullin scaffold and RING domain protein. CRLs recognise substrate protein *via* substrate receptor and ubiquitylate it using the E2 enzyme.

Cullin type ubiquitin ligases are highly regulated by different mechanisms such as neddylation by Nedd8 E3 ligase (DCN1), deneddylation by CSN and CAND1 inhibitor proteins and phosphorylation (Bulatov and Ciulli 2015). NEDD8 protein can attach to all CRL family members except for unusual Cullin RING E3 ligase subunit APC2 (anaphase-promoting complex-2). It is attached to the lysine residue near the RBX1/2 domain on the Cullin scaffold protein and enhances ubiquitylation activity of the Cullin protein. Neddylation and deneddylation cycles of CRLs is important for their function (Wu,

Lin et al. 2005, Watson, Irwin et al. 2011). One E1-Nedd8 complex can bind multiple Nedd8 E2 conjugating enzymes due to its conformational flexibility. While E2 UBE2F is specific for RBX2 RING domain, RBX1 is targeted by UBE2M (Huang, Ayrault et al. 2009). For example, RBX1 interacts with and also promotes UBE2M and Nedd8 binding to each other. Their closed confirmation is also stabilized by RBX1, allowing Need8's Ile44 hydrophobic patch binding to UBE2M. UBE2M and Nedd8 are recruited to CRL *via* supporting of RING E3 RBX1 and E3 ligase DCN1. Nedd8 is then transferred to the WHB domain of Cul1, which is located at the C terminal end of Cul1. After Nedd8 is bound through the isopeptide bond to WHB domain, this allows release of the RING domain of RBX1 into a flexible position and stimulates its ubiquitin transfer role (Baek, Scott et al. 2020). Neddylation of Cul1 protein hinders the neddylation inhibitor CAND1, so the complex of SCF (SKP1-CUL1-F-box) and its ubiquitylation activity is maintained (Liu, Furukawa et al. 2002, Welchman, Gordon et al. 2005). In contrast, CSN de-neddylates Cullin1, allowing CAND1 to bind Cul1 and inhibit its activity (Figure 1.7.) (Cope and Deshaies 2003, Schmidt, McQuary et al. 2009).

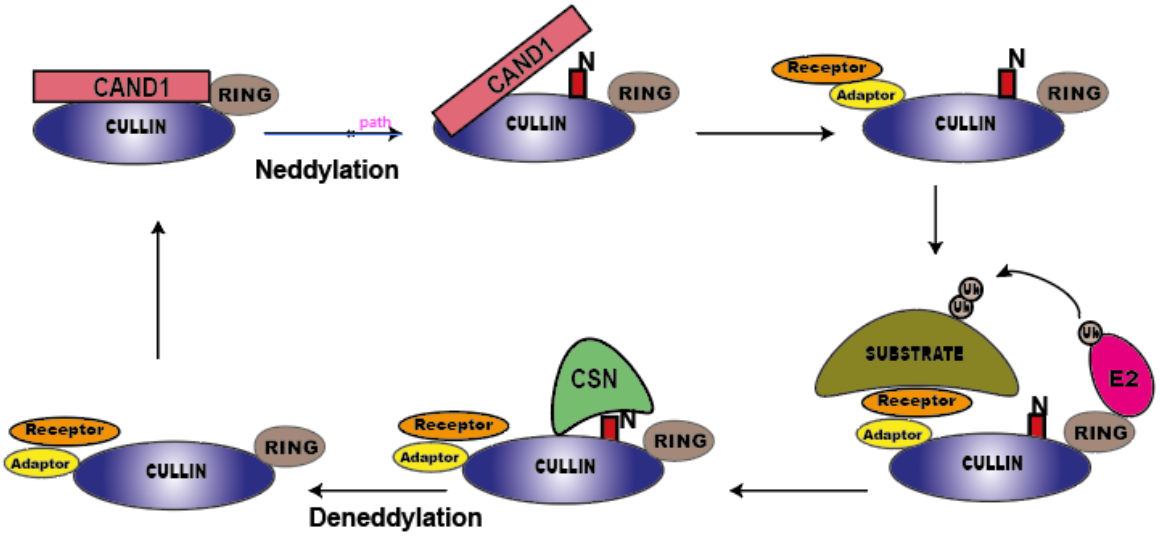

Figure 1. 7. Schematic representation of mechanism of CRLs regulation. Association of CAND1 inhibits neddylation of Cullin ligase. Neddylation of Cullin leads to disassociation of CAND1 and it allows binding of Adaptor-Receptor complex. Next the substrate is ubiquitylated by active CRL complex. After substrate displacement, CSN interacts with CRL and removes NEDD8 from CRL. NEDD8 protein is then recycled. Then, CRL2 is inactivated by binding of CAND1. Neddylation and de-neddylation provide a regulation cycle of Cullins. Adapted from Zhao et al, 2014 (Zhao, Morgan et al. 2014)

1.2. p97

1.2.1. The Structure of p97

p97, also known as VCP in metazoans, Cdc48 in yeast, CDC-48 in *Caenorhabditis elegans* and Ter94 in insects, is highly conserved from archaebacteria to metazoans (Ramadan, Halder et al. 2017). p97 belongs to the AAA family (ATPase associated with a variety of cellular activities), is a hexameric ATPase and forms a ring-like complex (Meyer, Bug et al. 2012). p97 can convert the energy of ATP hydrolysis to chemical energy to remodel or partially unfold substrate proteins. It consists of D1 and D2 ATPase domains, an N-terminal domain and a short flexible C-terminal tail (Figure 1.8.). The N and D1 domains are located on the cis side of p97, while the D2 domain and the C-terminal tail are present on the trans side of hexameric p97 (Twomey, Ji et al. 2019). The ATPase domains form two stacked rings with a pore in the centre and there is a link between the N-terminal and D1 domains (Bodnar and Rapoport 2017). While the N-terminal domain is important for interactions with cofactors and substrate proteins, the D1 and D2 ATPase domains are responsible for binding and hydrolysing ATP, which aids release of substrate proteins (D1) and provides the driving force (D2) for reactions.

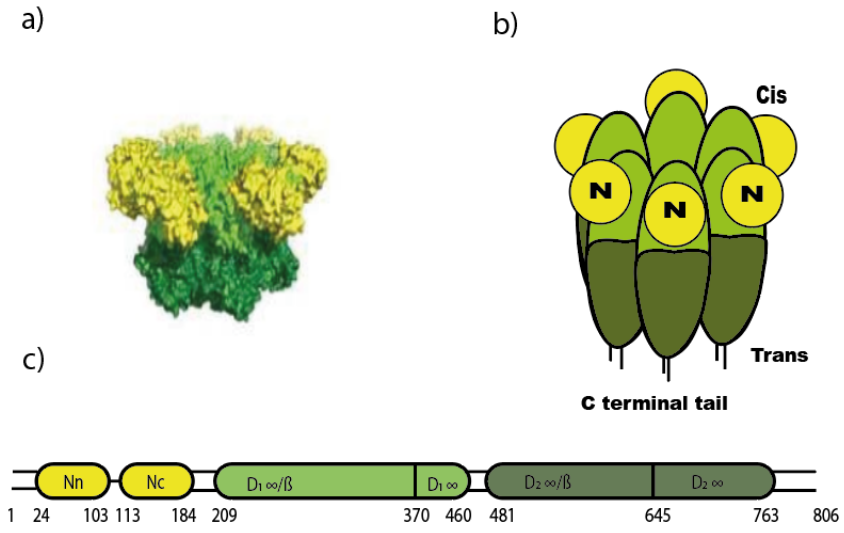

Figure 1. 8 Structure of p97. a) Side views of crystal and cryo-electron microscopy (cryo-EM) structure of p97 ATPase. b) The schematic representation of homo-hexamer p97. The N terminal domain of the hexameric ring is named as "cis side", while the C terminal tail side is called as the "trans side". c) Domain organisation of each subunits. Each subunit of p97 has an N terminal domain (yellow), D1 (light green), D2 (dark green) stacked AAA ATPase domains and C terminal tail (black). Taken and adapted from Stach et al. (Stach and Freemont 2017).

1.2.2. The Roles of p97

The cellular activities of p97 are diverse and depend on substrate localization or structure (Beskow, Grimberg et al. 2009). p97 works through binding proteins that are marked by ubiquitin and extracting them from membranes, cellular surfaces or protein complexes that they are interacting with (Meyer, Bug et al. 2012). p97 can also help to determine the fate of the substrate protein i.e. the ubiquitin chain(s) can either promote proteasomal degradation, or be edited or removed entirely, in which case the substrate protein is not degraded but instead recycled (Figure 1.9.) (Meyer, Bug et al. 2012) (Bodnar and Rapoport 2017) (Meyer and Weihl 2014). p97 assists degradation of not only polyubiquitylated proteins, but also monoubiquitylated substrates as in the case of UV-dependent RNA Pol II turnover (Meyer, Bug et al. 2012). p97 has also role ubiquitin independent disassembly which is driven Protein phosphatase-1 (PP1) holoenzymes. P37 interacts with Inhibitor-3 (I3) of PP1 without ubiquitylation, then p97 pull I3 out with ATPase energy which leads to disassembly of its partner and resulting in PP1 subunit exchange (Weith, Seiler et al. 2018).

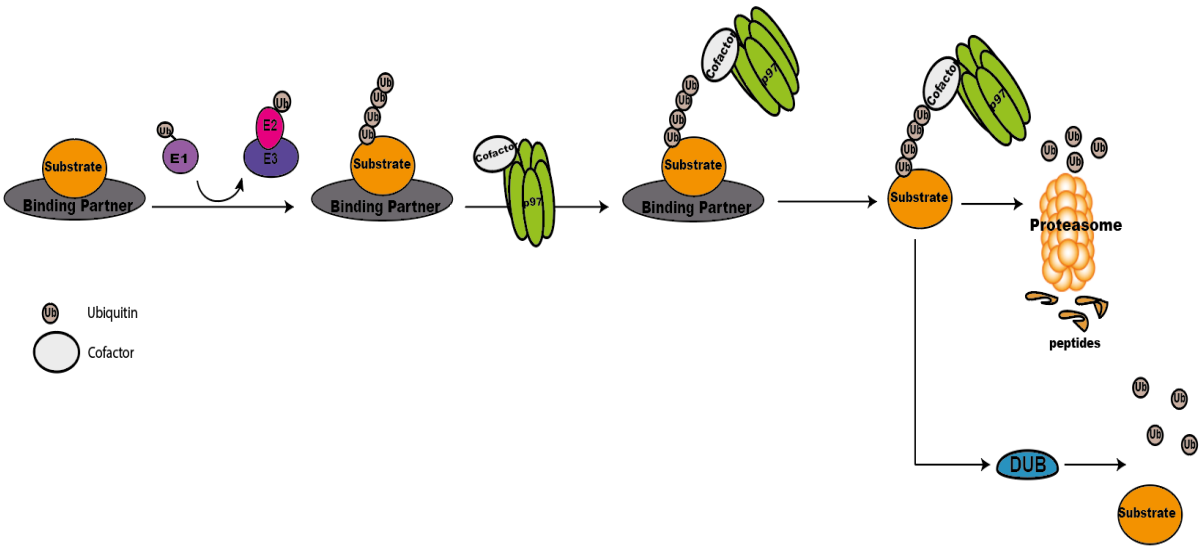

Figure 1. 9 A general model for Cdc48/p97 activity in extraction of ubiquitylated substrate. Substrate protein is ubiquitylated by ubiquitin machinery (E1, E2, E3 enzymes violet, pink and purple). A cofactor of Cdc48/p97, which has a ubiquitin binding domain, binds the ubiquitylated substrate and the substrate is transferred to the core of p97; thereby it is extracted from its binding complex (grey) such as protein complexes, membranes or chromatin by the ATPase activity of p97. After ubiquitylated substrates are extracted from their binding partners by p97 AAA ATPase, they are either degraded by the proteasome or recycled by deubiquitylating enzymes (DUBs).

The best known role of p97 in ubiquitin dependent proteasome degradation is endoplasmic reticulum (ER)–associated protein degradation (ERAD) (Stolz, Hilt et al. 2011). p97 with its cofactors removes

ubiquitylated misfolded proteins from Endoplasmic Reticulum for proteasomal degradation (Twomey, Ji et al. 2019). Other cellular processes, which require p97 segregase activity include mitochondrion-associated degradation (MAD), DNA repair, DNA replication, cell cycle regulation (Stach and Freemont 2017), DNA damage response (Dantuma and Hoppe 2012) (Franz, Ackermann et al. 2016), transcriptional and metabolic regulation and selective autophagy (Figure 1.10) (Stolz, Hilt et al. 2011). Besides these, p97 is also a central player in crucial signalling pathways (Meyer 2012) such as activation of NFκB (nuclear factor kappa-light-chain-enhancer of activated B cells, major transcription factor) to promote degradation of NFKBIA (DeLaBarre and Brunger 2003) and HIF1α (Hypoxia-inducible factor 1-alpha), the latter of which is a transcription factor and is expressed during normoxia

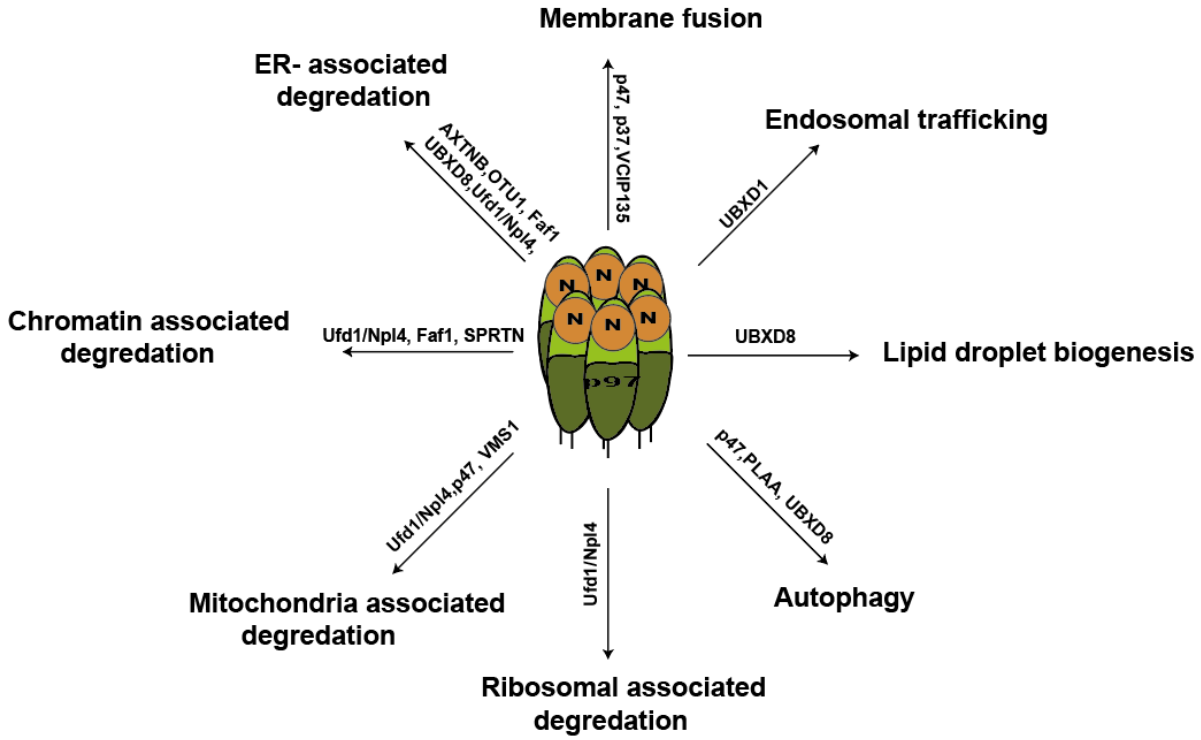

Figure 1. 10 p97 with its cofactors regulate different cellular process which are indicated. The p97 complex has a role in a variety of processes in the cell such as membrane fusion, endoplasmic reticulum associated degradation, chromatin associated degradation, mitochondria associated degradation, ribosomal associated degradation, autophagy, lipid droplet biogenesis and endosomal trafficking. The cofactors that facilitate p97 function in particular processes are listed by the arrows. Adapted from Ramadan et al, 2017 (Ramadan, Halder et al. 2017).

1.2.3. p97 Cofactors

The affinity of p97 to ubiquitin is weak and so adaptor proteins, which contain ubiquitin-binding domains, are needed for it to interact with ubiquitylated proteins (Ye 2006) (Stach and Freemont 2017). Cellular activities of p97 rely on a large number of protein cofactors. These cofactors have different roles; they can provide substrate specificity and can also change the length of ubiquitin chains, which are attached to the substrate (Bodnar and Rapoport 2017). p97 interacts with different sets of cofactors for each process (Figure 1.10) (Meyer 2012, Meyer, Bug et al. 2012).

There are two functional subclasses of p97 cofactors that provide the functional diversity of p97: (1) substrate-recruiting and (2) substrate-processing cofactors (Figu ´.11.). Substrate-recruiting cofactors help to select the different cellular substrates and these include p47, Ufd1/Npl4 and UBXD proteins like Ubxn7 and Faf1. In addition, the substrate recruiting cofactors have additional subclasses: (1) major cofactors, like UBXD1 (Vaz, Halder et al. 2013), p47 and Ufd1/Npl4, which always support p97 in particular type of activity e.g. ERAD, and (2) minor cofactors, which provide higher substrate specificity: e.g. Ubxn7, Faf1, UBXD8 (Faf2) and SAKS1. The substrate-processing cofactors, on the other hand, alter the enzymatic activities of p97-dependent reactions and include proteases such as Spartan (SPRTN) (Maskey, Kim et al. 2014), de-ubiquitylating enzymes such as YOD1 and Ataxin-3 , E3 such as GP78 (Stach and Freemont 2017)and E4 ubiquitin ligase UFD2 (human homolog is UBE4A and UBE4B) (Caren, Holmstrand et al. 2006, Hanzelmann and Schindelin 2011), which has role in multiubiquitin chain assembly, (Contino, Amati et al. 2004).

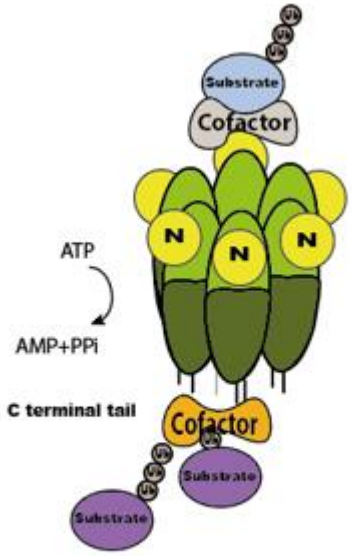

Figure 1. 11 Substrate recruiting and substrate processing cofactors of p97. p97/Cdc48 is presented in the middle with its D1/D2 domain, N terminal and C terminal tail. The domains of p97 cofactors for binding to p97 are showed on the left-hand side. Ubiquitylated substrate (blue) is detected by substrate recruiting cofactors (grey) and extracted from complex structures. Substrate processing cofactors (orange) activate polyubiquitylation of substrate (purple), inhibit it for polyubiquitylation or activate for deubiquitylation.

The cofactors bind to p97 either at its N-terminal domain or at the C-terminal tail. The largest group of cofactors, which interact with the N-terminal domain of p97, include proteins that contain ubiquitin-X (UBX), UBX-like (Meyer, Bug et al. 2012) (Meyer 2012), ubiquitin associated (binding) (UBA) (Meyer 2012), VCP-interacting motif (VIM), VBM (VCP-binding motif), and SHP (BS1, binding segment) domain (Hanzelmann and Schindelin 2011, Stach and Freemont 2017). Cofactors that bind the C-terminus of p97 typically interact through PUB (PNGase/ UBA- or UBX-containing proteins) and PUL (PLAA, Ufd3p and Lub1p) domains (Figure 1.11) (Stach and Freemont 2017).

Cofactor interactions with p97 are controlled by competition for binding position on N terminal domains (Figure 1.12.a), conformational changes (Figure 1.12.b), bipartite binding (Figure 1.12.c), and hierarchical binding (Figure 1.12.d) (Hanzelmann and Schindelin 2017, Twomey, Ji et al. 2019). The binding site on p97 that is recognised by UBX, UBX-L and VIM domains within the cofactors partly overlaps leading to competition for binding to p97. All these N domain cofactors bind the hydrophobic interdomain cleft placed between two lobes of N terminal domain of p97 (between Nn and Nc in Figure 1.8.c.) (Hanzelmann and Schindelin 2016) . SHP domain binds alternative part on the N domain of p97, different from hydrophobic interdomain cleft, but it may partially overlap with the site that UBX-L domains of NPL4 binds (Bruderer, Brasseur et al. 2004, Isaacson, Pye et al. 2007). p97 is a hexameric protein and therefore has six N domains, Ufd1/Npl4 binds to p97 through two adjacent N

domains and other cofactors could interact with the remaining N domains. Interestingly there are also hierarchical orders for cofactors binding with p97. For example, minor cofactors can only bind p97 after Ufd1/Npl4 heterodimers. While Ufd1/Npl4 does not directly interact with minor cofactors, its binding with p97 can induce a conformational change of p97 to allow tight binding of a minor cofactor (Hanzelmann, Buchberger et al. 2011).

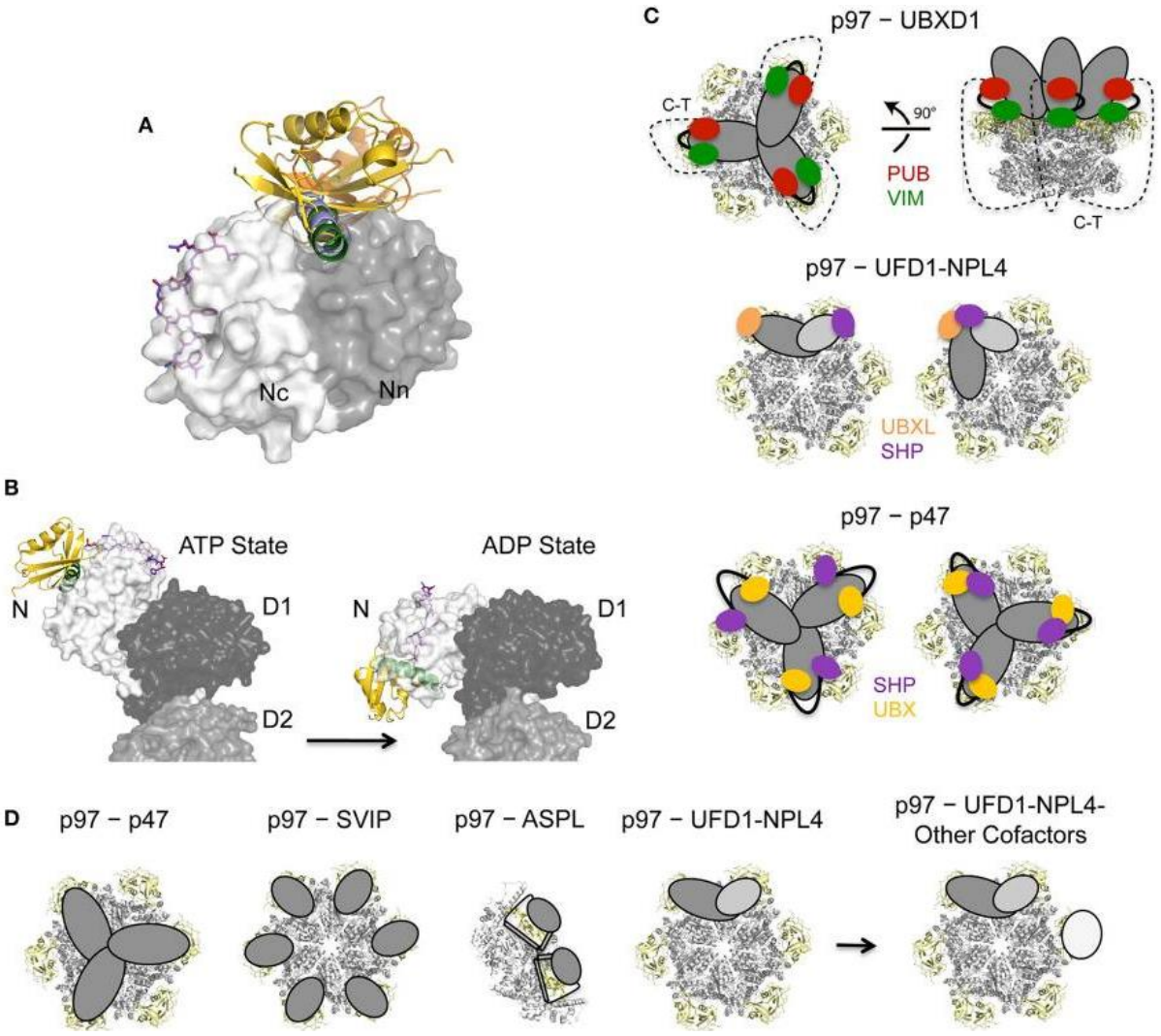

Figure 1.12 Binding mechanism of cofactors to N domain of p97 a) Competition of binding site. The cofactors position of p97 onto the N domain. Superposition of p97 N domain cofactor complexes: purple- SHP of UFD1, light green- VIM of gp78, light blue- VBM of RHBDL4, gold- UBX of FAF1, olive- UBXL of NPL4. Oval cartoons represent cofactors. Nn-in dark gray and Nc- in light gray are N domain of p97. b) Conformational changes of p97 through ATP binding and hydrolysing. p97 in the ATP- and ADP-bound states shows side position of p97 with its domains FAF1-UBX domain (gold), gp78 VIM (green), UFD1-SHP binding motif (purple) c) Bipartite binding of cofactors to p97. While UFD1-NPL4 heterodimer and p47 bind either the same or different N domains (shown

with yellow ribon), UBXD1 interacts to the N domain and the unstructured C terminal tail (C-T). d) Different oligomeric binding and hierarchical binding of cofactors (Hanzelmann and Schindelin 2017)

1.2.3.1. UBX proteins

UBX and UBX like (UBX-L) domains, which have similar structure to ubiquitin, allow for interaction with N terminal domain of p97 (Buchberger, Schindelin et al. 2015, Aguiar, Dumas et al. 2020). The human genome encodes approximately 30 UBX containing proteins (Stach and Freemont 2017). These proteins are divided into two groups according to the location of the ubiquitin related domain (Rezvani 2016). The first group of these proteins comprise both a UBX domain at the C-terminus and a UBA domain at the N-terminus; members include UBXD7 (UBXN7), UBXD8 (FAF2), UBXD10 (p47, NSFL1C), UBXD12 (FAF1), and UBXD13 (SAKS1, UBXN1) (Stach and Freemont 2017) (Rezvani 2016). Some of these members also have ubiquitin-related domains such as UIM (ubiquitin-interacting motif) and UBL (ubiquitin-like domain) (Figure 1.13 (Rezvani 2016). The cofactors that have UBA-UBX domains belong to substrate recruiting cofactors of p97 (Buchberger, Schindelin et al. 2015). Although these five proteins, which include UBX and UBA domains, can specifically recognise K11, K33, K48 and K63 linked

ubiquitin chains, recognition of K11 and K48 linked chains is more dominant (Stach and Freemont 2017).

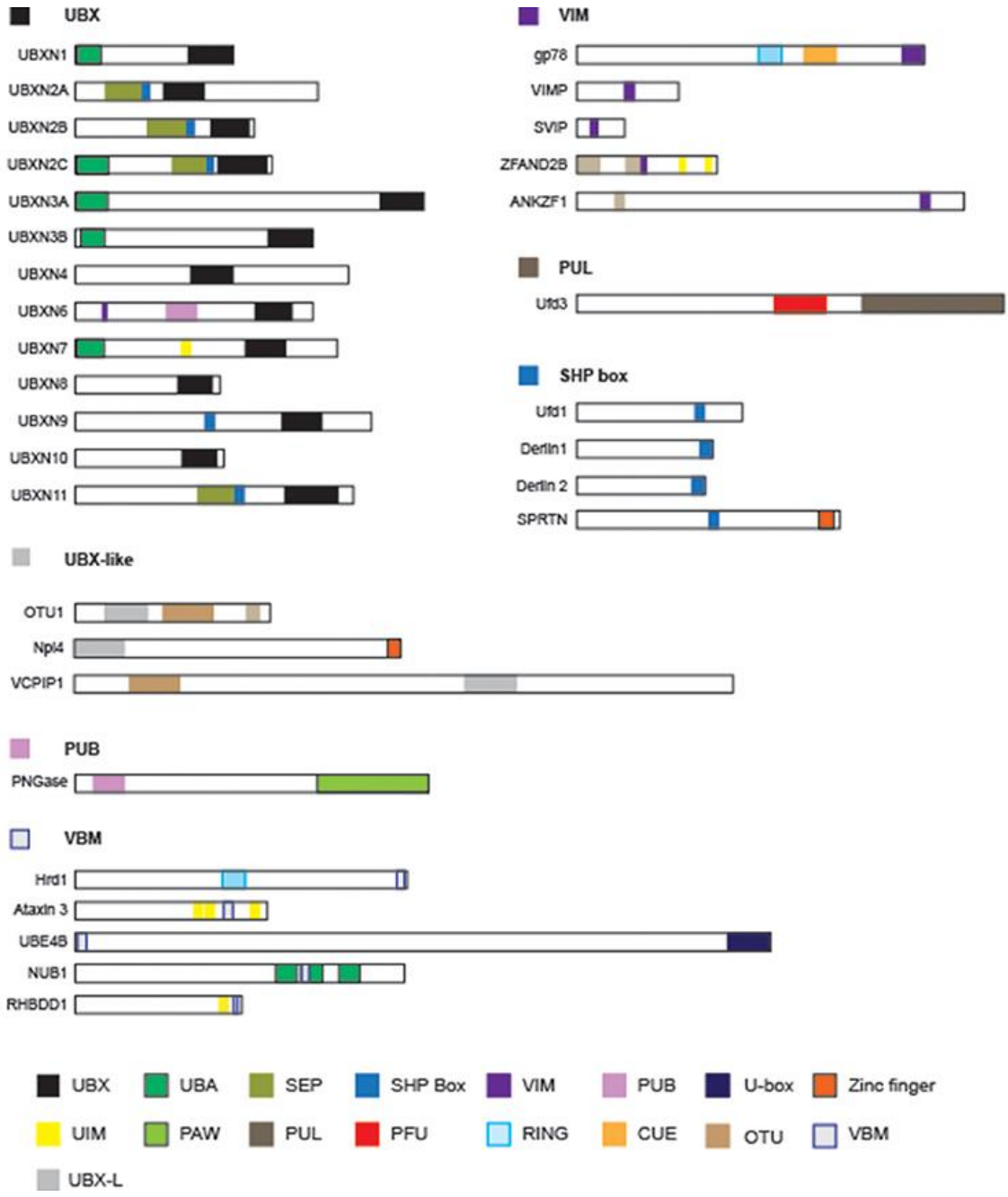

Figure 1.13 p97 cofactors. The UBA-UBX, UBX only and UBX-L domains containing cofactors, or short motifs containing the binding site 1 (SHP-BS1) interact with the p97 N-domain. UBX/UBX-like domain,UBA ubiquitin associated domain, SEP, Shp-eyc-p47 domain, VIM, VCP interacting domain, PUB, Peptid N-glycanase ubiquitin associated, ZF Zinc finger domain, UIM ubiquitin interacting motif, PAW, domain shows in PNGases and other worm proteins; PUL (PLAP, UFD3 and Lub1), PFU, PLAA family ubiquitin binding, RING, really interesting new gene, CUE (Coupling of ubiquitin to Endoplasmic reticulum degradation) domain, OTU (ovarian tumour) has deubiquitylating activity. UAS ubiquitin associated domain, UBL ubiquitin like domain, Taken from Ye, 2017 (Ye, Tang et al. 2017)**.**

The second group, members of which are: UBXD1 (UBXN6), UBXD2 (Erasin, UBXN4), UBXD3 (UBXN10), UBXD4 (UBXN2A), UBXD5 (Socius, COA-1, UBXN11), UBXD6 (Rep-8, UBXN8), UBXD9 (TUG, ASPL, ASPSCR1), and UBXD11 (P37, UBXN2B), carry only a UBX domain (Figure 1.13.).

While UBA domain of group 1 proteins facilitates their interactions with ubiquitylated substrates, all UBX family members are able to associate with p97 through their UBX domains. A common feature is that the UBX domain interacts with the hydrophobic cleft within N domain of p97 *via* a conserved FPR signature motif (Hanzelmann, Buchberger et al. 2011, Rezvani 2016). In addition p97 has a higher affinity for its ubiquitylated substrates when it binds first to the UBX domain of its cofactors

The p47 protein is one of the known cofactors of p97 (Meyer, Bug et al. 2012). As it is a member of the group 1 UBX family (UBA-UBX), it interacts with ubiquitylated proteins through its UBA domain but it also contains an SHP motif. This recently discovered motif provides an additional connection surface for the interaction between p97 and its cofactors (Rezvani 2016, Stach and Freemont 2017) and it can recruit p97 preferably to substrates containing K63 and M1 linked ubiquitin chains (Stach and Freemont 2017). p47 has an important role in the ERAD pathway, mitotic Golgi reassembly and membrane fusion (Rezvani 2016).

Another UBA-UBX family member protein is Faf1 (FAF Associated Factor1). The UBA domain of Faf1 generally binds K48-linked di-ubiquitin chains although it also can bind K63-linked chains (Kloppsteck, Ewens et al. 2012, Stach and Freemont 2017) suggesting that it has ubiquitin signalling roles apart from proteasomal degradation such as in the ERAD pathway (Kloppsteck, Ewens et al. 2012, Ewens, Panico et al. 2014) and chromatin-associated degradation (CAD) (Stach and Freemont 2017). In addition, Faf1 together with p97-Ufd1/Npl4 recognises K48-linked ubiquitin chain modified Ku80 protein and removes Ku70/80 heterodimer chromatin during NHEJ (van den Boom, Wolf et al. 2016). Besides this, UBXN-3 (*C.elegans* homolog of Faf1) interacts with CDT-1, which is a licencing factor during replication initiation. CDC-48/p97-UBXN3/Ufd1-Npl4 is required to extract CDT-1 from chromatin to complete DNA replication in *C.elegans*. Depletion of CDC-48/p97 or its cofactors leads to accumulation of CDT-1 and DNA replication abnormalities in *C.elegans* (Stach and Freemont 2017).

Ubxn7 (also called Ubxd7) has a role in HIF1α degradation in normoxia working with CUL2 ubiquitin ligase (Bandau, Knebel et al. 2012). Ubxn7 has three protein interaction domains, which mediate this: the UIM motif for binding with Cul2, the UBA domain for binding with Hif1-α (Bandau, Knebel et al. 2012) and the UBX domain for binding with p97 (Li, Wang et al. 2017). Ubxn7 binding to the substrate Hif1-α is independent of p97 (Alexandru, Graumann et al. 2008). p97-Ubxn7 extracts ubiquitylated Hif1-α and directs it for proteasomal degradation. As a result, when p97 was downregulated, endogenous Hif1-α accumulated (Alexandru, Graumann et al. 2008, Bandau, Knebel et al. 2012). While

the interaction of Ubxn7 with the Hif1-α and Cul2 is independent from p97/Ufd1/Npl4, the interaction of p97 with Hif1-α and Cul2 requires Ubxn7 as it links p97 to Hif1-α and Cul2 ligase (Alexandru, Graumann et al. 2008). Ubxn7 can bind Cul2 regardless of substrate ubiquitylation and substrate binding - it interacts with neddylated Cul2 by using its UIM domain that recognises the neddylation on Cul2. Moreover it has been shown that Ubxn7 plays as a negative regulator of Cul2. (Bandau, Knebel et al. 2012). Apart from its role in regulation of Hif1-α, Ubxn7 with p97-Npl4/Ufd1 has a role in the nucleotide excision repair (NER) pathway by extraction of DNA damage proteins DDB2 and XPC, which are Cullin4 substrates, in response to UV damage (Puumalainen, Lessel et al. 2014). Finally, Ubx5 (yeast homolog of UBXD7) upon binding Cullin3 is responsible for disassembly of RNA Pol II from chromatin with Cdc48-Ufd1/Npl4-Ubx4 in a UV dependent manner (Schuberth and Buchberger 2008, Verma, Oania et al. 2011). Furthermore, Ubxn7 RNA level has found increased with some cancer cell lines such as hepatocellular cancer, colorectal cancer, breast cancer and prostat cancer (https://www.proteinatlas.org/ENSG00000163960-UBXN7/pathology)

SAKS1 is another minor cofactor that has a role in the ERAD pathway, on which substrates it has inhibitory effects. It can recognize the substrates with K48 and K6-linked chains (Stach and Freemont 2017).

Ubxd8 is responsible for fatty acid storage regulation. Ubxd8 and Ubxd7 cofactors recognise K11, K48 and K63 linked ubiquitin chains on substrates (Stach and Freemont 2017).

ASPSCR1 (also called UBXD9, TUG or ASPL) cofactors directly interact with p97 without Ufd1/Npl4 heterodimeric complex (Hanzelmann and Schindelin 2017). It has roles in regulation of the glucose transporter GLUT4, Golgi assembly, ERAD and a variety of cellular processes (Bogan, Hendon et al. 2003, Yu, Cresswell et al. 2007). Importantly it acts as a negative regulator of p97: binding of ASPSCR1 to p97 leads to disassembly of the p97 hexamer (Hanzelmann and Schindelin 2017, Banchenko, Arumughan et al. 2019) and disrupts ATPase activity of the D2 linker of p97 (Banchenko, Arumughan et al. 2019).

1.2.3.2. UBX-L cofactors

Although the UBX-like (UBX-L) domain of cofactos has similar binding mechanism with UBX domain to p97, it is classified as a different subfamily due to lacks of multiple conserved residues which are important for binding to p97 (Isaacson, Pye et al. 2007). Moreover, a few p97 cofactors have UBX-L domain such as Npl4, which is a member of Ufd1-Npl4 heterodimer, OTU1(human hjomolog is YOD1) and VCIP135 (Buchberger, Schindelin et al. 2015).

The two major core cofactors for p97, which themselves form a heterodimer, are Ufd1 (ubiquitin fusion degradation 1) and Npl4 (nuclear protein localization homolog 4) (Stach and Freemont 2017). Npl4 contains a UBX-L domain, two ZN finger domains (not in yeast), an MPN domain and a C terminal domain. Ufd1 has an Ut3 domain, a flexible UT6 domain and two SHP motifs in mammals (Figure 1.14) (Sato, Tsuchiya et al. 2019, Twomey, Ji et al. 2019). Npl4 binds to the N-terminal domain of p97 via its UBX-L domain, while the SHP motif of Ufd1 further facilitates its interaction with p97 (Hanzelmann and Schindelin 2011). The Ufd1/Npl4 complex binds ubiquitylated proteins via the UT3 domain of Ufd1 and the NZF (NPL4 zinc finger) domain of Npl4 (Figure 1.13) (Stach and Freemont 2017, Bodnar, Kim et al. 2018). The CTD domain contributes to ubiquitin chain selectivity and initial attachment to the ubiquitin on the substrates (Sato, Tsuchiya et al. 2019). The sequence of the MPN domain, on the other hand, resembles the Rbp11 deubiquitylating enzyme, whose enzymatic activity is blocked by the UT3 region of Ufd1 (Twomey, Ji et al. 2019) . Even though MPN domain is not able to bind the K48 linked ubiquitin chains (Sato, Tsuchiya et al. 2019), it is required to interact with Ufd1. Moreover, Ufd1 interacts with Npl4 through its UT6 linker (Twomey, Ji et al. 2019). The Ufd1 and Npl4 heterodimer uses a bipartite mechanism to interact with p97 through two adjacent N domains of p97 (Hanzelmann and Schindelin 2016).

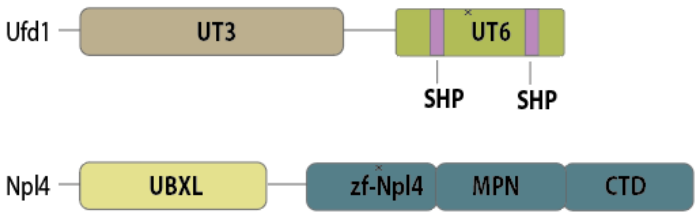

Figure 1.14 Domain structures of Ufd1 and Npl4. They bind to p97-N domain via SHP and UBX-Like (UBXL) domain, respectively. The Npl4 zinc finger (zf-Npl4) and UT3 are their ubiquitin binding domains.

Ufd1/Npl4 has a critical role primarily in ERAD, but also in chromatin association degradation and ribosome-associated degradation (Figure 1.10). Ubiquitylated proteins interact with the Ufd1/Npl4 complex (UN) through multiple ubiquitin binding sites (listed above) allowing p97 to unfold them (Twomey, Ji et al. 2019). First the ubiquitin chain is unfolded and then the substrate itself. The initiation of unfolding of the first ubiquitin is induced by association with the p97 complex itself but does not require D1 and D2 domains' activity. Once one ubiquitin in the chain is unfolded then the rest of the folded ubiquitin molecules are pulled through the p97 core (Twomey, Ji et al. 2019).

Other examples of p97 cofactors that have UBX-L domains are DUBs and YOD1. They interact with lysosomal autophagy and ERAD (Stach and Freemont 2017).

1.2.4. Substrate Translocation and Release From p97

The p97 hexameric complex has six D1 and six D2 domains, which form two stacked rings, and all twelve of them have active ATPase sites (Figure 1.8). The process of substrate recognition and translocation starts with the N domain of p97 once it is in the "down conformation". After the Ufd1/Npl4 (UN) complex binds the N terminus of p97, it attaches to the polyubiquitin chain of the substrate, which should consist of at least five ubiquitin moieties (Twomey, Ji et al. 2019). It is the UN complex that interacts with the polyubiquitin chain rather than p97 itself (Bodnar and Rapoport 2017). Recent studies have shown that after one ubiquitin from within the polyubiquitin chain firstly unfolds it then acts as a signal for substrate processing by p97. Ubiquitin binds to the Npl4 grove and the N terminus of ubiquitin inserts into the central pore of p97. The N terminal part of ubiquitin moves through the D1 domain of p97 and interacts with the D2 domain loop residues. This engagement with the D2 domain leads to formation of a staircase and pulls the rest of the unfolded ubiquitin molecules through the pore using energy from ATP binding and hydrolysis. However, this first initial unfolding within the D1 domain does not require ATP binding and ATP hydrolysis by the D2 domain. During ubiquitin translocation through the N-terminal part of p97, the D1 domain of p97 remains in the ATP bound state, as substrate binding inhibits ATP hydrolysis. The ubiquitin, which will unfold first, is at least three or four ubiquitins away from the distal end of the ubiquitin chain, while it could be one of the proximal ubiquitins that are attached to the substrate (Figure 1.15). The substrate is then unfolded while it is passed through the central pore of p97 from the D1 domain to the D2 domain. The process of this translocation then requires ATP hydrolysis by the D2 ring (Bodnar and Rapoport 2017).

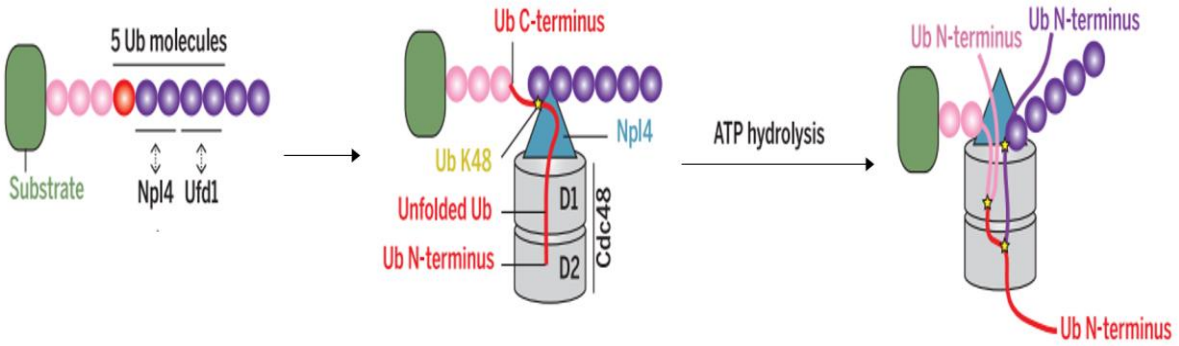

Figure 1.15 A model of substrate processing by p97. At least five ubiquitin molecules attached to the Ufd1/Npl4-p97 complex. First ubiquitin (red) unfolds and binds to the Npl4 groove. Translocation starts with the N terminal end of unfolded ubiquitin moving through the p97 core. Finally, ubiquitin molecules (pink) are pulled by p97 using energy from ATP hydrolysis until substrate becomes unfolded. In addition, the distal ubiquitin molecules (purple) are extracted by DUBs to release the substrate (Twomey, Ji et al. 2019).

ATP hydrolysis by the D1 domain has a role in substrate release from p97 and in some cases requires the interaction of a deubiquitylating enzyme (DUB) with ATPase (Stein, Ruggiano et al. 2014). OTU1 (in yeast; YOD1 in mammals) is a deubiquitylating enzyme, which binds the N domain of p97 *via* its UBX-like domain and helps to regulate efficient release of the polyubiquitylated protein (Twomey, Ji et al. 2019). In this step ATP hydrolysis of the D1 domain is critical, as the DUB cannot deubiquitylate the polyubiquitin chains whilst D1 is in an ATP bound state and the N domain is in the "up conformation". After substrate translocation has been initiated, the N domain moves back to the down conformation and DUBs can access the ubiquitin chain. The oligoubiquitylated substrate then moves entirely through the central pore (Figure 1.16). The oligoubiquitin chain may then be recycled by DUBs after translocation while the substrate is degraded by the proteasome (Bodnar and Rapoport 2017).

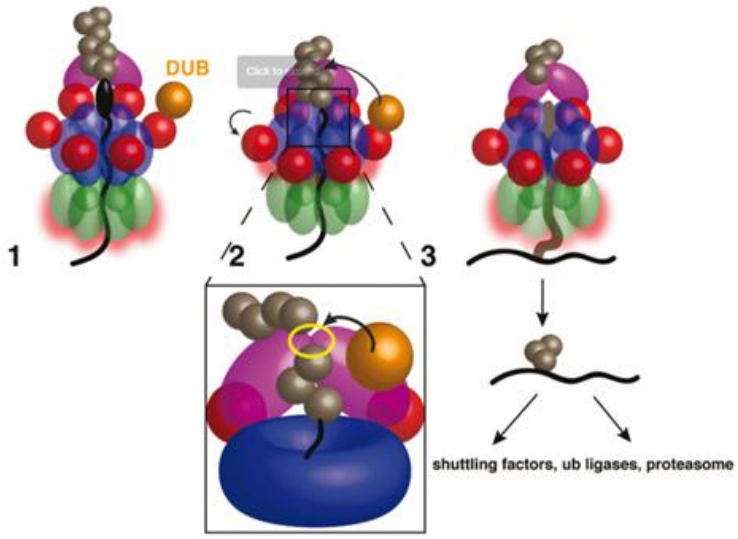

Figure 1.16 A model of substrate release from p97. Step 1: p97-Ufd1/Npl4 complex binds the polyubiquitylated substrate. The DUB binds to the N terminal domain of p97, which promotes removal of polyubiquitin chains from the substrate protein. D1 is in the ATP bound state and N domains are in the "up conformation". Step 2: Once N domains are in the "down confirmation" and substrate translocation is initiated following ATP hydrolysis of the D1 domain, the DUB can deubiquitylate the ubiquitin chain. Step 3: The oligoubiquitylated substrate is transferred through the pore and then to downstream factors. Taken from Bodnar et al, 2017 (Bodnar and Rapoport 2017).

1.3. The Function of p97 in Maintenance of Genome Stability

Many proteins are associated with chromatin and function to protect genome stability. Chromatin Associated Degradation (CAD) has emerged as an important process in maintaining genome stability and cellular homeostasis. The Ubiquitin Proteasome System (UPS), including p97, has crucial roles in

CAD (Vaz, Halder et al. 2013). These include remodelling and extraction of ubiquitylated chromatin-related proteins for recycling or degradation (Vaz, Halder et al. 2013, Meyer and Weihl 2014, Ramadan, Halder et al. 2017). This process works to regulate transcription, DNA replication, DNA repair, mitosis, cell division and chromatin associated degradation (Figure 1.17) (Torrecilla, Oehler et al. 2017). The next part of my introduction will focus therefore on the roles of p97 in DNA replication and repair, with wider introduction to the process of DNA replication and replisome disassembly, which is the subject of my research.

1.3.1. DNA Replication

The maintenance of genomic stability is essential for cell survival and development, prevention of carcinogenesis, regulation of aging and genomic alteration (Yao and Dai 2014). It is controlled by several mechanisms such as DNA damage checkpoint, DNA repair machinery and mitotic checkpoint (Giglia-Mari, Zotter et al. 2011, Yao and Dai 2014). DNA lesions can be created by exogenous sources such as ionizing radiation and ultraviolet light or endogenous sources such as reactive oxygen species. Moreover, oncogenes are activated upon increasing in DNA damage resulted in malignancy in the cells. (Abbas, Keaton et al. 2013, Vaz, Halder et al. 2013, Yao and Dai 2014). Moreover, every step of chromosomal replication must be executed in an error free manner to protect genome stability (Kang, Kang et al. 2017). Mistakes in DNA replication can lead to accumulation of mutagenic DNA lesions, genomic instability and chromosomal aberrations, which have been associated with many diseases, including cancer and premature aging (Figure 1.17) (Giglia-Mari, Zotter et al. 2011, Akopian and Rape 2017).

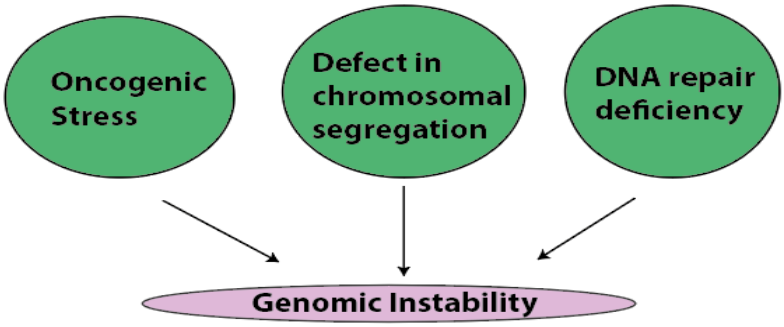

Figure 1.17 Genomic instability. It can be caused by defects in oncogenic stress, defects in chromosomal segregation, DNA repair deficiency.

1.3.1.1. The phases of DNA Replication

DNA replication initiates from certain regions of the genome, named replication origins (Cvetic and Walter 2005, Kang, Kang et al. 2017) . In eukaryotes DNA has to be replicated only once during each cell cycle (Machida, Hamlin et al. 2005). This process can be divided into four phases: origin licencing (MCM2-7 loading), initiation (origin firing), elongation and termination. These steps are carried out over two stages of the cell cycle, as explained below, and regulated by multiprotein complexes (Akopian and Rape 2017, Dewar, Low et al. 2017, Kang, Kang et al. 2017)

Accurate DNA replication must be performed in a hierarchical order at specific times in the cell cycle (Masai, Matsumoto et al. 2010, Fragkos, Ganier et al. 2015). The first step of DNA replication starts during late M phase and G1 phase of the cell cycle, when cyclin dependent kinase activity is low and involves assembly of the pre-replicative complexes (pre-RC) on DNA. Origins are determined by initial binding of the origin recognition complex (ORC), which is formed of Orc1/2/3/4/5/6. However, the molecular mechanisms of ORC are how to recruit to the chromatin is unknown. In yeast, origin selection of ORC is mainly depends on sequences (Bell and Labib 2016), although different mechanisms such as chromatin features and epigenetic mechanism are main responsible for ORC binding to origins in higher eukaryotes (Prioleau and MacAlpine 2016). For instance, it is thought that methylated Histone H4 influences origin selection by specifically interacting with Orc1 and facilitating ORC recruitment (10).

ORC together with Chromatin licensing and DNA replication factor (CDT1) and Cell Division Cycle 6 (CDC6) proteins loads two copies of the Mcm2-7 (Minichromosome maintenance 2,3,4,5,6,7) hexamer onto double-stranded DNA (Evrin, Clarke et al. 2009, Remus and Diffley 2009). Mcm2-7 is the core of the replicative helicase (Figure 1.18) (Kang, Kang et al. 2017). Together these factors constitute the pre-RCs and the process of their formation is called origin licensing (Moyer, Lewis et al. 2006, Moreno and Gambus 2015).

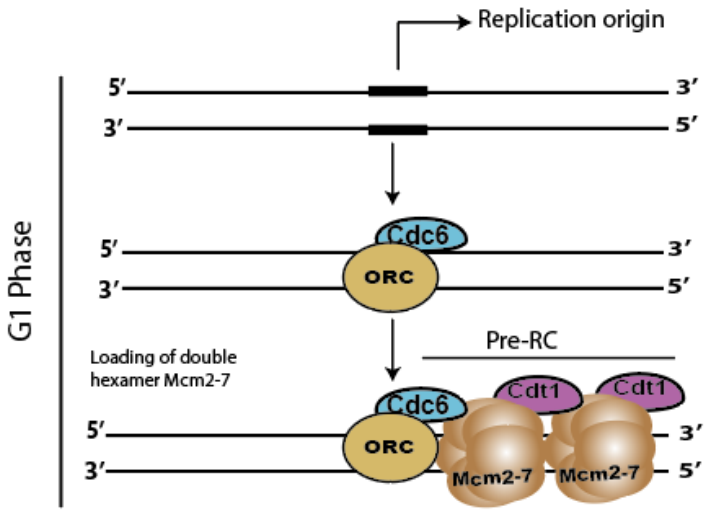

Figure 1.18 DNA origin licencing. During origin licencing, in G1 phase of the cell cycle, ORC, CDC6 and CDT1 load double hexamers of Mcm2-7 complexes on each origin of replication.

The initiation of DNA replication occurs during the S phase of the cell cycle, when CDK activity is high. In this process Cdc45 and the GINS complex (Go-Ichi-Ni-San, consisting of SLD5, PSF1, PSF2 and PSF3 or GINS1, 2, 3, 4) associate with Mcm2-7 to form the active replicative helicase, called CMG from the first letters of the components (Figure 1.9) (Kang, Kang et al. 2017) Formation of CMG is dependent on cyclin dependent kinase (CDK) and Dbf4 dependent kinase (DDK) activity. DDK helps the the recruitment of Sld3/7 and Cdc45 through phosphorylation of Mcm complex, whereas Sld2 and Sld3 are phosphorylated by CDK leading to GINS recruitment via their interaction with Dpb11, resulted in CMG complex formation (Deegan and Diffley 2016). After this activation process, each CMG complex travels in the opposite direction from one another away from the origin, unwinding DNA and providing the critical activity for DNA replication (Labib, Tercero et al. 2000, Pacek and Walter 2004, Kang, Kang et al. 2017). Mcm2-7 is an ATPase and its ATPase activity is required for unwinding of DNA but not for origin licensing (Ying and Gautier 2005).

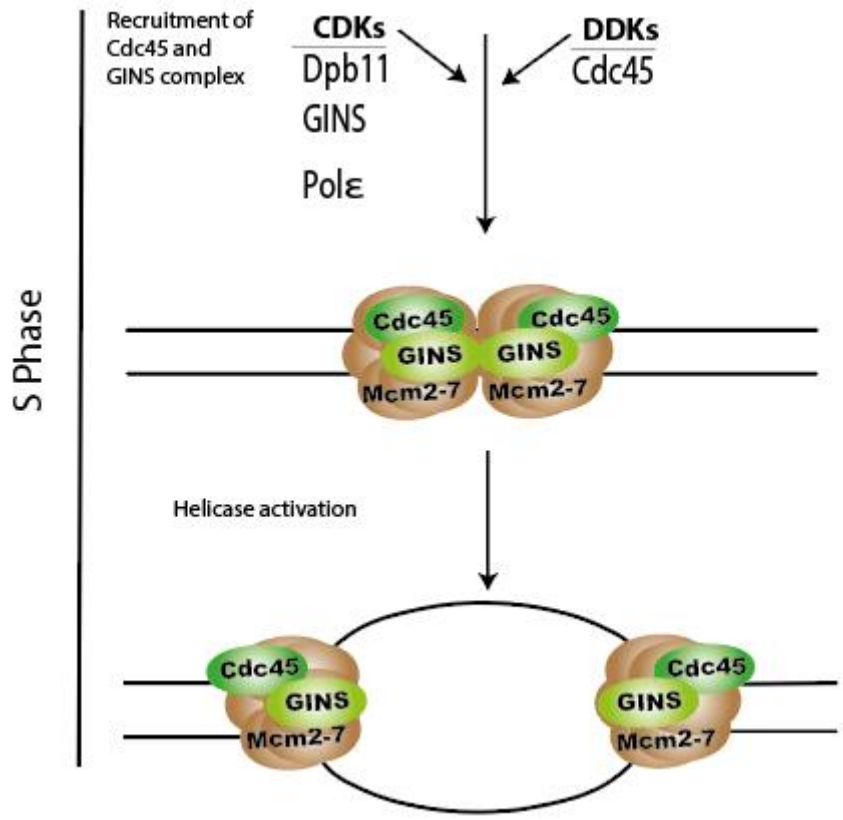

Figure 1.19 Replication initiation. Cdc45 and GINS complex are recruited to Mcm2-7 by CDKs and DDK activity during S-phase. Altogether Cdc45, Mcm2-7 and GINS form CMG complex that is an active replicative helicase.

During initiation, the CMG helicase melts DNA at the origin and remodels itself to encircle just one of the strands of DNA. In result after initiation CMG helicase encircles the leading strand template and moves along to unwind the double stranded DNA (Yardimci, Wang et al. 2012). Replication binding protein A (RPA) binds single strand DNA (ssDNA) and protects DNA from reannealing (Wold 1997, Zou, Liu et al. 2006). During elongation, DNA polymerase ε, which interacts with the CMG complex, synthesises the DNA on leading strand continuously in the same direction as the movement of the fork. However, as DNA is antiparallel, the other strand of DNA needs to be synthesised in the opposite direction to fork movement as short segments, called Okazaki fragments. The strand synthesised in the form of Okazaki fragments is called the lagging strand. To form Okazaki fragments, DNA polymerase α / primase complex makes a short RNA-DNA primer, which is then extended by DNA polymerase δ. DNA sliding clamp PCNA is loaded onto the DNA primer/template junction by the RFC complex and increases the activity of DNA polymerase δ. Once Okazaki fragments are completed, the RNA/DNA primers are removed by action of DNA polymerase δ and Fen1 endonuclease and the Okazaki fragments are joined together by DNA ligase (Bambara, Murante et al. 1997, Takisawa, Mimura et al. 2000, Burgers 2009, Dewar, Low et al. 2017) (Figure 1.20).

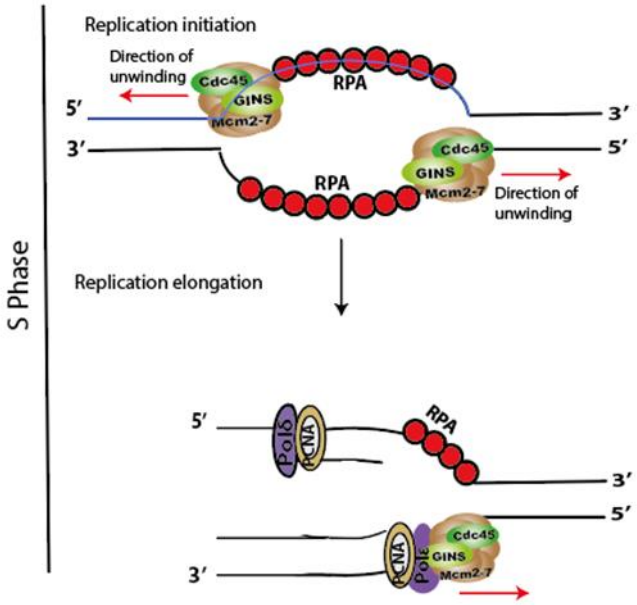

Figure 1.20 Replication elongation. During the elongation stage of DNA replication, the CMG helicase unwinds the DNA at the replication forks. DNA is synthesised as a leading and lagging strand by replication machinery (the replisome).

When two replication forks, which come from neighbouring origins, converge, the replication is terminated. It has been shown that the converging forks pass each other without significantly slowing (Dewar, Budzowska et al. 2015, Low, Chistol et al. 2020) . This can be explained by the fact that CMGs encircle the leading strand templates, therefore the CMG complexes converging at termination encounter each other on different strands (Figure 1.21) (Dewar, Budzowska et al. 2015, Dewar and Walter 2017). Upon convergence, the remaining DNA needs to be synthesised, replisomes need to be dissembled and sister chromatids detangled/decatenated (Moreno, Bailey et al. 2014, Bailey, Priego Moreno et al. 2015, Dewar and Walter 2017, Gambus 2017).

In human cells, about 30-50k replication origins are activated every S-phase. Origin position is not determined by particular DNA sequence. Origins fire stochastically in different cells, but following a spesific replication timing programme (Mechali 2010), which is regulated by chromatin organization and folding within the nucleus, the organization of transcriptional programmes and also existing of limiting replication factors (Fragkos, Ganier et al. 2015).

1.3.1.2. The role of p97 in replisome disassembly during replication termination

The segregase activity of p97 is important for disassembly of the CMG helicase complex (Maric, Maculins et al. 2014, Moreno, Bailey et al. 2014, Franz, Ackermann et al. 2016, Ramadan, Halder et al. 2017). This specific reaction does not require the proteasome (Moreno, Bailey et al. 2014). Disassembly of CMG at termination of replication forks is conserved in budding yeast (Maric, Maculins et al. 2014), worm (Sonneville, Moreno et al. 2017), frog (Moreno, Bailey et al. 2014) and in mouse (Villa, Fujisawa et al. 2021). Only one subunit of the terminated CMG is ubiquitylated – Mcm7 subunit. The polyubiquitin chain formed on Mcm7 at replication termination in S-phase is K48-linked (Maric, Maculins et al. 2014, Moreno, Bailey et al. 2014). There is a specialized ubiquitin ligase that ubiquitylates Mcm7 in budding yeast and in higher eukaryotes. Converging of CMG helicases at the end of replication promotes E3 ligase recruitment to CMG and ubiquitylation of Mcm7 (Dewar, Low et al. 2017, Sonneville, Moreno et al. 2017). Mcm7 is polyubiquitylated by the E3 ligase SCF-Dia2 in budding yeast *S.cerevisiae*, (Maric, Maculins et al. 2014, Maculins, Nkosi et al. 2015, Sonneville, Moreno et al. 2017), Cul2-Lrr1 in Xenopus (Dewar, Low et al. 2017, Dewar and Walter 2017, Gambus 2017, Sonneville, Moreno et al. 2017), in *C.elegans* (Sonneville, Moreno et al. 2017) and in mouse (Villa, Fujisawa et al. 2021). p97 has substrate specificity, which is driven by cofactors i.e. at DNA replication termination, the Ufd1-Npl4 cofactor complex has been found to help recruit p97 to the terminating CMG helicase in budding yeast (Maric, Mukherjee et al. 2017), in worms and in *Xenopus* (Sonneville, Moreno et al. 2017), and in mouse (Villa, Fujisawa et al. 2021).

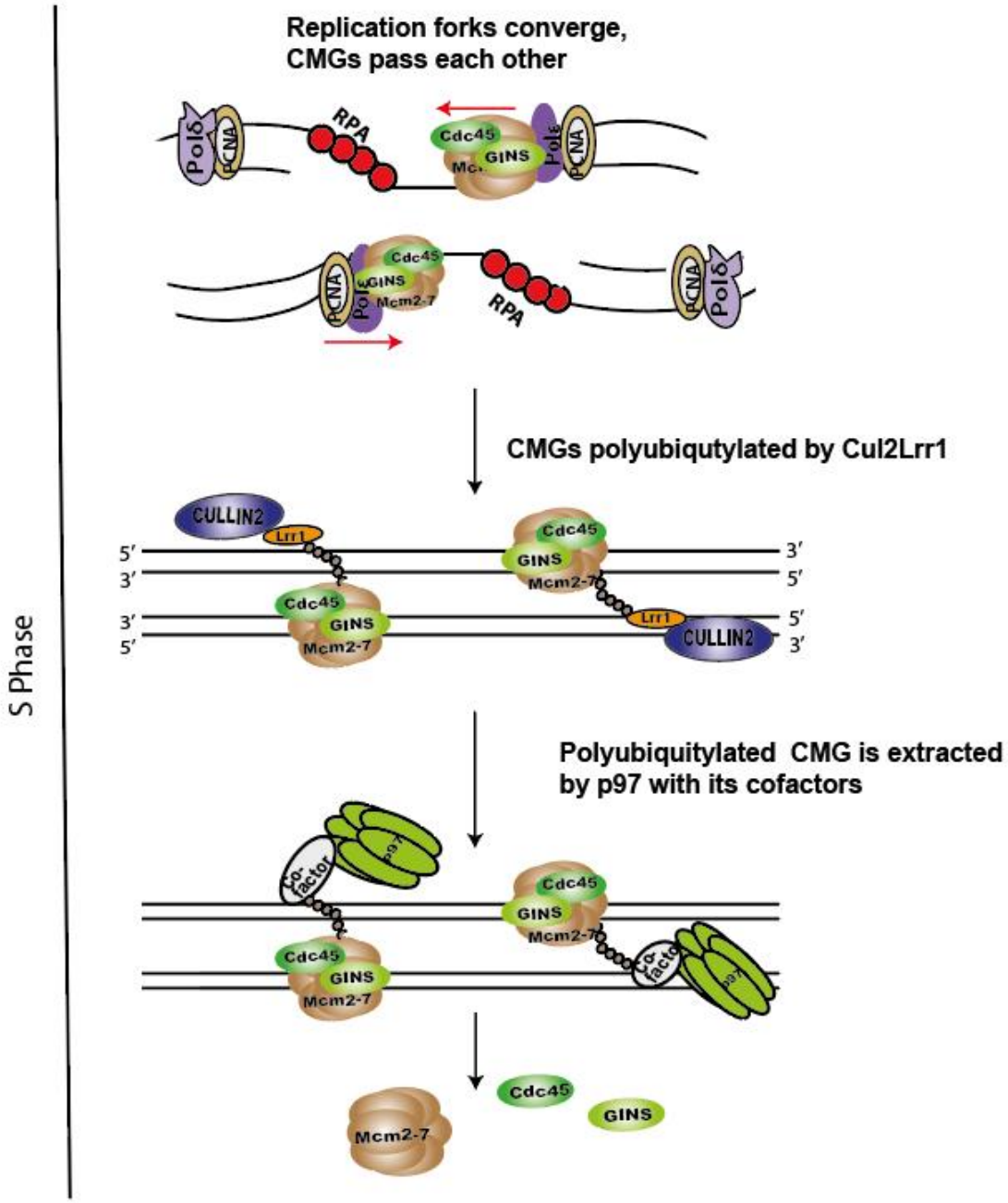

Figure 1.21 Replisome disassembly in higher eukaryotes. The two terminating forks, which come from neighbouring origins, converge, pass each other, and replisome is disassembled after DNA replication has been completed. $Cul2^{Lrr1}$ E3 ubiquitin ligase ubiquitylates CMG complex on Mcm7. p97 ubiquitin segregase with Ufd1/Npl4 cofactors recognizes polyubiquitylated Mcm7. CMG complex is unloaded from chromatin by p97 complex.

p97-Ufd1/Npl4 complex recognises polyubiquitylated Mcm7 substrate and extracts the entire CMG complex (Mcm2-7, Cdc45, GINS) from the chromatin using its ATP hydrolysing energy (Figure 1.1). In budding yeast, long ubiquitin chains promote efficient unloading of CMG, with a 5 ubiquitin-long chain

as minimum to allow for Mcm7 unloading by p97 (Deegan, Mukherjee et al. 2020). While Mcm7 stays bound to p97-Ufd1/Npl4 complex after disassembly, the rest of the CMG helicase: Mcm2-6, GINS complex and Cdc45 stay together. Most probably the unfolded Mcm7 is degraded by proteasome. However, the fate of GINS complex and Cdc45 is not yet known (Deegan, Mukherjee et al. 2020).

In budding yeast lacking SCF Dia2 complex (Dia2 is not essential for yeast viability), terminated helicases accumulate on chromatin until next G1 phase of the cell cycle (Maric, Maculins et al. 2014). However, in *C.elegans* embryos, in the absence of $Cul2^{Lrr1}$ the CMG helicase remains bound to the chromatin until the prophase of mitosis, at which point it is removed by p97 and its cofactor UBXN-3 (orthologous to Faf1 in human (Figure 1.22) (Gaggioli and Zegerman 2017, Sonneville, Moreno et al. 2017). Moreover p97 dependent replisome disassembly in mitosis has been then shown to work in *Xenopus* egg extract, in *C.elegans* embryos (Deng, Wu et al. 2019, Priego Moreno, Jones et al. 2019, Sonneville, Bhowmick et al. 2019) and in mouse embryonic cells (Villa, Fujisawa et al. 2021). In all the model systems Mcm7 is ubiquitylated in mitosis by TRAIP ubiquitin ligase. In *Xenopus* egg extract Mcm7 is ubiquitylated with K6 and K63 linked ubiquitin chains during mitotic helicase removal (Deng, Wu et al. 2019, Priego Moreno, Jones et al. 2019).

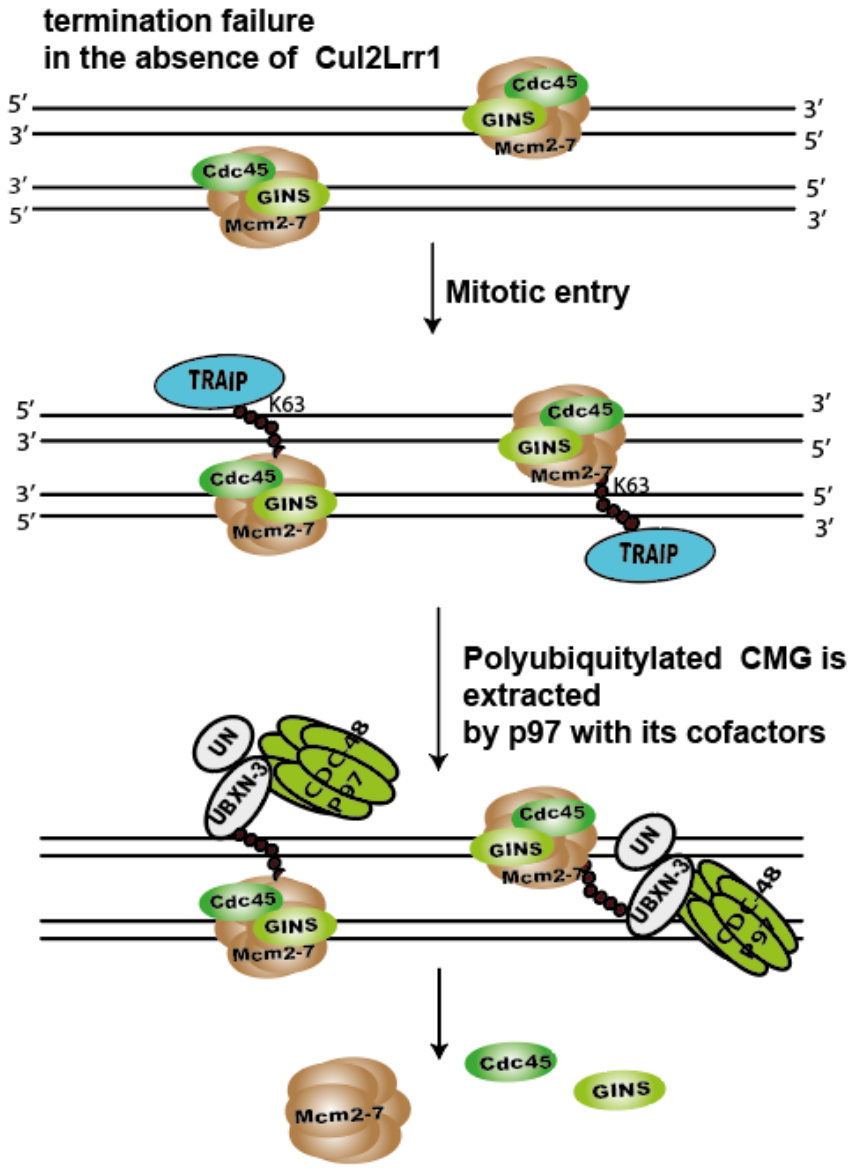

Figure 1.22 Back-up mitotic pathway of CMG helicase unloading. When the S-phase replisome disassembly is inhibited, the back-up CMG removal pathway in late prophase is dependent on CDC-48/p97 in mouse, *Xenopus*, *C.elegans* and cofactors Ufd1/Npl4 and UBXN3 shown, in *C.elegans* embryos (Sonneville, Moreno et al. 2017).

1.3.1.3. Other roles of p97 during DNA Replication and replication stress

The role of p97 in DNA synthesis was first shown in the *C.elegans* model system. Inactivation of the CDC-48-Ufd-1/Npl-4 complex resulted in reduced DNA synthesis, and a replication checkpoint-dependent delay in S phase progression (Franz, Orth et al. 2011, Raman, Havens et al. 2011). It has been reported recently that both *C.elegans* CDC-48 and human p97 regulate DNA replication by

degradation of the Cdt1/CDT-1 in S phase after initiation of DNA replication (Franz, Orth et al. 2011, Dantuma and Hoppe 2012, Franz, Ackermann et al. 2016). CDT-1 is a DNA licensing factor required for DNA replication initiation and depletion of CDC-48, Ufd-1/Ufd1, or Npl-4/Npl4 protein from cells in *C.elegans* embryos or from *Xenopus* egg extract results in accumulation of CDT-1/Cdt1 on mitotic chromatin (Franz, Orth et al. 2011, Franz, Ackermann et al. 2016).

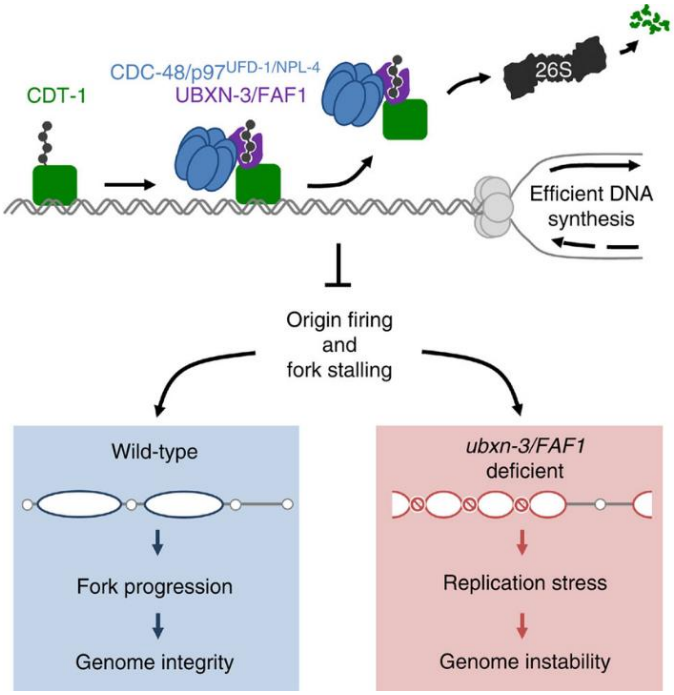

Figure 1.23 The role of Ubxn3/Faf1 in DNA replication progress. p97 core complex with Ubxn7/Faf1 extracts the ubiquitylated replication factor CDT-1 from chromatin. Then, it is degraded by the 26S proteasome. Regulation of chromatin associated CDT-1 is critical for protection of genome stability (Franz, Pirson et al. 2016).

Consequently, it was shown that also UBXN-3 (Faf1 homolog in *C.elegans,* FAF1 homolog in *human*) (Sonneville, Moreno et al. 2017) is important for CDT-1 degradation (Figure 1.23) (Franz, Pirson et al. 2016) . Once UBXN-3/Faf1 is inactive, CDT-1 and Cdc45/GINS are stabilised on chromatin. These result in replication stress i.e. a decrease in replication fork velocity, an increased number of stalled forks and an increase in newly fired origins, which leads to genotoxic DNA breaks and genome instability. Then the replication checkpoint and DNA repair machinery are activated (Franz, Pirson et al. 2016).

p97 may regulate further steps during DNA synthesis and DNA replication stress by directly interacting with several helicases including the Werner protein and HIM-6 (in *C.elegans*), which are members of the RecQ DNA helicase family and have 3'-5' DNA helicase activities (Partridge, Lopreiato et al. 2003, Caruso, Jenna et al. 2008, Jung, Lee et al. 2014). WRN and HIM-6 have multiple roles to provide genomic stability including in DNA replication and DNA repair. Mutation of WRN is responsible for

Werner syndrome and a variety of cancer types in human cells (Ramadan, Halder et al. 2017), while a mutation of HIM-6 leads to Bloom syndrome (Caruso, Jenna et al. 2008). WRN can directly interact with replisome components: its interaction with DNA pol δ leads to increase of DNA pol δ processivity and localisation in the nucleus, while its binding to RPA stimulates helicase activity of WRN in *C.elegans* (Hyun, Park et al. 2012). p97 provides recruitment of WRN to the stalled fork during DNA replication stress (Indig, Partridge et al. 2004, Ramadan, Halder et al. 2017). HIM-6 with WRN binding to the CRN-1 (homolog of human FEN-1) stimulates HIM-6 activity in *C.elegans* (Jung, Lee et al. 2014). HIM-6 and CDC-48 are substrates of ATM kinase. CDC-48 may play a role as a scaffold between HIM-6 and ATM that regulates gene transcription in ER stress (Caruso, Jenna et al. 2008).

Another protein that is regulated by p97 upon DNA replication stress is RPA. RPA is a single stranded binding protein and consists of three subunits: RPA1, RPA2 and RPA3 (Oakley and Patrick 2010) (Bochkareva, Korolev et al. 2002, Arunkumar, Stauffer et al. 2003, Oakley and Patrick 2010). During replication initiation, Mcm10, which interacts with the Mcm2-7 complex, is responsible for recruitment of RPA to the replication forks. RPA1 is responsible for interaction of RPA with Polymerase α whose activity and processivity is increased by RPA (Oakley and Patrick 2010). Ubiquitylation of RPA1 and RPA3 is increased upon UV DNA damage, in contrast to RPA2. In addition, ubiquitylation of RPA was induced by stalled replication forks upon UV treatment and it is processed by p97, however, it does not promote proteasomal degradation due to mixed linkage ubiquitin chains (Elia, Wang et al. 2015). Moreover, RFWD3 ubiquitin ligase drives ubiquitylation of RPA and RAD51 and consequent removal from chromatin by p97 in response to mitomycin C (MMC)-induced DNA damage. This unloading of RPA and Rad51 leads to their proteasomal degradation and allows for homologous recombination to fix the DNA damage (Elia, Wang et al. 2015, Inano, Sato et al. 2020). RPA stimulates also Polymerase epsilon activity resulting in its interaction with PCNA (Loor, Zhang et al. 1997, Dianov, Jensen et al. 1999). Many studies show that PCNA monoubiquitylation is catalysed onto the RPA-coated ssDNA by RAD18 (Huttner and Ulrich 2008) (Hedglin and Benkovic 2017) and then deubiquitylated by USP1 upon DNA damage. PCNA monoubiquitylation at lysine164 (K164) in yeast, *Xenopus,* chicken, and mammals (Kannouche, Wing et al. 2004, Friedberg 2006, Fox, Lee et al. 2011), and polyubiquitylation at K164 with K63 linked ubiquitin chains in budding yeast are important during DNA replication to maintain genomic stability (Kannouche and Lehmann 2004, Waters, Minesinger et al. 2009, Fox, Lee et al. 2011). In addition, Dvc1 (SPRTN), which localises to the DNA damage lesions, interacts with PCNA and recruits p97 to DNA damage sites; thereby, it regulates translesion synthesis (TLS) (Davis, Lachaud et al. 2012, Ghosal, Leung et al. 2012, Vaz, Halder et al. 2013). However, it has not been recorded whether PCNA is regulated by p97 through proteasomal degradation.

Finally, p97 is crucial for repair of inter-stand crosslinks (ICLs). ICL covalently links the two strands of DNA and blocks DNA replication forks (Wu, Semlow et al. 2019). Removal of CMG replicative helicase is essential during inter-strand crosslink repair (Mirsanaye, Typas et al. 2021). Inter-strand crosslinks on DNA lead to two distinct repair pathways in *Xenopus* egg extract system and both pathways require Traip E3 ligase. In response to a stalled replication fork at an ICL, CMG helicase is ubiquitylated by Traip. However, while short ubiquitin chains on CMG are recognised by NEIL3 DNA glycosylase base excision repair enzyme, CMG with long ubiquitin chains, which are mixed ubiquitin chains, is unloaded by p97 for ICL repair through the FA pathway (Wu, Semlow et al. 2019, Li, Wang et al. 2020). This promotes disassembly of replisome from the ICL site in order to induce DNA repair mechanisms as the downstream repair factors can access the region of DNA damage (Fullbright, Rycenga et al. 2016).

1.3.2. p97 roles in DNA damage and DNA repair

Cells are exposed to a multitude of DNA lesions every day including products of cellular metabolism, ionizing radiation, UV light exposure, chemical exposure and DNA replication errors. p97 has a variety of roles in DNA damage and DNA repair mechanisms. A ubiquitin-dependent process is required to resolve stalled replication forks and p97 is an irreplaceable part of this process.

1.3.2.1. Response to double strand breaks (DSBs)

Non-Homologous End-Joining (NHEJ) and Homologous Recombination (HR) are two main pathways that repair DSBs in eukaryotic cells. NHEJ can be executed at any stage of the cell cycle, while HR is only active during late S- and G2-phases as it requires access to homologous sister chromatid template. Importantly p97 acts in both of these DSB repair pathways.

1.3.2.2. The role of p97 in homologous recombination (HR)

It is known that RNF8 and RNF168 ubiquitin ligases are responsible for ubiquitylation with K63 linked ubiquitin chains during DSB repair. However, this has been changed with identification of the p97 role in DSB repair mechanism (Aquila and Atanassov 2020). The activity of the p97-Ufd1/Npl4 complex at the sites of DSBs depends on RNF8. Depletion of both RNF8 and RNF168 removed K48 and K63-linked chains at DSB site, whereas downregulation of specifically RNF168 only removed K63-linked chains. Moreover, the absence of p97 activity led to accumulation of K48-linked ubiquitin chains at DSB site.

This data revealed that while K48-linked ubiquitylated substrates by RNF8 recruit p97 to the DSB sites, it is independent from RNF168 activity and K63-linked chains (Meerang, Ritz et al. 2011, Ramadan 2012, Vaz, Halder et al. 2013). RNF8 ubiquitin ligase modifies proteins with K48-linked ubiquitin chains and then p97 is recruited to disassemble them from chromatin. For example, following treatment of cells with ionising radiation, RNF8 ubiquitylates the signalling and repair proteins BRCA1 and Rad51, at sites of DSBs. BRCA1 and Rad51 are essential for HR. Following repair, these proteins are extracted from chromatin by the p97 complex (Meerang, Ritz et al. 2011, Vaz, Halder et al. 2013).

After binding of MRE11/RAD50/NBS1 (MRN) complex with the DSB end (van den Bosch, Bree et al. 2003), ATM is activated and recruited to the chromatin to initiate the signalling of DDR (Blackford and Jackson 2017). This recruitment results phosphorylation of a variety of proteins, which have role in cell cycle checkpoint activation and recruitment of additional DDR factors at damaged sites (Vitor, Huertas et al. 2020). MRE11 has endonuclease and 3'-5' exonuclease activities. Its excision to double-stranded DNA leads to make single-stranded DNA (ssDNA). Thereby Homolog recombination repair is activated in the S/G2 phase (Nieminuszczy, Broderick et al. 2019). it has been shown that after the cells exposed to IR, p97 association with MRE11 and extraction of it from chromatin resulted in generation of ssDNA by MRE11. However, MRE11 accumulated on chromation upon P97 inactivation in IR treated cells, leads to accumulation of ssDNA creation and deficient of Homolog recombination (Figure 1.24). Therefore, it has been suggesting that p97 interaction with MRE11 is critical for efficient HR, 53BP1 foci recruitment and cell survival (Kilgas, Singh et al. 2021) **.**

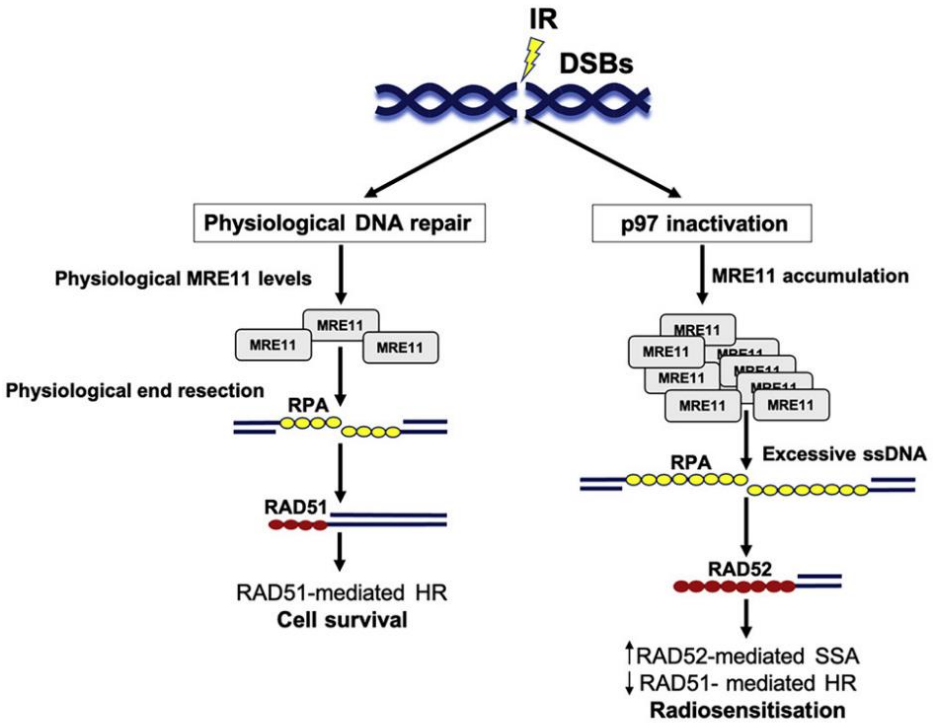

Figure 1.24 Schematic representation of p97 in DSB repair pathway choice. Left shows that MRE11 a part of MRN complex initiates RAD51 mediated HR repair upon excision of DSB sites. Then it is disassembled from chromatin by p97 ATPase activity. In addition, RPA, which binds to single strand DNA to protect the 3'-ssDNA, relocated with RAD51, leading to error free error-free DNA repair in S and G2 phases of the cell cycle. Right MRE11 accumulated on the DSBs sites when p97 is inactive resulted in overabundant 5'-DNA end resection and thereby HR abnormalities created. This leads to increasing of mutagenic RAD52 mediated single-strand annealing (SSA) repair pathway. Taken from Kilgas et al (Kilgas, Singh et al. 2021).

1.3.2.3. The role of p97 in Non-Homologous End-Joining (NHEJ)

One of the important roles of p97 in NHEJ is to aid recruitment of the central DNA repair molecule 53BP1 to DSB sites. In undamaged chromatin, the polycomb protein L3MBTL1 binds with high affinity to di-methylated K20 in histone H4 (H4K20me2). Upon DNA damage, ubiquitin ligases RNF8 and RNF168 catalyse ubiquitylation of L3MBTL1 with K63-linked ubiquitin chain, which is subsequently extracted from the chromatin by p97-Ufd1/Npl4. This allows 53BP1 to bind H4K20me2 and for the repair process to proceed (Figure 1.25) (Franz, Pirson et al. 2016); (Dantuma and Hoppe 2012).

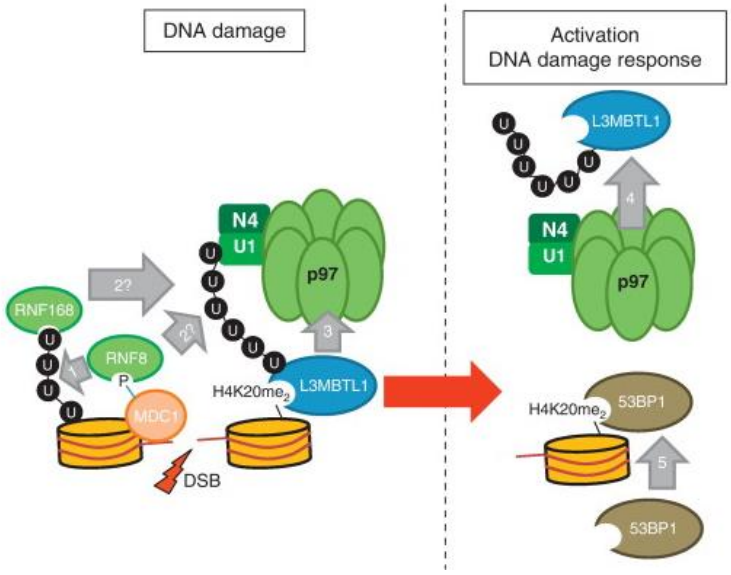

Figure 1.25 p97 controls DNA damage induced histone modifications. RNF8 and RNF168 ubiquitylate L3MBTL1 after DNA damage and p97 core complex extracts it from H4K20me2. Then, 53BP1 binds H4K20me2 to facilitate the DNA repair process. Taken from Dantuma et al., 2012 (Dantuma and Hoppe 2012).

p97 is also essential to complete DSB repair through NHEJ pathway (Ramadan 2012). KU70/80 complex plays a role in both HR and NHEJ repair as binding of KU to the DSBs promotes downstream protein binding. In addition, it is required to remove KU70/80 from DNA damage sites in order to allow binding of RPA to the ssDNA, thereby promote HR repair (Ramadan 2012). The KU70/80 complex is interlocked on the DNA during DNA DSB repair and needs to be removed once the damage is repaired. After repair is completed, KU80 is ubiquitylated with K48-linked ubiquitin chains by RNF8 E3 ligase (Feng and Chen 2012) in human cells and Cul1 E3 ligase in *Xenopus* (Postow, Ghenoiu et al. 2008) and removed from chromatin by p97-Ufd1/Npl4 -FAF1 (Figure 1.26) (Feng and Chen 2012, van den Boom, Wolf et al. 2016, Torrecilla, Oehler et al. 2017). Ku70 may be removed by a similar mechanism but this is not yet known (Torrecilla, Oehler et al. 2017).

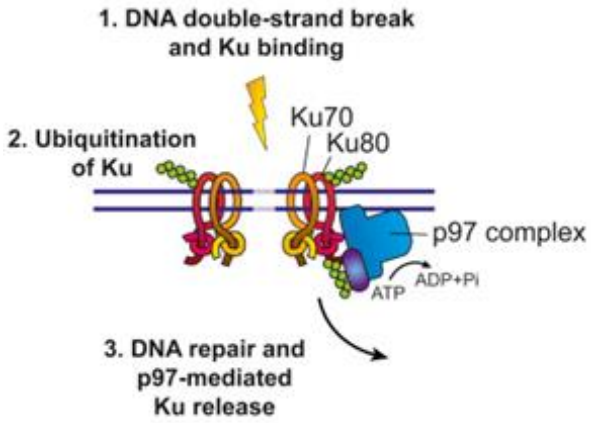

Figure 1.26 The role of p97 in DSB repair. The Ku70/80 heterodimer complex binds to the end of the broken DNA double strands. Hence, it is protected from extensive end resection. Following repair by non-homologous end joining, KU80 is modified by K48 linked ubiquitin chains and is disassembled from DNA by p97 complex in an ATP dependent manner. Taken from Van der et al., 2012 (van der Veen and Ploegh 2012).

1.3.2.4. The role of p97 in nucleotide excision repair (NER)

The bulky DNA lesion that is induced by UV light or some cancer chemotherapeutic agents is removed by Nucleotide Excision Repair (NER). UV-induced DNA lesions like pyrimidine-pyrimidone photoproducts (6-4PPs) and cyclobutane pyrimidine dimers (CPDs) are removed by NER to protect genome integrity. It is classified as either global genome NER (GG-NER) or transcription-coupled NER (TC-NER), which selectively removes UV lesions from actively transcribed genes (Scharer 2013, Osakabe, Tachiwana et al. 2015).

RNA Pol II transcribes a number of genes. When transcriptional elongating RNA Pol II stalled at DNA damage sites, e.g., at photo lesions, first it should stabilize association with Cockayne syndrome B (CSB). NER is promoted upon interaction of RNA Pol II with CSB. RNA Pol II disassembly is then needed for the lesion to be accessible by NER proteins. Rpb1 is the largest subunit of this RNA polymerase ll. Ubiquitylated Rpb1 is selectively extracted by p97 and its cofactors Ufd1-Npl4-UBX4-UBX5 in DNA damage response (Dantuma and Hoppe 2012, Franz, Ackermann et al. 2016). The ATP-dependent chromatin remodelling complex INO80 is also necessary for p97 driven RNA polymerase II extraction (Lafon et al., 2015). This process is important in protecting chromatin against severe damage because at this point NER proteins are activated and can repair the lesion (Figure 1.27) (Dantuma and Hoppe 2012).

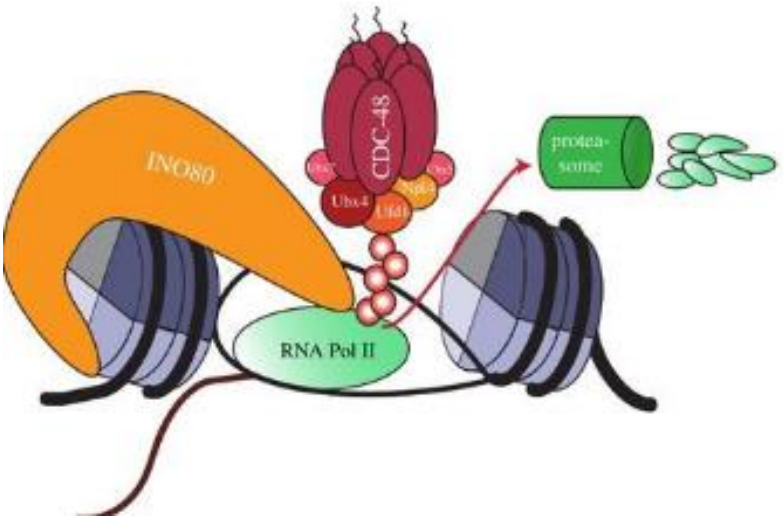

Figure 1.27 Schematic drawing of UV-induced proteasomal degradation of RPB1 subunits of RNA polymerase II. RNA polymerase II is ubiquitylated with K48-linked ubiquitin chains and unloaded from chromatin by INO80 and Cdc48 with its cofactors Ufd1-Npl4 –UBX4-UBX5. Finally degraded by the proteasome in budding yeast. Taken from Torrecilla et al., 2017 (Torrecilla, Oehler et al. 2017).

The global-genome NER main sensors are DDB2 (Damaged DNA-binding 2) and XPC (Xeroderma pigmentosum group C), which extract UV lesions from both transcribed and non-transcribed genes (Blackford and Jackson 2017). Following UV radiation exposure, DDB2 and XPC are ubiquitylated by the activity of CUL4A/B ubiquitin ligase and are removed from DNA damaged site by the helping of p97 and its cofactors Ufd1/Npl4 heterodimer (Ruthemann, Pogliano et al. 2016)and UBXD7 (Ubxn7) (Puumalainen, Lessel et al. 2014). It has been shown that once p97 activity was impaired, removal of ubiquitinated DDB2 or XPC failed, thereby leading to accumulation of these two damage sensors in chromatin and deficient the NER pathway. Therefore p97 and its cofactors have critical importance to complete of efficient GG-NER reaction and protect chromosomal aberrations after UV radiation (Puumalainen, Lessel et al. 2014).

1.4. *Xenopus* Egg Extract Model System

Genetic research in a mammalian organism has been restricted due to existing tools. Therefore, a number of lower eukaryotic model oraganism systems has been an alternative for the research of DNA replication and repair pathways (Lebofsky, Takahashi et al. 2009). The single cell eukaryote, budding yeast *S.cerevisiae* is a model organism extensively used to study DNA replication using genetic approaches due to easy manipulation in haploid and diploid form, as well as fast growth compared to the animal models. Its genome was first fully sequenced among all eukaryotes (Botstein and Fink 2011). *S.cerevisiae* initiates DNA replication at 400 origins in every S phase of the cell cycle (Arias and Walter 2007). Many biological pathways, including the cell cycle, are significantly conserved between yeast and human (Botstein and Fink 2011).. However, some replication proteins such as geminin are lacking compared to human cells (Lee, Cheung et al. 2021).

Nematode worm, *C.elegans*, is the simplest multicellular model eukaryotic organism used in DNA replication research. The genome of *C.elegans* is fully sequenced. Moreover, genetic manipulation methods such as RNAi, transgenesis, genome editing, and mutagenesis are comparatively straightforward (Kovalchuk and Kovalchuk 2016). Significantly, DNA repair mechanisms and DNA damage agents are highly conserved from worms to humans. *C.elegans* produces 300 eggs by self-fertilization (Rieckher, Bujarrabal et al. 2018). Although DNA repair and signalling pathways in the meiotically and mitotically dividing *C.elegans* germ cells are redily researched, somatic cells of adult *C.elegans* have resistance against most DNA damage drugs and they are fully postmitotic.

Unlike budding yeast, humans contain multiple types of different cells that divide at distinct times. There are approximately between 7000 and 100,000 replication origins in human cells (Prioleau and MacAlpine 2016). Although there are many advantages to studying DNA replication in human cell lines, difficulties with synchronization, manipulations of the genome, redundancy between protein factors and frequent mutation of cell cycle and checkpoint pathways in cancerous cell lines, make studies of DNA replication in human cell lines rather challenging.

The cell-free *Xenopus* egg extract is made from unfertilised eggs of *Xenopus laevis*, which is a species of South African clawed frog. *Xenopus laevis* egg extract contains all proteins required to drive DNA replication and DNA repair. Importantly, DNA replication and repair processes are highly conserved between *Xenopus laevis* and mammalian cells (Kornbluth, Yang et al. 2006). Indeed, egg extracts have been used to investigate a number of complex cellular processes such as the control of cell cycle progression, apoptosis, nuclear formation, nucleocytoplasmic transport, spindle microtubule dynamics, chromatin structure, sister chromatid cohesion, the regulation of DNA replication and DNA

repair (Gillespie, Neusiedler et al. 2016). Following addition of demembranated sperm DNA and ATP to the extract, a nuclear membrane is assembled around the DNA and then DNA replication takes place. The extract is also treated with cyclohexamide to prevent further cell cycle progression following completion of DNA replication.

The advantages of this system include the fact that it is a synchronised without remarkable transcription (Newport and Kirschner 1982)and cell-free system and that it is easy to manipulate. Therefore, the egg extract system is ideal for studying DNA replication and cell cycle regulated processes at the biochemical level (Kornbluth, Yang et al. 2006, Gillespie, Gambus et al. 2012, Hoogenboom, Klein Douwel et al. 2017). The quantity and quality of Xenopus laevis material in biology is high compared to other organisms. For example, the ovary of the one Xenopus frog is equal to one thousand the ovary of the mouse (Gurdon 2006). The large and several hundreds of oocytes can easily acquire (Gillespie, Neusiedler et al. 2016). Moreover, Oocytes have contain all RNA and proteins which is required from the first stages of development to early embryogenesis. In addition, transcriptional activity does not occur till the mid-late blastula stage (Collart, Owens et al. 2014). Oogenesis and maturation period is highly conserved in mammals (Fisher 2011) although size is different, resulting extensively using this system for cell cycle researches.

1.5. Aim of the project

p97 functions as a ubiquitin segregase, binding ubiquitylated substrates and extracting them from different cellular structures including protein complexes, membranes and chromatin. It regulates many different cellular processes in the cells. The functional diversity of p97 is attributable to its wide variety of cofactors, which help to recognise different ubiquitylated substrates.

The aim of this project is to characterize in detail the role of p97 during DNA replication termination, specifically during the process of replisome disassembly.

We wanted to determine the particular cofactors required during DNA replication, especially in the termination process. A previous PhD student in the Gambus lab, Dr Sara Priego Moreno found that the terminated helicase is interacting with p97 and a number of p97 cofactors (Sonneville, Moreno et al. 2017), including Ubxn7 and Faf1, which are two more novel and interesting cofactors that could potentially regulate replisome disassembly

The aims of my project were therefore to confirm that Ubxn7 and Faf1 indeed interact with p97 during replisome disassembly and determine if they have roles in DNA replication termination. I aimed also to determine how Ubxn7 regulates the activity of Cul2 ubiquitin ligase and removal of the CMG helicase from chromatin by p97.

Moreover, different types of ubiquitin chains on Mcm7 regulate CMG terminated helicase disassembly in S-phase and mitosis. While K48-linked chains formed on Mcm7 support replisome unloading in S-phase, K6 and K63-linked chains are able to drive unloading of Mcm7 in mitosis. This suggests that p97 segregase activity in the CMG removal pathway is highly regulated not only by the substrate but also by specific types of ubiquitin chains (Horn-Ghetko, Krist et al. 2021). It is likely, therefore, that different groups of p97 cofactors recognise different ubiquitin chain types on substrates. Thus, my aim was to identify which p97 cofactors needed for replisome disassembly in mitosis.

2 MATERIALS AND METHODS

2.1. Tables

Table 1. Table of solutions

2x ANIB100: 100 ml stock is kept at 4°C.
100 mM HEPES pH 7.6 200 mM KAc 20 mM MgAc 5 mM Mg-ATP (added from a stock of: 250 mM ATP; 250 mM $MgCl_2$; pH 6.7 with NaOH) 1 mM spermidine 0.6 mM spermine 2 µg/ml of each aprotinin, leupeptin and pepstatin 50 mM β-glycerophosphate 0.2 mM Na_3VO_4 0.2 µM microcystin-LR
1x ANIB100 with additions: required volume of it is prepared freshly before starting the chromatin isolation protocol and kept on ice during the experiment.
prepared by mixing 1 volume of 2x ANIB100 with 1 volume of H2O 0.1% Triton X-100 0.1 mM PMSF Optional: 20 mM Iodoacetamide; 10 mM 2-chloroacetamide
Cysteine solution:
2.2% cysteine 5 mM EGTA pH to 7.6 with KOH
LFB1/50
10% sucrose 50 mM KCl 40 mM HEPES pH 8 20 mM K phosphate pH 8 2 mM $MgCl_2$ 1 mM EGTA 2 mM DTT 1 µg/ml of each: aprotinin, leupeptin and pepstatin
MMR (10x): 3 L are prepared one day before eggs collection. 1 L of 1x MMR is prepared from this stock and kept at 4°C for using next day in egg extract preparation. This buffer is warmed at RT in the same morning before eggs collection
1 M NaCl 20 mM KCl 10 mM $MgCl_2$ 20 mM $CaCl_2$ 1 mM EDTA

50 mM HEPES Adjust pH to 7.8 with NaOH
PBST
1x PBS 0.1% Tween 20
Stop-C: Stored at 37°C to prevent SDS precipitation.
5 mM EGTA 0.5% SDS 20 mM Tris-HCl pH7.5
5% TCA
5% w:v TCA 0.5% w:v $Na_4P_2O_7$ x 10 H_2O
10% TCA: 10 L stock is prepared and kept at 4°C
10% w:v TCA 2% w:v $Na_4P_2O_7$ x 10 H_2O
UEB: 1 L is prepared one day before eggs collection and kept at 4°C for using next day in egg extract preparation. This buffer is warmed at RT in the same morning before eggs collection
50 mM KCl 50 mM HEPES 5 mM MgCl2 5 mM EGTA pH to 7.6 with KOH

Table 2. Inhibitors added to X.laevis egg extract. Final concentration in the extract, addition timing and provider are specified

Inhibitors	Preparation and addition to *X. laevis* egg extract
MLN4924 (A01139, Active Biochem) (Cullin inhibitor)	Dissolved in DMSO at 20 mM and used at 10 µM. Added 15 minutes after sperm DNA addition
NMS873 (17674, Cayman Chemical Company) (p97 inhibitor)	Dissolved in DMSO at 10 mM and used at 50 µM. Added 15 minutes after sperm DNA addition
Caffeine (C8960, Sigma)	Dissolved in water at 100 mM and used at 5 mM. Added together with sperm DNA

Table 3. Recombinant proteins added to X. laevis egg extract. Final concentration in the extract, addition timing and provider are specified.

Recombinant proteins	Addition to *X. laevis* egg extract
His-*X.laevis* Ubxn7 wt (purified in the lab)	Added together with sperm DNA at 0.06 mg/ml or 0.3 mg/ml.
His-*X.laevis* Ubxn7 ΔUBX (purified in the lab)	Added together with sperm DNA at 0.3 mg/ml.
His-*X.laevis* Ubxn7 ΔUIM (purified in the lab)	Added together with sperm DNA at 0.3 mg/ml.
His-Ubiquitin (U-530, Boston Biochem)	Dissolved in LFB1/50 at 10 mg/ml and added together with sperm DNA at 0.5 mg/ml
His-UbiNOK (UM-HNOK, Boston Biochem)	Dissolved in LFB1/50 at 10 mg/ml and added together with sperm DNA at 0.5 mg/ml
His-tagged *X.laevis* cyclin A1 NΔ56 (purified in the lab as in(Strausfeld, Howell et al. 1996))	Added together with sperm DNA at 826 µM

Table 4. Antibodies used for western blotting. Dilution, species in which the antibodies were raised in and provider are specified.

Antibody	Dilution (specie raised in)	Provider
α-MCM7	1:500 (rabbit)	Previously described (Priego Moreno, Jones et al. 2019)
α-Cdc45	1:500 (sheep)	Previously described (Gambus, Khoudoli et al. 2011)
α-Psf2	1:500 (sheep)	Previously described (Gambus, Khoudoli et al. 2011)
α-p97	1:1000 (mouse)	65278, Progen Biotechnik
α-cullin2	1:1000 (rabbit)	EPR3104, Abcam (Sonneville, Moreno et al. 2017)
α-cullin2 (SA206)	1:1000 (sheep)	SA206
α-PCNA	1:2000 (mouse)	P8825, Sigma
α-LRR1 (S962D)	1:100 (sheep)	S962D (Sonneville, Moreno et al. 2017)
α-p97	1:1000 (sheep)	This study
α-Ufd1	1:1000 (rabbit)	Kindly provided by Prof Stemmann (Heubes and Stemmann 2007)

α-Npl4	1:1000 (rabbit)	Kindly provided by Prof Stemmam (Heubes and Stemmann 2007)
α-Ubxn7	1:1000 (sheep)	This study
α-His	1:500 (mouse)	H1029, Sigma
HRP-sheep-IgG	1:10000	A34151ML, Sigma
HRP-rabbit-IgG	1:25000	A05451ML, Sigma
HRP-mouse-IgG	1:5000	A52781ML, Sigma

Table 5. Antibodies used for immunoprecipitations. Antibody quantities used per beads in IP

Antibody	Antibody quantities per beads	Immunoprecipitation
α-p97	1 µg for 15 µl Protein G Dynabeads™ (Invitrogen™)	Extract
α-Ubxn7 (purified ab)	1 µg for 15 µl Protein G Dynabeads™ (Invitrogen™)	Extract
α-p97 (purified ab)	20 µg for 30 Dynabeads M-270 epoxy (14302D, Invitrogen)	S phase chromatin
α-Ubxn7 (purified ab)	20 µg for 30 µl Dynabeads M-270 epoxy (14302D, Invitrogen)	S phase chromatin
α-p97 (purified ab)	20 µg for 30 µl Dynabeads M-270 epoxy (14302D, Invitrogen)	Mitotic chromatin
α-cullin2 (SA206)	10 µg for 50 µl Protein G Dynabeads™ (Invitrogen™)	S phase chromatin
HIS-Tag isolation (10104D, Invitrogen)	30 µl of extract	Extract
Sheep-IgG (I5131, Sigma)	1 µg for 15 µl Protein G Dynabeads™ (Invitrogen™)	Extract
Sheep-IgG (I5131, Sigma)	20 µg for 30 µl Dynabeads M-270 epoxy (14302D, Invitrogen)	S phase and mitotic chromatin

Table 6. Buffers used for Purification of p97

Lysis Buffer
150 mM sodium phosphate pH 7.4 300 mM NaCl 10mM imidazole 1 mM $MgCl_2$ 5 mM β-mercaptoethanol 0.1 mM PMSF 1 µg/ml of each aprotinin, pepstatin and leupeptin
Wash buffer
50 mM sodium phosphate pH 7.4 300 mM NaCl 60 mM imidazole 5 mM β-mercaptoethanol 0.1 mM PMSF 1 µg/ml of each aprotinin, pepstatin and leupeptin
Elution buffer
50 mM HEPES pH 7.4 100 mM KCl 1mM MgCl2 150 mM sucrose 250 mM imidazole 1 mM DTT 0.1 mM PMSF 1 µg/ml of each aprotinin, pepstatin and leupeptin

Table 7. Buffers used for Purification of Ubxn7

Lysis Buffer: LFB1/50
10% sucrose 50 mM KCl 40 mM HEPES pH 8 20 mM K phosphate pH 8 2 mM $MgCl_2$ 1 mM EGTA 2mM DTT 1 µg/ml of each: aprotinin, leupeptin and pepstatin
Wash Buffer: LFB1/50 (1st, 3rd wash) and LFB1/200 (2nd, 4th wash)
10% sucrose 50 mM KCl (for LFB1/50), **20**0 mM KCl (for LFB1/200) 40 mM HEPES pH 8 20 mM K phosphate pH 8 2 mM $MgCl_2$ 1 mM EGTA 2mM DTT 1 µg/ml of each: aprotinin, leupeptin and pepstatin
Elution buffer:
LFB1/50 250 mM imidazole 0.1 mM PMSF 1 µg/ml of each aprotinin, pepstatin and leupeptin

Table 8. Buffers used for Purification of p97 and Ubxn7 antibodies

Antigen elution Buffer:
25 mM Tris Base 192 mM Glycine 0.1% SDS
Coupling Buffer:
0.1 M $NaHCO_3$ 0.5 M NaCl, pH 8.3
Blocking Buffer:
0.5 M ethanolamine 0.5 M NaCl, pH 8.3
Wash Buffer:
PBS 0.5 M NaCl, pH 8.3
Storage Buffer:
1 X PBS 55% Glycerol

2.2. Working with *Xenopus laevis* egg extract

2.2.1. Preparation of inactivated *X.laevis* egg extract

X.laevis egg extract is arrested at metaphase II of meiosis and the protocol for preparation was described previously (Gillespie, Gambus et al. 2012). *X.laevis* egg extract is made from unfertilised female frog eggs. 10 frogs were primed with 150 units of follicle stimulating hormone, Folligon (Intervet) 2-7 days before eggs were required, leading to an increase in the number of mature, stage 6 oocytes. In the afternoon prior to egg collection, frogs were injected with 400-600 units of serum gonadotropin, Chorulon (Intervet), and transferred to laying tanks containing 2.5 l of 1x MMR. Frogs were kept in the tanks to lay eggs over-night at ≤ 23°C. The good quality eggs, which are dark coloured animal pole is larger than light coloured vegetal pole (Gillespie, Gambus et al. 2012), from different frogs were collected the next morning in a 1 l glass beaker. Any apoptotic eggs, white, immature or string-arranged eggs, were not collected.

Eggs, firstly, were rinsed with 1x MMR and then de-jellied in cysteine solution approximately 5 minutes (3 changes of the cysteine solution). They were rinsed again in 1x MMR and then washed in UEB buffer supplemented with 2 mM DTT (A3668, PanReac AppliChem). During this process, white apoptotic eggs that collected on the top were removed with a Pasteur pipette. Remaining eggs were then transferred to Ultra Clear 18 x 95 mm centrifuge tubes (1870261 Greiner Bio-One) containing 1 ml of UEB buffer supplemented with 10 µg/ml each of the protease inhibitors leupeptin, pepstatin and aprotinin (AppliChem Lifesciences), 50 µg/ml of cytochalasin D (C8273-5MG, Sigma) and 2 mM DTT. They were packed by centrifuging at 3,000 rpm in a swinging bucket JS13.1 rotor (Optima centrifuge) for 1 minute at RT. After the spin, the buffer and white apoptotic eggs that floated on the surface were removed as much as possible with a Pasteur pipette.

The eggs were then spin-crushed by centrifugation at 12,000 RPM in the same centrifuge for 10 min at RT. This centrifugation separated the egg mixture into a grey insoluble pellet, a brownish cytoplasmic fraction and a yellow lipid plug. From this point onwards, the egg extract was kept on ice. The cytoplasmic fraction was carefully removed using a 20-G needle and a 1 ml syringe and transferred to a 15 ml Falcon tube. Then, 10 µg/ml of leupeptin, pepstatin and aprotinin, 10 µg/ml of cytochalasin D and 15% of LFB1/50 were added and mixed gently. The egg extract was transferred to SW50 ultracentrifuge tubes (326819, Beckman Coulter), and centrifuged at 30,000 RPM in a pre-cooled ultracentrifuge in a SW55 rotor (326819, Beckman Coulter) for 20 min at 4°C.

After the spinning, the yellow lipid plug was removed from the top of the tube with a clean spatula, and the golden yellow cytoplasmic fraction was collected, taking extra care to not disturb the layer below. This layer contains mitochondria, which will lyse after freeze-thawing the extract and will promote apoptosis, making the extract useless. 1% v: v of glycerol was supplemented and the extract was frozen in liquid nitrogen in approximately 20 µl beads by pipetting it drop wise with a pre-cut p200 tip. These beads were then collected using Millipore forceps and stored in 2 ml cryovials at -80°C.

2.2.2. Use of *X.laevis* egg extract and demembranated sperm DNA for DNA replication experiments

2.2.2.1. Activation of *X.laevis* egg extract

X.laevis egg extract needs to be activated to efficiently complete DNA replication. *X.laevis* eggs are arrested in metaphase of meiosis II and addition of $CaCl_2$ (final concentration 0.3 mM) to the extract, mimics the Ca^{2+} wave that is induced at fertilisation and allow extracts to exit from meiosis and enter into interphase. Moreover, DNA replication requires a continuous energy supply, which is provided by supplementing the extract with 1/40 volume of energy regenerator solution (ER: 600 µg/ml creatine phosphokinase (10127566001, Roche), 1 M phosphocreatine (13810831, Roche) and 10 mM HEPES KOH 7.6). Finally, to block protein synthesis and to impede synthesis of cyclins so as to block cell cycle progression following completion of DNA replication, cycloheximide (CHX, Sigma) was added to the extract at 250 µg/ml.

2.2.2.2. Chromatin isolation time-course

This assay was performed to study the chromatin-binding pattern of replication factors during a replication reaction time-course after subjecting the extract to different drug treatments, as described previously (Gillespie, Gambus et al. 2012).

Extract was thawed and subsequently activated as described above in section 2.2.2.1. After 15 min activation, 30 µl of extract was transferred to a 1.5 ml Treff tube (9607811903, TreffLab), acting as a negative control (no DNA). The remainder of the extract was supplemented with demembranated sperm nuclei to 5-10 ng/µl final concentration and any indicated treatments. The reactions were split

into 30 µl aliquots in 1.5 ml Treff tubes, having as many aliquots as the number of time-points to be examined, and were incubated at 23°C for the duration of the time-course.

At each pre-determined time-point, the 30 µl reaction was stopped by addition of 0.5 ml ice cold Acetate Nuclear Isolation Buffer (ANIB100) buffer and then mixed thoroughly. This mixture stops the reaction due to dilution of the extract and decreasing its density. 100 µl of ANIB100 containing 20% sucrose was carefully under-laid in the bottom of the tube, creating a sucrose cushion. The tubes were then centrifuged in a pre-cooled micro-centrifuge with swinging bucket rotor at 2,500 g for 5 min at 4°C. The buffer above the sucrose cushion was removed, and the tube walls and top of the cushion washed twice with 100 µl of ANIB100 to reduce contamination within the chromatin sample. Most of the sucrose cushion was removed except approximately 20 µl. The tube was centrifuged at maximum speed in a micro-centrifuge with a fixed angle rotor for 2 min at RT to isolate the pellet. The important point is that hinges of the tubes were placed facing outwards; therefore, the chromatin pellet could be localised. After the final spinning, the remaining liquid was removed, leaving behind the chromatin pellet. The isolated pellet was finally re-suspended in 45 µl of 2x NuPAGE LDS loading buffer (NP0008, Novex by Life Technologies) and boiled for 5 min. The negative control sample(s) (no DNA) were processed in the same way to provide a chromatin specificity control. The samples were separated on SDS PAGR gel and bottom of the gel cut and stained with SimplyBlue™ SafeStain (Invitrogen™) to use as a loading control (described in section 2.4.1.)

Chromatin binding pattern of p97 and Ubxn7 during replication termination in S phase

X.laevis egg extract was supplemented with ER, CHX and $CaCl_2$, as explained in section 2.2.2.1., for 15 min at RT for activation, after which 10 ng/µl of demembranated sperm nuclei was added. At this point, 0.5 mg/ml UBI-NOK (dissolved in LFB1/50) or LFB1/50 buffer was added if used in the experiment. Finally, the reaction was optionally subjected to 5 mM MLN4924 (10 mM stock dissolved in DMSO) or 50 mM NMS873 (1 mM stock dissolved in DMSO) or equal volume of DMSO as the control at 15 min after sperm adding. The reaction was then mixed well after each addition and incubated at 23°C for indicated amounts of time. At each set time, the reaction was diluted with ANIB100, carefully underlaid with the ANIB100 20% sucrose cushion and chromatin isolated as described in section 2.2.2.2. (Gillespie, Gambus et al. 2012).

Competing endogenous Ubxn7 protein by adding recombinant Ubxn7 proteins in S-phase

Interphase egg extract, as explained in section 2.2.2.1., was supplemented with 10 ng/µl of demembranated sperm nuclei. The extract was optionally treated with LFB1/50 buffer or 0.3 mg/ml recombinant Ubxn7$^{\Delta UBX}$, Ubxn7$^{\Delta UIM}$ or Ubxn7^{wt}. At indicated time-points, samples were collected for the chromatin isolation procedure as explained in section 2.2.2.2.

Examining interaction of Ubxn7 with chromatin in mitosis

Interphase egg extract was supplemented with 10 ng/µl of demembranated sperm nuclei and incubated for 15 min at 23°C. The extract was then treated with 5 mM MLN4924 (A01139; Active Biochem) and DNA synthesis allowed to reach completion during 90 min incubation at 23°C. Half of the reaction was then treated with 826 nM cyclin A1 NΔ56 and treated optionally with 10 µM NMS873 or DMSO and optionally with 0.5 mg/ml recombinant His-tagged ubiquitin or Ubi-NOK (Boston Biochem, dissolved in LFB1/50 buffer at 10 mg/ml). Samples were isolated at indicated time points as described in section 2.2.2.2. (Gillespie, Gambus et al. 2012).

Chromatin binding pattern of replication factors in Ubxn7 depleted extract

Interphase Ubxn7 depleted extract (described in section 2.2.2.9.) and mock depleted extract were supplemented with ER for energy supply and 5 ng/µl of demembranated sperm nuclei. Chromatin was isolated at indicated time points as explained in 2.2.2.2.

Rescue of Ubxn7 depleted extract with Ubxn7^{wt} protein

Interphase Ubxn7 depleted extract and mock depleted extract were supplemented with ER for energy supply and 5 ng/µl of demembranated sperm nuclei. The depleted extracts were optionally treated with 0.06 mg/ml recombinant Ubxn7^{wt} or LFB1/50 buffer. At 100 min, when terminating CMG was unloaded from chromatin in the mock depleted extract, samples were isolated for the chromatin isolation procedure as explained in 2.2.2.2.

2.2.2.3. TCA replication assay

The efficiency of DNA replication in the prepared in *X.laevis* egg extract was measured through incorporation of radiolabelled nucleotide into nascent DNA during a time course using the TCA replication assay. This assay was also described previously (Gillespie, Gambus et al. 2012).

First, the volume of extract required was activated with ER, CHX and $CaCl_2$ as described in section 2.2.2.1. Then immediately 16.5 nM α-[P^{32}]dATP (NEG512H250UC, Perkin Elmer) was added to the extract along with demembranated sperm nuclei to 10-15 ng/µl. At this point reactions were optionally subjected to the indicated concentrations of recombinant Ubxn7$^{\Delta UBX}$, Ubxn7$^{\Delta UIM}$ and Ubxn7^{wt}, or LFB1/50 buffer. Reactions were then separated into 5 µl aliquots in 0.5 ml tubes and were incubated at 23°C for the duration of the time-course.

At each pre-determined time-point, the 5 µl reaction was stopped by addition of 160 µl of Stop-C buffer supplemented with 0.2 mg/ml proteinase K (740506, Macherey Nagel) (added from stock: 10 mM Tris-HCl, 20 mg/ml proteinase K, 50% v:v glycerol, pH 7.5) and incubated at 37°C for at least 30 min to ensure all of the proteins were degraded.

The samples were transferred to 5 ml Falcon tubes containing 4 ml of 10% TCA solution for precipitation of DNA and incubated at 4°C for a minimum time of 30 min. The TCA samples were then filtered through 25 mm glass fibre filters (11512083, Fisherbrand) under vacuum on a manifold (Millipore). To ensure that all DNA was deposited on the glass fibre filters, the tubes were washed once with 5 ml of 10% TCA solution (as above) and then 8 ml of 5% TCA solution, and finally rinsed with 70% ethanol. A 40 µl aliquot was taken from each sample prior to filtering and deposited onto a 25 mm Whatmann paper filter (1001-025, GE healthcare life sciences) providing a measure of the total radiation level in each sample. All of the glass fibre and Whatmann paper filters were subsequently left to dry under an infrared lamp for 10-15 min. Finally, each filter was inserted into a scintillation counter tube which was supplemented with 0.5 ml of the scintillant Ultima Gold F (6013179, Perkin Elmer), and radiation levels quantified in a scintillation counter.

After counting, the level of signal of ^{32}P incorporated into the precipitated DNA samples on the glass fibre filters was divided by the total ^{32}P on the paper filter, giving the total ^{32}P levels of each sample. The total DNA synthesized in each reaction (ng replicated DNA / µl extract) can be then calculated by multiplying the normalised values by 0.654. This value is calculated under the assumption that an average molecular weight of dNMPs, which is 327 Da, the extract contains endogenous pools of dNTPs of around 50 µM and same amount of 4 dNTPs are incorporated into DNA (Gillespie, Neusiedler et al. 2016) (Blow and Laskey 1986).

Monitoring DNA synthesis in Ubxn7 depleted extract

In this process, the Ubxn7 depleted extract had already been activated with $CaCl_2$ during its making (see section2.2.2.7.) so in this case it only required supplementation with ER for energy. As in section 2.2.2.3. 16.5 nM of α-[P32] dATP and demembranated sperm nuclei to 5-10 ng/µl was added to the depleted extract. DNA synthesis reactions were incubated at 23°C, stopped at indicated time-points and DNA synthesis analysed as explained above.

2.2.2.4. Immunoprecipitation of Ubxn7 and p97 from *X.laevis* egg extract

The required volume of metaphase II arrested egg extract (considering that each IP requires 100 µl extract) was thawed in a 1.5 ml Eppendorf tube and activated with ER, $CaCl_2$ and CHX to release it into interphase as explained in section 2.2.2.1. The extract was then supplemented with 400 µl of LFB1/50 per 100 µl of extract and spun down at max speed for 15 min at 4°C. The supernatant was split into four Eppendorf tubes, each containing 100 µl aliquots. At this point also, the input sample was prepared by mixing 50 µl of supernatant with 50 µl of 2x NuPAGE LDS loading buffer. The four tubes were then supplemented with different antibodies which are 1 µg of sheep IgG, 1 µg of purified p97 antibody, 1 µg of purified Ubxn7 antibody, 1 µg of purified UBXN7 antibody (Table 5) . The tubes were incubated on ice for one hour. In the meantime, 60 µl of Protein G Dynabeads™ (Invitrogen™) was aliquoted into a 1.5 ml Eppendorf tube and washed, first with 1 ml PBS once, then with 1 ml of LFB1/50 twice. These tubes were vortexed after adding each buffer, centrifuged briefly, then placed on a magnetic rack enabling removal of the entire buffer. Following the washes, beads in LFB1/50 were aliquoted into 4 tubes. The input from the tubes incubated on ice was added to the tubes containing the beads, and rotated for 1 hour at 4°C. After rotation, the samples were then centrifuged in a mini centrifuge and placed on the magnetic rack in order to separate the beads from the liquid. At this point, 20 µl of depleted samples from each tube was taken and mixed with 20 µl of 2x NuPAGE LDS loading buffer. Then the remaining buffer was removed from the tubes and the beads were washed with 1 ml of LFB1/50 thrice. Finally, after the entire buffer was removed, samples were centrifuged briefly, and all remaining buffer was removed, beads boiled in 30 µl of 2x NuPAGE LDS loading buffer for 5 min and the tubes were then placed on the magnetic rack to transfer all the liquid into new tubes. The new tubes contained IP samples. Samples were analysed with immunoblotting (section 2.4.1).

2.2.2.5. Small scale immunoprecipitation of chromatin interacting proteins

The required volume of metaphase II arrested egg extract (each IP requires 100 µl extract) was activated as explained in section 2.2.2.1. The interphase egg extract was then mixed with 10-15 ng/µl demembranated sperm nuclei and optionally supplemented with the indicated treatments. The reaction was incubated at 23°C for the indicated time. At this stage chromatin was isolated by first diluting the reaction with 10 volumes of ice cold ANIB100 containing 10 mM 2-chloroacetamide (616036000, Millipore) and underlying the mixture with ANIB100 containing 20% sucrose (1 ml in a 15 ml tube and 2.5 ml in a 50 ml tube). Each tube was centrifuged at 3,500 RPM in a swinging bucket rotor for 5 min at 4°C. The spinning program was repeated until a clear white chromatin pellet was detected at the bottom of the tube without any white threads going up the cushion. The buffer above the sucrose cushion was aspirated, and the top of the cushion was washed three times with 1 ml ANIB100 (+chloroacetamide). After the washes, the sucrose cushion was removed and the pellet transferred to a 1.5 ml tube. The samples were then re-suspended in the same volume of original extract of ANIB100 containing 20% sucrose. After that, protein complexes were released from chromatin by digestion with 2 U/µl of Benzonase nuclease (E1014-25KU, Sigma) with 20 min incubation at RT. Then the samples either sonicated for 5 min using a Diagenode sonicator with settings: 15s on, 15s off, medium settings or salt concentration increased to 300 Mm. The protein complexes were then subsequently incubated with either IgG, p97, Ubxn7 or cullin2 antibodies for immunoprecipitation, as explained below.

Immunoprecipitation of p97 from X.laevis S-phase chromatin

X.laevis interphase egg extract was supplemented with 10 ng/µl demembranated sperm nuclei as explained in section 2.2.2.1. and treated with 50 mM p97 inhibitor NMS-873 (from 1 mM stock) 15 min after sperm addition. Chromatin was isolated in the middle of S-phase, as described above in 2.2.2.2., and protein complexes released from chromatin by digestion of DNA using 2 U/µl Benzonase for 20 min. The input sample was prepared by mixing 20 µl of digested chromatin with 6.5 µl 4x NuPAGE LDS loading buffer. 30 µl of Dynabeads M-270 epoxy (14302D, Invitrogen) previously coupled covalently to 20 µg of either mouse affinity purified p97 antibody or IgG from mouse serum (A52781ML, Sigma) (antibodies were coupled to Dynabeads M-270 epoxy as described in section 2.2.2.8.) were incubated with 100 µl digested chromatin at 4°C for one hour with rotation. Following the incubation time, beads were washed for 5 min rotating at 4°C twice with ANIB100, once with

ANIB100 containing an additional 0.1% Triton X-100 and finally twice with ANIB100 buffer. Each sample was prepared by boiling in 30 µl of 2x NuPAGE LDS loading buffer for 5 min.

Immunoprecipitation of Ubxn7 from X.laevis S-phase chromatin

X.laevis interphase egg extract was supplemented with 10 ng/µl demembranated sperm nuclei as explained in section 2.2.2.1. and treated with 50 mM NMS-873 and caffeine 15 min after sperm adding, to promote accumulation of p97 and CMG helicase on chromatin. Protein complexes were released from chromatin by digestion of DNA using 2 U/µl benzonase for 20 min and sonication for 5 min using a Diagenode sonicator with settings: 15s on, 15s off, medium settings. 50 µl of 2M KAc was then added to the samples in order to raise salt concentration from 100 mM to 300 mM to increase solubility of digested protein. The samples were centrifuged at maximum speed for 5 min at 4°C. Following centrifugation, the input sample was prepared by mixing 20 µl of supernatant with 6.5 µl of 4X loading buffer. Protein complexes isolated from 200 µl of extract were incubated optionally with 30 µl of Dynabeads M-270 epoxy (14302D, Invitrogen) previously coupled covalently to 20 µg of either sheep affinity purified Ubxn7 antibody or IgG from sheep serum (I5131, Sigma) (antibodies were coupled to Dynabeads M-270 epoxy as described in section 2.2.2.8.). After 1-hour rotation at 4°C, tubes were placed on a magnetic rack to isolate beads and 20 µl of the depleted input (supernatant) was collected and mixed with 6.5 µl 4x NuPAGE LDS loading buffer. Beads were then rotated for 5 min at 4°C twice with ANIB100, once with ANIB100 supplemented with 0.1% Triton X-100, and again twice with ANIB100. Each sample were prepared by boiling in 30 µl of 2x NuPAGE LDS loading buffer for 5 min.

Immunoprecipitation of Cul2 from S-phase chromatin

Interphase extract was supplemented with 15 ng/µl demembranated sperm nuclei as described in 2.2.2.1., after 15 min sperm adding treated with NMS-873 and caffeine to promote accumulation of Cul2, p97 and Ubxn7 on chromatin. After chromatin was isolated end of the S-phase, protein complexes were released from chromatin as described in 2.2.2.4. The samples were sonicated for 5 min using the Diagenode cold water sonicator with settings: 15s on, 15s off, medium settings, to agitate protein complexes in solution. Salt concentration was then increased from 100 mM to 300 mM by adding 50 µl of 2M KAc to increase solubility of digested protein. After centrifugation at max speed at 4°C, the input sample was prepared by mixing 30 µl of supernatant with 13 µl of 4X loading buffer. Each sample was mixed with 50 µl of Dynabeads coupled with affinity purified Cul2 antibody (SA206) or IgG antibody from sheep (I5131, Sigma) for two hours at 4°C. Coupling of antibodies to Dynabeads was performed as described in section 2.2.2.8. Beads were then washed with 1 ml of PBS-T ice cold

buffer (+ 2-chloroacetamide) (thrice) and 1ml ANIB 300 buffer (once) with rotation for 5 min at 4°C. Each sample was prepared by boiling in 30 µl of 2x NuPAGE LDS loading buffer for 5 min.

2.2.2.6. Large scale IPs of p97 in S phase for mass spectrometry analysis

1.9 ml metaphase egg extract for each IP samples was released into interphase as explained in section 2.2.2.2., supplemented with 10 ng/µl demembranated sperm nuclei and optionally subjected p97 inhibitor NMS-873, to accumulate p97 and replisome components on S-phase chromatin. Following incubation at 23°C, chromatin was isolated at the time point in which p97 was present on the chromatin at high levels in S-phase. The extract was then diluted with 38 ml of ice cold ANIB100 supplemented with 10 mM 2-chloroacetamide (616036000, Millipore). The diluted extract was also underlaid with 2.5 ml per 50 ml tube ANIB100 containing 20% sucrose and chloroacetamide and then spun down for 5 min at 3,500 RPM in a swinging bucket rotor at 4°C. Following centrifugation, the buffer above the sucrose cushion was aspirated and the top of the sucrose cushion was washed three times with 1 ml ANIB100 (+ 2-chloroacetamide). The top of the cushion was then removed and the pellet transferred to a 1.5 ml tube. The samples were then re-suspended in 500 µl ANIB100 containing 20% sucrose and chloroacetamide. After that, protein complexes were released from chromatin by digestion with 2 U/µl of Benzonase nuclease (E1014-25KU, Sigma) for 20 min at room temperature with occasional mixing. After centrifugation at max speed in a micro-centrifuge with fixed angle rotor for 10 min at 4°C, the protein complexes were subsequently incubated with 125 µl of beads mixing at 4°C (antibodies were coupled to Dynabeads M-270 epoxy as explained in section 2.2.3.10). After two hours rotating at 4°C, beads were washed 5 times with rotation for 5 min at 4°C twice with ANIB100, once with LFB1/50 supplemented with 0.1% Triton X-100, and again twice with ANIB100. Immunoprecipitated material was eluted by boiling each sample in 60 µl of 2x NuPAGE LDS loading buffer for 5 min, followed by mixing by vortex and a final 5 min boiling and analysed by mass spectrometry as explained (Sonneville, Moreno et al. 2017) with the collaboration of Dr Richard Jones from MS Bioworks LLC. Signpost 2.4.5 here for SDS-PAGE.

2.2.2.7. Large scale IPs of p97 in mitosis for mass spectrometry analysis

Interphase extract was supplemented with 10 ng/µl demembranated sperm nuclei as explained in 2.2.2.1. and treated with Cul2 inhibitor MLN4924 to stop S-phase replisome disassembly, caffeine to maximise chromatin-bound replisome components and NMS-873 to accumulate p97 on S-phase chromatin. DNA replication was completed with incubation at 23°C for 90 min, following which cyclin

A1Δ was added to the extract to promote entry into mitosis. Chromatin was isolated from mitotic extract when most of the p97 was accumulated at 30 min. Protein complexes were released as described in 2.2.2.6. The samples were sonicated for 5 min using the diagenode cold water sonicator with settings: 15s on, 15s off, medium settings, to agitate protein complexes in solution. Solubility of the protein was increased by adding potassium acetate to increase salt concentration to 300 mM. Chromatin bound protein complexes were then incubated with 125 µl Epoxy beads mixing at 4°C (antibodies were coupled to Dynabeads M-270 epoxy as explained in section 2.2.3.10). After two hours rotating at 4°C, beads were washed 5 times with rotation for 5 min at 4°C, twice with ANIB100, once with LFB1/50 supplemented with 0.1% Triton X-100, and again twice with ANIB100. Immunoprecipitated material was eluted by boiling each sample in 60 µl of 2x NuPAGE LDS loading buffer for 5 min, followed by mixing with vortex and a final 5 min boiling and analysed by mass spectrometry as explained (Sonneville, Moreno et al. 2017) with the collaboration of Dr Richard Jones from MS Bioworks LLC. Signpost 2.4.5 here for SDS-PAGE.

2.2.2.8. Pull-down of HIS-tagged proteins from X.laevis egg extract

120 µl egg extract (each pull-down requires 30 µl) was activated with ER, CHX and $CaCl_2$ as explained in 2.2.2.1. for 15 min at RT. Interphase egg extract was then supplemented with 10 ng/µl of demembranated sperm nuclei and optionally supplemented with LFB1/50, or 0.3 mg/ml of recombinant Ubxn7$^{\Delta UBX}$, Ubxn7$^{\Delta UIM}$ or Ubxn7^{wt} proteins.

The replication reaction was stopped with LFB1/50 Buffer supplemented with 0.1% Triton X-100mix and chloroacetamide in the middle of the S phase when the bulk of replication has completed. The samples were sonicated for 5 min using the Diagenode cold water sonicator with settings: 15s on, 15s off, medium settings. After taking the extract samples, centrifuged at max speed for 10 min at 4°C, and the supernatant carefully removed. 15 µl of the resultant supernatant was subsequently taken and mixed with 15 µl of 2x NuPAGE LDS loading buffer as the input sample. Rest of the supernatant from 30 µl of extract was incubated with 60 µl Dynabeads HIS-Tag isolation (10104D, Invitrogen) and incubated for 2 hour with rotation at 4°C. Beads were subsequently washed 2 times with LFB1/50 Buffer supplemented with 0.1% Triton X-100 mix and chloroacetamide with rotation for 5 min at 4°C. Pulled-down His-tagged proteins were eluted by boiling the beads in 30 µl of 2x NuPAGE LDS loading buffer for 5 min.

2.2.2.9. Immunodepletion of Ubxn7 protein from *X.laevis* egg extract

600 µl of interphase egg extract was incubated with 600 µl of Dynabeads Protein G coupled to 360 µg of affinity purified sheep Ubxn7 antibody for two rounds of 1 hour incubation at 4°C to generate Ubxn7 immunodepleted extract. The same volume of extract was incubated with Dynabeads coupled to IgG from sheep serum in parallel to generate the mock depleted extract. Coupling of antibodies to Dynabeads was prepared as described below in section 2.2.2.10

As soon as possible, the depleted extract was frozen in liquid nitrogen in approximately 10 µl drops. These beads were then collected using Milipore forceps and stored in 2 ml cryovials at -80°C.

2.2.2.10. Coupling antibodies to Dynabeads

Coupling Cul2 antibody to Protein G Dynabeads

Protein G Dynabeads (for antibodies raised in sheep) were coupled with Cul2 antibody before performing Immunoprecipitations of Cul2.

10 µg of Cul2 antibody was coupled to 50 µl of Dynabeads Protein G (10003D, Invitrogen) or IgG from sheep serum (I5131, Sigma). 50 µl Protein G Dynabeads were transferred to a 1.5 ml tube, placed on a magnetic rack and all the supernatant was removed. The beads were washed with water and phosphate buffered saline-tween (1xPBS-T supplemented with 0.1% Triton X-100), following which 10 µg of affinity purified Cul2 antibody (SA206) or IgG from sheep (I5131, Sigma) were added. Cul2 antibody was coupled to Protein G dynabeads with incubation at RT for 2 hours.

Before incubation with input, dynabeads were washed three times with PBS-T.

Coupling Ubxn7 antibody to Protein G Dynabeads

Protein G Dynabeads (10003D, Invitrogen) were coupled with Ubxn7 antibody on the day before performing immunodepletion of Ubxn7. The beads were washed with 100 mM Hepes pH 7.6. 120 µg of affinity purified Ubxn7 antibody or a same quantity of IgG antibody from sheep (I5131, Sigma) were added to the beads. IgG volume was made equal to the volume of Ubxn7 antibody used with 100 mM Hepes pH 7.6. Protein G beads were incubated with antibodies overnight at 4°C.

The next day, the antibody coupled beads were washed once with 100 mM Hepes pH 7.6 (first and third wash), 100 mM Hepes pH 7.6 + 1 µl PMSF with 15 min rotation at RT (second wash) and finally with LFB1/50. With the last wash, the reaction was transferred into 2 tubes, placed on a magnetic rack and all supernatant removed.

Covalent coupling of α-p97 antibodies to Dynabeads M-270 epoxy for p97 IP from S-phase and mitotic chromatin and Ubxn7 IP

This experiment was based on the Invitrogen Dynabeads M-270 epoxy beads preparation protocol. 250 µl of Dynabeads M-270 epoxy (14302D, Invitrogen) was covalently coupled with 83 µg of either the p97 antibody or the IgG mouse (I5381, Sigma) antibody and either Ubxn7 or IgG sheep (I5131, Sigma) antibody.

2 ml of DMF was mixed with Dynabeads M-270 epoxy ($2x10^9$ beads/ml) and mixed by vortexing, after which 450 µl of beads solution was taken out and placed on a magnetic rack and DMF solvent removed. Beads were incubated with 1 ml 0.1 M sodium phosphate pH 7.4 for 10 min at RT, twice with fresh sodium phosphate buffer. After incubation, the buffer was exchanged with 300 µl of 3 M ammonium sulphate in phosphate buffer pH 7.4 and subsequently 300 µg of chosen antibody was added. The mixture was then topped up with sodium phosphate buffer pH 7.4 to 900 µl final volume. This mixture was rotated for two days at 4°C. After incubation, beads were washed with 1 ml PBS four times and once incubated with 1 ml PBS containing 0.5% Triton X-100 for 10 min at RT. Finally, beads were incubated with 1 ml PBS three times for 5 min at RT. Once all washes were complete, beads were re-suspended in 900 µl of PBS with 0.05% sodium azide and stored at 4°C until the experiment was to be performed.

2.3. Working with bacteria

2.3.1. Transformation

100 ng of plasmid DNA was added to 10 µl aliquot of competent cells, which was defrosted on ice, and then the tube was left on ice for 30 min. Cells were then heat shocked by placing them in a 42°C water bath for 45 sec and then put on ice for 2 min. 250 µl of rich SOC media (pre-warmed at 37°C) was then added to the cells and they were incubated in a shaking incubator at 37°C for 1 hour. After this period, the cells were plated on LB agar plates with appropriate antibiotics and left to grow over night in a 37°C incubator.

Five different bacterial strains were used during my project for protein expression of $p97^{wt}$, $Ubxn7^{wt}$, Ubxn7 P458G and Ubxn7 L286E A289Q S293A (Prokhorova and Blow 2000):

1- Rosetta (DE3) pLysS Competent Cells (Novagen by Merck Millipore)
2- BL21- (DE3) Competent Cells (Fisher Scientific)
3- C41 (DE3) pLysS SOLOs Competent Cells (Lucigen)

4- Transetta (DE3) Competent Cells (Merck Millipore)

2.3.2. Testing expression of recombinant proteins

Before performing large scale recombinant protein expression and purification, a pilot experiment was carried out to determine whether the protein could be expressed efficiently after induction with IPTG. The plasmid carrying the gene of interest was transformed into Rosetta, BL21, C41 and Transetta cells (as mentioned in section 2.3**.1**). One colony was then picked, used to inoculate 10 ml of LB with selective antibiotics and grown over night in a shaking incubator at 37°C. To make glycerol stocks, 500 µl of 50% glycerol was mixed with 500 µl from this liquid culture. The day after the fresh culture was started, a 1:100 culture was prepared in 10 ml of LB media with antibiotics and grown in an incubator at 37°C. This culture was shaken until the optical density (OD) of the culture reached approximately 0.5 OD600. At this point, an un-induced sample was taken: 1000 µl of the culture was centrifuged at max speed for 5 min. Following removal of the supernatant, the cell pellet was re-suspended in 50 µl of 1x NuPAGE LDS loading buffer. In order to induce protein expression in the remainder of the culture, 1 mM IPTG was added and it was left in the shaking incubator at 37°C.

After two hours 500 µl was collected from the culture as an induced sample, then processed in the same way as the un-induced sample. Induced and un-induced samples were boiled at 95°C for 5 min, run on a polyacrylamide gel and examined by staining the gel with Coomassie Brillant Blue (described in General procedures).

2.3.3. Purification of recombinant proteins

2.3.3.1. Purification of p97

Expression constructs containing genes for *X.laevis* p97 (pQE80 p97, ampicillin resistance) were kindly provided by Prof Stemmann and proteins purified as described (Heubes and Stemmann 2007).
20 ml over-night cultures were grown from glycerol stocks. 2x 1 L liquid cultures with antibiotics were then inoculated with 1/100 volume of the overnight cultures and grown in a shaking incubator at 37°C until OD600 reached 0.5. Then the culture was induced by addition of 1 mM IPTG for approximately 2.5 hours. Cell cultures were transferred to 500 ml Nalgene centrifuge tubes and spun down at 6,000 g for 10 min at 4°C to pellet the cells which were kept at -80°C until the protein was to be purified.
Cell pellets were firstly thawed, and then re-suspended in 30 ml of lysis buffer. Homogenates were transferred to 45 ml Nalgene centrifuge tubes, 25 U/ml of benzonase nuclease (SIGMA) was added,

and the samples incubated at RT for 20 min. Homogenates were centrifuged at 14,000 g for 30 min at 4°C, and supernatants containing soluble proteins were then incubated with 2 ml of pre-washed Super Ni-NTA Affinity Resin (SUPER-NINTA100, Generon) for 2 hours, rotating at 4°C.

10 µl of supernatant of homogenates was taken and mixed with 20 µl 2x NuPAGE SDS loading buffer as an input sample before adding the supernatant from the cell lysate to the beads. After incubation with beads, the tubes were spun down at 1,000 RPM for 1 minute at 4°C. 10 µl of supernatant was taken and processed in the same manner as the input samples. The beads were then washed twice with 30 ml wash buffer.

The beads were transferred to 10 ml columns (Poly-Prep Chromatography Column, Bio-Rad). In order to elute the protein from the beads, 1 ml of elution buffer was added to the columns and allowed to drop into 1.5 ml tubes as 1 ml fractions. This was repeated a further 10 times. 10 µl from each fraction was removed and mixed with 10 µl 2x NuPAGE SDS loading buffer. All samples were boiled at 95°C for 5 min. The concentration of the purified proteins was quantified by Bradford Assay or/and BSA Gel Assay and evaluated with SDS-PAGE and Coomassie Staining (described in general methods).

2.3.3.2. Purification of Ubxn7

pET28a containing the wild type *X.laevis* Ubxn7 gene was previously prepared in Gambus lab. In the first construct, the Ubxn7 gene contains a single mutation, P458G, which mutates the UBX domain and blocks the interaction with p97. The second construct contains a triple mutant of Ubxn7: L282E, A285Q and S289A and this mutates the UIM domain to block the interaction with Cul2.

A 25 ml culture of BL21-codon Plus (DE3)-RIPL competent cells, transformed with pET28a-Ubxn7, pET28a-Ubxn7-P458G, pET28a-Ubxn7-L282E/A285Q/S289A vector, was grown with appropriate antibiotics. 2x 1 L cultures with antibiotics were inoculated with 1/100 volume of overnight culture and were shaken in an incubator at 37°C for 2 hours until it reached 0.3 OD600. The temperature was then lowered to 20°C and the cultures were grown until OD600 reached 0.6. The expression of recombinant proteins was subsequently induced by addition of 1 mM IPTG followed by incubation over night at 20°C. The following day, cell cultures were transferred to 500 ml Nalgene centrifuge tubes and centrifuged at 6,000 g for 10 min at 4°C. Supernatant was removed and pellets kept at -80°C.

Purification of Ubxn7^{wt}, Ubxn7-P458G and Ubxn7-L282E/A285Q/S289A proteins was performed following the same protocol as explained before for p97 in section 2.2.1.1, but using buffers indicated in the table and washing beads 4 times for Ubxn7 proteins.

2.3.4. Purification of Antibody

In order to purify antibodies, an affinity column is needed to be made. For this purpose, first the purified protein should be dialysed into a column coupling buffer; then the column is incubated with the purified protein and the protein becomes bound to the beads. The serum which contains antibody is run through the column. After the washing step, the antibody is eluted.

2.3.4.1. Dialysis of p97 and Ubxn7 proteins

A Pur-A-Lyzer ^{TM} dialysis tube (Sigma Aldrich) was filled with 3 ml of ultrapure water and incubated for 5 min at RT. After removal of the water, 1 ml of the eluted fraction (containing the highest concentration of purified protein of p97 and Ubxn7) was loaded into the dialysis tube and left overnight in 1 L of coupling buffer, stirring at 4°C. The samples were then transferred from the dialysis tube to clean 1.5 ml tubes.

2.3.4.1.1. Purification of p97 and Ubxn7 antibody

The antigen column-HiTrapTM NHS-activated HP (GE Healthcare) was washed with 6 ml of ice-cold 1 mM HCl using a 10 ml syringe. Carefully the column was loaded with dialysed protein immediately without creating any air bubbles and incubated at RT for 30 min. The liquid was removed from the column, washed, and incubated for 30 min with 10 ml blocking buffer to block unreacted NHS groups. Then, the column was washed with 10 ml of 10 mM Tris-HCl pH 8 (1st and 3rd washes), then with 10 ml of 0.1 M Glycine pH 2.0 and finally with 10 ml of 0.1 M trimethylamine pH 11.5. All the washes were repeated once more, then washed with 30 ml of 2XPBS using a peristaltic pump at 4°C.

After antiserum was thawed, it was supplemented with 0.1% NaN_3, split and mixed with equal volume of 1x PBS. The solution was filtered using a 0.2 mm Stericup filter (Millipore) and recirculated through the column for at least 3 hours. Next, the column was washed with 50 ml of washing buffer (PBS, 0.5M NaCl, 0.1% Triton X 100), then with 2 X PBS. The antibody binding to the column was eluted with 0.1

M Glycine pH 2.0 and 1 ml fractions were collected in 1.5 ml tubes containing 100 µl of 2 M Tris-HCl pH 8.5. Finally, the column was washed with 50 ml of 10 mM Tris-HCl pH 8.0 and 50 ml of PBS and stored at 4°C.

2.4. General procedures

2.4.1. Immunoblotting

Protein samples were separated by SDS-polyacrylamide gel electrophoresis using either self-prepared gels or precast NuPAGE 4-12% gradient Midi Bis-Tris gels (WG1403BOX, Invitrogen), depending on the proteins being investigated. The precast gels were run at 160 volts for 75 min with NuPAGE MOPS SDS buffer (NP000102, Novex by Life technologies). 3 µl of the pre-stained protein marker PageRulerTM Plus Prestained Protein Ladder (Thermo Scientific) was loaded at the beginning and end of each gel.

After running, gels were either stained with Coomassie or transferred to PVDF membrane (IPVH00010, Merck Millipore) using the wet transfer system from Bio-Rad at 100 volts for 90 min. However, to detect histones for chromatin isolation assay, the bottom of the chromatin gel was cut off and firstly washed with deionised water 3 times for 5 min each and then stained in SimplyBlue™ SafeStain (Invitrogen™) overnight, and finally destained with deionised water.

Membranes with transferred proteins were first blocked with 5% milk in TBST and then incubated with the respective primary antibodies diluted in 3% BSA in TBST supplemented with 0.02% NaAzide, at 4°C over-night with rotation. If the membranes needed to be cut into appropriate fragments, this was done before incubating with primary antibodies.

The dilutions used for different primary antibodies are listed in Table 2.7. Secondary antibodies used were: Anti-sheep IgG from donkey, conjugated to horseradish peroxidase (HRP) (A3415-1ML Sigma-Aldrich), Anti-mouse IgG from goat conjugated to peroxidase (A5278-1ML, Sigma-Aldrich), Anti-rabbit IgG (H+L) from goat (10082602, Sigma-Aldrich). Western Bright™ ECL-spray (Advansta) was used for detection of chemiluminescent signals.

2.4.2. Bradford Assay

Standards were prepared by serially diluting 1 mg/ml Bovine Serum Albumin (BSA) in deionised water, so the volume of final diluted protein was 100 µl. 1 ml of Pierce™ Coomassie Plus (Bradford) Assay

Reagent was added and mixed very well in a cuvette (Fisher Brand). For analysis, 1 µl of the protein sample was mixed with 99 µl H_2O and 1 ml Coomassie reagent. The absorbance at 595 nm was measured in a spectrometer and a standard curve generated using the absorbance for the standards. Concentrations of the protein samples were determined by plotting sample absorbance against the standard curve.

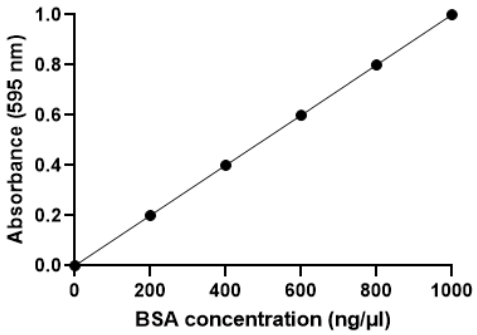

Figure 2.1 A symbolic example of standard curve for the Bradford Protein assay shows concentration versus absorbance. The protein standards Bovine serum albumin (BSA) was diluted at the fallowing concentrations: 0, 250, 500, 750, 900 ng/µl. Absorbance was measured at 595 nm. This standard curve of Protein concentration vs absorbance used to calculate the approximate protein concentrations of diluted proteins.

2.4.3. BSA Gel Assay

1 mg/ml BSA was serially diluted using LFB1/50 to desired concentrations at 2 mg/ml, 1 mg/ml, 0.5 mg/ml, 0.25 mg/ml, 0.125 mg/ml, 0.0625 mg/ml and mixed with 2x NuPAGE LDS Sample Buffer for standard references. Purified protein samples were also serially diluted in 1x NuPage LDS Sample Buffer. All samples were run on a 12% SDS-PAGE gel and stained with Coomassie for analysis.

2.4.4. Coomassie staining

Gels were stained with Coomassie Stain solution (1g Coomassie Brilliant Blue R-250, 400ml methanol, 100ml acetic acid, 500ml H2O). After 30 mins, they were washed with destaining solution (400 ml methanol, 100 ml acetic acid, 500 ml dH_20) until the bands were visible. Gels were sealed in acetate and scanned.

2.4.5. Preparation of gels for mass spectrometry

40 µl of large scale immunoprecipitated material (explained in sections 2.2.3.5) were resolved by SDS-PAGE. 10-wells NuPAGE 4-12% Midi Bis-Tris gels (Invitrogen, NP0335BOX) were run in NuPAGE MOPS SDS buffer at 160 volts for 10 min. Protein bands were visualized with staining by SimplyBlue SafeStain (LC6060, Invitrogen) and each lane subsequently cut into 10 bands. Gel bands were placed into individual wells in a 96 well reaction plate (40.010, Intavis), supplemented with water to avoid gel dehydration. The 96 well reaction plate was covered with an Axygen sealing mat (AM96PCRRD, Scientific Laboratory Supplies). Protein samples were analysed by mass spectrometry with the collaboration of Dr Richard Jones from MS Bioworks LLC.

3. RESULTS

3.1. The interaction of p97 with chromatin during replication reaction.

3.1.1. Introduction

The segregase activity of p97 is important for disassembly of the CMG helicase complex during DNA replication termination (Maric, Maculins et al. 2014, Moreno, Bailey et al. 2014, Dewar, Budzowska et al. 2015). Only one subunit of the terminated CMG is ubiquitylated – the Mcm7 subunit (Maric, Maculins et al. 2014, Moreno, Bailey et al. 2014). In higher eukaryotes, Mcm7 is polyubiquitylated by the E3 ligase $Cul2^{Lrr1}$ in *Xenopus* egg extract (Dewar, Budzowska et al. 2015, Sonneville, Moreno et al. 2017), in *C.elegans* embryos (Maric, Maculins et al. 2014) and in mouse (Villa, Fujisawa et al. 2021). The polyubiquitin chain formed on Mcm7 at termination is K48-linked (Maric, Maculins et al. 2014, Moreno, Bailey et al. 2014). p97-Ufd1/Npl4 complex recognizes this polyubiquitylated Mcm7 substrate and extracts the entire CMG complex from the chromatin using the energy from ATP hydrolysis (Maric, Mukherjee et al. 2017).

The aim of this project is to characterize in more detail the regulation of p97 function during DNA replication termination. The segregase activity of p97 towards CMG requires major cofactors Ufd1 and Npl4 (Sonneville, Moreno et al. 2017, Bodnar, Kim et al. 2018). During this investigation, we would also like to identify and characterise any other cofactors required for this p97 function.

3.1.2. Results

3.1.2.1. Characterisation of p97 chromatin binding pattern upon inhibition of replication termination at different stages

In order to analyse p97 binding to chromatin during DNA replication, I isolated chromatin from replication reactions set up in *Xenopus laevis* egg extract and followed p97 interaction with chromatin by western blotting (Figure 3.1.a.). I also quantified the efficiency of nascent DNA synthesis (Figure 3.1.b.).

The double hexamer of Mcm2-7 proteins is a core of the replicative DNA helicase that is loaded onto chromatin in G1 phase of the cell cycle in an inactive form. It is activated by interaction with Cdc45 and GINS complex during S phase. We can see therefore that Mcm7 (part of Mcm2-7) interacts with

chromatin from the earliest time points and decreases in abundance as replication progresses (Figure 3.1.a.). On the other hand, Cdc45 and Psf2 (GINS subunit) appear on chromatin at 45 minutes when extract is replicating DNA very efficiently as seen by exponential increase of produced DNA at this time (Figure 3.1.a and b). By 60 minutes most of the bulk of DNA is already replicated (Figure 3.1.b.) and Cdc45 and Psf2 are barely visible on chromatin (Figure 3.1.a.). This is due to disassembly of terminated helicase (CMG complex) during DNA replication termination. As we can see, Mcm7 is polyubiquitylated at 45 and 60 min, while Cdc45 and Psf2 are removed from chromatin at the same time points. Only a small proportion of Mcm7 on chromatin is ubiquitylated as only a small proportion forms active helicase – most of Mcm7 is on chromatin in the form of inactive double hexamers, which are displaced from chromatin in a way that does not involve ubiquitylation of Mcm7 (Moreno, Bailey et al. 2014). PCNA, which is a polymerase clamp, and thus another replisome component, is present mostly on the chromatin when the bulk of the replication happens, but stays on a little longer as it is involved in Okazaki fragments maturation and post-replicative DNA repair (Thakar, Leung et al. 2020). Importantly, p97 interacts with chromatin at the same time when ubiquitylated Mcm7 is visible on chromatin and remains on it for a little longer (Figure 3.1.a.).

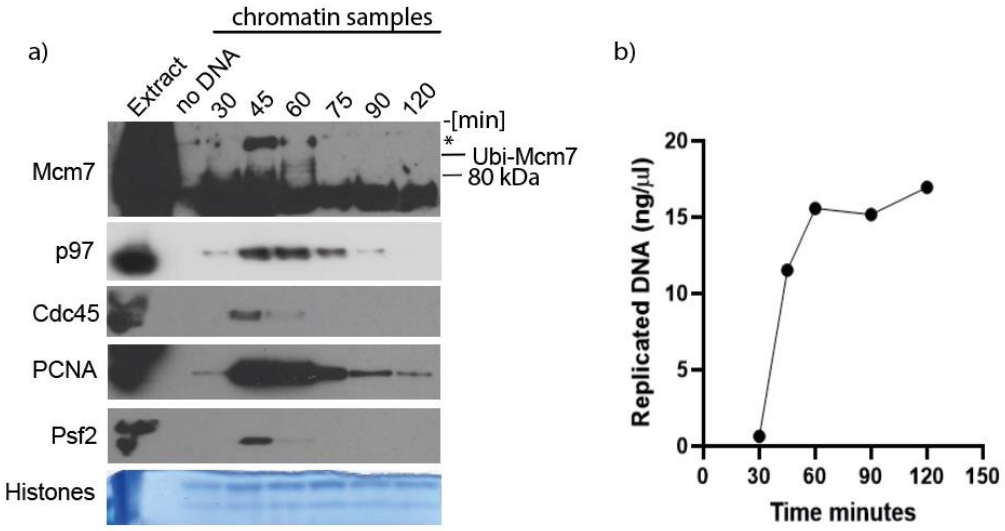

Figure 3. 1 p97 interacts with chromatin during replication reaction. (a) Interphase egg extract was supplemented with demembranated sperm nuclei. Chromatin was isolated at indicated time points, separated by SDS-PAGE and Western blotted using the indicated antibodies. Histones are stained on the gel to act as a loading control. An extract sample without addition of DNA was analysed in parallel to other chromatin samples to provide a chromatin specificity control. * I*t is a band that does not disappear when polyubiquitylation is blocked with Ubi-NOK. This is a* representative gel of at least 10 experiments performed. (b) Interphase extract was supplemented with demembranated sperm nuclei and α-[P32]dATP, and DNA synthesis was monitored at indicated time points by measuring incorporation of radiolabelled nucleotides into newly synthesised DNA. The experiment was performed every time a new extract prep was used.

3.1.2.1.1. The ATPase activity of p97 is not required for its recognition of terminated CMG complex

In order to understand what regulates chromatin binding of p97, we decided to block replication termination in different ways. ATPase activity of p97 allows it to pull out and process ubiquitylated substrates from cellular structures such as chromatin (Ramadan, Bruderer et al. 2007, Mouysset, Deichsel et al. 2008). I optionally blocked the activity of p97 by using the small molecule inhibitor NMS-873. NMS-873 binds at the D1-D2 interdomain linker and prevents ADP release from D2, and in this way, the ATPase activity of D2 is inhibited (Magnaghi, D'Alessio et al. 2013, Xia, Tang et al. 2016, Ding, Zhang et al. 2019) . In such a way, NMS-873 prevents p97 from extracting ubiquitylated protein from their complex structures. It has been shown previously that treatment with NMS-873 causes p97 to accumulate on chromatin, because it can still bind to its substrates (e.g., ubiquitylated Mcm7) during DNA replication. To check that this is the case in my hands, chromatin was isolated at indicated time points during the replication reaction in egg extract and analyzed by western blotting using the indicated antibodies (Figure 3.2.a.). In control reaction, DMSO was added, as NMS-873 was dissolved in it. As expected, we saw the replication factors (Cdc45 and PCNA) binding the chromatin at 45 and 60 min in the control conditions when the bulk of replication happens. p97 and Ufd1, however, start binding at around that time but remain bound to chromatin for longer (Figure 3.2.a DMSO).

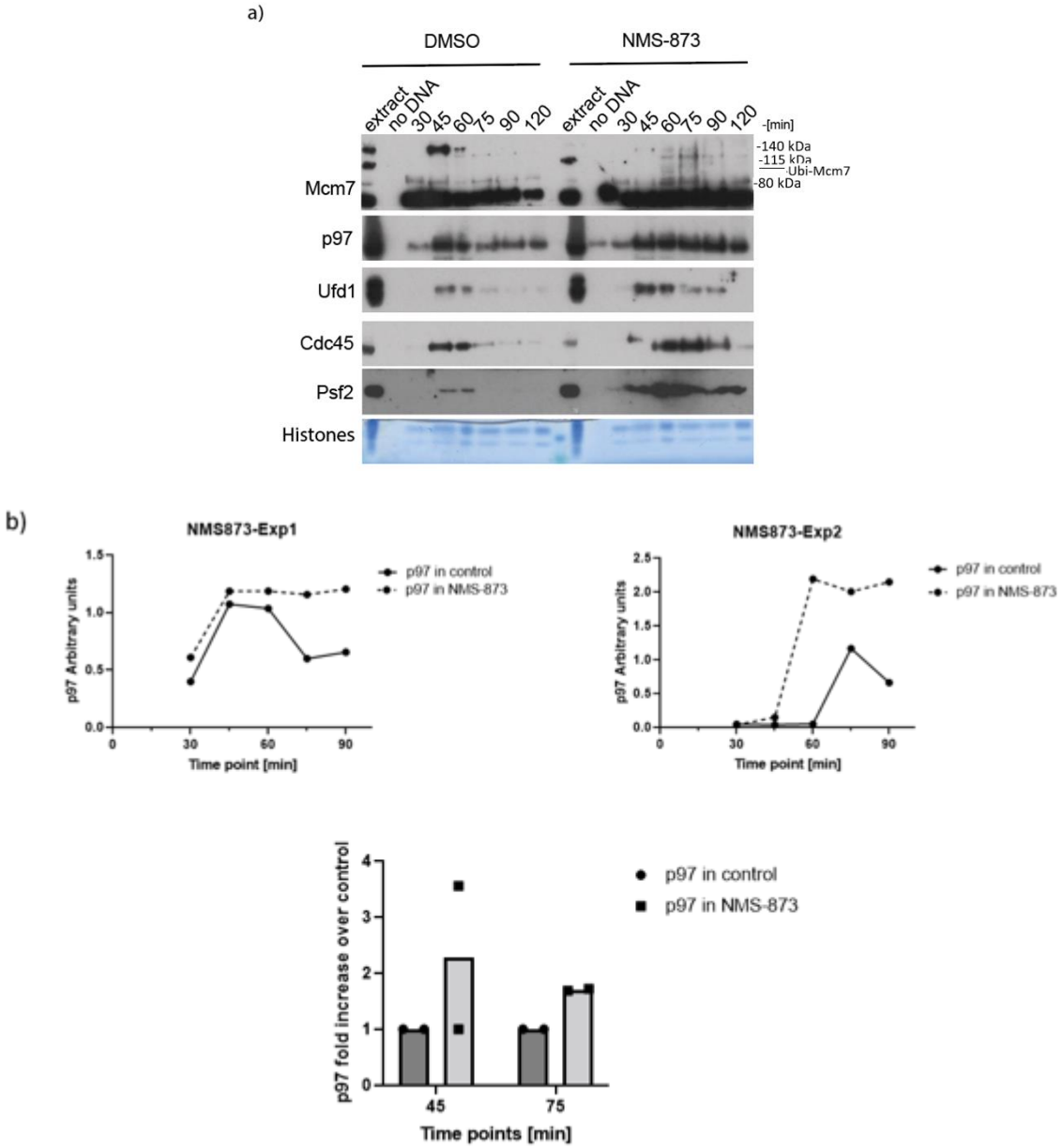

Figure 3. 2 Blocking ATPase activity of p97 does not stop its chromatin binding during replication. a) Interphase egg extract was supplemented with demembranated sperm nuclei and optionally with NMS-873. Chromatin was isolated at indicated time points, separated by SDS-PAGE and Western blotted using the indicated antibodies. Histones are stained on the gel with colloidal coomassie to act as a loading control. An extract sample without addition of DNA was analysed in parallel to other chromatin samples to provide a chromatin specificity control. * It is a band that does not disappear when polyubiquitylation is blocked with Ubi-NOK. This experiment represents one of two biological repeats. b) The graphs showing abundance of p97 on chromatin were created from measuring band (pixel) densities of p97 using Image J and represent arbitrary units of two different experiments. Blots in (a) correspond to experiment 1. c) The mean fold increase of p97 in two experiments in independent extracts.

It has been previously shown, that addition of NMS-873 to the egg extract does not affect the efficiency of nascent DNA synthesis during DNA replication (Sonneville, Moreno et al. 2017).

Importantly, when the activity of p97 was blocked with the NMS-873 inhibitor, it led to a defect in the replication fork termination and prevented disassembly of the components of the CMG helicase (Cdc45, Psf2); therefore, they accumulated on the chromatin, which has been observed previously (Dewar, Low et al. 2017). In addition, there was an increase in the signal for ubiquitylated Mcm7, which indicates that polyubiquitylated Mcm7 could not be removed from chromatin. Finally, treatment with NMS-873 caused p97 to accumulate on chromatin along with its cofactor Ufd1. This is most likely due to accumulation of p97 substrate on chromatin: ubiquitylated Mcm7. I measured levels of p97 in two independent experiments by Image J and plotted as graphs of signal (Figure 3.2.b.). They show both different kinetics due to different extract used and imperfections of this technique, however both show the same trend of increased p97 chromatin association upon inhibition of its ATPase activity (Figure 3.2.c.). I chose to compare level of p97 at 45 and 75 min, as 45 min timepoint represents the peak of nascent DNA synthesis and accumulation of active replication forks on chromatin, while 75 min timepoint corresponds to time after which active replication forks should be gone and only terminated replisome retained on chromatin. This result therefore suggests that when ATPase activity of p97 is inhibited, it is still able to recognize its substrates and is thus still able to bind chromatin.

3.1.2.1.2. When Mcm7 polyubiquitylation is blocked by inhibiting activity of $Cul2^{Lrr1}$ ubiquitin ligase, p97 level decreases on chromatin during replication termination

I next wanted to test how p97 interaction with chromatin is affected when polyubiquitylation of Mcm7 is blocked by impairment of activity of Cul2Lrr1. Cul2Lrr1 ubiquitin ligase drives Mcm7 polyubiquitylation during replication termination in higher eukaryotes allowing p97, together with Ufd1 and Npl4, to unload it from chromatin. Cullin ubiquitin ligases are activated by neddylation. MLN4924 blocks the activity of Cullin type ubiquitin ligases by inhibiting their neddylation through inactivation of the NEDD8 activating enzyme (NAE) (Brownell, Sintchak et al. 2010). The activity of Cul2Lrr1 can be therefore blocked through addition of the drug MLN4924 into the extract. Preventing Mcm7 polyubiquitylation by MLN4924 leads to accumulation of terminated CMG on chromatin (Moreno, Bailey et al. 2014), while the overall nascent DNA synthesis is not affected (Moreno, Bailey et al. 2014). My hypothesis was that treatment with MLN4924 would cause decreased protein levels of p97 on chromatin, because one of p97's main substrate on chromatin (Mcm7) could not be polyubiquitylated by Cul2Lrr1 during DNA replication termination. Samples were taken throughout

the replication reaction in egg extract at indicated time points after optional MLN4924 addition and analysed by western blotting using the indicated antibodies (Figure 3.3.a.).

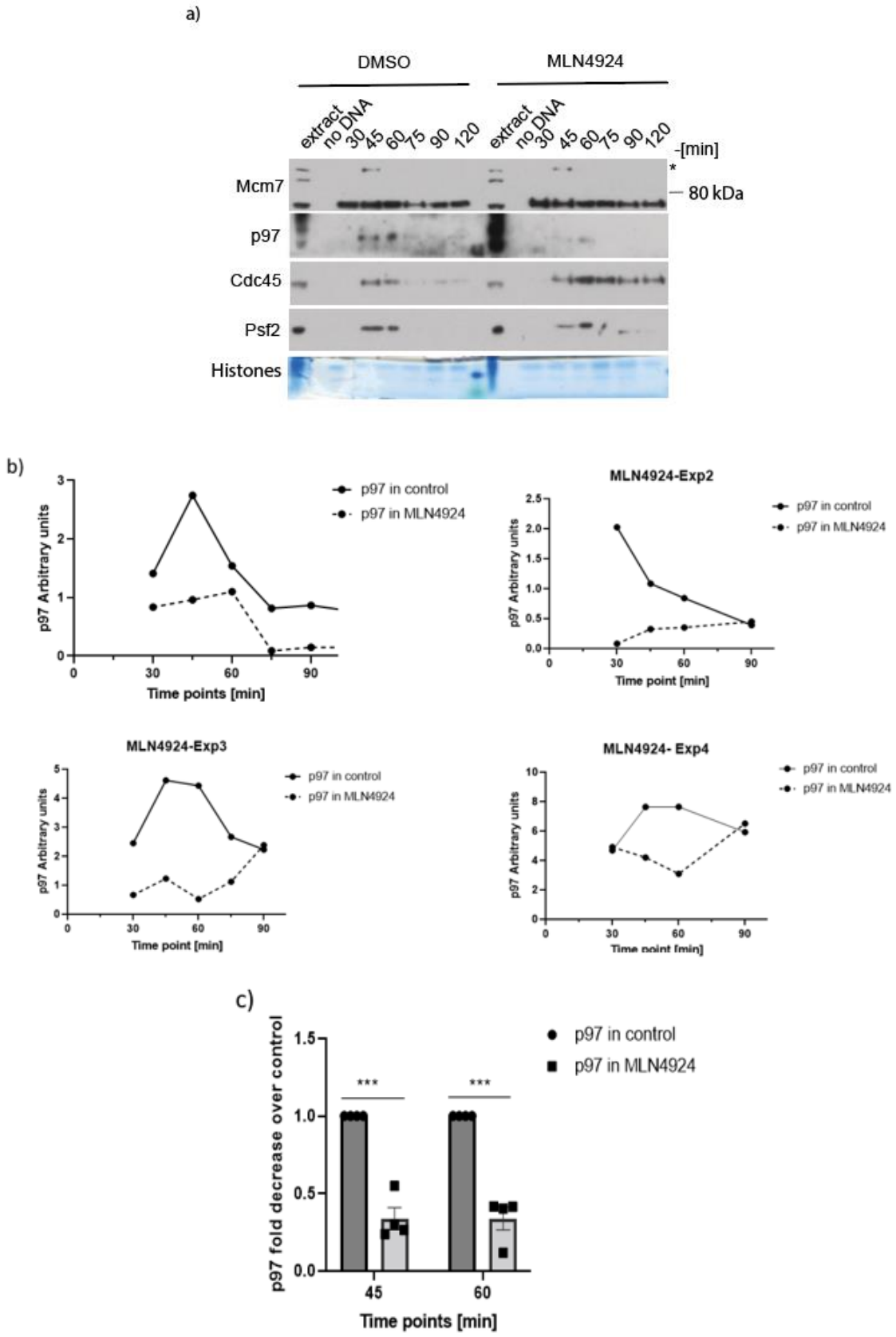

Figure 3. 3 p97 chromatin interaction is reduced when Cul2^{Lrr1} E3 Ubiquitin ligase is inactive. a) Interphase egg extract was supplemented with demembranated sperm nuclei and optionally with MLN4924 inhibitor. Chromatin was isolated at indicated time points, separated by SDS-PAGE and Western blotted using the indicated antibodies. Histones were stained in the gel with colloidal coomassie to act as a loading control. An extract sample without addition of DNA was analysed in parallel to other chromatin samples to provide a chromatin specificity control. * It is a band that does not disappear when polyubiquitylation is blocked with Ubi-NOK. This experiment represents one of four biological repeats. b) The density of p97 was measured by using Image J. The graphs represent arbitrary units of p97 signal at indicated time points from 4 independent experiments performed in different extracts. The blots in (a) correspond to experiment 1 in (b). c) The average fold decrease of p97 at 45 and 60 minutes quantified with SEM. Statistical analyses were performed with Multiple T Test. P value *<0.5, **<0.05, ***<0.005.

In unchallenged replication reaction, replication factors bind to chromatin at 45 and 60 min and the majority of replication is completed by 75 min. Therefore, CMG subunits (Cdc45 and Psf2) are bound to the chromatin at 45 and 60 min in the control conditions. p97 also binds at this time (Figure 3.3.a DMSO). Importantly when the neddylation and activity of Cul2^{Lrr1} was blocked by MLN4924 this led to accumulation of chromatin bound CMG components (Cdc45 and Psf2) in samples treated with the inhibitor. Nevertheless, despite accumulation of the terminated replisomes on chromatin, p97 does not accumulate on chromatin when Cullin neddylation is blocked (Figure 3.3.a.). I have quantified chromatin bound p97 over number of experiments to show that this trend is reproducible. I have also calculated the fold change of p97 signal for a couple of time points to do statistical analysis. I chose 45 and 60 min time points for the analysis as they represent the time points when there are replication forks elongating and terminating on chromatin and p97 binding to chromatin at these times most likely represents its interaction with Mcm7. This result suggests that ubiquitylation of substrates on chromatin by Cullin type ubiquitin ligases is important for p97 chromatin binding. In absence of Mcm7 ubiquitylation, despite accumulation of post-termination replisome on chromatin, p97 cannot recognise such unmodified replisome.

3.1.2.1.3. p97 accumulates on the chromatin upon inhibition of all polyubiquitylation during DNA replication

p97 is known to extract ubiquitylated protein substrates from chromatin (Ramadan, Bruderer et al. 2007). In the previous section I have shown that p97 binding to chromatin was decreased when Cul2^{Lrr1} activity was blocked. In order to learn how chromatin binding of p97 is affected when global polyubiquitylation is blocked, I blocked polyubiquitylation by using the Ubi-NOK recombinant protein. Ubi-NOK is a recombinant ubiquitin that inhibits polyubiquitylation as all of its lysines are mutated to arginine, thus it is defective in ubiquitin chain formation. We have shown previously that it inhibits Mcm7 ubiquitylation and replisome disassembly (Moreno, Bailey et al. 2014). My hypothesis was that

treatment with Ubi-NOK would lead to decreased levels of p97 on chromatin as all potential p97 substrates not just Mcm7, could not be efficiently polyubiquitylated.

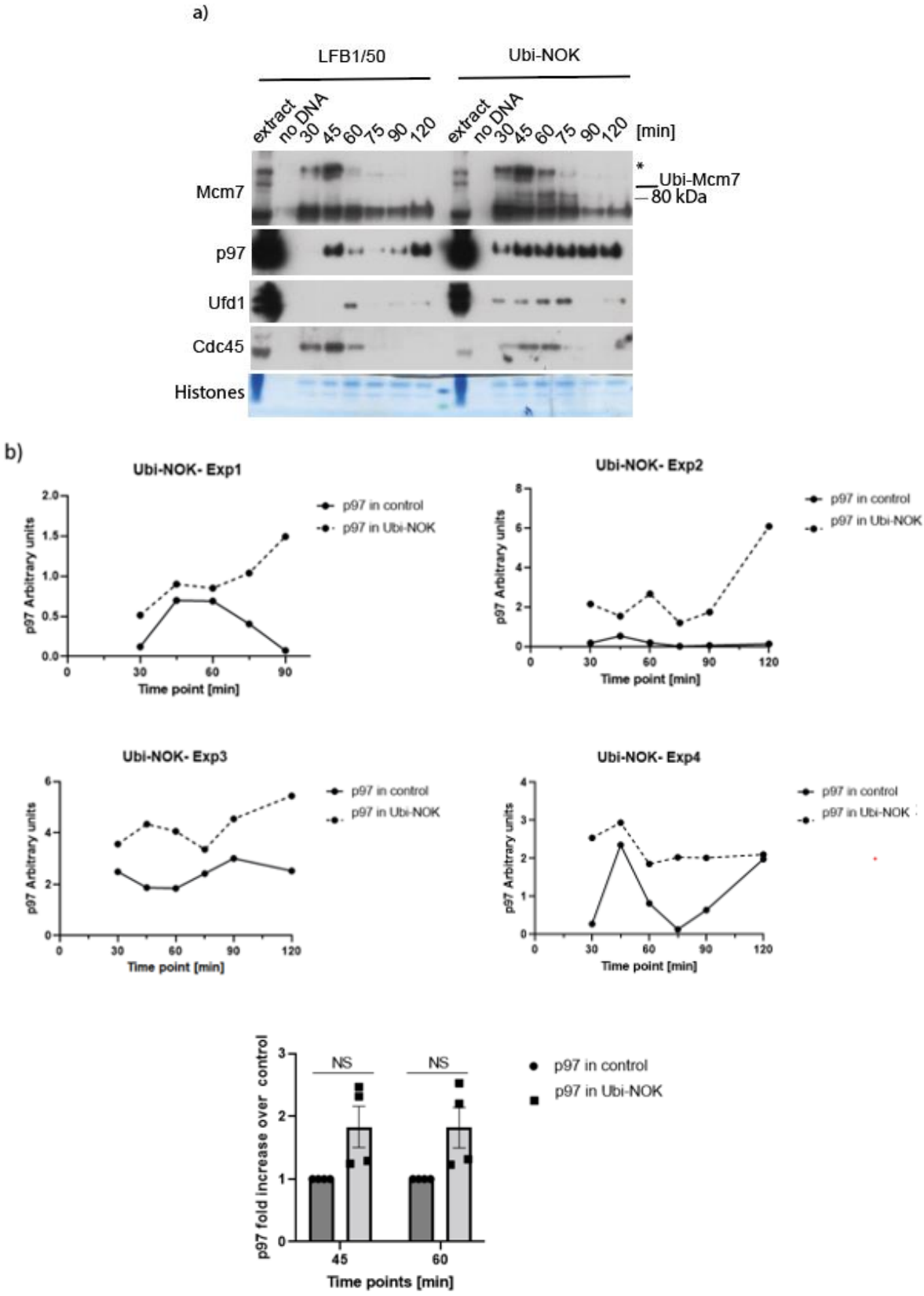

Figure 3. 4 p97 accumulated on chromatin upon inhibition of polyubiquitylation of substrates. a) Interphase egg extract was supplemented with demembranated sperm nuclei and optionally with Ubi-NOK. Chromatin was isolated at indicated time points, separated by SDS-PAGE and Western blotted using the indicated antibodies. Histones are stained on the gel with colloidal coomassie to act as a loading control. An extract sample without addition of DNA was analysed in parallel to other chromatin samples to provide the chromatin specificity control. * It is a band that does not disappear when polyubiquitylation is blocked with Ubi-NOK. This experiment represents one of four biological repeats. b) p97 on chromatin was quantified using Image J. The graphs represent arbitrary units of p97 quantification in 4 different experiments performed in different extracts. The figure in (a) corresponds to Experiment 4. c) The fold increase of p97 at 45 and 60 minutes quantified with SEM. Statistical analysis have done with Multiple T Test. P value *<0.5, **<0.05, ***<0.005.

Chromatin samples were isolated throughout the replication reaction in egg extract at indicated time points after optional addition of Ubi-NOK and analysed by western blotting using the indicated antibodies (Figure 3.4.). LFB1/50 buffer was added into the control reaction as Ubi-NOK protein was dissolved in it. As expected, control reaction samples behaved as observed previously (Figure 3.1.). Addition of Ubi-NOK to the replication reaction does not affect the ability of extract to replicate DNA, as shown previously (Moreno, Bailey et al. 2014), whilst it resulted in prolonged association of the replicative helicase with chromatin as seen by increased and prolonged association of Cdc45 with chromatin (Figure 3.4.a.) as described previously (Moreno, Bailey et al. 2014). Moreover, we can observe accumulation of monoubiquitylated Mcm7 on chromatin as Ubi-NOK can be attached to substrates and monoubiquitylate them, but it does not have lysines to attach further ubiquitins in the chains. This monoubiquitylation is most likely created by $Cul2^{Lrr1}$ at DNA replication termination (Figure 3.4.a.). The non-specific MCM7 high Mw band also could be seen. However, we do not have an antibody that can immunodeplete mcm7 to check if this band would disappear. Although, this band shows chromatin binding dynamics similar to replication fork protein and if it recognizes some other replication factor it would also disappear when mcm7 is depleted as mcm2-7 is essential for replication and establishment of replisome on chromatin.

We expected to see a decreased level of p97 chromatin binding upon egg extract treatment with Ubi-NOK during replication as there are no polyubiquitylated factors that can be detected by p97 core complex (p97-Ufd1/Npl4) for extraction from chromatin. However, surprisingly, the amount of p97 and Ufd1 binding on chromatin was increased (Figure 3.4.a.). I quantified p97 levels over a number of experiments to show reproducibility of this observation (Figure 3.4.b.), then l chose a couple of time points to do statistical analysis (Figure 3.4.c.). Although the difference in fold increase of p97 upon inhibition of polyubiquitylation is not statistically significant due to much divergence between experiments, in all experiments we could consistently see higher p97 signal on chromatin when its substrates could not be polyubiquitylated. This surprising result suggests that p97/Ufd1/Npl4 is not brought to the chromatin during DNA replication in *Xenopus* egg extract just by directly recognizing

and binding its polyubiquitylated substrates. It suggests, that p97 complexes can be recruited to the chromatin in alternative ways e.g., with the use of cofactors that recognize other components of replicating chromatin. I decided therefore to identify such cofactors.

3.1.2.2. p97 antibody purification

My aim was to see what cofactors interact with p97 on chromatin during replication termination. For that I need to immunoprecipitate p97 from chromatin during termination and send the sample for analysis by mass spectrometry. To be able to do it I needed high-affinity antibodies against *Xenopus* p97.

p97 antibody had already been raised in the lab and so my first job was to purify them from whole sera and characterise them. To purify p97 antibody, an antigen column needed to be prepared. Therefore, the first task was to express and purify p97 protein from bacteria. BL21 *E. coli* cells were thus transformed with plasmids containing a His-p97 insert and a large culture was grown. p97 protein was then purified using nickel beads, following the protocol in section 2.3.3.1. The success of purification was determined by Coomassie staining (Figure 3.5.). The elution fraction with the highest concentration of purified protein, which was elution 2, was used for antibody purification. Fraction 2 was dialyzed into the column-coupling buffer (as described in section 2.3.4.1.). The concentration of p97 purified protein was quantified by Bradford assay and was found to be 6.12 mg/ml.

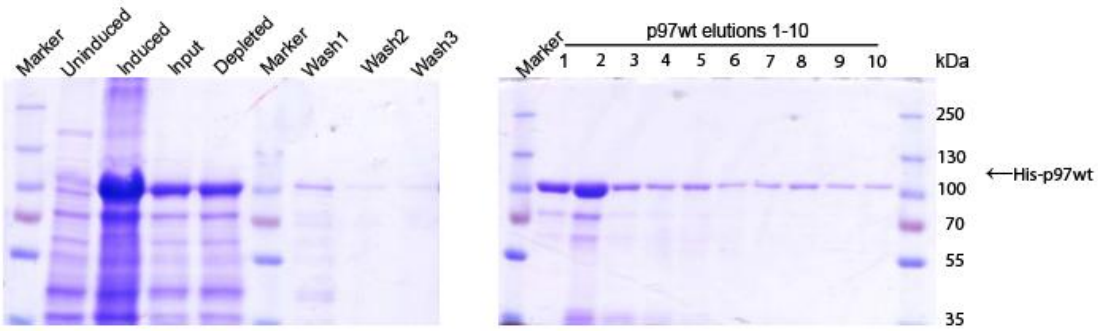

Figure 3. 5 Recombinant *X.laevis* His-tagged p97 (His-p97) was purified. BL21 bacteria cells containing His-p97 plasmid were grown in large culture. His-p97 was induced with IPTG and then purified using nickel beads. Samples from each step of purification protocol were resolved by SDS-PAGE prior to staining with Coomassie Blue.

3.1.2.2.1. Purification of p97 antibody

Antibodies against p97 were purified following the protocol in section 2.3.4.2. and eluted with low pH. The quality of the purified antibody was then tested by Western Blotting with samples of egg extract

and compared with the whole serum (non-purified antibody) (Figure 3.6.). The purified antibody was much cleaner and more specific as it produced bands of the expected size and fewer non-specific bands. The p97 sera has a varieties concentration of unlabeled antibodies. Therefore, it could be useful if we also measured the binding affinity of p97 antibody in the sera by competitive binding assay to confirm the p97 antibody in sera recognized the purified p97 protein is not a nonspecific protein.

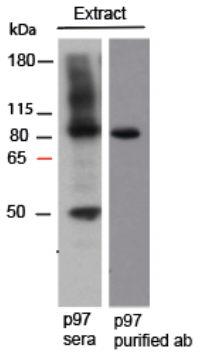

Figure 3. 6 The purified p97 antibody against p97 was more specific than non-purified p97 sera. Samples of egg extract were resolved on an SDS-PAGE gel and western blotting was performed using purified and non-purified (sera) antibody against p97**.** Samples were run on same gel and transferred onto same membrane

3.1.2.3. p97 immunoprecipitation from chromatin during replication termination

We know that the purified p97 antibody specifically recognizes one band of correct size using western blotting of *Xenopus* egg extract (Figure 3.6.) However, to further test this antibody, i.e., to determine whether it recognizes natively folded proteins and co-immunoprecipitate its cofactors from the extract, I used it to immunoprecipitate p97 from *Xenopus* egg extract (section 2.3.5.) (Figure 3.7.a).

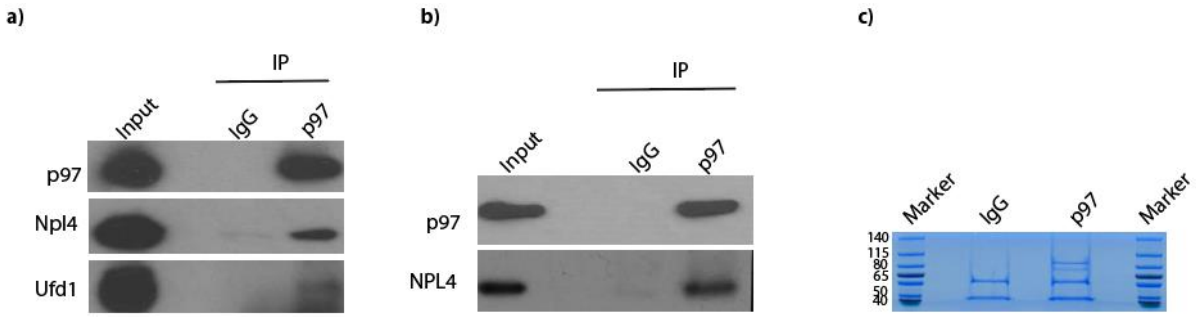

Figure 3. 7 Purified p97 antibodies can immunoprecipitate p97 from *Xenopus* egg extract and from chromatin. a) p97 was immunoprecipitated from whole egg extract using purified antibodies. Immunoprecipitated samples were tested by western blotting with indicated antibodies. b) p97 immunoprecipitation from chromatin assembled in S-phase extract treated with p97 inhibitor NMS-873. Interphase *X.laevis* egg extract was supplemented with demembranated sperm nuclei and NMS-8734. Chromatin containing high levels of terminated CMGs was isolated at 60 min, when most of the DNA had been replicated. Chromatin samples were subjected to benzonase treatment to release protein complexes from chromatin and purified p97 or commercial non-specific IgG antibodies used for immunoprecipitation. Immunoprecipitated materials were tested by western blotting with indicated antibodies. c) Large scale immunoprecipitation samples like in (b) were resolved in an SDS-PAGE and stained with colloidal coomassie. Each lane was cut into 10 bands and protein content analysed by mass spectrometry. The experiment was performed once.

The purified p97 antibody was incubated with the interphase egg extract and protein G dynabeads used to capture antibody-p97 complex. Immunoprecipitated p97 complex was analysed by western blotting. When we immunoprecipitate p97, firstly we can see that the antibody immunoprecipitates p97 protein as expected and secondly that it can co-immunoprecipitate p97 major interactors: Npl4 and Ufd1 (Figure 3.7.a). This shows that our antibody can recognize natively folded p97 protein.

To identify the cofactors that may be working with p97 during CMG complex removal from chromatin at replication termination, we needed to immunoprecipitate p97 from chromatin sample with terminated replisomes. Replication reaction was established in egg extract and p97 ATPase activity inhibitor (NMS-873) was added to the reaction to accumulate high levels of replisomes and p97 on chromatin. Based on our observations in Figure 3.2.a, we expected that p97 would still interact with the polyubiquitylated CMG helicase and other substrates upon treatment with the NMS-873 inhibitor, but that the interactions would be stabilized as such substrates could not be subsequently removed from the chromatin. Chromatin was isolated at 60 min when most of the DNA replication has been completed. Protein complexes were released from chromatin by digestion of DNA with Benzonase and immunoprecipitated with p97 or non-specific IgG beads. Samples were analyzed through western blotting and we were able to see that the p97 antibody could immunoprecipitate p97 from chromatin in S phase and could co-immunoprecipitate the major cofactor Npl4 (Figure 3.7.b.). In this experiment we expected to see the major cofactors Npl4 and Ufd1, as these have previously been shown to work

in this process (Maric, Mukherjee et al. 2017), but we also hoped to identify any minor cofactors, which may provide better substrate specificity and explain how p97 may be recruited to chromatin in absence of polyubiquitylated substrates. To identify such cofactors, the majority of material from a large-scale p97 immunoprecipitation from chromatin was resolved by SDS-PAGE and whole gel lanes were cut into 10 slices (Figure 3.7.c.) and sent for mass spectrometry analysis.

Analysis of the obtained mass spectrometry data has shown that p97 was successfully immunoprecipitated, as seen by the identification of 935 peptides of p97 in p97 IP sample (Table 3.1.). I then analysed the proteins identified in p97 and control IP and firstly looked for proteins involved in ubiquitin-proteasome system: p97 cofactors or potential cofactors (proteins containing ubiquitin binding domains), ubiquitin ligases, deubiquitylating enzymes and Sumo conjugation enzymes. A previous PhD student in the Gambus lab, Dr Sara Priego Moreno, immunoprecipitated terminated replisomes through Mcm3 immunoprecipitation and analyzed co-immunoprecipitated proteins by mass spectrometry (Sonneville, Moreno et al. 2017). To block replisome disassembly and accumulate terminated replisomes Sara added a p97 mutant, that contains mutations within the two AAA+ ATPase domains required for the binding (D1 domain) and hydrolysis (D2 domain) of ATP (p97mut) (Heubes and Stemmann 2007)). She also used caffeine **,** which blocks ATR/ATM checkpoint signaling and allows for firing of more replication origins (Marheineke and Hyrien 2004). I have compared, therefore, my p97 immunoprecipitation results with her mass spectrometry data to establish whether factors that I identify are also able to interact with terminated replisomes in S-phase. 128 peptides of p97 were found co-immunoprecipitated with terminated replisome in Sara's data (Table 3.1.).

Table 3. 1 p97 and its cofactors, ubiquitin ligases, Sumo related proteins and DUBs interacting with p97. Table presenting mass spectrometry analysis results of peptides identified following p97 immunoprecipitation from chromatin (with NMS-873) or Mcm3 IP (p97 mutant and caffeine). Total spectral count (TSC), which is a number of peptides for each protein identified, is indicated with the percentage of protein coverage in brackets. Proteins are sorted from higher to lower TSC in the p97 IP. Proteins identified with at least 2 peptides are shown.

		IP from chromatin assembled in extract treated with and NMS873		IP from chromatin assembled in extract treated with p97 mut and caffeine	
	Protein (kDa)	IgG TSC (coverege)	α-p97 TSC (coverege)	IgG TSC (coverege)	α-Mcm3 TSC (coverege)
p97 and co-factors	p97 (89 kDa)	8 (7%)	935 (80%)	0	128 (75%)
	Npl4 (69 kDa)	0	203 (58%)	0	80 (36%)
	Ufd1 (35 kDa)	0	97 (63%)	0	24 (53%)
	Ubxn7 (55 kDa)	0	6 (12%)	0	51 (23%)
	Faf1 (74 kDa)	0	5 (4%)	0	8 (10%)
	p47 (40 kDa)	0	5 (12%)	0	0
	Faf2b (52 kDa)	0	15 (23%)	0	0
	Faf2a (53 kDa)	0	14 (23%)	0	0
Ubiquitin ligases	Brca1 (176 kDa)	0	90 (23%)	0	0
	Bard1 (87 kDa)	0	2 (2%)	0	0
	E6ap (105 kDa)	0	11 (11%)	0	0
	Cullin1 (90 kDa)	0	9 (8%)	0	0
	Cullin9 (241 kDa)	0	2 (1%)	0	0
	Wwp2 (85 kDa)	0	6 (7%)	0	0
	Rnf31 (118 kDa)	0	5 (3%)	0	0
	Uhrf1 (87 kDa)	0	4 (1%)	0	0
	Hectd1 (281 kDa)	0	3 (5%)	0	0
	Rnf115 (33 kDa)	0	2 (6%)	0	0
	Cul2 (87 kDa)	0	0	0	131 (53%)
Sumo related proteins	Ranbp2 (315 kDa)	0	106 (25%)	52 (6%)	23 (4%)
	Sumo3 (11 kDa)	0	12 (35%)	0	0
DUBs	Usp9x (291 kDa)	0	4 (1%)	0	0
	Usp5 (93 kDa)	0	18 (20%)	0	0

We identified six p97 cofactors in immunoprecipitation of p97: Ufd1, Npl4, p47, Ubxn7, Faf1, Faf2a and Faf2b. However, only four of them were found to interact with terminated replisome as well: Ufd1, Npl4, Ubxn7 and Faf1 (Table 3.1.). Ufd1 and Npl4 form a heterodimer and are the major cofactors for p97 known to function on the chromatin. p47 has role in Golgi and ER formation in cell cycle, membrane fusion (Stach and Freemont 2017), Faf2a and Faf2b, are active in ER-associated degradation (ERAD) pathways that regulate ubiquitin dependent degradation of misfolded or unfolded endoplasmic reticulum proteins (Xia, Yan et al. 2014). They are mainly localized to the lipid droplets and endoplasmic reticulum (https://www.proteinatlas.org/ENSG00000113194-FAF2/subcellular). Moreover, they did not interact with the replisome in Mcm3 IP. For this reason, we chose not to investigate them further.

Most interestingly, this experiment revealed two minor cofactors, Ubxn7 and Faf1, interacting both with p97 and post-termination replisomes on chromatin (Priego Moreno, Jones et al. 2019). These data suggest that Ufd1-Npl4, Ubxn7 and Faf1 might be working with p97 in the disassembly of the CMG helicase during replication termination. Ubxn7 has been found previously to act as an important linker protein for interactions between the ubiquitin ligase $Cul2^{VHL}$, p97 and its substrate: ubiquitylated Hif1-α (Bandau, Knebel et al. 2012). In *X.laevis* egg extract and in *C.elegans* embryos during replication termination Mcm7 is ubiquitylated by Cul2 ubiquitin ligase (Sonneville, Moreno et al. 2017) and p97 unloads it (Moreno, Bailey et al. 2014). We therefore have the same components as in HIF1-α regulation and so we hypothesized that there may be a similar mechanism. On the other hand, *C.elegans* ortholog of Faf1 (UBXN-3) has been shown to be important for CMG disassembly in mitosis when $Cul2^{Lrr1}$ is defective in S phase (Gaggioli and Zegerman 2017, Sonneville, Moreno et al. 2017). Given that we have seen the same cofactors in replisome IP, we decided to further investigate the interaction between Ubxn7 and Faf1 and p97 during replisome disassembly, which is driven by polyubiquitylation by $Cul2^{Lrr1}$.

p97 is known to interact with deubiquitylating enzymes and ubiquitin ligases that can process substrates recognized by p97 (Alexandru, Graumann et al. 2008). I have therefore analysed them too and l found a number of ubiquitin ligases: Brca1, Bard1, E6ap2, Cullin1, Cullin9, Wwp2, Rnf31, Uhrf1, Hectd1, and Rnf11. Similarly, a couple of deubiquitylating enzymes: Usp9x and Usp5 were found associated with the p97 on the chromatin during termination in the mass spectrometry analysis. Most of them were found only in p97 immunoprecipitation and not in terminated replisome, suggesting that they may be involved in other replication related roles of p97 or contamination of soluable p97 in our chromatin fraction.

Table 3. 2 DNA replication and DNA damage related proteins interacting with p97. Table presenting proteins identified following p97 IP (with NMS-873) or Mcm3 IP (p97 mutant and caffeine) and mass spectrometry analysis, as in Table 3.1. This table shows replisome components, DNA replication and DNA damage related proteins. Number of peptides identified for each protein in the different samples is indicated (Total spectral count, TSC), with the protein coverage in brackets. Proteins are sorted from higher to lower TSC and also combined in known complexes in the p97 IP. Only proteins identified by at least 2 peptides are shown.

		IP from chromatin assembled in extract treated with NMS873		IP from chromatin assembled in extract treated with p97 mut and caffeine	
	Protein (kDa)	IgG TSC (coverege)	α-p97 TSC (coverege)	IgG TSC (coverege)	α-Mcm3 TSC (coverege)
Mcm Complex	Mcm2 (100 kDa)	0	67 (31%)	14 (12%)	957 (72%)
	Mcm3 (90 kDa)	0	3 (2%)	22 (10%)	1133 (84%)
	Mcm4 (97 kDa)	0	28 (21%)	4 (3%)	945 (78%)
	Mcm5 (82 kDa)	0	30 (31%)	29 (27%)	862 (84%)
	Mcm6 (93 kDa)	0	49 (32%)	33 (19%)	828 (83%)
	Mcm7 (82 kDa)	0	42 (34%)	23 (16%)	884 (77%)
Replisome components	Rpa1 (67 kDa)	0	149 (38 %)	0	1 (13%)
	Rpa3 (13 kDa)	0	3 (36%)	0	0
	PCNA (29 kDa)	19 (48%)	54 (66%)	0	6 (7%)
	Dnmt1 (168 kDa)	0	50 (19%)	0	53 (19%)
	Spt16 (118 kDa)	0	25 (15%)	25 (15%)	0
	Ctf4 (125 kDa)	0	23 (16%)	0	0
	Rfc2 (38 kDa)	0	8 (22%)	0	6 (18%)
	Rfc3 (40 kDa)	0	20 (38%)	4 (11%)	14 (38%)
	Rfc4 (40 kDa)	0	13 (28%)	0	0
	Pol3 (125 kDa)	0	2 (6%)	0	0
	Polα1 (165 kDa)	0	9 (5%)	0	66 (24%)
	Polε (261 kDa)	0	3 (1%)	0	316 (37%)
	Topbp1-α (169 kDa)	0	11 (71%)	0	0
	Orc2 (62 kDa)	0	8 (12%)	0	39 (29%)
	Orc3 (81 kDa)	0	7 (9%)	0	31 (32%)
	Orc4 (50 kDa)	0	2 (6%)	0	20 (22%)
	Dna2 (120 kDa)	0	6 (5%)	0	0
	Fen1-a (43 kDa)	0	3 (9%)	0	0
DNA replication and DNA damage response proteins	Sall4 (114 kDa)	0	20 (27%)	0	0 (9%)
	Rif1 (257 kDa)	0	108 (21%)	0	6 (3%)
	Arid1a (206 kDa)	0	82 (17%)	0	0
	Arid1b (148 kDa)	0	16 (10%)	0	0
	Smarca5 (122 kDa)	0	45 (29%)	2 (2%)	372 (63%)
	Smarca4 (181 kDa)	0	21 (9%)	0	0
	Smarce1 (47 kDa)	0	17 (26%)	0	0
	Smarcb1 (43 kDa)	0	11 (24%)	0	0
	Cenpe (339 kDa)	0	41 (6%)	0	0
	Rrm1 (91 kDa)	0	29 (8%)	0	0
	Baz1b (166 kDa)	0	27 (11%)	0	150 (34%)
	Rad50 (154 kDa)	0	19 (8%)	0	0
	Rbbp7 (48 kDa)	0	15 (23%)	0	0
	Smc3 (141 kDa)	0	14 (12%)	0	22 (22%)
	Hdac1-b (55 kDa)	0	12 (22%)	0	0
	Etaa1 (90 kDa)	0	11 (12%)	0	0
	Ehmt2 (65 kDa)	0	11 (11%)	0	0
	H3.3 (15 kDa)	4 (21%)	8 (36%)	0	22 (69%)

p97 segregase plays an important role in homeostasis of proteins on chromatin and is a key player of protein-induced chromatin stress (PICHROS) (Vaz, Halder et al. 2013). An increasing number of proteins is suggested to be regulated by p97 during DNA damage response (Acs, Luijsterburg et al. 2011, Meerang, Ritz et al. 2011). However, fewer DNA replication substrates of p97 are known. Some of the proteins that p97 interacts with in our samples may represent potential substrates that are regulated by p97. I have analyzed, therefore, my mass spectrometry data and focused first on interacting proteins involved in processes of DNA replication and DNA damage (Table 3.2).
Mcm2-7 are the core components of the CMG helicase complex, and these were detected in the p97 IP. The remaining subunits of the CMG complex however, GINS complex and Ccdc45, were not identified in the analysis. One explanation could be that GINS complex and Cdc45 proteins are much smaller and therefore much more difficult to detect by mass spectrometry (Table 3.2.).

Most of the replication machinery components remain bound to chromatin when CMG disassembly is blocked during termination (Sonneville, Moreno et al. 2017). I have detected many replication factors in my p97 immunoprecipitation: Rpa1, Rpa3, PCNA, Dnmt1, Spt16, Ctf4, Rfc2, Rfc3, Rfc4, Pol3, Polα1, Polε, Topbp1-α, Orc2, Orc3, Orc4, Dna2, Fen1-α (Table 3.2.). We saw more enrichment of RPA1 than RPA2 and RPA3. It might be due to direct interaction of RPA1 with the p97 and chromatin but not RPA2 and RPA3. Interestingly, we found RPA1 to be strongly enriched and PCNA to be increased in the p97 IP. This suggests that these two replication factors may directly interact with p97 either solely or as a member of a complex and could be potential p97 substrates.

p97 segregase is a key factor that controls DNA repair mechanisms to correct errors during DNA replication (Meerang, Ritz et al. 2011, van den Boom, Wolf et al. 2016). We could see that Smarca5 and Baz1b proteins are found more abundantly in the Mcm3 IP rather than p97 IP suggesting that they interact more with replisome components. However, Arid1a, Rif1 and Cenpe proteins appear to be more enriched in the p97 IP in comparison to the replisome IP (Table 3.2.). This suggests that the latter proteins may directly associate with p97. We would therefore like to hypothesize that these proteins might be substrates of p97 or regulate p97 in a process independent from CMG unloading at termination.

Table 3. 3 Other proteins associated with p97 on chromatin upon inhibition of replisome disassembly. Other proteins that are found associated with p97 in the same mass spectrometry analysis as Table 3.1. and Table 3.2. The number of peptides for each protein is indicated (Total spectral count, TSC), with protein coverage in brackets. This table only shows those proteins enriched in the p97 IP (at least 2-fold enrichment in p97 IP), and only proteins with more than 10 peptides identified in the p97 IP are shown. Proteins are sorted from higher to lower TSC. A short description of listed proteins' functions is also provided.

		IP from chromatin assembled in extract treated with NMS873		
	Protein (kDa)	IgG TSC (coverege)	α-p97 TSC (coverege)	Description
Other proteins	Nup214 (209 kDa)	0	109 (17%)	Nuclear pore complex components, essential for nuclear transport
	Nup205 (228 kDa)	0	41 (11%)	
	Nup160 (142 kDa)	0	12 (7 %)	
	Nup155 (155 kDa)	0	13 (6%)	
	Nup153 (165 kDa)	0	16 (5%)	
	Nup107 (105 kDa)	2	29 (19%)	
	Nup93 (93 kDa)	0	19 (15%)	
	Nup88 (82 kDa)	0	38 (29%)	
	Nup85 (128 kDa)	0	14(14%)	
	Nup37 (37 kDa)	2 (4%)	10 (26%)	
	Cct2 (58 kDa)	0	64 (31%)	TCP1 complex folds different proteins upon ATP hydrolyses, helps to regulate telomere maintenance
	Cct3 (61 kDa)	7(10%)	42 (34%)	
	Cct4 (58 kDa)	2 (2%)	28 (36%)	
	Cct5 (60 kDa)	0	50 (38%)	
	Cct6a (66 kDa)	0	26 (34%)	
	Cct8 (59 kDa)	0	58 (63%)	
	Tcp1(60 kDa)	6(8%)	41 (11%)	
	Eif3a (169 kDa)	0	49 (19%)	Eukaryotic translation initiation factors, initiate protein synthesis
	Eif4enif1 (85 kDa)	0	45 (30%)	
	Kpnb1 (97 kDa)	0	45 (21%)	Karyopherin subunits, important for nucleocytoplasmic transport
	Kpna1 (58 kDa)	0	25 (20%)	
	Psmd2 (99 kDa)	3 (7%)	23 (17%)	Proteasome subunits, regulates ATP-dependent degradation of ubiquitinated proteins
	Psmd14 (35 kDa)	0	16 (24%)	
	Eef1g (50 kD)	0	20 (31%)	Eukaryotic elongation factors, required for protein synthesis
	Eef1d (29 kd)	2 (3%)	12 (31%)	
	Cad (205 kDa)	0	63 (15%)	Involved in pyrimidine biosynthesis
	Cltc (191 kDa)	0	133 (24%)	Acting as inter-microtubule bridge in mitotic spindle
	Pard3 (142 kDa)	28 (14%)	82 (30%)	Asymmetrical cell division,cell polarization processes
	Xsal-3 (114 kDa)	0	70 (26%)	Nucleic acid binding
	Hsp90ab1 (83 kDa)	0	68 (39%)	Molecular chaperone, transcription activity
	Pdcd6ip (96 kDa)	0	60 (39%)	Apoptotic process, mitotic cytokinesis
	Wrd33 (177 kDa)	0	59(19%)	Regulation of RNA pol 2
	Pkm2 (58 kDa)	0	59(32%)	Pryvate kinase acting in glycolysis
	Prpf40a (103 kDa)	0	41 (11%)	Regulation of cell morphology, cytoskeletal organiz.
	Ttf22 (132 kDa)	0	40 (19%)	Acting in termination of RNA pol 2
	Copa (139 kDa)	0	32 (19%)	Protein transport from ER to Golgi
	Copb2 (103 kDa)	0	18 (3%)	
	Ffa1 (161 kDa)	0	31 (16%)	Regulation of calcium ion transport, glucose homeos.

		IP from chromatin assembled in extract treated with NMS873		
	Protein (kDa)	IgG TSC (coverege)	α-p97 TSC (coverege)	Description
Other proteins	Igf2bp3-b (65 kDa)	0	29 (33%)	Regulator of mRNA transport and localization
	Xlzpc (50 kDa)	2	28 (5%)	Binding of sperm to zona pellucida of egg
	Tjpl (197 kDa)	0	28 (8%)	Tight junction adaptor protein
	Atp5a1 (60 kDa)	0	25 (34 %)	Generate mitochondrial ATP synthesis
	Snd1 (101 kDa)	0	21 (18%)	Endonuclease, regulates mRNAs (G1-to-S transition)
	Pak7 (74 kDa)	0	21 (25%)	Ser/Thr protein kinases, regulation of cytoskeletal dynamics
	Eprs (170 kDa)	0	21 (10%)	tRNA aminoacylation for protein translation
	Pgam5 (kDa)	0	20 (34%)	Phosphatase act. for Ser/Thr res., acting in necroptotic proc.
	Ythdf1 (61 kDa)	15 (19%)	19 (27%)	Regulator of mRNA translation efficiency
	Ap2b1 (106 kDa)	0	19 (15%)	Function in protein transport via vehicles
	Cttn (60 kDa)	6 (10%)	18 (20%)	Role in intracellular protein transport and endocytosis
	Zp4 (60 kDa)	0	16 (12%)	Component of the zona pellucida, prevents post-fertilizati.
	Rplp0 (34 kDa)	5 (5 %)	15 (34%)	Subunit of the ribosome
	Gapdh (36 kDa)	0	15 (23%)	Playing a role in glycolysis and nuclear functions
	Cand1 (136 kDa)	0	14 (9%)	Inhibitor of cullin nedd, SCF assembly and ligase activity
	Znf609 (153 kDa)	0	14 (6%)	Transcription factor
	Epabp (71 kDa)	0	14 (19%)	Stimulates the translation of mRNAs
	Padi2 (74 kDa)	0	14 (19%)	Catalyzes the deimination of arginine residues of proteins
	Ttc37 (175 kDa)	0	14 (5%)	RNA degredation by the exosome complex
	Gcn1l1 (294 kDa)	0	13 (4%)	Stimulating EIF2AK4/GCN2 kinase activity
	Rangap1 (63 kDa)	0	13 (16%)	Participates in the regulation of nuclear transport
	Pklr (58 kDa)	0	13 (9%)	Pyruvate Kinase, key role in glycolysis
	Kif2c (83 kDa)	0	12 (14%)	Promoting mitotic chromosome segregation
	Trafd1 (68 kDa)	0	11 (19%)	Negative regulation of innate immune response
	Tax1bp1 (89 kDa)	0	11 (11%)	Kinase binding, inhibits TNF-induced apoptosis

To complete my analysis of the p97 interactors, Table 3.3. presents the rest of the proteins found to interact with p97 in our mass spectrometry analysis. The interaction of these proteins with p97 may be explained by different functions of p97 during S-phase and replication e.g. nuclear transportation. Others may be potential substrates for p97 or be recruited to the chromatin as a result of impaired CMG disassembly.

3.1.2.4. Purification of Ubxn7 protein and antibody

Having identified Ubxn7 and Faf1 as potential secondary p97 cofactors, I wanted to confirm their interaction with p97 on chromatin by western blotting. I have a commercial Faf1 antibody that can recognise *Xenopus* Faf1, however a commercial Ubxn7 antibody was not available so I purified antibodies against Ubxn7 raised in the lab. I expressed His-tagged Ubxn7 in *E.coli* and purified recombinant wild type Ubxn7 (His-Ubxn7). His-Ubxn7 was expressed in Rosetta cells, a derivative of BL21 *E.coli* and purified following the protocol in (section 2.3.3.2.). Rosetta cells contain a plasmid expressing tRNAs for codons that are used in eukaryotic cells but are rare in prokaryotes (Kopanic, Al-

Mugotir et al. 2013). As a result, Rosetta strain is better at expressing eukaryotic proteins that are not codon optimised. The purification result was analysed using Coomassie Blue (Figure 3.8.). Purified protein, Elution 2 was dialysed overnight in 1l of antigen column coupling buffer (0.1 M NaHCo3, 0.5 M NaCl, pH 8.3).

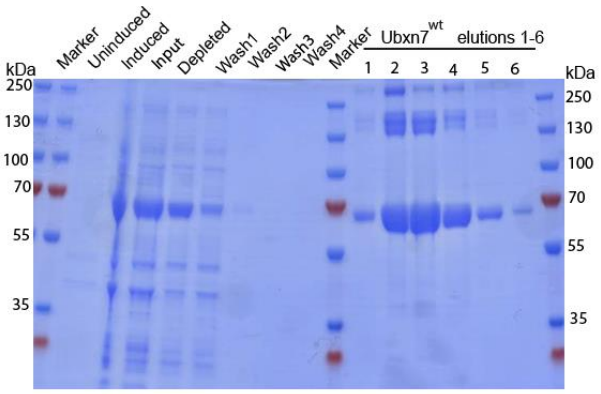

Figure 3. 8 The recombinant *X.laevis* His-tagged Ubxn7 (His-Ubxn7) was purified. Rosetta bacterial cells containing His-Ubxn7 plasmid were grown in large culture. His-Ubxn7 was expressed upon IPTG induction and purified using nickel beads. Samples from different purification steps were resolved by SDS-PAGE prior to staining with Coomassie Blue.

I then used the purified His-Ubxn7 protein for making an antigen column and purified Ubxn7 sera following the protocol described in section 2.3.4. After purification, I tested whether the purified Ubxn7 antibody specifically recognises Ubxn7 protein in the *Xenopus* egg extract by western blotting. It clearly recognised a band of a correct size and was much cleaner than the full sera (Figure 3.9.).

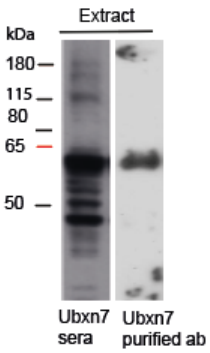

Figure 3. 9 The purified antibody against Ubxn7 is more specific than non-purified Ubxn7 sera. Samples of egg extract were resolved on an SDS-PAGE gel and western blotting was performed using purified and non-purified (sera) antibody against Ubxn7. Samples were run on the same gel and transferred onto the same membrane

3.1.2.5. p97 interacts with Ubxn7 and Faf1 on chromatin

To start confirming my mass spectrometry data, I first tested the interaction between p97 and Ubxn7 in whole egg extract, and Ubxn7 and Faf1 on chromatin. Firstly, I tested whether p97 can interact with Ubxn7 in egg extract and could see Ubxn7 interacting with p97 (Figure 3.10.a.). Secondly, I tested whether p97 interacts with Faf1 and Ubxn7 on chromatin with accumulated terminated replisomes. A DNA replication reaction was started by adding sperm DNA into the interphase egg extract. The extract was treated with NMS-873 to accumulate terminated replisomes on chromatin. After the majority of the replication was completed, chromatin was isolated, protein complexes released from DNA with Benzonase and p97 immunoprecipitated. Then, I tested whether I can detect Ubxn7 and Faf1 co-immunoprecipitating with p97 from chromatin sample. Figure 3.10.b. shows that both Ubxn7 and Faf1 interact with p97 on late S-phase chromatin as confirmed by western blotting. This result suggests that these two novel cofactors, Ubxn7 and Faf1, may regulate p97 binding to S-phase chromatin.

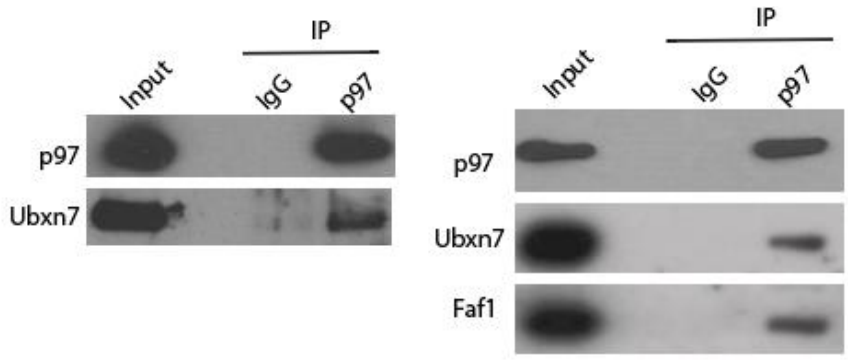

Figure 3. 10 p97 interacts with Ubxn7 and Faf1. a) IgG or purified p97 antibody was used to immunoprecipitate p97 from interphase egg extract. Immunoprecipitated samples were tested by western blotting with p97 and Ubxn7 purified antibodies. b) p97 interacts with Ubxn7 and Faf1 on S phase chromatin. Interphase *Xenopus laevis* egg extract was supplemented with demembranated sperm nuclei, treated with NMS-873 and chromatin was isolated at 60 min. Chromatin samples were subjected to Benzonase treatment to release protein complexes (input) and p97 or non- specific antibodies used for immunoprecipitation. Immunoprecipitated material was tested by western blotting with indicated antibodies.

3.1.3. Discussion

3.1.3.1. Regulation of p97 recruitment to chromatin during replication termination

p97 AAA-ATPase, which is a highly conserved ubiquitin segregase (Dantuma and Hoppe 2012, Meyer and Weihl 2014), regulates many different cellular processes in the cells although its role in the process of DNA replication is still not fully characterised. Our lab has shown previously that p97 is essential for replisome disassembly during DNA replication termination. The aim of my project therefore was to characterise the regulation of p97 during DNA replication termination.

In order to characterise p97 interaction with chromatin during DNA replication termination, we set up replication reactions in *X.laevis* egg extract using different treatments to block replisome disassembly at different stages of the process. p97 is one of the most abundant proteins in the cells (Meyer and Weihl 2014) and egg extract (Peters, Walsh et al. 1990). It is therefore clearly visible in my results that only a very small pool of p97 existing in the extract binds to chromatin at any time. As a result, it is a difficult protein for chromatin isolation as any small contamination of chromatin sample with extract fraction makes a big difference to the result. I made sure therefore, that I repeated the key experiments numerous times to ensure their reproducibility.

Inhibition of p97 activity led to an accumulation of CMG with ubiquitylated Mcm7 on chromatin (Figure 3.2.a.) (Moreno, Bailey et al. 2014, Dewar, Low et al. 2017), but also p97 and its cofactor Ufd1, possibly due to accumulation of the substrate, polyubiquitylated Mcm7, on the chromatin. When $Cul2^{Lrr1}$ activity was inhibited, I observed CMG accumulation on chromatin as expected (Moreno,

Bailey et al. 2014). However, the chromatin binding of p97 was decreased upon inhibition of Cullins (Figure 3.3.a.). This suggests that p97 could not recognize its substrate Mcm7 without polyubiquitin chains. Finally, when all of the polyubiquitylation was blocked with addition of Ubi-NOK, Mcm7 was not polyubiquitylated (Moreno, Bailey et al. 2014), and this led to accumulation of chromatin bound CMG. However, surprisingly, the protein levels of chromatin bound p97/Ufd1 increased (Figure 3.4.a.). This suggests that the recruitment of p97 to chromatin is not only directly through binding to the polyubiquitylated substrates on chromatin during DNA replication in *Xenopus* egg extract. It may be due to novel cofactors, which recruit p97 to chromatin independently from presence of polyubiquitylated substrates.

3.1.3.2. Potential cofactors of p97 during replication termination

We wanted to investigate the potential specific cofactors, which play roles during the DNA replication termination process. To identify which cofactors p97 may be working with during CMG complex disassembly at replication termination, we immunoprecipitated p97 specifically from chromatin in S phase, in conditions where replisome disassembly was blocked. The immunoprecipitated material was then analysed by mass spectrometry. We have then compared the results of p97 IP with results obtained previously in a similar experiment but immunoprecipitating Mcm3. These were two different experiments which have been performed separately and their comparison was used just as a suggestion of specificity of interaction, that needs to be validated in properly controlled experiments later. Themass spectrometry experiments performed are not quantitative due to the specifics of *Xenopus leavis* model organism. Powerful methods of quantitative mass spectrometry exist in human cells such as SILAC or iTRAQ. They cannot however be adapted for *Xenopus* system. To make our comparison of two immunoprecipitations more comparable, the input material could be the same for immunoprecipitation of either p97 or Mcm3 upon preparing one very large sample of S phase and mitotic chromatin. Such an experiment would require usage of large quantity of egg extract: about 10 ml when including preliminary experiments to set up best conditions for chromatin isolation. Standard yield of egg extract preparation is 5-10 ml. We decided therefore to compare two separate experiments and follow them with more controlled smaller scale experiments to validate our findings.

Our mass spectrometry analysis revealed that p97 interacts with several substrate recruiting cofactors Ufd1, Npl4, Faf2a, Faf2b, p47, Faf1 and Ubxn7 (Table 3.1.).

Ufd1 and Npl4 work together as a heterodimer and are the major known cofactors for p97 functions on the chromatin and their role is conserved from worms to human (Franz, Orth et al. 2011, Raman,

Havens et al. 2011). Importantly have already been shown to work in disassembly of the CMG helicase at the end of DNA replication (Maric, Mukherjee et al. 2017).

Faf2a and Faf2b (UBXD8) have known roles in Endoplasmic associated protein (ERAD). Neither they interact with post-termination replisome on chromatin (Sonneville, Moreno et al. 2017), nor their interaction with p97 on chromatin or Cul2 E3 ligase has not been reported. Therefore, we did not continue investigate further in this project.

We were also able to identify two more cofactors in this experiment: Ubxn7 and Faf1, which are minor substrate specific cofactors. Their interaction with p97 in this process is novel and interesting to investigate as the same two cofactors were found to interact with a post-termination replisome on chromatin by Dr Sara Priego Moreno (Sonneville, Moreno et al. 2017).

Faf1 plays a critical role in maintaining replication fork stability in worms and in human cell lines (Franz, Pirson et al. 2016). It has been shown that UBXN3 (homologous of human FAF1) is essential for CMG replisome unloading in mitotic prophase in *C. elegans* (Xia, Fujisawa et al. 2021) (Sonneville, Moreno et al. 2017) and human (Franz, Valledor et al. 2021) (Table3.1.). Franz et al has recently showed that Faf1 works with p97-Ufd1/Npl4 specifically disassembly of DNA replication factors from chromatin during DNA replication upon cooperation with USP7 in human cells (Franz, Valledor et al. 2021).
Ubxn7 has been found previously to act as an important linker protein for interactions between the ubiquitin ligase $Cul2^{VHL}$, which ubiquitylates Hif1-α, and p97 segregase to process ubiquitylated Hif1-α (Figure 3.11.) (Alexandru, Graumann et al. 2008, Bandau, Knebel et al. 2012). Ubxn7 depletion in cells unexpectedly leads to a reduced level in both full length Hif1-α and ubiquitylated Hif1-α, while overexpression of Ubxn7 leads to increased levels of non-ubiquitylated Hif1-α (Alexandru, Graumann et al. 2008). This suggests therefore that binding of Ubxn7 to neddylated Cul2 blocks its activity, not allowing for full activation through Nedd8 modification. Therefore, Ubxn7 is a negative regulator of ubiquitin ligase activity of Cul2. It was also suggested that reduced Cul2 activity stimulates binding of p97 through the UBX domain of Ubxn7. Ubxn7 first binds to neddlated-Cul2, regulates its substrate ubiquitylation and then changes its action towards docking p97 (Bandau, Knebel et al. 2012).

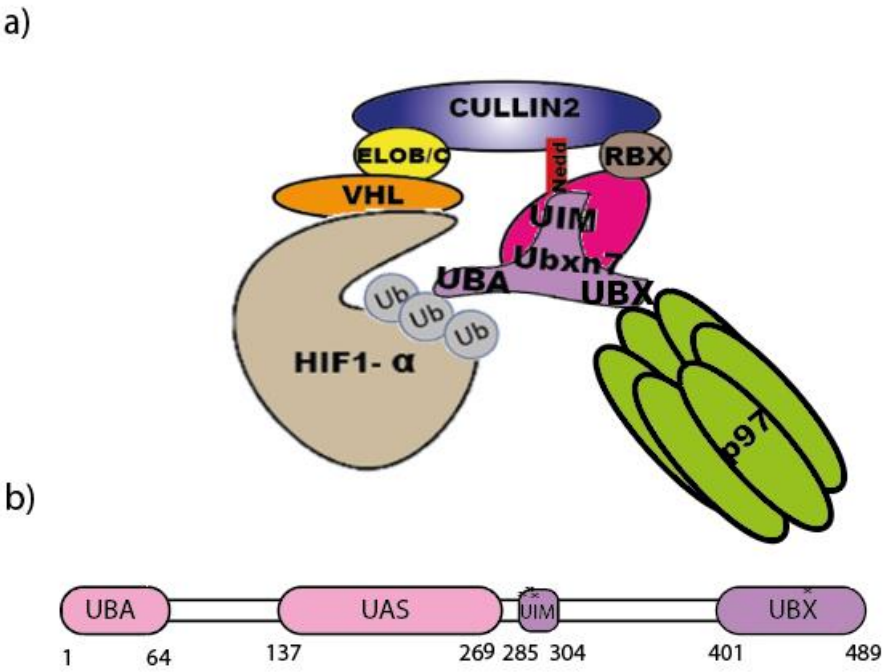

Figure 3. 11 The representation of human Ubxn7 in Hif1-α degradation. a) Ubxn7 regulates degradation of Hif1-α together with neddylated Cullin2 E3 ligase and p97, (b) Domain organisation of Ubxn7. Ubxn7 is interacting with neddylated Cul2, ubiquitylated substrate and p97 through different domains as indicated in (a).

In our project, we have similar components: the substrate Mcm7 is polyubiquitylated by Cul2 and extracted by p97 in the DNA replication termination process. It will be very interesting to see whether Ubxn7 has a role during the DNA replication termination process and whether it is a negative regulator of $Cul2^{Lrr1}$ activity as described above.

Both Ubxn7 and Faf1 cofactors may recruit p97 core complex for binding to ubiquitylated substrates on chromatin at the end of DNA replication termination. To confirm these interactions, we found that p97 antibody could co-immunoprecipitate Ubxn7 protein from egg extract (Figure 3.10.a.). Further to this, we found that p97 interacts with Ubxn7 and Faf1 on chromatin. This suggests that Ubxn7 and Faf1 act as secondary cofactors for p97, and have roles in CMG extraction from chromatin at the end of replication.

In the next chapter we further investigate whether these two cofactors have a role during CMG extraction by p97 from chromatin.

3.1.3.3. Other UPS related interactors of p97 on S-phase chromatin

Our mass spectrometry data also revealed that p97 interacts with a number of ubiquitin ligases (Table 3.2.). Many of them have been previously linked with p97 such as BRCA1 is a tumour suppressor gene (Chang, Wang et al. 2011) whose mutations and abnormal expression in cells leads to breast and ovarian cancer (Miki, Swensen et al. 1994). It forms a heterodimer with BARD1 to form an E3 ubiquitin ligase that maintains genomic stability. Other ubiquitin ligases have also been identified as chromatin associated p97 interactors in our analysis: WWP2, Rnf31, Ranbp2 and Usp5. They may act as cofactors or substrates of p97 but need to be further investigated.

RanBP2 is localized in the nuclear pore (Vetter, Nowak et al. 1999) and is responsible for sumoylation of the target protein (Pichler, Gast et al. 2002). While p97 is able to bind RanBP2 during nuclear import (Delphin, Guan et al. 1997), their interaction on the chromatin is not yet known. However, it is known that nuclear pore complexes are formed and are built into the nuclear membrane through their interaction with Mcm2-7 on chromatin in *Xenopus* egg extract (Gillespie, Khoudoli et al. 2007). RanBP2 and p97 are linked together due to replisome components interaction with nuclear pore complex, it is possible that p97 plays some role in proper nuclear membrane formation.

3.1.3.4. Other interactors of p97 on S-phase chromatin that could be p97 substrates

p97 interacts with many replication factors on chromatin upon inhibition of CMG helicase disassembly at the end of the replication: Rpa1, Rpa3, PCNA, Dnmt1, Spt16, Ctf4, Rfc2, Rfc3, Rfc4, Pol3, Polα1, Polε, Topbp1-α, Orc2, Orc3, Orc4, Dna2, Fen1-α are all detected interacting with p97 (Table 3.2.). Most of these factors could be linked to p97 through retained terminated replisome on chromatin, which is a p97 substrate. However, RPA1 peptides are much more abundant in the p97 IP than in the Mcm3 IP, suggesting that they can be potential substrates of p97. RPA as a single stranded binding protein is essential for DNA replication and DNA damage repair (Bochkareva, Korolev et al. 2002, Arunkumar, Stauffer et al. 2003, Oakley and Patrick 2010). RFWD3 E3 ubiquitin ligase was shown to drive ubiquitylation of RPA and RAD51 in response to mitomycin C (MMC)-induced DNA damage. Such modified RPA is removed from chromatin by p97 for proteasomal degradation (Inano, Sato et al. 2020) and promotes homologous recombination (Elia, Wang et al. 2015, Inano, Sato et al. 2020). RPA might therefore be a potential substrate of p97 during unchallenged DNA replication, too.

p97 also interacts with a number of other DNA damage response (DDR) and DNA replication proteins (Table 3.2.). Ubiquitylation controls DNA replication, DDR and DNA repair pathways by regulating

assembly and disassembly of certain proteins on chromatin (Ulrich and Walden 2010, Lehmann 2011). We have seen that levels of the SALL4, Arid1a, RIF and CENPE proteins are much higher in the p97 IP compared with the replisome (Mcm3) IP.

Finally, a variety of nuclear pore components (NUP) were also identified in the p97 IP, specifically a number of Nup107-160 complex members. It is possible that p97 plays some role in proper nuclear membrane formation potentially via interaction with RanBP2.

3.2. Ubxn7 forms a bridge between Cul2 and p97 during replisome disassembly in S phase

3.2.1. Introduction

In the previous chapter, I have shown that p97 does not bind to chromatin just through interaction with ubiquitylated substrates and we have identified possible co-factors that may regulate p97 during replication termination. These are Ubxn7 and Faf1. Ubxn7 seems especially interesting as a connector protein between the E3 ubiquitin ligase Cul2, p97 and ubiquitylated substrate, based on previous work with Hif1α (Bandau, Knebel et al. 2012). Thus, it is possible that Ubxn7 associates with $Cul2^{Lrr1}$, p97 and Mcm7 during CMG helicase removal during DNA replication termination. For this reason, we wanted to test whether this cofactor plays a role during replication termination.

3.2.2. Results

3.2.2.1. Ubxn7 is present on chromatin during DNA replication reaction

In order to determine whether Ubxn7 has a role in DNA replication and especially replication termination, I wanted first to analyse whether it binds to chromatin during DNA replication reaction. I isolated chromatin from replication reactions and tested Ubxn7 association with chromatin by western blotting (see materials and methods, section 2.2.2.2.) (Figure 3.12.).

CMG helicase is present on chromatin at 45 and 60 min when the bulk of DNA replication is happening, after which components of CMG disappeared from chromatin, as they are unloaded. There is still a strong Mcm7 signal on chromatin at later time points due to the fact that most of the Mcm2-7 complexes on chromatin are inactive and not all nuclei in the reaction mix undertake replication (Moreno, Bailey et al. 2014). I could also see that p97 and Ubxn7 start binding at this time but remain bound to chromatin for longer.

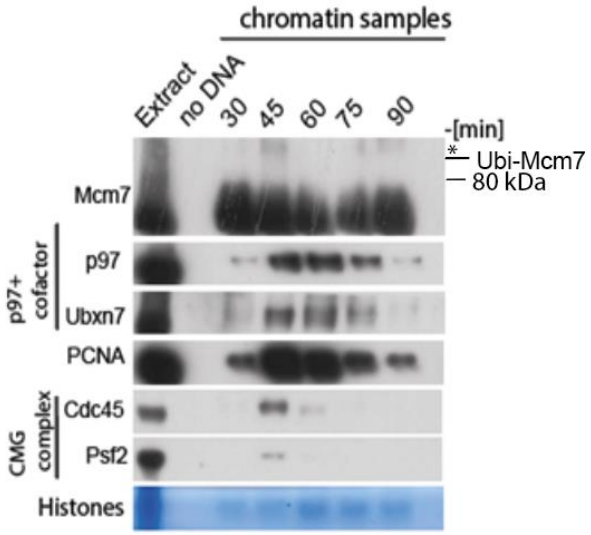

Figure 3. 12 Ubxn7 interacts with chromatin during replication reaction. Interphase egg extract was supplemented with demembranated sperm nuclei. Chromatin was isolated at indicated time points, separated by SDS-PAGE and Western blotted using the indicated antibodies. Histones are stained on the gel to act as a loading control. An extract sample without addition of DNA was analysed in parallel to other chromatin samples to provide a chromatin specificity control. * It is a band that does not disappear when polyubiquitylation is blocked with Ubi-NOK. This is a representative gel of at least 10 biological replicates.

3.2.2.2. Ubxn7 accumulates on chromatin when p97 activity and replisome unloading is blocked

l wanted next to analyse chromatin association of Ubxn7 when replication termination was blocked at different stages. Firstly, l optionally blocked the ATPase activity of p97 by using the drug NMS-873 which leads to accumulation of ubiquitylated replisome and p97 on chromatin. The control reaction was treated with DMSO, in which NMS-873 was dissolved. Chromatin was isolated at indicated time points during replication reaction in egg extract and tested by western blotting using the indicated antibodies (Figure 3.13.a.).

At 45 and 60 min, I could see Cdc45, Psf2, and Cul2 assembled on chromatin, and then unloading was observed. Lrr1 is difficult to visualize in the control, most probably due to transient interaction with the chromatin. Similarly, Ufd1, Faf1 and Ubxn7 can be detected binding to chromatin when the bulk of DNA replication happens, and forks are present on chromatin. p97, however, starts binding earlier and remains bound to chromatin for longer (Figure 3.13.a.).

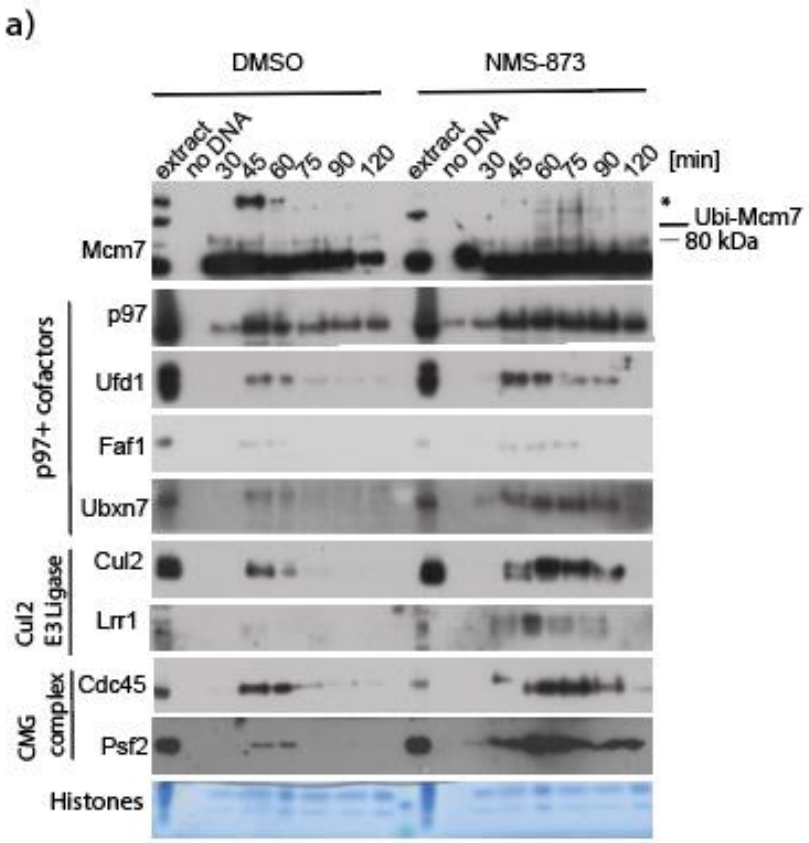

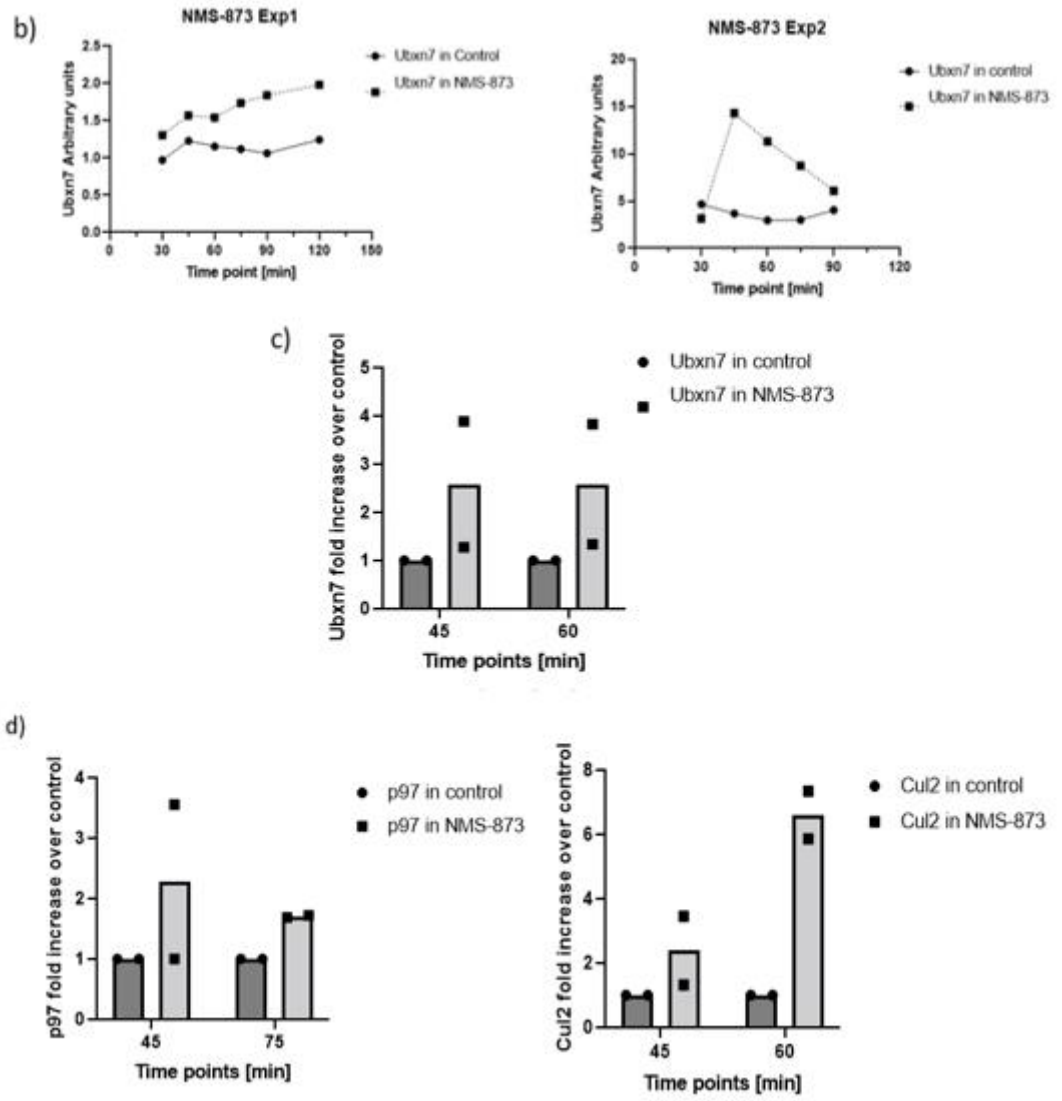

Figure 3. 13 Ubxn7 interacts with chromatin during DNA replication termination. a) Interphase egg extract was supplemented with demembranated sperm nuclei and optionally with p97 inhibitor NMS-873. Chromatin was isolated at indicated time points, separated by SDS-PAGE and Western blotted using the indicated antibodies. Histones are stained on the gel to act as a loading control. An extract sample without addition of DNA was analysed in parallel to other chromatin samples to provide a chromatin specificity control. This experiment represents one of two biological replicates. * It is a band that does not disappear when polyubiquitylation is blocked with Ubi-NOK. Faf1 was analysed in only one experiment. Part of these data has already been presented in Figure 3.2. b) The graphs showing abundance of Ubxn7 on chromatin were created from measuring band (pixel) densities of Ubxn7 using Image J and represent arbitrary units of two different experiments in independent extracts. Blots in (a) correspond to experiment 1 in (b). (c) The mean of the fold increase of Ubxn7 in two experiments in independent extracts at 45 and 60 min. d) The mean of the fold of increase of p97 and Cul2 at indicated time points.

Upon treatment with NMS-873, components of the CMG helicase (Cdc45, Psf2) accumulate on the chromatin together with ubiquitylated Mcm7, which indicates that polyubiquitylated Mcm7 and the rest of the replisome could not be removed from chromatin, which has been observed previously

(Sonneville, Moreno et al. 2017). Additionally, the ubiquitin ligase Cul2 (Figure 3.12.a and 3.12.d) and Lrr1 can be seen enriched on chromatin due to accumulation of their substrates (terminated replisomes) (Sonneville, Moreno et al. 2017). Finally, treatment with NMS-873 causes p97 to accumulate on chromatin along with its cofactor Ufd1 as shown in Chapter 1. Importantly, both Faf1 and Ubxn7 also accumulate in this situation (Figure 3.13.a, 3.13.b and 3.13.c). These data suggest that Ubxn7 and Faf1 may indeed play a role in DNA replication termination, as they show similar patterns of chromatin binding as known factors. Moreover, even though p97 is not active, Ubxn7 is still able to bind on chromatin.

3.2.2.3. Ubxn7 accumulation on chromatin is restricted when $Cul2^{Lrr1}$ is not neddylated

In order to learn whether the chromatin binding of Ubxn7 depends on either $Cul2^{Lrr1}$ or p97 during DNA replication termination, I first blocked the activity of $Cul2^{Lrr1}$ by using the drug MLN4924. MLN4924 blocks the activity of Cullin type ubiquitin ligases by inhibiting their neddylation through inactivation of the NEDD8 activating enzyme (NAE) (Soucy, Smith et al. 2009). It was shown previously that treatment with MLN4924 leads to accumulation of $Cul2^{Lrr1}$ on chromatin in its deneddylated form, because although its activity is inhibited, it can still interact with its substrate Mcm7 at DNA replication termination (Sonneville, Moreno et al. 2017). Samples were taken throughout the replication reactionin egg extract at indicated time points after optional DMSO or MLN4924 addition and analysed by western blotting using the indicated antibodies (Figure 3.14.a).

As we have seen previously, active CMG subunits (Cdc45 and Psf2) are bound to the chromatin at 45 and 60 min in the control conditions. p97 and Ubxn7 bind chromatin at these times too. Importantly, when the neddylation and activity of $Cul2^{Lrr1}$ was blocked by MLN4924, this led to accumulation of chromatin bound CMG components (Cdc45 and Psf2) but not p97 as shown in chapter 1 (Figure 3.14.d.). Although $Cul2^{Lrr1}$ was not active, it still could recognise and bind CMG complex on the chromatin, which results in accumulation of Cul2 itself (Figure 3.14.d). Interestingly, while we observed a possibly increased level of Faf1 on chromatin during S phase upon the inactivation of Cul2 ligase, there appears to be a reproducible reduction in protein levels of Ubxn7 (Figure 3.14.c.). This suggests that either Ubxn7 is recruited to chromatin through interaction with neddylated Cul2, or that it interacts with p97 to extract polyubiquitylated CMG termination helicases during the termination process. Faf1 likely has a different mechanism of interaction with chromatin independently of Ubxn7, although the pattern of Faf1 interaction with chromatin needs to be reproduced in more experiments (Figure 3.14).

a)

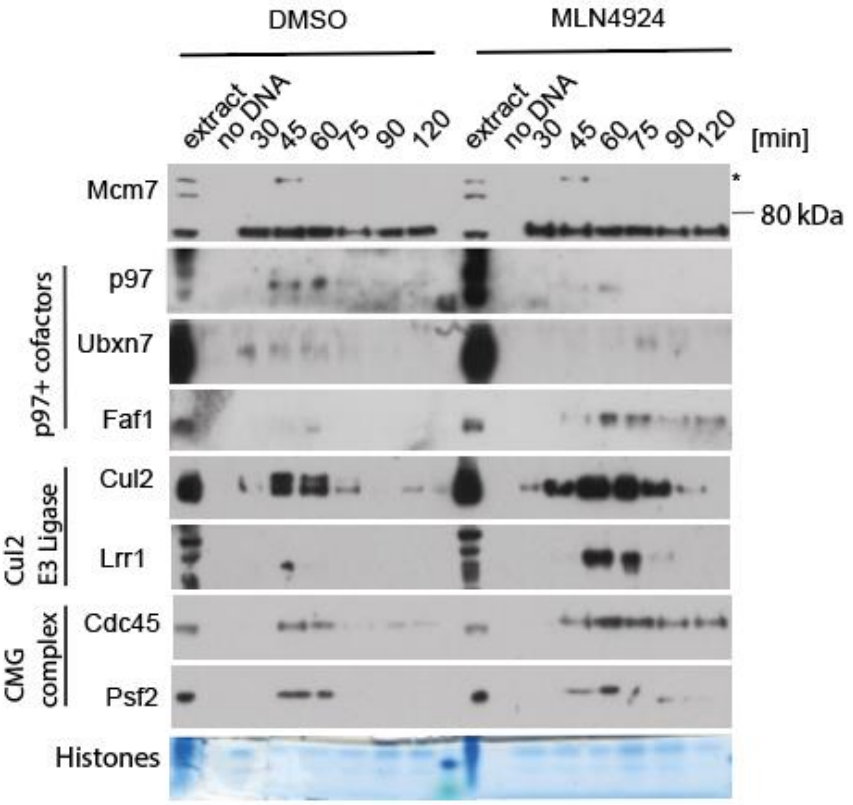
DMSO
MLN4924
extract
no DNA
30
45
60
75
90
120
extract
no DNA
30
45
60
75
90
120
[min]
Mcm7
*
80 kDa
p97+ cofactors
p97
Ubxn7
Faf1
Cul2 E3 Ligase
Cul2
Lrr1
CMG complex
Cdc45
Psf2
Histones

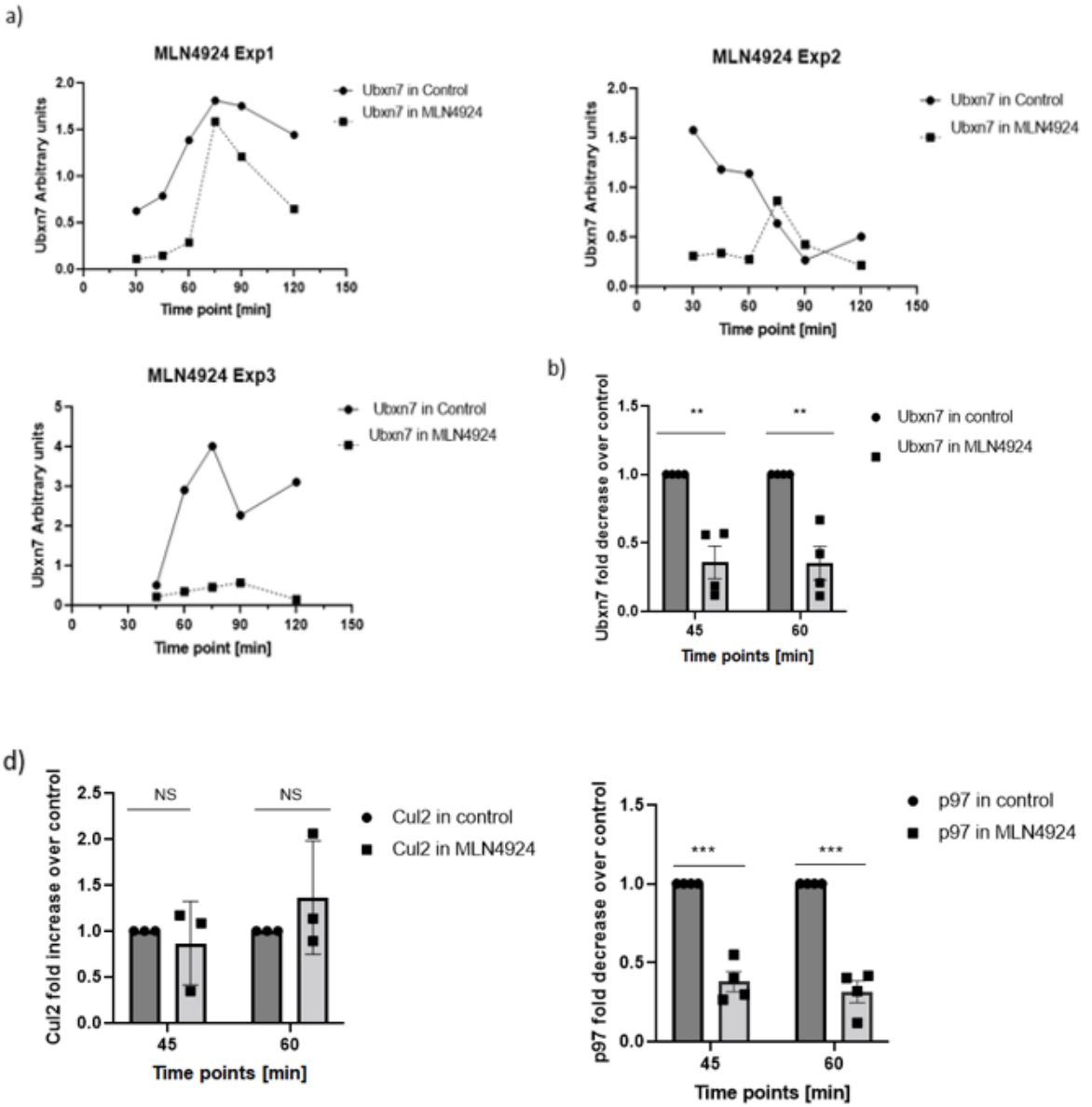

Figure 3. 14 Ubxn7 interaction with chromatin is inhibited upon inhibition of Cul2 activity. a) Interphase egg extract was supplemented with demembranated sperm nuclei and optionally with MLN4924. Chromatin was isolated at indicated time points, separated by SDS-PAGE and Western blotted using the indicated antibodies. Histones are stained in the gel to act as a loading control. An extract sample without addition of DNA was analysed in parallel to other chromatin samples to provide a chromatin specificity control. * It is a band that does not disappear when polyubiquitylation is blocked with Ubi-NOK. This experiment represents one of three biological repeats. Faf1 was analysed in only one experiment. b) The graphs were created from measuring band (pixel) densities of Ubxn7 using Image J and represent arbitrary units of three different experiments in independent extracts. Blots in (a) correspond to experiment 1 in (b). (c) The average fold decrease of Ubxn7 at 45 and 60 minutes quantified with a SEM. Statistical analysis is done with Multiple T Test. P value *<0.5, **<0.05, ***<0.005. d) The density of p97 and Cul2 was measured by using Image J. The average fold change of p97 and Cul2 at 45 and 60 minutes quantified with SEM. Statistical analysis as in (c).

3.2.2.4. Ubxn7 accumulates on chromatin upon inhibition of polyubiquitylation

In order to learn how blocking polyubiquitylation affects chromatin binding of Ubxn7 during DNA replication termination, I blocked polyubiquitylation by using the Ubi-NOK recombinant protein. My hypothesis was that treatment with Ubi-NOK would cause $Cul2^{Lrr1}$ to accumulate on chromatin, but not p97. $Cul2^{Lrr1}$ should still be able to bind in its active neddylated form to its substrate Mcm7 at DNA replication termination but would be unable to catalyse the formation of ubiquitin chains. Samples were taken throughout the replication reaction in egg extract at indicated time points after optional addition of Ubi-NOK and analysed by western blotting using the indicated antibodies (Figure 3.15.a.)

LFB1/50 was added to the control reaction samples as Ubi-NOK protein was dissolved in this buffer. As expected, control reaction samples behaved as observed previously (Figure 3.13.a and 3.14.a.) with most of replication forks present on chromatin at 45 min. Addition of Ubi-NOK to the replicating extract resulted in prolonged association of the replicative helicase with chromatin, while Mcm7 accumulated on chromatin in a monoubiquitylated form, as described previously (Moreno, Bailey et al. 2014). Similarly, chromatin-bound $Cul2^{Lrr1}$ significantly increased (Figure 3.15.d.) upon treatment with Ubi-NOK as the E3 ligase recognises its substrate Mcm7 but is unable to catalyse the formation of ubiquitin chains due to the presence of the Ubi-NOK mutant. It is also visible that Cul2 accumulates in its active neddylated form, which runs a bit higher on the gel than unneddylated Cul2.

As seen in chapter 1, the amount of p97 and Ufd1 binding on chromatin was increased in Ubi-NOK samples (Figure 3.15.d.). Similarly, Ubxn7 binding was increased upon inhibition of polyubiquitylation. It is possible, therefore, that the p97 core complex is primarily brought to chromatin by Ubxn7 binding to neddylated Cul2 rather than through direct binding to polyubiquitylated proteins.

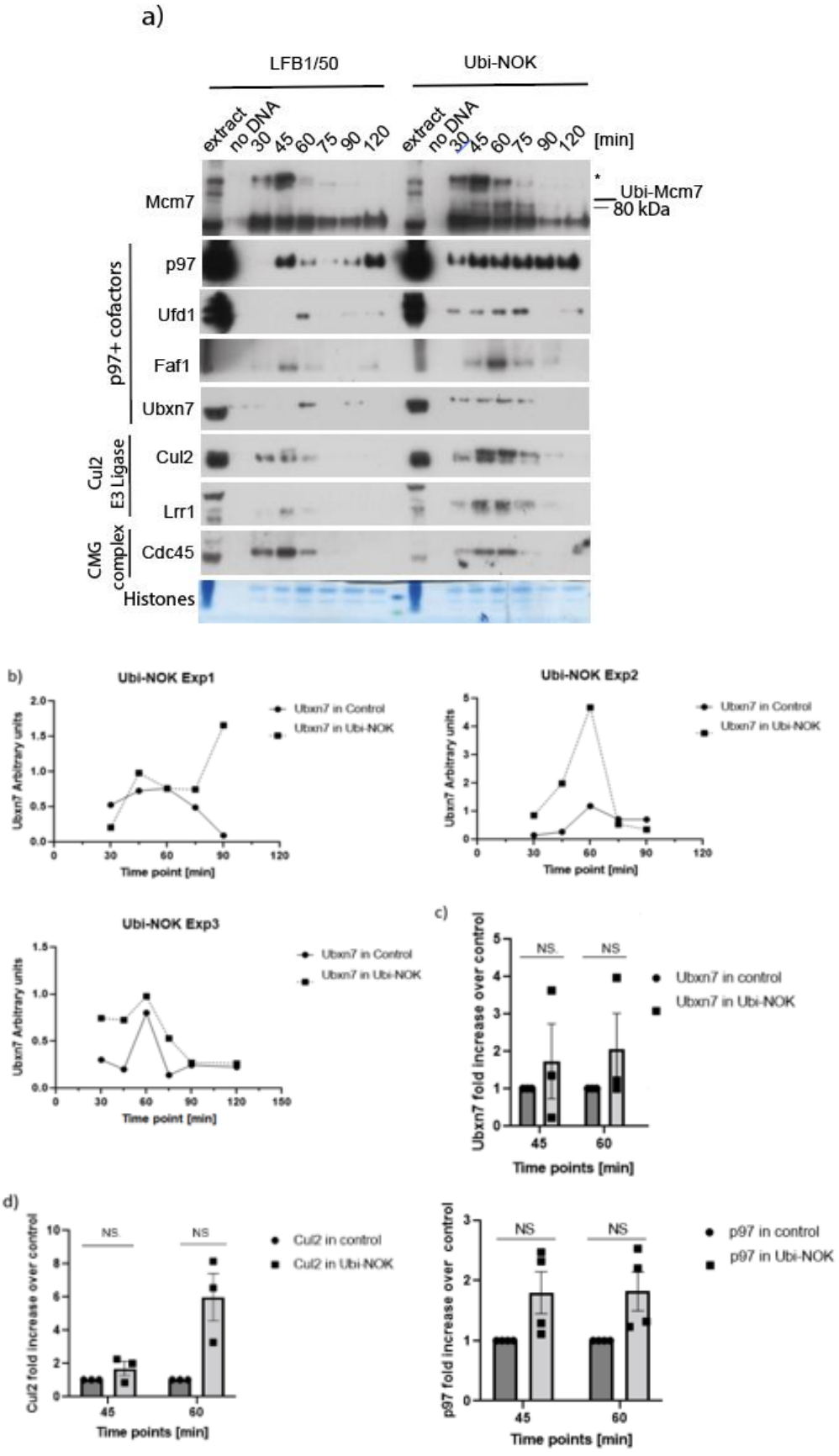
a)
LFB1/50
Ubi-NOK
extract
no DNA
30
45
60
75
90
120
[min]
Mcm7
Ubi-Mcm7
80 kDa
p97+ cofactors
p97
Ufd1
Faf1
Ubxn7
Cul2 E3 Ligase
Cul2
Lrr1
CMG complex
Cdc45
Histones
b)
Ubi-NOK Exp1
Ubi-NOK Exp2
Ubi-NOK Exp3
Ubxn7 Arbitrary units
Time point [min]
Ubxn7 in Control
Ubxn7 in Ubi-NOK
c)
Ubxn7 fold increase over control
NS
Time points [min]
Ubxn7 in control
Ubxn7 in Ubi-NOK
d)
Cul2 fold increase over control
Cul2 in control
Cul2 in Ubi-NOK
p97 fold increase over control
p97 in control
p97 in Ubi-NOK

Figure 3. 15 Ubxn7 accumulates on chromatin upon inhibition of polyubiquitylation. a) Interphase egg extract was supplemented with demembranated sperm nuclei and optionally with Ubi-NOK. Chromatin was isolated at indicated time points, separated by SDS-PAGE and Western blotted using the indicated antibodies. Histones are stained in the gel to act as a loading control. An extract sample without addition of DNA was analysed in parallel to other chromatin samples to provide a chromatin specificity control. This experiment represents one of three biological repeats. B) The graphs were created from measuring band (pixel) densities of Ubxn7 using Image J and represent arbitrary units of three different experiments in independent extracts. The figure in (a) corresponds to Experiment 3. C) The average fold increase of Ubxn7 at 45 and 60 minutes quantified with SEM. Statistical analysis through Multiple T Test. P value *<0.05, **<0.005, ***<0.0005 d) The density of p97 and Cul2 was measured by using Image J. The average fold change of p97 and Cul2 at 45 and 60 minutes quantified with SEM. Statistical analysis as in (c).

3.2.2.5. Ubxn7 and Cul2 interact on chromatin, while they do not associate in the extract

We hypothesised that $Cul2^{Lrr1}$ may be working together with p97 through Ubxn7. To support this hypothesis, we decided to analyse Ubxn7 interaction with each of these proteins. To identify proteins that interact with Ubxn7 in the *Xenopus* egg extract, we used affinity purified polyclonal Ubxn7 antibody to immunoprecipitate Ubxn7. Purified Ubxn7 antibodies were added to the interphase egg extract, and the resulting antibody-protein(s) complex precipitated from the mixture with Protein G dynabeads. Immunoprecipitated Ubxn7 was then analysed by western blotting. We found that this antibody could precipitate Ubxn7 protein efficiently and co-immunoprecipitate p97 and its interactors: Npl4 and Ufd1. Interestingly, Cul2 did not co-immunoprecipitate with Ubxn7 from the untreated extract (Figure 3.15.a.).

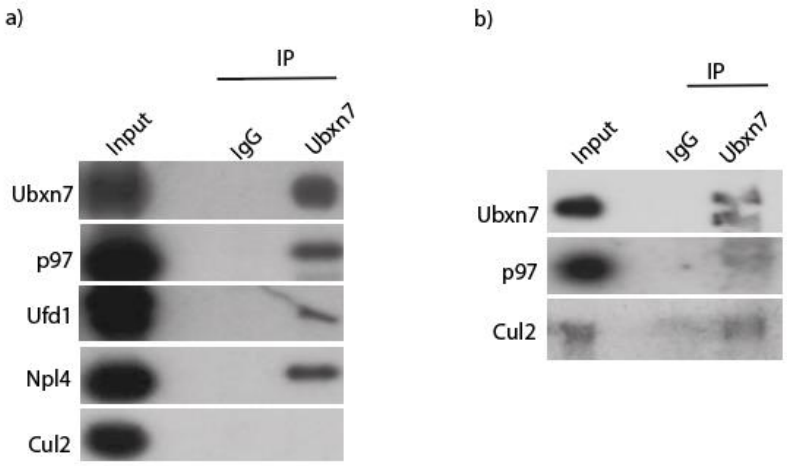

Figure 3. 16 Ubxn7 can interact with p97 core complex in *Xenopus* egg extract and chromatin, while it associates with Cul2 only on chromatin. a) The egg extract was activated into interphase and Ubxn7 was immunoprecipitated. Immunoprecipitated samples were tested by western blotting with indicated antibodies. Experiment were performed once. B) Ubxn7 immunoprecipitation from chromatin assembled in S-phase extract treated with p97 inhibitor NMS-873. Interphase *X.laevis* egg extract was supplemented with demembranated sperm nuclei and NMS-873. Chromatin containing high levels of terminated CMGs was isolated at 60 min. Chromatin samples were subjected to benzonase treatment to release protein complexes from chromatin and Ubxn7 or non-specific antibodies used for immunoprecipitation. Western blotting with indicated antibodies tested immunoprecipitated materials. Experiment was performed once.

If Ubxn7 does not interact with Cul2 in the extract, does replication induce their interaction? Neddylation induces Cul2 activity, and ubiquitylation and unloading of CMG helicases needs neddylated active Cul2 (Sonneville, Moreno et al. 2017). In addition, it is known that Ubxn7 interacts with Cul2 once it is in active neddylated form (Bandau, Knebel et al. 2012). To answer this, we immunoprecipitated Ubxn7 from S-phase chromatin. The extract was supplemented with p97 inhibitor NMS-873 to inhibit replisome disassembly and to increase the level of terminated replisomes on chromatin. Protein complexes were released from chromatin by digesting with Benzonase and then subsequently incubated with magnetic beads covalently coupled to either Ubxn7 or nonspecific IgG. Immunoprecipitated material was analysed by western blotting. It can be seen that Ubxn7 interacts with p97 and Cul2 on S phase chromatin with terminated replisomes (Figure 3.16.b.).

Ubxn7 interaction with Cul2 could not be seen in the cytoplasmic egg extract, as Cul2 exists there in its inactive, unneddylated form, while Cul2 accumulated on chromatin upon inhibition of p97 activity in its active neddylated form and could interact with Ubxn7. This is consistent with the idea that Ubxn7, as a cofactor of p97, may stimulate p97 interaction with polyubiquitylated CMG helicase through its interaction with Cul2 E3 ligase, similarly to the Hif1α degradation mechanism (Alexandru, Graumann et al. 2008, Bandau, Knebel et al. 2012) (see more detail in Discussion 3.2.). Moreover, we also observed two molecular size bands of Ubxn7 - the top band of Ubxn7 may represent a post -

translational modification of Ubxn7 such as phosphorylation. A phosphorylation modification within the UIM domain of UBXN7 at Ser287, Ser297 (phosphosite.org) and Ser288 was identified in human (Kim, Tannenbaum et al. 2005, Imami, Sugiyama et al. 2008). However, phosphorylation at Ser288 does not seem of critical importance for UIM binding to Cul2 (Bandau, Knebel et al. 2012) .

To further validate the interaction between Ubxn7, p97 and Cul2 on the chromatin, I next immunoprecipitated Cul2 from digested chromatin when disassembly of the terminated CMGs was inhibited by addition of p97 inhibitor NMS-873, whilst caffeine was added to increase origin firing. The immunoprecipitated samples were then analysed by western blotting. Cul2 was successfully immunoprecipitated (Figure 3.17.a.). Moreover, Cul2 co-immunoprecipitated Psf2, which confirms that Cul2 associates with the terminated replisome machinery on chromatin (Sonneville, Moreno et al. 2017). Based on our observations in Figure 3.16.b, we expected Cul2 to associate with Ubxn7 on chromatin during S phase. This interaction was indeed observed, but there was no detectable interaction between Cul2 and p97.

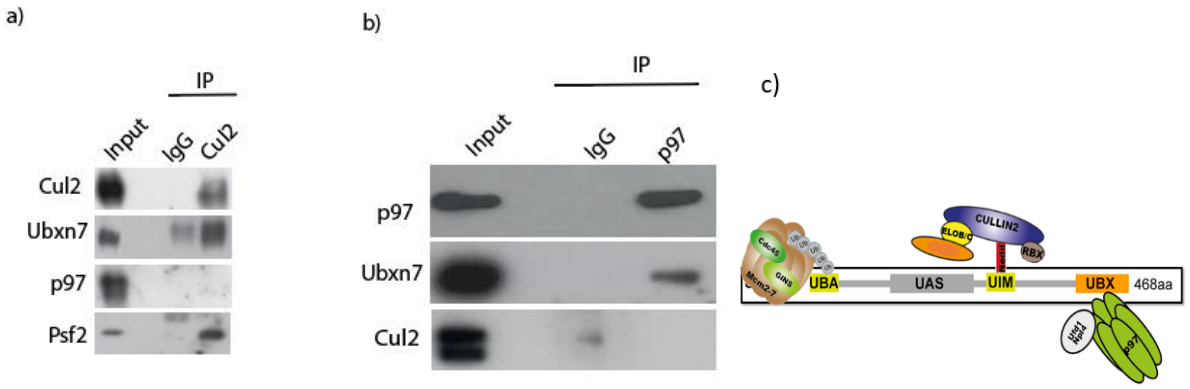

Figure 3. 17 Cul2 and p97 interaction is not stable on chromatin. (a) Interphase extract was supplemented with demembranated sperm nuclei, and treated with NMS-873 and caffeine to accumulate terminated replisomes on chromatin. Chromatin was isolated in middle of S-phase, and DNA digested with Benzonase to release protein complexes from chromatin (input) and Cul2 or non-specific IgG antibodies as a negative control used for immunoprecipitation. Immunoprecipitated materials were tested by western blotting with indicated antibodies. The experiments were performed once. (b) As in (a) but p97 antibodies were used instead of Cul2 antibodies. c) Model of Ubxn7 binding to replisome and regulate p97 and Cul2 activity.

To confirm this result, we re-analysed the immunoprecipitated p97 sample from S phase chromatin (Figure 3.10.b) by blotting with Cul2 antibody. p97 immunoprecipitation from chromatin also did not co-precipitate Cul2, while there was co-precipitation of Ubxn7 (Figure 3.17.b.).

3.2.2.6. Immunodepletion of Ubxn7 from egg extract postpones replisome unloading from chromatin

The results presented above suggest that Ubxn7 interacts with Cul2 and p97 for stimulation of CMG disassembly during replication termination. To address this hypothesis, I wanted to analyse the requirement for Ubxn7 for DNA replication and replisome disassembly. Moreover, we would like to understand whether Ubxn7 is needed for Cul2 and p97 binding to chromatin during replication termination. In order to do this, I immunodepleted Ubxn7 from *Xenopus laevis* egg extract using affinity purified polyclonal Ubxn7 antibodies (described above in 2.3.4.2.). In order to efficiently immunodeplete Ubxn7 from the extract, I performed two rounds of 45-minute incubations with Dynabeads coupled to the purified Ubxn7 antibodies. Alongside this, I used a non-specific IgG antibody coupled to Dynabeads with the same incubation protocol, for use as a negative control (mock) (Figure 3.18.a.).

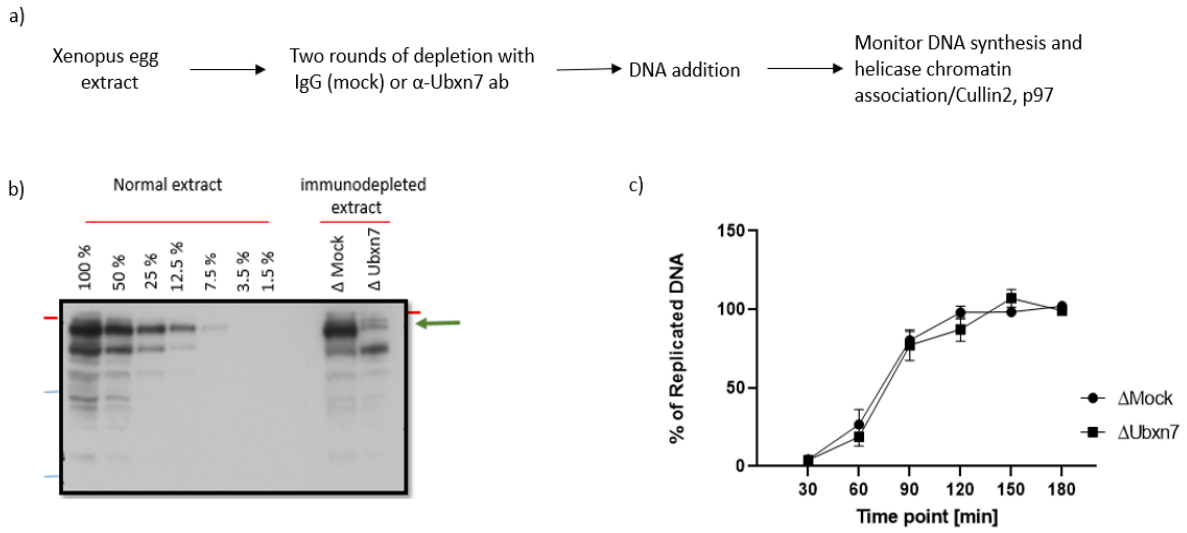

Figure 3. 18 Immunodepletion of Ubxn7 from Xenopus egg extract does not inhibit DNA replication. a) The scheme shows Ubxn7 or mock immunodepletion from egg extract using non-specific IgG or purified Ubxn7 antibodies. b) Ubxn7 is immunodepleted from the egg extract. Mock or Ubxn7 depleted extracts were analysed by western blotting using Ubxn7 antibody. c) Interphase mock and Ubxn7 depleted extracts were supplemented with demembranated sperm nuclei and α-[P32] dATP, and DNA synthesis was monitored at indicated time points by measuring incorporation of radiolabelled nucleotides into newly synthesised DNA. The mean level of replication in mock and Ubxn7 depleted extract of the five experiments in independent extracts was averaged with standard error of the mean (SEM). For each experiment the highest number of ng/ul of replicated nascent DNA was set as 100% of replication in the experiment and other values normalise to that point.

When we compare normal and mock depleted extract with Ubxn7 depleted extract, It could clearly be seen that Ubxn7 was immunodepleted, with less than 10% of Ubxn7 remaining in the extract

comparing to the serial dilution of normal extract (Figure 3.18.b.). Depletion of Ubxn7 from the extract does not affect the ability of the extract to complete the bulk of DNA synthesis, as the graphs of accumulation of nascent DNA in ΔMock and ΔUbxn7 extract do not differ (Figure 3.18.d.).

I next wanted to test whether immunodepletion of Ubxn7 affects unloading of terminated replisomes from chromatin and chromatin interaction of $Cul2^{Lrr1}$ and p97. Replicating chromatin in mock or Ubxn7 immunodepleted extract was isolated during the replication reaction at indicated time points after adding DNA and analysed by western blotting using the indicated antibodies (Figure 3.19.a.).
In mock depleted extract we observed that Cdc45 and Psf2 started binding DNA at 45 minutes, peaked at 60 minutes and were being unloaded from chromatin after 90 minutes. As expected, p97, Ubxn7 and Cul2 are seen on the chromatin when the majority of replication is taking place (Figure 3.19.a.).

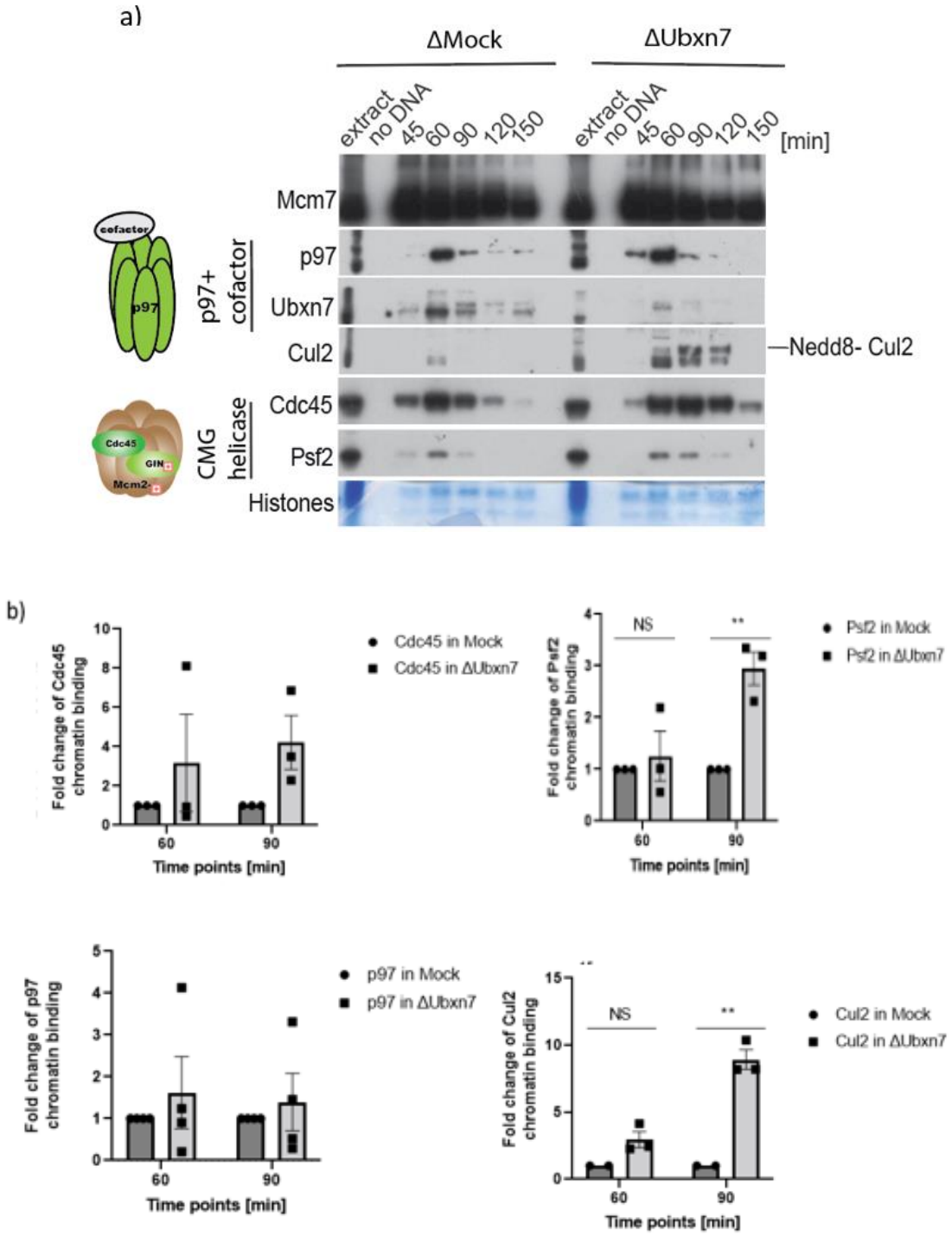

Figure 3. 19 Replisome disassembly was delayed in the absence of Ubxn7 in the extract. (a) Mock and Ubxn7 depleted extracts were supplemented with demembranated sperm nuclei. Chromatin was isolated at indicated time points after DNA addition and association of CMG components, p97 and Cul2 monitored by western blotting using the indicated antibodies. This experiment represents one of four biological repeats. b) The level of western blot signal of Cdc45, Psf2, p97 and Cul2 at indicates time points were quantified in three independent experiments performed in three Ubxn7 immunodepleted extracts. The average fold change of was quantified with SEM. Statistical analysis through Multiple T Test. P value *<0.05, **<0.005, ***<0.0005

In Ubxn7 depleted extract the chromatin-bound Ubxn7 protein levels were much reduced compared with the mock control extract as expected. I did see a delay in the chromatin disassembly of CMG components in Ubxn7 depleted extract in comparison to the mock-depleted extract (Figure 3.19.a.). We did observe that replication started slightly later (lower signal at 45 min of Cdc45 and Psf2) and unloading of the replisome shifted to 120 minutes in the Ubxn7 depleted extract. Interestingly, we could see considerably higher levels of Cul2 on the chromatin after immunodepletion of Ubxn7 in the extract (Figure 3.19.a. and 3.19.b.). Importantly most of this chromatin bound Cul2 was in its active neddylated form (higher band on Cul2 blot).

I measured levels of Cdc45, Psf2, Cul2 and p97 in four independent experiments by Image J and plotted as graphs of signal. Normalized to loading control and compared to buffer control. I chose to quantify them at 60 minutes as this is at the peak of replication and represents active replication forks, and 90 minutes because the bulk of DNA synthesis is finished by then in mock depletion (Figure 3.19.b.) and the remaining CMGs on chromatin should be mostly terminated by this point (Figure 3.19.b.).

These results suggest therefore that Ubxn7 is not necessary for replisome unloading but regulates the efficiency of this process. We cannot, however, exclude the possibility that the level of depletion of Ubxn7 in our extract is not sufficient and the remaining Ubxn7 slowly provides its activity. Interestingly, not having Ubxn7 can stimulate chromatin binding and activity of Cul2. Ubxn7 was suggested as a negative regulator of $Cul2^{VHL}$ in regulation of Hif1α degradation (Bandau, Knebel et al. 2012) and may act similarly here. The increased activity of $Cul2^{Lrr1}$ could compensate for not having Ubxn7 to bridge with p97 as longer chains on ubiquitylated Mcm7 could more efficiently attract p97 to extract it (Deegan, Mukherjee et al. 2020).

3.2.2.7. Ubxn7 is needed for efficient replisome disassembly

In order to confirm that observed phenotypes of Ubxn7 depletion were due to the absence of Ubxn7 and not co-immunodepletion of an unrelated factor, I aimed to rescue these phenotypes by adding back recombinant *Xenopus* Ubxn7. I first had to characterise the amount of recombinant protein, which should be added back to the extract, so that it rescues the endogenous levels and does not disrupt DNA replication. I added Ubxn7 to the normal extract at different concentrations and tested the levels by western blot using Ubxn7 antibodies. The extract sample without adding any recombinant protein showed endogenous Ubxn7 protein level. The recombinant Ubxn7 contains only additional 6His tag so it is of a very similar size to the endogenous protein. Based on the blot in Figure

3.20.a. we can estimate that the amount of endogenous Ubxn7 protein in the extract is less than 0.06 mg/ml, most likely about 20 µg/ml. I tested therefore addition of 0.06 mg/ml of recombinant Ubxn7 protein (a bit higher level than endogenous) to confirm that it will not affect DNA replication reaction in the extract on its own. We observed that the extracts to which we added 0.06 mg/ml of the recombinant Ubxn7 protein could efficiently support DNA replication.

Mock and Ubxn7 depleted egg extracts were supplemented with sperm DNA and either LFB1/50 buffer (Ubxn7 protein was dialyzed into this buffer) or recombinant Ubxn7 were optionally added to the extract. Chromatin was isolated at 100 minutes after sperm DNA addition when CMG helicase should already be removed in mock depleted extract, while it should stay on chromatin in Ubxn7 depleted extract (based on Figure 3.19) and analysed by western blotting using the indicated antibodies (Figure 3.20.c). Under such conditions, in mock-depleted extract Cdc45 and Psf2 no longer interacted with chromatin with or without addition of recombinant Ubxn7 (lane 1 and 2 in Figure 3.20.c). However, as seen before, they remained chromatin bound in Ubxn7 depleted extract (lane 3 in Figure 3.20.c.), while adding back recombinant Ubxn7 led to a successful rescue in restoring efficient CMG removal from chromatin (lane 4 in Figure 3.19c, Cdc45 and Psf2). This confirms that Ubxn7 is required for efficient disassembly of replisome during DNA replication termination.

As we noticed before (Figure 3.19. a. and 3.19.c.), Cul2 binding on chromatin is much higher in the Ubxn7 depleted extract in comparison to the mock depleted extract. Importantly, reproducibly, we observed that neddylated Cul2 accumulated on chromatin in Ubxn7 depleted extract, while adding back Ubxn7 to the Ubxn7 depleted extract abrogated this accumulation (Figure 3.20.c.). Three different experiments reproducibly suggest that when there is less Ubxn7 available, chromatin-bound Cul2 binds chromatin at higher level in its neddylated, active form. This supports the hypothesis that Ubxn7 has a role in negatively regulating Cul2 (Bandau, Knebel et al. 2012).

a)

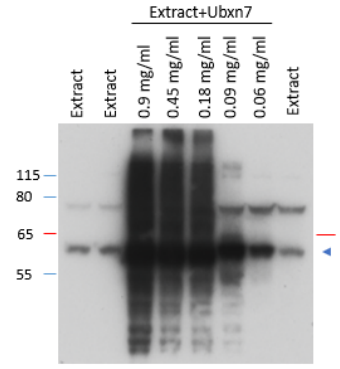
Extract+Ubxn7
Extract
Extract
0.9 mg/ml
0.45 mg/ml
0.18 mg/ml
0.09 mg/ml
0.06 mg/ml
Extract
115
80
65
55

b)

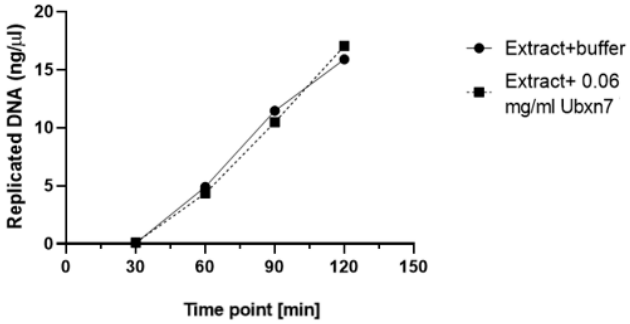
Replicated DNA (ng/µl)
20
15
10
5
0
0
30
60
90
120
150
Time point [min]
Extract+buffer
Extract+ 0.06 mg/ml Ubxn7

c)

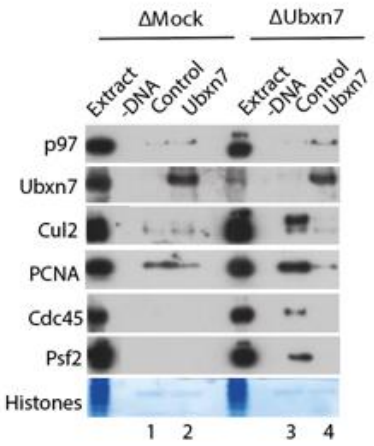
ΔMock
ΔUbxn7
Extract
-DNA
Control
Ubxn7
Extract
-DNA
Control
Ubxn7
p97
Ubxn7
Cul2
PCNA
Cdc45
Psf2
Histones
1
2
3
4

d)

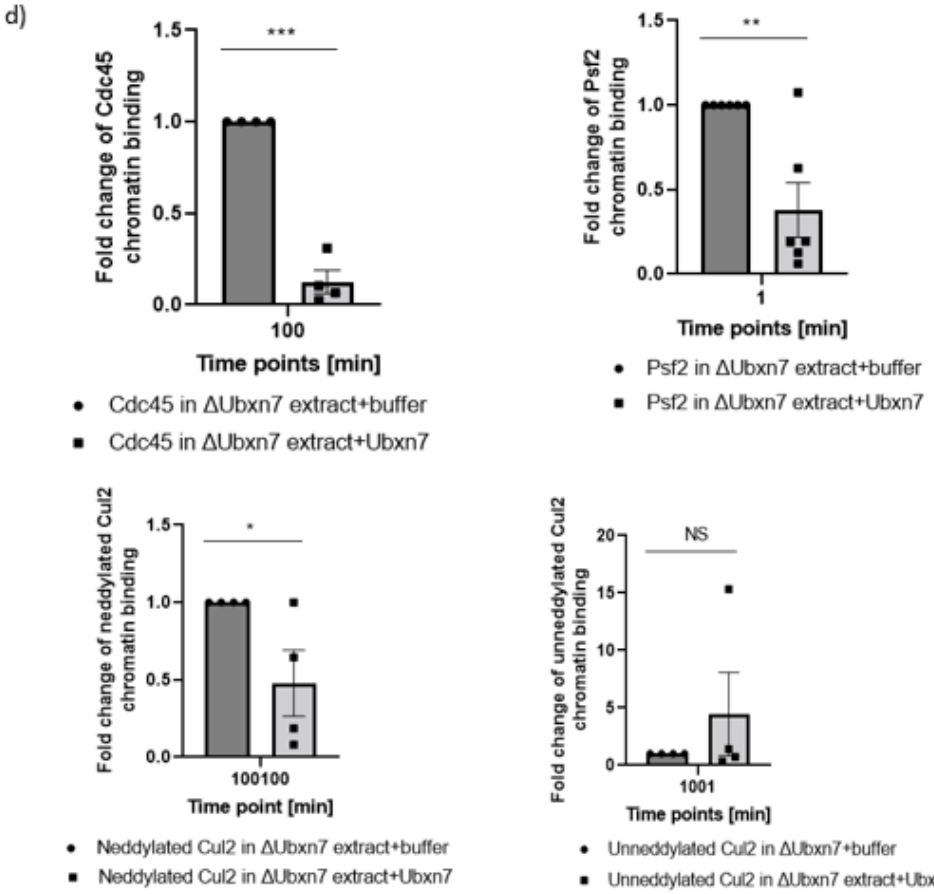
Fold change of Cdc45 chromatin binding
1.5
1.0
0.5
0.0
***
100
Time points [min]
Cdc45 in ΔUbxn7 extract+buffer
Cdc45 in ΔUbxn7 extract+Ubxn7
Fold change of Psf2 chromatin binding
1.5
1.0
0.5
0.0
**
1
Time points [min]
Psf2 in ΔUbxn7 extract+buffer
Psf2 in ΔUbxn7 extract+Ubxn7
Fold change of neddylated Cul2 chromatin binding
1.5
1.0
0.5
0.0
*
100100
Time point [min]
Neddylated Cul2 in ΔUbxn7 extract+buffer
Neddylated Cul2 in ΔUbxn7 extract+Ubxn7
Fold change of unneddylated Cul2 chromatin binding
20
15
10
5
0
NS
1001
Time points [min]
Unneddylated Cul2 in ΔUbxn7+buffer
Unneddylated Cul2 in ΔUbxn7 extract+Ubxn7

Figure 3. 20 Addition of recombinant Ubxn7 protein to the ΔUbxn7 extract can rescue efficient CMG unloading and Cul2 chromatin levels. a) Different concentrations of recombinant purified Ubxn7 protein were added to the extract and analysed by western blotting with Ubxn7 antibody. b) Interphase egg extracts were supplemented with demembranated sperm nuclei, α-[P32]dATP and optionally with LFB1/50 buffer or recombinant Ubxn7 protein. DNA synthesis was monitored at indicated time points by measuring incorporation of radiolabelled nucleotides into newly synthesised DNA. c) Mock and Ubxn7 depleted extracts were supplemented with demembranated sperm nuclei and LFB1/50 buffer or Ubxn7 were added optionally. Chromatin was isolated at 100 minutes after DNA addition and monitored by western blotting using the indicated antibodies. The experiment represents one of three biological repeats. d) The average fold change of Cdc45, Psf2, p97, neddylated and unneddylated Cul2 at 100 minutes quantified with SEM. Statistical analysis have done with Multiple T Test. P value *<0.05, **<0.005, ***<0.0005

3.2.2.8. Separation of interaction mutants of Ubxn7

3.2.2.8.1. Purification of recombinant Ubxn7 mutants

We wanted next to generate mutants of Ubxn7 that will inhibit its ability to interact with either p97 or Cul2, as we would like to test whether they are able to rescue phenotypes in immunodepleted extracts and thus determine the mechanism by which Ubxn7 acts during replisome disassembly in S phase. Ubxn7-P458G point mutation in UBX domain blocks the interaction with p97 and Ubxn7, while L286E/A289Q/S293A Ubxn7 has mutated UIM domain to abolish the interaction with $Cul2^{Lrr1}$ as described before in human cells (Bandau, Knebel et al. 2012, Abbas, Keaton et al. 2013). *Xenopus laevis* Ubxn7 protein (488 amino acids) has a high level of similarity with *Homo sapiens* Ubxn7 (489 amino acids). The amino acids mutated previously in human Ubxn7 studies are conserved in the *Xenopus* sequence but have a slightly different number: mutation of UIM is 282E, 285Q and 289A and mutation of UBX is P458 (Figure 3.21.b.).

pET28 plasmids containing these mutants (poly-histidine tagged) were transformed into BL21 *E.coli* strain. Large cultures of BL21 bacterial cells containing *Xenopus* HIS-Ubxn7-P458G and HIS-Ubxn7-L282E/A285Q/S289A expression plasmids were grown. The proteins expressed in bacteria were then purified using nickel beads, as explained in section 2.3.3.2. The success of the purification was determined by analysing samples on an SDS-PAGE gel stained with Coomassie (Figure 3.21.c and 3.21.d.). Elution 2 from each protein contained the highest concentration of protein and was dialysed into LFB1/50 buffer. The concentration of HIS-Ubxn7-P458G and HIS-Ubxn7-L282E/A285Q/S289A was quantified by comparison to BSA standard on the gel and resulted in final concentrations of 13.5 mg/ml and 7.5 mg/ml, respectively (Figure 3.21.e.)

a)

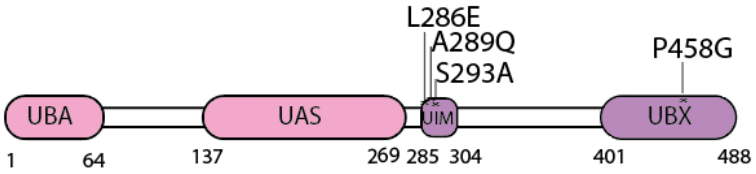

b)

```
x.l.|Q6NTX4|Q6NTX4_XENLA    MEKDGG-----VSQQLLREFTAITGATDSVAKHMLEACNHNLEMAVTMFLDGGGIPDEPS    55
h.s.|O94888|UBXN7_HUMAN     MAAHGGSAASSALKGLIQQFTTITGASESVGKHMLEACNNNLEMAVTMFLDGGGIAEEPS    60
                            *  .**     . : *:::**:****::**.********:*************** :***

x.l.|Q6NTX4|Q6NTX4_XENLA    TSSAGSSTARPAPDLSDDVRAPIPQKQEILVEPE-IFGAPKRRRPARSIFDGFRDFQTET    114
h.s.|O94888|UBXN7_HUMAN     TSSASVSTVRP--HTEEEVRAPIPQKQEILVEPEPLFGAPKRRRPARSIFDGFRDFQTET    118
                            ****. **.**  . .::*************** :************************

x.l.|Q6NTX4|Q6NTX4_XENLA    IRQEQELRNGGAVDKKLTTLADLFRPPIDLMHKGSFETAKQFGQLHNKWLMINIQNVQDF    174
h.s.|O94888|UBXN7_HUMAN     IRQEQELRNGGAIDKKLTTLADLFRPPIDLMHKGSFETAKECGQMQNKWLMINIQNVQDF    178
                            ***********:*************************: **::***************

x.l.|Q6NTX4|Q6NTX4_XENLA    ACQCLNRDIWSNDAIKTLIREHFIFWQVYHDSEEGQRYIQFYKLPEFPYVSILDPRTGQK    234
h.s.|O94888|UBXN7_HUMAN     ACQCLNRDVWSNEAVKNIIREHFIFWQVYHDSEEGQRYIQFYKLGDFPYVSILDPRTGQK    238
                            ********:***:*:*.:************************ :***************

x.l.|Q6NTX4|Q6NTX4_XENLA    LVEWHKLDPNSFVEQVTGFLGEMGQLDGLSSSPPKKRLRSESLIDASEDSQLEAAIRASL    294
h.s.|O94888|UBXN7_HUMAN     LVEWHQLDVSSFLDQVTGFLGEMGQLDGLSSSPPKKCARSESLIDASEDSQLEAAIRASL    298
                            *****:** .**::***********************  **********************

x.l.|Q6NTX4|Q6NTX4_XENLA    QETHFDSAVNKETPRREEESESELYSGSEEFISVCGSDHEEDEERPVIESSAEPDSCGKS    354
h.s.|O94888|UBXN7_HUMAN     QETHFDSTQTKQDSRSDEESESELFSGSEEFISVCGSDEEEEVENLA-----------KS    347
                            *******: .*:  * :*******:*************.**: *. .           **

x.l.|Q6NTX4|Q6NTX4_XENLA    KKSTSKDPNHRKEEVGRTH--PVVVEE---TSNHQSPE---DTASSEEHHRESGCSVAVS    406
h.s.|O94888|UBXN7_HUMAN     RKSPHKDLGHRKEENRRPLTEPPVRTDPGTATNHQGLPAVDSEILEMPPEKADGVVEGID    407
                            :**  ** .***** *    * * :  ::***.     .  .  .: .*   .:.

x.l.|Q6NTX4|Q6NTX4_XENLA    DNGPKAKLMLRYPDGKKEQIALPEQAKLLALVRHVQLKGYPNERFELLTNFPRRKLSHLD    466
h.s.|O94888|UBXN7_HUMAN     VNGPKAQLMLRYPDGKREQITLPEQAKLLALVKHVQSKGYPNERFELLTNFPRRKLSHLD    467
                             *****:*********:***:***********:*** ************************

x.l.|Q6NTX4|Q6NTX4_XENLA    YDVTLQEAGLCPQETVFVQERN    488
h.s.|O94888|UBXN7_HUMAN     YDITLQEAGLCPQETVFVQERN    489
                            **:********************
```

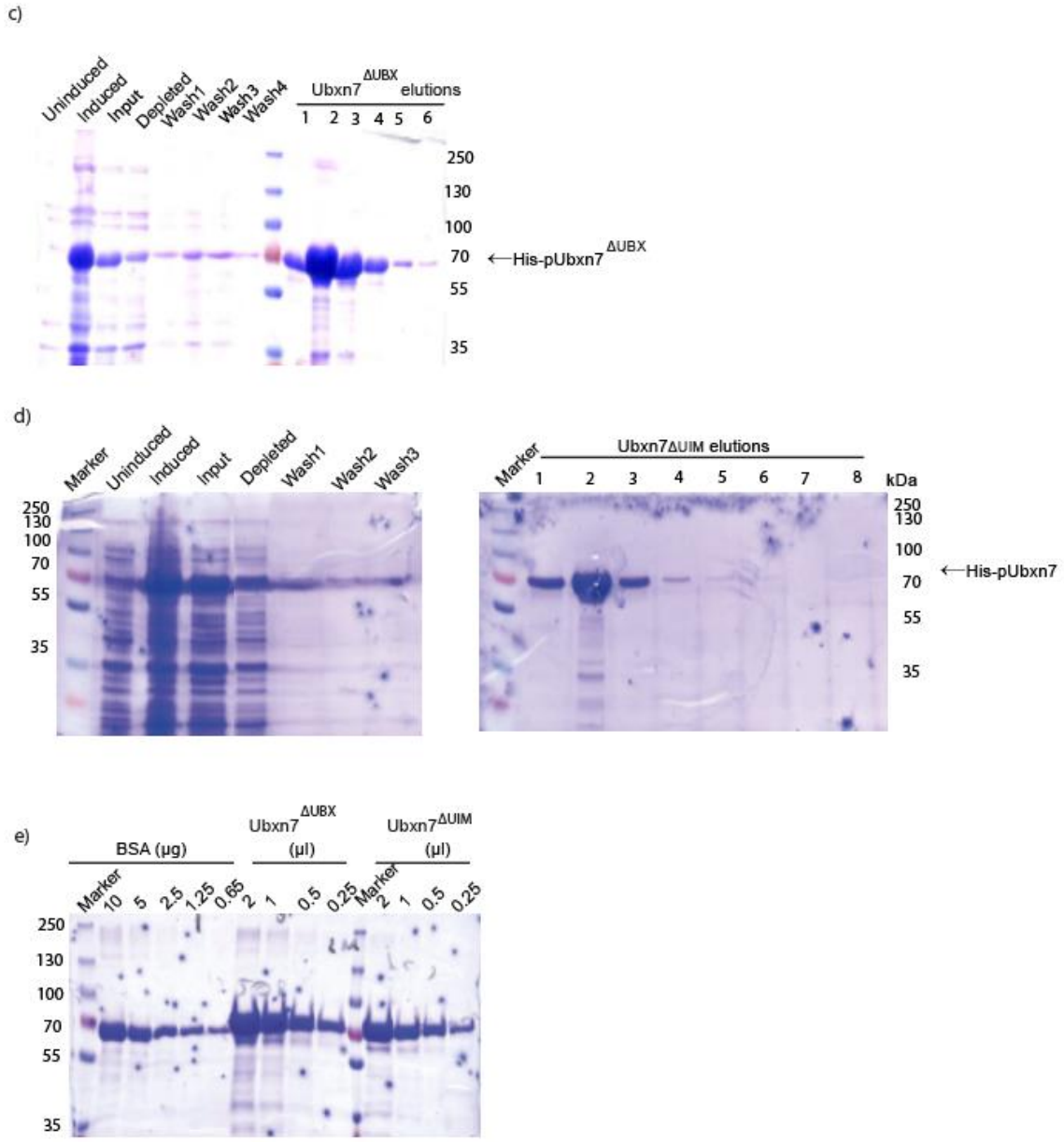

Figure 3. 21 The recombinant X. laevis His-tagged Ubxn7-P458G (Ubxn7$^{\Delta UBX}$) and Ubxn7-L282E/A285Q/S289A (Ubxn7$^{\Delta UIM}$) proteins were purified. a) Model of Ubnx7 with various domains and indicated mutations disrupting particular activities in human protein**.** b) Xenopus laevis and human Ubxn7 protein sequence was compared. Red colour represents UBA domain, green colour is UAS domain, purple colour is UIM domain and blue colour is UBX domain. c) His-Ubxn7-P458G was expressed in BL21 E.coli cells. His-tagged protein was then purified using nickel beads and samples from purification protocol were resolved by SDS-PAGE prior to staining with Coomassie. d) As in b) but His-Ubxn7-L282E/A285Q/S289A was purified. e) The quantification of the purified proteins by BSA standard gel.

3.2.2.9. Ubxn7 interacts with p97 through UBX domain

Having purified Ubxn7 mutants that should specifically disrupt one of the two key interactions of Ubxn7, I wanted next to confirm whether Ubxn7 interacts with p97 through its UBX domain and associate with Cul2 *via* its UIM domain, as predicted from previous studies (Bandau, Knebel et al. 2012). As I have shown in Figure 3.16, Ubxn7 interacts in egg extract (whole cell extract) with p97 but not with Cul2, while interaction with Cul2 is observed only on chromatin.

In order to examine the ability of different mutants of Ubxn7 to interact with p97, I have taken advantage of the fact that recombinant Ubxn7 proteins are tagged with six consecutive histidine residues (6His tag) that can be pulled down by Nickel Magnetic Beads. To be able to compete with endogenous Ubxn7, I supplemented *Xenopus* extract with a higher concentration of recombinant Ubxn7 proteins than in rescue experiments. Egg extract was supplemented with sperm DNA and optionally with buffer (negative control), Ubxn7^{wt} (positive control), Ubxn7$^{\Delta UBX}$ mutant or Ubxn7$^{\Delta UIM}$ mutant. After most of the replication reaction had been completed (60 min), the extract was incubated with HIS-pull down dynabeads. The precipitated material was then analysed by western blot using anti-HIS and anti-p97 antibodies. We did not blot for Cul2, as Ubxn7 does not interact with Cul2 in the *X. laevis* egg extract (Figure 3.16.a.).

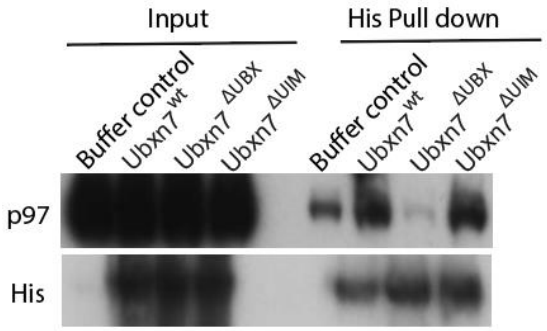

Figure 3. 22 Ubxn7 interacts with p97 in the extract through its UBX domain. a) Interphase extract was supplemented with demembranated sperm nuclei and optionally with LFB1/50, 0.3 mg/ml Ubxn7^{wt}, Ubxn7$^{\Delta UBX}$ or Ubxn7$^{\Delta UIM}$. HIS pull down dynabeads were incubated with the extract in late S-phase (60 min). The precipitated material was then analysed by western blot using anti-HIS and anti-p97 antibodies.

We blotted the samples with HIS antibody to detect the pulled-down HIS-tagged Ubxn7 recombinant proteins – in all three samples containing recombinant protein added there was a similar level of

protein pulled-down on the beads. I could see that p97 was enriched in the sample containing wild type Ubxn7 and in Ubxn7$^{\Delta UIM}$ mutant. Most importantly, we observed that p97 interaction with Ubxn7$^{\Delta UBX}$ mutant was inhibited, which indicates that Ubxn7 interacts with p97 through its UBX domain in the *X.laevis* egg extract (Figure 3.22). Unfortunately, I have run out of the time to test whether Ubxn7$^{\Delta UIM}$ mutation will abolish interaction of Ubxn7 with Cul2 on chromatin.

3.2.2.10. Adding recombinant Ubxn7 mutants to extract to compete with endogenous Ubxn7

In order to characterise further the importance of Ubxn7's interactions with Cul2 and p97, I decided to add purified recombinant Ubxn7 mutants to *X.laevis* egg extract to compete with endogenous Ubxn7. The concentration of endogenous Ubxn7 in the extract is less than 0.06 mg/ml as shown before in Figure 3.20.a. I wanted therefore to add a larger amount of the Ubxn7 mutants. I tested DNA replication kinetics of the extract with different high concentrations of Ubxn7^{wt} (0.23 mg/ml, 0.3 mg/ml or 0.43 mg/ml) at two different time points to see if it affects replication (Figure 3. 23. a.). My result suggests that a high concentration of Ubxn7 does not affect replication. Therefore, I chose a mid-range concentration (0.3 mg/ml) and assessed that adding Ubxn7 mutants at that concentration also does not affect replication. DNA synthesis of the extract was not significantly affected by addition of this concentration (0.3 mg/ml) of either Ubxn7^{wt}, Ubxn7$^{\Delta UBX}$ or Ubxn7$^{\Delta UIM}$ proteins, as seen by the incorporation of radioactive nucleotides into nascent DNA (Figure 3.23.b.).

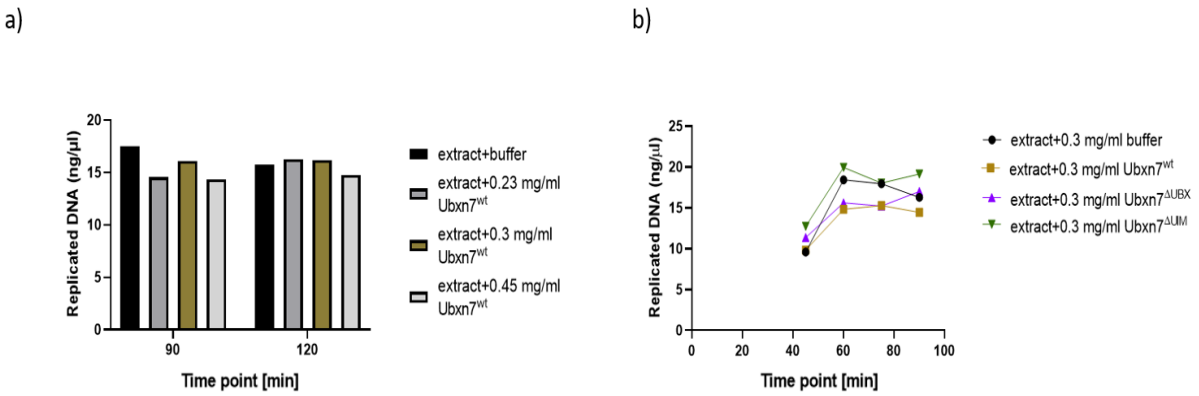

Figure 3. 23 Addition of high concentration of recombinant Ubxn7 does not inhibit progression of DNA replication. a) The extracts were supplemented with demembranated sperm nuclei and optionally: LFB1/50 or different concentrations of Ubxn7^{wt}. Then α-[P32]dATP was added and DNA synthesis was monitored at two time points by measuring the incorporation of radiolabelled nucleotides into the nascent DNA. The experiment was repeated twice. b) Optionally, LFB1/50 or 0.3 mg/ml of recombinant Ubxn7 proteins were added to the extract with sperm DNA and α-[P32]dATP. DNA replication was monitored at indicated time points by measuring the incorporation of radiolabelled nucleotides into newly synthesised DNA. The experiment carried out once.

Knowing that addition of Ubxn7^{wt} and mutant recombinant proteins at high concentration does not affect the bulk of DNA synthesis in the extract (Figure 3.23.b), I wanted to test if they affect replisome disassembly and chromatin binding of p97 and Cul2^{Lrr1}. Following sperm DNA addition to interphase egg extract, LFB1/50 buffer, Ubxn7^{wt}, Ubxn7$^{\Delta UBX}$ or Ubxn7$^{\Delta UIM}$ were added optionally to the reaction. Chromatin was isolated at indicated time points during the replication reaction and samples analysed by western blotting using the indicated antibodies (Figure 3.23).

Adding a high concentration of Ubxn7 recombinant proteins led to a much higher level of Ubxn7 on chromatin, both the wild type but also mutants, suggesting that both mutants can still interact with the chromatin. The "no DNA" sample was isolated in parallel to chromatin samples from extract containing recombinant Ubxn7 proteins and indicates that the bands present in chromatin samples are not just precipitated recombinant protein. Nevertheless, in the presence of all recombinant Ubxn7 proteins, Cdc45 was still efficiently removed from chromatin.

Ubxn7$^{\Delta UIM}$ mutant should disrupt the interaction between Ubxn7 and Cul2, while not disrupting p97 interaction. I have previously shown that immunodepletion of Ubxn7 leads to a very prominent accumulation of Cul2 on chromatin in its neddylated active form (Figure 3.19.a.). We confirmed this data upon addition of a high concentration of recombinant Ubxn7$^{\Delta UIM}$ mutant to normal egg extract, mimicking overexpression experiments. The addition of Ubxn7$^{\Delta UIM}$ to the replication reaction lead to accumulation of Cul2 on chromatin (Figure 3.24.a). To analyse Cul2 binding to chromatin upon addition of a high concentration of Ubxn7 mutants, I measured levels of Cul2 accumulated on chromatin at 45 min in three independent experiments with Image J and plotted graphs of signal (Figure 3.24.b). Addition of Ubxn7 wt protein resulted in the lowest amount of Cul2 binding to chromatin, suggesting that high level of Ubxn7 leads to high turnover of Cul2 on chromatin. To analyse specifically neddylated Cul2, I measured the top band of the Cul2 blot on its own, which is neddylated form of Cul2. Only two experiments were quantified in this case as the neddylated and unneddylated bands of Cul2 were not resolved and separated enough in the third experiment. In conclusion, we observed that when Ubxn7 cannot interact with Cul2^{Lrr1} upon addition of the Ubxn7$^{\Delta UIM}$ mutant, levels of Cul2 and especially the neddylated Cul2^{Lrr1} increase on chromatin (Figure 3.24.a and 3.24.b).

Interestingly, mutation of the UBX domain in Ubxn7, which disrupts its interaction with p97 reproducibly led to less binding of p97 to the chromatin (Figure 3.23.a). Moreover, p97 bind similarly on chromatin when there are more Ubxn7$^{\Delta UBX}$ mutant or more Ubxn7$^{\Delta UIM}$ mutant, supports our hypothesis that Ubxn7 along with Cul2 brings p97 to the chromatin, as we could see before (Figure 3.15.a).

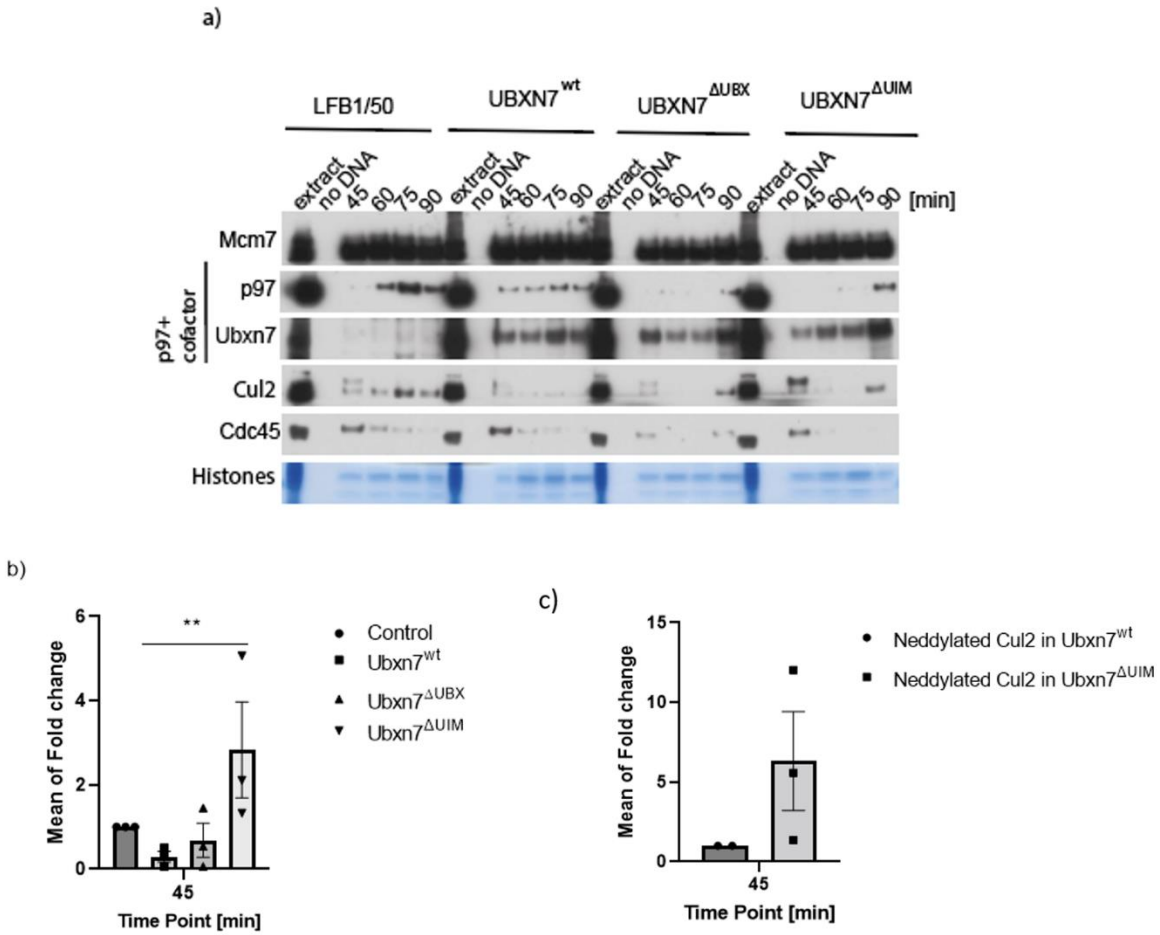

Figure 3. 24 Neddylated Cul2^{Lrr1} increased on chromatin when high concentration of Ubxn7$^{\Delta UIM}$ mutant was added to the replication reaction. a) Interphase egg extract was supplemented with demembranated sperm nuclei and optionally: LFB1/50 buffer, 0.3 mg/ml Ubxn7^{wt}, Ubxn7$^{\Delta UBX}$ or Ubxn7$^{\Delta UIM}$. Chromatin was isolated at indicated time after DNA addition and analysed by western blotting using the indicated antibodies. b) Cul2 density was quantified by Image J in three independent experiments performed in different extracts, the average fold change of Cul2 at 45 min quantified with SEM. Multiple T Test used for statistical analysis. ***<0.005 c) Neddylated Cul2 density was quantified using Image J in two biological repeats performed in different extracts. The average fold change of Neddylated Cul2 at 45 min quantified.

3.2.3. Discussion

3.2.3.1. Ubxn7 binds chromatin during replisome disassembly

It is known that the CMG helicase is ubiquitylated by $Cul2^{Lrr1}$ and extracted from chromatin by the p97 remodeller in *Caenorhabditis elegans (Sonneville, Moreno et al. 2017), Xenopus laevis* (Dewar, Low et al. 2017, Sonneville, Moreno et al. 2017) and in mouse embryonic stem cells (Villa, Fujisawa et al. 2021). However, the mechanism of p97 recruitment to the chromatin at the end of DNA replication is not yet known. In the previous chapter, we found that polyubiquitylation of chromatin substrates is not necessary for recruitment of p97 to chromatin during DNA replication. Instead, it seems that the p97-Ufd1/Npl4 core complex is recruited to chromatin for CMG helicase unloading by cofactors rather than direct binding to polyubiquitylated substrates. Based on our mass spectrometry result, Ubxn7 and Faf1 might be the possible cofactors that regulate p97 activity during replication termination. Ubxn7 especially may be an important cofactor playing a role in CMG disassembly, providing a link between Cul2, p97 and ubiquitylated substrate, based on its role in Hif1α degradation (Alexandru, Graumann et al. 2008, Bandau, Knebel et al. 2012).

To start analysing the role of Ubxn7 in DNA replication termination we first checked that Ubxn7 cofactor binds to chromatin during DNA replication, especially at the termination stage, using the chromatin isolation experiment. The pattern of Ubxn7 binding resembles that of p97: it is increased upon p97 activity inhibition, decreased upon inhibition of Cullin activity and slightly increased upon inhibition of polyubiquitylation with Ubi-NOK. Ubxn7 chromatin interaction may be therefore regulated by p97 chromatin binding or *vice versa*, p97 may be recruited to chromatin by Ubxn7.

Bandau et al., 2012, had shown that Ubxn7 exclusively interacts with neddylated Cul2 in the cell lysate (Bandau, Knebel et al. 2012). Mutants of two Cullin proteins (Cul1 and Cul2), which cannot be neddylated, show minimal binding to Ubxn7 (den Besten, Verma et al. 2012). The NEDD8-E1 inhibitor MLN4924 causes de-neddylation of Cul2 and so Ubxn7 cannot bind it (den Besten, Verma et al. 2012). Furthermore, Emberley et al., 2012, shown that Ubxn7 interaction with Cul2 prevents Cul2 de-neddylation by CSN (Emberley, Mosadeghi et al. 2012). These observations strongly support the conclusion that Ubxn7 can interact only with active, neddylated Cul2 and it is tempting to speculate that Ubxn7 may recruit p97 through its interaction with neddylated Cullin2. However, chromatin binding of p97 may not represent binding only to the replisome, as there may be other substrates on chromatin for p97. Therefore, it is important to confirm this pattern of interactions with chromatin through IPs with replisome. However, I have run out of time to complete these experiments.

3.2.3.2. Ubxn7 interacts with Cul2 on chromatin

To validate whether Cul2 interaction with p97 is dependent on Ubxn7, we first showed that Ubxn7 interacts with p97, Ufd1 and Npl4 but not with Cul2 in the extract, as we expected, due to the fact that Ubxn7 associates only with neddylated, active Cul2. Cul2 in whole cell extract is stable in a de-neddylated form (Emberley, Mosadeghi et al. 2012) and becomes neddylated and active in order to polyubiquitylate CMG terminated helicase during replication termination. Indeed, immunoprecipitation of Ubxn7 from late S-phase chromatin revealed interaction with Cul2 and p97 (Figure 3.16.b). This data thus supports the idea that Ubxn7 can link p97 only with active Cul2 on chromatin as in the case of Hif1α degradation (Bandau, Knebel et al. 2012).

I immunoprecipitated also Cul2 from chromatin with accumulated terminated replisomes and confirmed that Cul2 interacts with CMG helicase on the chromatin as shown before (Sonneville, Moreno et al. 2017). However, while Cul2 interacts with Ubxn7 on chromatin, it does not interact with p97 (Figure 3.18.a.). In order to understand this interaction in more detail, we also re-analysed p97 IP from chromatin. Importantly, we could show that p97 can interact with Ubxn7 on chromatin but cannot co-precipitate Cul2 as in Cul2 IP.

This data can be explained in one of two ways: firstly, Ubxn7 interacts individually with Cul2 and p97, so there are two different pools of complexes formed on chromatin; secondly, Ubxn7, p97 and Cul2 are interacting together in one complex but p97 and Cul2 do not directly interact as Ubxn7 is placed between them. This complex may be dynamic and not very stable in the conditions of the immunoprecipitation, therefore, when we pull down Cul2 we are not able to co-precipitate p97 and *vice versa* (Figure 3.17.c). We used 300 mM KAc salt concentration when preparing input for Cul2 immunoprecipitation and 100 mM KAc in p97 chromatin lysis buffer, to retain solubility of protein complexes released from chromatin. It is possible that p97 interactions are salt sensitive. Indeed, Besche et al., 2009, revealed that 150 mM NaCl in the buffer reduced the interaction between the RAD23 (DNA damage sensor protein) UBL domain and p97 (Besche, Haas et al. 2009). Besides this, p97 was shown to interact with ubiquitin conjugated proteins through UIM and UBL domain of its cofactors only in the absence of salt (Besche, Haas et al. 2009). Finally, 150 mM NaCl in the proteasome isolation buffer abolished proteasome interaction with p97 and its cofactors such as Ufd1, Npl4 and FAF1. This suggests that the correct ionic strength of the buffer may be essential for preserving the interactions between Ubxn7/Cul2 and p97. When we decrease salt concentrations of the buffer, we may have direct interactions between Cul2 and p97.

3.2.3.3. Ubxn7 deficiency leads to delay in disassembly of replisomes and accumulation of active Cul2 on chromatin

When we immunodepleted Ubxn7 in the *Xenopus* egg extract using our new antibodies, we determined that the lack of Ubxn7 does not affect the ability of extract to synthesise the bulk of nascent DNA. A control inhibitor that is known to block DNA replication was not used when we quantified the effect of Ubxn7 during DNA synthesis by using TCA replication assay. This technic, which is incorporation of radiolabelled nucleotide into nascent DNA during a time course, has been used previously to show blocking of DNA synthesis by replication drugs such as DNA polymerase inhibitor; aphidicolin or an inhibitor of DNA topoisomerase; camptothecin, (Moreno, Bailey et al. 2014, Moreno, Jones et al. 2019).

Despite a delay in unloading of replisome components, ubiquitylated Mcm7 and Cdc45 were still eventually unloaded from chromatin, suggesting that Ubxn7 is not essential for replisome disassembly at termination, but regulates the efficiency of unloading. However, we could not 100% deplete Ubxn7 and so even small amounts of Ubxn7 might enable its activity. Importantly, we could rescue the phenotype of delayed terminated helicase unloading in Ubxn7 depleted extract by adding recombinant Ubxn7 protein.

Interestingly, we observed much higher Cul2 binding on chromatin reproducibly in Ubxn7 depleted extract compared to the mock depleted extract. Critically, more neddylated Cul2 was observed in the Ubxn7 depleted extract, while adding back recombinant Ubxn7 to the Ubxn7 depleted extract led to more Cul2 protein in the unneddylated form. This supports the idea therefore, that Ubxn7 acts as a negative regulator of Cul2 and without Ubxn7, there is more active, neddylated Cul2 bound to the chromatin. It is possible therefore that lack of Ubxn7 is compensated for by an increased level of active Cul2 ligase accumulated on the chromatin. The accumulated Cul2, without the hindrance of Ubxn7, may be super active, build very long chains on Mcm7 and allow for subsequent unloading of the replisome. To support our data, the Labib's lab has recently explored that longer ubiquitin chains on Mcm7 increased the stability of p97 interaction and efficiency of replisome unloading (Deegan, Mukherjee et al. 2020).

Alexandru et al showed that upon p97 depletion in human cells, Ubxn7 association with Hif1α or Cullin2 did not dramatically change; however, Ubxn7 interaction with Ufd1/Npl4 is significantly reduced. It suggests that Ubxn7 binding to polyubiquitylated substrate and Cul2 is independent of p97-Ufd1/Npl4 (Bandau, Knebel et al. 2012). Depletion of Ubxn7 by siRNA had a negative effect on co-immunoprecipitation of p97 with ubiquitylated Hif1α and Cul2 (Alexandru, Graumann et al. 2008). In addition, it speculates that Hif1α does not interact with p97 in the absence of Ubxn7. On the contrary,

our results showed that the target substrate of Mcm7 in DNA replication is still ubiquitylated and disassembled from chromatin by p97 when Ubxn7 is depleted.

While p97 depletion in human cells leads to accumulation of Hif1α level, Ubxn7 depletion results in reduced levels of HIF1α. However, increased HIF1α levels was expected due to Ubxn7's role as a cofactor for p97. This suggested that Ubxn7's role in HIF1α regulation is complicated (Bandau, Knebel et al. 2012). Deshaies and colleagues suggested that Ubxn7 binding to Cul2 is inhibiting substrate ubiquitylation in yeast (Emberley, Mosadeghi et al. 2012). Moreover, Alexandru and colleagues revealed that overexpressed Ubxn7 in the cell caused accumulation of mostly non ubiquitylated Hif1-α and neddylated Cul2 in human cells (Bandau, Knebel et al. 2012). These observations are in agreement with our observation that Ubxn7 interaction with Cul2 negatively affects activity of chromatin bound Cul2. However, in contrast to these studies, we still do not know how Ubxn7 and Cul2 interaction affects substrate ubiquitylation. We could test whether Mcm7 is ubiquitylated with longer ubiquitin chains when Ubxn7 is depleted: we can supplement egg extract with His-tagged ubiquitin and pull-down ubiquitylated proteins under denaturing conditions in both mock and Ubxn7 depleted extract. Ubiquitin chain length on Mcm7 can then be analysed through western blotting.

In addition, the protein level of chromatin bound Cul2 did not change in the mock depleted extract with additional Ubxn7 added. This suggests that gentle overexpression of Ubxn7 did not change neither replisome disassembly nor binding of Cul2 on chromatin. However, adding wild type Ubxn7 at a high concentration to the normal extract leads to less Cul2 binding on chromatin (mentioned below). This is unlike in human cells as Bandau et al., 2012 (Bandau, Knebel et al. 2012) and Besten et al., 2012 (den Besten, Verma et al. 2012) showed that overexpression of Ubxn7 leads to increased levels of neddylated Cul2 in cells. It is most likely that high level of Ubxn7 in the extract leads to faster turnover of Cul2 on chromatin – Cul2 recognises and ubiquitylates Mcm7 and Ubxn7 brings p97 very quickly and efficiently leading to unloading of replisome and Cul2 from chromatin at faster paste.

3.2.3.4. Different domains of Ubxn7 have different roles

We wanted to understand better the importance of the interactions between Ubxn7, p97 and Cul2, and we generated mutations within the Ubxn7 protein to hinder these interactions and analyse their phenotypes in DNA replication. There are four different domains in Ubxn7: UBA, UAS, UIM, UBX (Bandau, Knebel et al. 2012, den Besten, Verma et al. 2012). I have purified Ubxn7-P458G protein (Alexandru, Graumann et al. 2008, Bandau, Knebel et al. 2012), which contains a single mutation within the UBX domain to block interactions with p97. Moreover, I have purified Ubxn7-

L282E/A285Q/S289A protein (Bandau, Knebel et al. 2012), which contains a triple mutation in the UIM domain to block the interaction with Cul2.

Recombinant His-tagged Ubxn7^{wt}, Ubxn7$^{\Delta UBX}$ or Ubxn7$^{\Delta UIM}$ mutant proteins were added to egg extract at high concentration to compete with endogenous Ubxn7 protein. Alexandru and colleagues (Alexandru, Graumann et al. 2008) presented in their data that Ubxn7 with mutated UBX domain not only failed to interact with p97 but also ubiquitylated substrates but was not affected in its binding to CRL. We confirmed that Ubxn7 could interact with p97 through its UBX domain in *Xenopus* egg extract (Figure 3.22).

Bandau et al. (Bandau, Knebel et al. 2012) in human cells and Besten et al. (den Besten, Verma et al. 2012) in yeast found that Ubxn7's (yeast ortholog Ubx5) ability to bind with Cul2 was lost upon depletion of the UIM domain. UIM domain of Ubxn7 detects ubiquitin *via* ubiquitin's hydrophobic surface (Hicke, Schubert et al. 2005). Sequences of Ubiquitin and NEDD8 are 60% identical (Kamitani, Kito et al. 1997). Besides this, the hydrophobic patch of ubiquitin, which interacts with ubiquitin binding domains, is the same in NEDD8 (Swanson, Kang et al. 2003). UIM domains are therefore able to interact with neddylated Cul2 due to the same hydrophobic patch on Nedd8 (Bandau, Knebel et al. 2012). We know that endogenous Ubxn7 does not interact with Cul2 in the *Xenopus* egg extract, therefore we did not test the interaction of the UIM mutant in the extract. Unfortunately, I also ran out of time to test the interaction between Cul2 and the Ubxn7 UIM mutant on chromatin.

3.2.3.5. Cul2 interaction with chromatin is dependent upon the UBXN7 UIM domain

We added 0.3 mg/ml recombinant Ubxn7 mutants to extract, which did not affect the ability of egg extract to replicate nascent DNA, to compete with endogenous Ubxn7 and tested the chromatin binding patterns of the proteins. We confirmed that all three recombinant Ubxn7 proteins could bind to the chromatin. In addition, Cdc45 was unloaded from chromatin in all conditions, suggesting none of the mutants strongly affected replisome disassembly. p97 interaction with chromatin was reduced however in the presence of the Ubxn7$^{\Delta UBX}$ mutant. As we know that Ubxn7 associates with p97 by its UBX domain (Alexandru, Graumann et al. 2008, Bandau, Knebel et al. 2012). Furthermore, p97 binding to chromatin was decreased upon addition with Ubxn7$^{\Delta UIM}$ mutant. Altogether, this is in agreement with our earlier theory that Ubxn7 and Cul2 recruit p97 to the chromatin. As seen in the Ubxn7 depleted extract, we revealed that neddylated Cul2 binding on the chromatin is reproducibly much higher in the presence of the Ubxn7$^{\Delta UIM}$ mutant. We therefore propose that Ubxn7, *via* its UIM domain, is a negative regulator protein of Cul2^{Lrr1} just like in case of Cul2^{VHL} (Alexandru, Graumann et al. 2008, den Besten, Verma et al. 2012). It will be important to confirm the interactions of variant

mutants with replisome and $Cul2^{Lrr1}$ through immunoprecipitation of endogenous Ubxn7 and to add them back to immunodepleted extract so that I can see fully their phenotype rather than seeing what they do on the background of endogenous Ubxn7 present in the egg extract.

In summary, the results in this chapter suggest that during replisome disassembly, $Cul2^{Lrr1}$ recognises terminated helicase and active, neddylated $Cul2^{Lrr1}$ interacts with Ubxn7. Ubxn7 in turn restricts $Cul2^{Lrr1}$ activity but also bridges binding to p97. Without Ubxn7, unloading of replisomes is postponed, while $Cul2^{Lrr1}$, which is unrestricted in its activity due to the absence of Ubxn7, accumulates on chromatin.

The role of Ubxn7 as a specific linker of Cul2Lrr1 and p97 during S-phase also suggest an explanation for surprising specificity of p97 to Mcm7 modified with K48-linked ubiquitin chains in S-phase. It has been shown that K48-linked ubiquitin chains on Mcm7 specifically drive unloading in S phase (Moreno, Bailey et al. 2014). The bridging of Cul2Lrr1 and p97 by Ubxn7 may explain why p97 preferentially unloads helicase modified with K48-linked ubiquitin chains made by Cul2Lrr1 and why inhibition of polyubiquitylation of all substrates with Ubi-NOK allows for accumulation of p97 on chromatin. We know (Gambus lab unpublished data) that when replisome unloading is blocked in S-phase, Mcm7 is ubiquitylated with K6 linked chains, driven by TRAIP ubiquitin ligase. However, K6-chains do not promote replisome unloading in S-phase. In mitosis, however, p97 unloads post-termination replisome in which Mcm7 is ubiquitylated with K63 and K6 linked ubiquitin chains by TRAIP E3 ubiquitin ligase (Priego Moreno, Jones et al. 2019). Intriguingly, although K48 linked chains are formed on Mcm7 in mitosis they are not able to drive unloading. Therefore, next, we would like to understand whether p97 drives replisome unloading with different cofactors that recognize different ubiquitin chains on CMG helicase in mitosis.

3.3. p97 in mitotic replisome disassembly

3.3.1. Introduction

It has been shown that Mcm7 is ubiquitylated within the terminated CMG helicase complex by $Cul2^{Lrr1}$ in *X. laevis* egg extract (Dewar, Low et al. 2017, Gambus 2017), in *C. elegans* embryos (Maric, Maculins et al. 2014) and in mouse (Villa, Fujisawa et al. 2021) during DNA replication termination in S phase. CMG is then disassembled by p97, allowing the whole replisome to be removed from the chromatin (Moreno, Bailey et al. 2014). If there is a defect in either replisome removal at termination or are obstacles to fork convergence, then the helicase complexes fail to be unloaded in S phase. Notably, it has been shown that an alternative backup pathway for replisome disassembly works in mitosis and this requires a different E3 ubiquitin ligase, TRAIP. This second alternative replisome disassembly pathway still depends on p97 activity (Priego Moreno, Jones et al. 2019, Villa, Fujisawa et al. 2021, Wu, Pellman et al. 2021).

3.3.2. Results

3.3.2.1. p97 association with chromatin during replisome disassembly in mitosis

S-phase replisome disassembly depends on K48-linked ubiquitin chains, while Mcm7 is ubiquitylated in mitosis with K48, K63 and K6-linked ubiquitin chains. Interestingly only K6 and K63-chains support replisome unloading during mitosis, while K48-chains are not able to drive unloading. This suggests that p97 activity is very strictly controlled by different types of ubiquitin chains (Priego Moreno, Jones et al. 2019). Although it is known that p97 cofactors bind substrates with different ubiquitin chains (Alexandru, Graumann et al. 2008, Meyer and Weihl 2014), it is not known which cofactors provide p97 specificity for non- 48 linked ubiquitin chains. Our aim, therefore, was to investigate how p97 interacts with chromatin during mitosis and identify which cofactors may direct it to the K6 and K63-linked ubiquitylated Mcm7 in this stage of the cell cycle.

Firstly, I wanted to analyse chromatin binding of p97 upon induction of mitosis. $Cul2^{Lrr1}$ activity was blocked with MLN4924 in interphase extract in order to block the S-phase pathway of replisome disassembly and accumulate post-termination replisomes on chromatin. To keep synchronicity in the *Xenopus laevis* egg extract system, we block protein synthesis with cycloheximide, which prevents the extract from entering mitosis (Gillespie, Gambus et al. 2012). Therefore, to analyse p97 and its cofactors in the mitotic replisome disassembly pathway in *Xenopus* egg extract, we induced mitosis in the extract with addition of purified HIS-tagged *X.laevis* Cyclin A1Δ56 (Cyclin A1Δ), following

completion of DNA replication (90 min post sperm DNA addition) (Strausfeld, Howell et al. 1996). This has been shown previously to cause the extract to enter mitosis (Priego Moreno, Jones et al. 2019). At this point, half of the sample was treated optionally with DMSO or the p97 inhibitor, NMS-873. It has been shown that adding NMS-873 along with Cyclin A1Δ does not affect entry into mitosis (Priego Moreno, Jones et al. 2019).

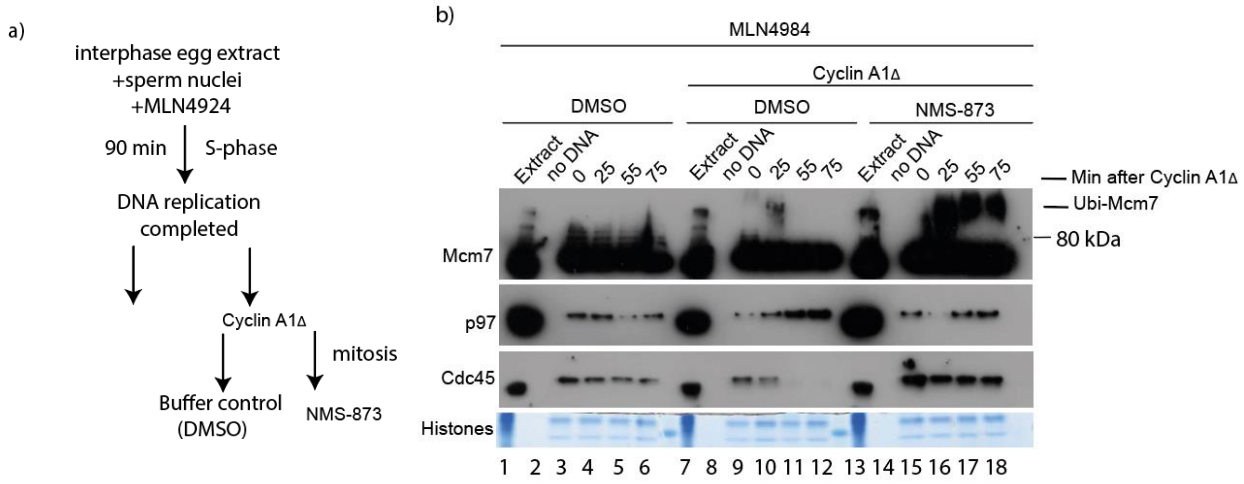

Figure 3. 25 p97 interacted with chromatin in mitosis. a) **Experimental design driving egg extract from S phase to mitosis.** b) Interphase egg extract was supplemented with demembranated sperm nuclei and with MLN4924. After DNA synthesis was completed (90 minutes post addition of sperm DNA), Cyclin A1Δ was optionally added to the extract to drive entry into mitosis. The extract was then optionally treated with either DMSO or NMS-873. Chromatin was isolated at indicated time points, separated by SDS-PAGE and Western blotted using the indicated antibodies. Histones are stained on the gel to act as a loading control. An extract sample without addition of DNA was analysed in parallel to other chromatin samples to provide a chromatin specificity control. Time "0" sample represents the time at which Cyclin A1Δ was added, after DNA synthesis was completed. This experiment represents one of two biological repeats.

Lanes 3-6 (Figure 3.25) represent samples from late S-phase (LFB1-50 buffer addition) as these do not include Cyclin A1Δ. In this case, addition of MLN4924 has blocked replisome disassembly, shown by retention of Cdc45 on the chromatin, which forms part of the active helicase. We also see a low level of Mcm7 ubiquitylation (short ubiquitin chains), due to the blocking activity of $Cul2^{Lrr1}$. In mitosis however, upon the addition of Cyclin A1Δ, Cdc45 is unloaded, with noticeable ubiquitylation of Mcm7 (Figure 3.25, lane 10). We also observed longer ubiquitin chains on Mcm7, which has been observed before and could indicate that long ubiquitin chains are necessary for mitotic replisome unloading (Priego Moreno, Jones et al. 2019). In mitotic samples treated with the p97 inhibitor NMS-873 (Figure 3.25, lanes 15-18) we can see accumulation of Cdc45 on the chromatin and accumulation of Mcm7 ubiquitylation, indicating inhibition of mitotic replisome disassembly. p97 associates with chromatin at all of these different stages, (Figure 3.25, lanes 9-12).

3.3.2.2. p97 binding to chromatin in mitosis is likely to be stimulated by ubiquitylation of substrates

We hypothesise that in S-phase p97 is recruited to the chromatin at terminating replication forks by Ubxn7 and $Cul2^{Lrr1}$, rather than directly and primarily binding by polyubiquitylated Mcm7. In order to determine whether polyubiquitylated substrates, including Mcm7, bring p97 to the chromatin during mitotic replisome disassembly, I wanted to block polyubiquitylation in mitosis and observe p97 interaction with chromatin. I first blocked replisome disassembly in S-phase with Cul2 inhibitor MLN4924. Then I optionally added LFB1/50 buffer or Cyclin A1Δ to the extract to drive entry into mitosis. Half of the mitotic sample was then optionally supplemented with wt ubiquitin (Ubi) or Ubi-NOK, in which all lysines are mutated and which therefore blocks polyubiquitylation of all proteins, including Mcm7.

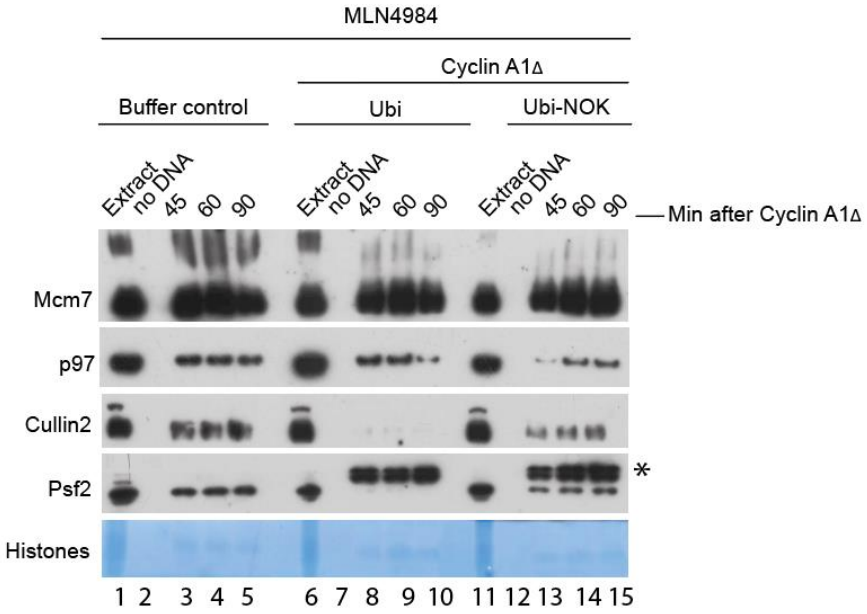

Figure 3. 26 p97 interaction with chromatin in mitosis. Interphase egg extract was supplemented with sperm DNA. DNA synthesis was completed in the presence of Cul2 inhibitor MLN4924 and optionally supplemented with LFB1-50 or Cyclin A1Δ. Mitotic samples were then also supplemented optionally with recombinant wt ubiquitin or Ubi-NOK. Chromatin was isolated at indicated time points, separated by SDS-PAGE and Western blotted using the indicated antibodies. Histones are stained on the gel to act as a loading control. An extract sample without addition of DNA was analysed in parallel to other chromatin samples to provide a chromatin specificity control. The band marked with asterix in Psf2 blot represent the recombinant Cyclin A1Δ, which is recognised with Psf2 antibody. This experiment was performed once.

In this experiment, we could detect accumulation of Psf2 in late S-phase due to blocked $Cul2^{Lrr1}$ activity (Figure 3.26, lane 3-5), which was then unloaded in mitosis (lanes 7-10 – by the first time point of 45

min Psf2 is unloaded). Of note, the dense band above Psf2 (marked with *), represents recombinant Cyclin A1Δ, which is recognised by the Psf2 antibody (Lanes 7-10 and 13-15). In the presence of Ubi-NOK, we observed that the replisome component Psf2 stayed on chromatin due to inhibition of ubiquitin chain formation (Figure 3.26, lane 13-15). Interestingly, we found decreased levels of p97 on chromatin at 45 min, likely due to the reduced level of polyubiquitylated substrates, which suggests that these substrates do help the recruitment of p97 to chromatin in mitosis. We cannot however compare this experiment directly to our data from S-phase, as to block the S-phase pathway of replisome disassembly I have added Cullin inhibitor MLN4924, which is then present in the extract throughout the experiment. As my results in Results Chapter 2 suggest, inhibition of neddylation of Cullin2 stops its interaction with Ubxn7. This link of p97 with Cul2 through Ubxn7 would have been blocked in this experiment.

3.3.2.3. p97 may interact with different cofactors for replisome disassembly in mitosis

While we know that the p97 cofactor Ubxn7 recognises K48-linked ubiquitin chains (Alexandru, Graumann et al. 2008, Cilenti, Di Gregorio et al. 2020) and works in the S-phase replisome disassembly pathway, the distinct ubiquitin chains used in the mitotic pathway are likely to be recognised by alternative p97 cofactors. In order to identify potential cofactors of p97 acting during replisome disassembly in mitosis, we decided to immunoprecipitate chromatin-bound p97 in mitosis and investigate all the interacting proteins by mass spectrometry. A replication reaction was set up in which replisome disassembly in S-phase was blocked by treating egg extract with the Cullin inhibitor MLN4924. Additionally, the egg extract was treated with caffeine to activate more replication forks during replication initiation. As a result of caffeine treatment there are more replisomes on chromatin and therefore more substrates for p97. It has been shown previously that inhibition of checkpoint by caffeine does not affect the efficiency of DNA replication termination and replisome disassembly. At 90 min, at which point DNA synthesis is complete, mitosis was induced by adding Cyclin 1AΔ to the reaction. To have more substrate and more p97 on the chromatin, the mitotic replisome disassembly was blocked with p97 inhibitor NMS-873 and chromatin was isolated in mitosis at 45 min when p97 is accumulated on chromatin. Protein complexes were released from DNA through digestion with Benzonase, insoluble material spun out and soluble material incubated with p97 or non-specific IgG beads. A fraction of the immunoprecipitated p97 sample was analysed by Western blotting with p97 antibody. As expected, p97 antibodies can immunoprecipitate p97 protein from mitotic chromatin (Figure 3.27.a.). The rest of the immunoprecipitated samples were resolved by SDS-PAGE, gel lanes were cut into 10 slices (Figure 3.27.b.) and analysed by mass spectrometry.

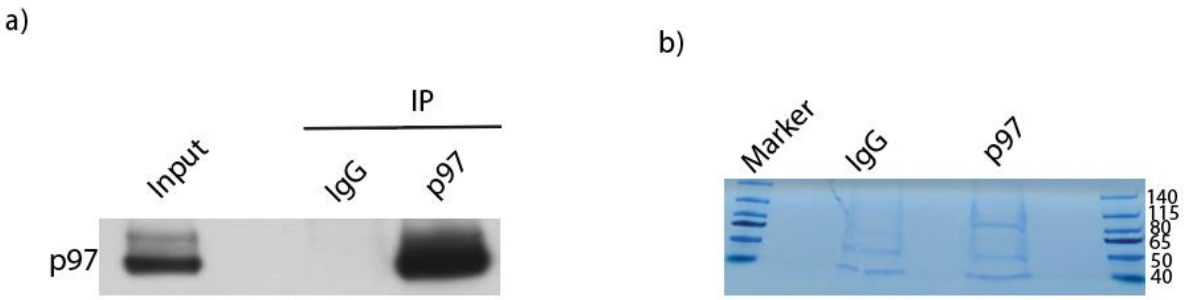

Figure 3. 27 Purified p97 antibodies can immunoprecipitate p97 from mitotic chromatin. a) Interphase egg extract was supplemented with demembranated sperm nuclei, caffeine (to increase origin firing) and MLN4924 (to impede CMG unloading from chromatin). Then at 90 min Cyclin A1Δ (to induce mitotic entry) and NMS-873 (to increase the amount of p97 on chromatin) were added. Chromatin containing high levels of terminated CMGs was isolated in mitosis at 45 min after Cyclin A1Δ addition, proteins released from DNA by benzonase treatment and p97 immunoprecipitated. Immunoprecipitation of p97 was confirmed by western blot analysis. b) Immunoprecipitated material was resolved by SDS-PAGE and stained with colloidal coomassie. Each lane was cut into 10 bands and protein content analysed by mass spectrometry. The experiment was performed once.

Mass spectrometry data revealed that p97 was successfully immunoprecipitated, as seen by the identification of 1076 peptides of p97 in the p97 IP sample (Table 3.4.). I then went on to search through the list of proteins identified in immunoprecipitated material for any involved in the ubiquitin-proteasome system: p97 cofactors or potential cofactors (proteins containing ubiquitin binding domains) and ubiquitin ligases.

A previous PhD student in the Gambus lab, Dr Sara Priego Moreno, immunoprecipitated Mcm3 from mitotic chromatin and analysed the interacting factors by mass (Priego Moreno, Jones et al. 2019). To increase the number of terminating replisomes on chromatin, to aid analysis, replisome disassembly was blocked by addition of p97 inhibitor NMS-873. She also treated the reaction with caffeine to promote DNA replication initiation and increase the number of active forks. Thus, I have compared my mass spectrometry data with her replisome IP in mitosis.

Table 3. 4 Mass spectrometry analysis of immunoprecipitated p97 in mitosis. Table presenting mass spectrometry analysis results of peptides identified following p97 immunoprecipitation from mitotic chromatin (caffeine to increase replication origin, MLN4984 to block CMG disassembly in S-phase, Cyclin A1Δ to induce entry into mitosis and NMS873 to have more p97) or Mcm3 IP (caffeine, NMS873 and Cyclin A1Δ). This table shows p97 and its co-factors and ubiquitin ligases. Total spectral count (TSC), which is a number of peptides for each protein identified, is indicated, with the percentage of protein coverage in brackets. Proteins are sorted from higher to lower TSC in the p97 IP. Proteins identified with at least 2 peptides are shown.

		IP from mitotic chromatin assembled in extract treated with NMS-873		IP from mitotic chromatin assembled in extract treated with NMS-873	
	Protein (kDa)	IgG TSC (coverege)	α-p97 TSC (coverege)	IgG TSC (coverege)	α-Mcm3 TSC (coverege)
p97 and co-factors	p97 (89 kDa)	0	1076 (83%)	15 (16%)	40 (36%)
	Ubxn7 (55 kDa)	0	83 (34%)	2 (4.7)	0
	Aspscr1 (63 kDa)	0	30 (25%)	0	0
	Npl4 (69 kDa)	0	27 (24%)	8 (14%)	0
	Ufd1 (35 kDa)	0	9 (31%)	0	12 (31%)
	p47 (41 kDa)	0	2 (6.5%)	0	0
	Faf1 (74 kDa)	0	0	0	3 (41%)
Ubiquitin ligases	E6AP(105 kDa)	0	4 (3.2%)	2 (1.9%)	0

In both sets of data, six p97 cofactors were found: Ufd1, Npl4, Ubxn7, Aspscr1 and p47 (Table 3.4.). Ufd1 and Npl4 are heterodimeric major cofactors of p97 and they have a role in CMG disassembly from chromatin during mitosis (Maric, Mukherjee et al. 2017, Sonneville, Moreno et al. 2017). My previous chapters revealed that $Cul2^{Lrr1}$ interacts with Ubxn7 and these together with p97 unload CMG from chromatin in S-phase. Another cofactor p47 is required for membrane fusion by p97 (Totsukawa, Matsuo et al. 2013) and degrades ER substrates during the ERAD pathway (Endoplasmic reticulum associated pathway) (Besche, Haas et al. 2009). Aspscr1 (also Ubxn9) has a UBX domain and has a role in disassembly of p97 targeted substrates in membrane trafficking. However, neither p47 nor Aspcr1 have been found previously to have a role during DNA replication and neither interacts with the replisome in mitosis.

In the p97 IP we also detected components of the CMG complex: Mcm2-7 and Cdc45. Interestingly however, the GINS complex was not detected, which may be due to the fact that it is a complex of much smaller proteins (Table 3.5).

Inhibition of replisome disassembly in mitosis results in accumulation of many replisome components on chromatin during mitosis (Table 3.5, Mcm3 IP). We observed many of these to also interact with

p97 during mitosis: Rpa1, Rpa2, Rpa3, Topbp1-α, Spt16, Dnmt1s, Ssrp1, Rfc3 and Polε. While Rpa1 and Topbp1-α associate more with p97, Spt16, Dnmt1s, Ssrp1 and Rpa3 interacted more strongly with the replisome (Mcm3 IP) rather than p97, during mitosis. Interestingly, Rfc3 and Polε only interacted with p97 and not with Mcm3 in mitosis. This result suggests that Rfc3 and Polε directly interact with p97 and could therefore be potential substrates of p97 in mitosis.

As is known, p97 has critical roles in DNA repair to protect the cell from death (Bennett, Lewis et al. 1993). Indeed, many DNA damage response proteins were found to interact with p97 in mitosis (Table 3.5), although H1foo, H2A, H2b1.1, H3.3, H4, Smarca5, Smc2, Smc4, Fancd2 and Cyclin A2 were more enriched in the Mcm3 IP, suggesting they interact more strongly with the replisome. Smarcal1 and GAPDH were, however, found to interact with p97 approximately two-fold more than with Mcm3, suggesting that they might be potential substrates of p97 or are regulated by p97 during mitosis. Moreover, WRN DNA helicase, Casein Kinase 2 α (CKII α), Casein Kinase 2 β (CKII β), and Aurora B, which initiates mitotic exit (Cao, Nakajima et al. 2003) were found to interact only with p97 and not with the replisome (Table 3.5). We hypothesise therefore that these proteins may directly interact with p97 and are also possible substrates of p97.

Table 3. 5 CMG helicase, DNA replication and DNA damage related proteins interacting with p97. Table presenting proteins identified following p97 IP from mitotic chromatin or Mcm3 IP as in Table 3.4. This table shows replisome components, DNA replication and DNA damage related proteins. Number of peptides identified for each protein in the different samples is indicated (Total spectral count, TSC), with the protein coverage in brackets. Proteins are sorted from higher to lower TSC and also combined in known complexes in the p97 IP. Proteins are only shown if they have at least 2 peptides in p97 IP over control (IgG) IP.

		IP from mitotic chromatin assembled in extract treated with NMS873		IP from mitotic chromatin assembled in extract treated with NMS873	
	Protein (kDa)	IgG TSC (coverege)	α-p97 TSC (coverege)	IgG TSC (coverege)	α-Mcm3 TSC (coverege)
CMG Complex	Mcm2 (100 kDa)	136 (44%)	231 (54%)	364(46%)	1348 (78%)
	Mcm3 (90 kDa)	17 (14%)	124(43%)	222 (55%)	1610 (90%)
	Mcm4 (97 kDa)	72 (28%)	201(55%)	198 (45%)	1277 (85%)
	Mcm5 (82 kDa)	13 (13%)	149 (57%)	70 (59%)	720 (88%)
	Mcm6 (93 kDa)	65(23%)	162 (52%)	196 (60%)	964 (91%)
	Mcm7 (82 kDa)	25 (20%)	120 (41%)	160 (52%)	1082 (84%)
	Cdc45 (66 kDa)	0	6 (6.7%)	18 (26%)	187 (46%)
Replisome components	Rpa1 (67 kDa)	0	236(38 %)	80 (53%)	107 (48%)
	Rpa2 (29 kDa)	29 (17%)	27(28%)	13 (22%)	30(55%)
	Rpa3 (13 kDa)	0	2 (36%)	6 (52%)	10 (92%)
	Topbp1-α (169 kDa)	0	71 (24%)	0	43(7%)
	Spt16 (118 kDa)	0	25 (15%)	109 (23%)	431(61%)
	Dnmt1.s (168 kDa)	0	9 (1%)	5 (1.7%)	65 (25%)
	ssrp1 (79 kDa)	0	3 (5.6%)	19 (8%)	224(45%)
	Rfc3 (40 kDa)	0	3 (9.8%)	0	0
	Polε (188 kDa)	0	3 (24%)	0	0
DNA replication and DNA damage response proteins	ATR (301 kDa)	0	56 (125 %)	46 (13%)	182 (27%)
	H1foo (15 kDa)	0	17(24%)	87(33%)	210 (73%)
	H2A (15 kDa)	3(22%)	5 (23%)	4 (28%)	29 (63%)
	H2b1.1 (14 kDa)	27 (56%)	31(68%)	0	6 (3%)
	H3.3 (15 kDa)	11 (29%)	27 (43%)	0	51 (88%)
	H4 (11 kDa)	15 (51%)	24 (52%)	35 (11%)	86 (28%)
	Smarca5 (122 kDa)	0	30 (14%)	0	372 (63%)
	Smarcal1 (107 kDa)	0	18 (8.9%)	9 (6.2%)	9 (7.4%)
	Fanci (150 kDa)	0	26 (11%)	47 (17%)	87 (30%)
	Gapdh (144 kDa)	0	14 (13%)	5 (14%)	6 (16%)
	CKII α (45 kDa)	0	12 (12%)	0	0
	CKII β (25 kDa)	0	5 (14%)	0	0
	Smc2 (136kDa)	0	2 (2.2%)	91 (33%)	65 (35 %)
	Smc4 (147 kDa)	0	10 (6.4%)	118 (36%)	100 (44%)
	Fanc d2 (163 kDa)	0	10 (4.9%)	36 (8.7%)	136 (48%)
	Aurora B (41 kDa)	0	5 (9.7%)	0	0
	Wrn (162 kDa)	0	5 (2.6 %)	0	0
	Cyclin A2 (147 kDa)	3 (3.9%)	4 (3.9%)	2 (8.2)	4 (11%)

Table 3.6 Comparison of p97 interactors on chromatin upon inhibition of replisome disassembly in S phase and mitosis. The number of peptides for each protein is indicated (Total spectral count, TSC), with protein coverage in brackets. This table only shows those proteins enriched in the p97 IP (at least 2-fold enrichment in mitotic p97 IP over IgG IP), and only proteins with more than 10 peptides identified in the S phase and mitotic p97 IP are shown. Proteins are sorted from higher to lower TSC in the p97 IP.

		IP from S-phase chromatin assembled in extract treated with NMS873		IP from mitotic chromatin assembled in extract treated with NMS-873	
	Protein (kDa)	IgG TSC (coverege)	α-p97 TSC (coverege)	IgG TSC (coverege)	α-p97 TSC (coverege)
p97 and co-factors	p97 (89 kDa)	8 (7%)	935 (80%)	0	1076 (83%)
	Npl4 (69 kDa)	0	203 (58%)	0	27 (24%)
	Ufd1 (35 kDa)	0	97 (63%)	0	9 (31%)
	Ubxn7 (55 kDa)	0	6 (12%)	0	83 (34%)
	Faf1 (74 kDa)	0	5 (4%)	0	0
	p47 (40 kDa)	0	5 (12%)	0	2 (6.5%)
	Faf2b (52 kDa)	0	15 (23%)	0	0
	Faf2a (53 kDa)	0	14 (23%)	0	0
	Aspscr1 (63 kDa)	0	0	0	30 (25%)
Ubiquitin ligases	Brca1 (176 kDa)	0	90 (23%)	0	0
	Bard1 (87 kDa)	0	2 (2%)	0	0
	E6ap (105 kDa)	0	11 (11%)	0	4 (3.2%)
	Cullin1 (90 kDa)	0	9 (8%)	0	0
	Cullin9 (241 kDa)	0	2 (1%)	0	0
	Wwp2 (85 kDa)	0	6 (7%)	0	0
	Rnf31 (118 kDa)	0	5 (3%)	0	0
	Uhrf1 (87 kDa)	0	4 (1%)	0	0
	Hectd1 (281 kDa)	0	3 (5%)	0	0
	Rnf115 (33 kDa)	0	2 (6%)	0	0
	Cul2 (87 kDa)	0	0	0	0
Sumo related proteins	Ranbp2 (315 kDa)	0	106 (25%)	0	0
	Sumo3 (11 kDa)	0	12 (35%)	0	0
DUBs	Usp9x (291 kDa)	0	4 (1%)	0	0
	Usp5 (93 kDa)	0	18 (20%)	0	0

		IP from S-phase chromatin assembled in extract treated with NMS873		IP from mitotic chromatin assembled in extract treated with NMS-873	
	Protein (kDa)	IgG TSC (coverege)	α-p97 TSC (coverege)	IgG TSC (coverege)	α-p97 TSC (coverege)
CMG Complex	Mcm2 (100 kDa)	0	67 (31%)	136 (44%)	231 (54%)
	Mcm3 (90 kDa)	0	3 (2%)	17 (14%)	124(43%)
	Mcm4 (97 kDa)	0	28 (21%)	72 (28%)	201(55%)
	Mcm5 (82 kDa)	0	30 (31%)	13 (13%)	149 (57%)
	Mcm6 (93 kDa)	0	49 (32%)	65(23%)	162 (52%)
	Mcm7 (82 kDa)	0	42 (34%)	25 (20%)	120 (41%)
	Cdc45 (66 kDa)	0	0	0	6 (6.7%)
Replisome components	Rpa1 (67 kDa)	0	149 (38 %)	0	107 (48%)
	Rpa2 (29 kDa)	0	0	0	30(55%)
	Rpa3 (13 kDa)	0	3 (36%)	0	10 (92%)
	PCNA (29 kDa)	19 (48%)	54 (66%)	0	0
	Dnmt1 (168 kDa)	0	50 (19%)	0	65 (25%)
	Spt16 (118 kDa)	0	25 (15%)	0	431(61%)
	Ctf4 (125 kDa)	0	23 (16%)	0	9 (1%)
	Rfc2 (38 kDa)	0	8 (22%)	0	0
	Rfc3 (40 kDa)	0	20 (38%)	0	0
	Rfc4 (40 kDa)	0	13 (28%)	0	0
	Pol3 (125 kDa)	0	2 (6%)	0	0
	Polα1 (165 kDa)	0	9 (5%)	0	0
	Polε (261 kDa)	0	3 (1%)	0	0
	Topbp1-α (169 kDa)	0	11 (71%)	0	0
	Orc2 (62 kDa)	0	8 (12%)	0	0
	Orc3 (81 kDa)	0	7 (9%)	0	0
	Orc4 (50 kDa)	0	2 (6%)	0	0
	Dna2 (120 kDa)	0	6 (5%)	0	0
	Fen1-a (43 kDa)	0	3 (9%)	0	0
	ssrp1 (79 kDa)	0	0	0	3 (5.6%)

		IP from S-phase chromatin assembled in extract treated with NMS873		IP from mitotic chromatin assembled in extract treated with NMS-873	
	Protein (kDa)	IgG TSC (coverege)	α-p97 TSC (coverege)	IgG TSC (coverege)	α-p97 TSC (coverege)
DNA replication and DNA damage response proteins	Sall4 (114 kDa)	0	20 (27%)	0	0
	Rif1 (257 kDa)	0	108 (21%)	0	0
	Arid1a (206 kDa)	0	82 (17%)	0	0
	Arid1b (148 kDa)	0	16 (10%)	0	0
	Smarca5 (122 kDa)	0	45 (29%)	0	372 (63%)
	Smarca4 (181 kDa)	0	21 (9%)	0	0
	Smarce1 (47 kDa)	0	17 (26%)	0	0
	Smarcb1 (43 kDa)	0	11 (24%)	0	0
	Cenpe (339 kDa)	0	41 (6%)	0	0
	Rrm1 (91 kDa)	0	29 (8%)	0	0
	Baz1b (166 kDa)	0	27 (11%)	0	0
	Rad50 (154 kDa)	0	19 (8%)	0	0
	Rbbp7 (48 kDa)	0	15 (23%)	0	0
	Smc3 (141 kDa)	0	14 (12%)	0	0
	Hdac1-b (55 kDa)	0	12 (22%)	0	0
	Etaa1 (90 kDa)	0	11 (12%)	0	0
	Ehmt2 (65 kDa)	0	11 (11%)	0	0
	H3.3 (15 kDa)	4 (21%)	8 (36%)	0	51 (88%)
	ATR (301 kDa)	0	0	0	182 (27%)
	H1foo (15 kDa)	0	0	0	210 (73%)
	H2A (15 kDa)	0	0	0	29 (63%)
	H2b1.1 (14 kDa)	0	0	0	6 (3%)
	H4 (11 kDa)	0	0	0	86 (28%)
	Smarcal1 (107 kDa)	0	0	0	9 (7.4%)
	Fanci (150 kDa)	0	0	0	87 (30%)
	Gapdh (144 kDa)	0	0	0	6 (16%)
	CKII α (45 kDa)	0	0	0	0
	CKII β (25 kDa)	0	0	0	0
	Smc2 (136kDa)	0	0	0	65 (35 %)
	Smc4 (147 kDa)	0	0	0	100 (44%)
	Fanc d2 (163 kDa)	0	0	0	136 (48%)
	Aurora B (41 kDa)	0	0	0	0
	Wrn (162 kDa)	0	0	0	0
	Cyclin A2 (147 kDa)	0	0	0	4 (11%)

When comparing p97 IP in S phase with mitosis, it can be seen that Ufd1/Npl4 and Ubxn7 are the potential cofactors which may have roles in replisome disassembly both in S phase and mitosis. However, interaction of p97 with Ufd1/Nlp4 is strongly decreased in mitosis, Ubxn7 interaction with p97 is increased. This might be either due to posttranslational modifications (PTMs) of p97 or due to IP conditions (see in discussion).

3.3.2.4. Immunoprecipitated p97 interacts with Ubxn7 and Faf1 on mitotic chromatin

We aimed next to confirm p97 interaction with Ubxn7, Aspcrc1 and Faf1 during the mitotic pathway of replisome disassembly. We set up a reaction in a similar way as for our mass spectrometry analysis: replisome disassembly in S-phase was blocked by adding Cul2 inhibitor MLN4924. Moreover, origin firing was induced with the presence of caffeine, and p97 accumulated on chromatin by addition of p97 inhibitor NMS873. The reaction was then supplemented with cyclin A1Δ after DNA replication was completed (90 min post addition of sperm DNA) to induce the extract to enter mitosis. After 45 min in mitosis chromatin was isolated, chromatin bound protein complexes were released by digestion with Benzonase and then immunoprecipitation performed with p97 antibody or non-specific IgG beads.

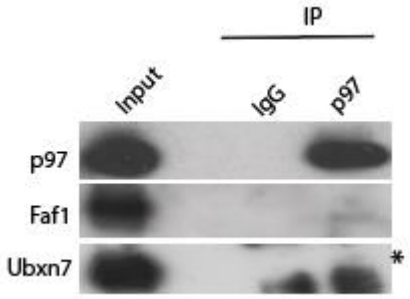

Figure 3. 28 p97 interacts with Faf1 and Ubxn7 on mitotic chromatin. p97 was immunoprecipitated from mitotic chromatin treated with caffeine, MLN4984 and p97 inhibitor NMS873. The extract was driven to enter mitosis by supplementation with Cyclin 1AΔ. Chromatin, containing high levels of terminated CMGs was isolated at 45 minutes after Cyclin 1AΔ addition. Immunoprecipitated materials were tested by western blotting with indicated antibodies. * Shows Ubxn7 Xenopus protein. The experiment was performed once.

In order to confirm association between p97 and its cofactors under such conditions, I analysed the immunoprecipitated p97 sample by western blotting with Ubxn7, Faf1 and Aspscr1. I could detect faint bands for Faf1 and Ubxn7 co-immunoprecipitated with p97. The top band (*) refers to co-immunoprecipitated Ubxn7 *Xenopus* protein. Interestingly, although a high number of Ubxn7 peptides were identified interacting with p97 in mitosis through mass spectrometry analysis, it was very difficult to detect Ubxn7 by western blotting. It suggests that either the mass spectrometry method is more sensitive and so l can detect certain levels by mass spectrometry but not see them by western blotting or some modifications of Ubxn7 in mitosis prevent the antibodies to bind to co-immunoprecipitated Ubxn7 (Figure 3.28.). We detected also that mitotic p97 interacted slightly with Faf1 protein in contrary to the mass spectrometry analysis. When we blotted with two different

Aspscr1 commercial antibodies, we did not have any signal even in the extract (data not shown), suggesting that they do not recognise *Xenopus* Aspscr1.

3.3.2.5. Posttranslational modifications of p97 may promote cell cycle specific functions

Posttranslational modifications on p97 such as ubiquitylation, acetylation, sumoylation, parylation and phosphorylation enable p97 to regulate many diverse cellular functions (Fang, Zhang et al. 2016). Moreover, these modifications regulate the stabilization of p97 interactions with its cofactors in specific processes (Mori-Konya, Kato et al. 2009). I therefore analysed the mass spectrometry data obtained from p97 immunoprecipitation from S phase (presented in Results Chapter 1) and mitosis (presented here) for posttranslational modifications (Figure 3.29.).

a)

Post-translational modifications	IP from S-phase chromatin assembled in extract treated with NMS-873 (TSC)						IP from mitotic chromatin assembled in extract treated with NMS-873 (TCS)					
	Amino acid number, name	PTM sites in contex of sequence	Confidents* of identification	Number of peptides unmodified	Number of peptides modified	if this aminoacid is conserved in similar position in human	Amino acid number, name	PTM sites in contex of sequence	Confidents* of identification	Number of peptides unmodified	Number of peptides modified	if this aminoacid is conserved in similar position in human
Phosphorylation	S5 T7 S9 - -	MASGSDTKSD MASGSDTKSD MASGSDTKSD	(100%) (95%) (95%)	21 21 28	1 1 1	n/a n/a n/a	S5 - - S702 S718	MASGSDSKSD RDRQTNPSAM ESIENEIRRE	(100%) (99%) (95%)	- 41 18	1 1 5	n/a conserved conserved
Acetylation	A2	MASGSDTKSD	(99%)	3	19	conserved	A2 (23)	MASGSDTKSD	(99%)	-	23	conserved
Ubiquitylation	- - K 295	EEAEKNAPAI	(100%)	16	2	conserved	K 425 (1) K 426 (1) -	QAIRKKMDLI QAIRKKMDLI	(99%) (99%)	30 40	1 1	conserved conserved

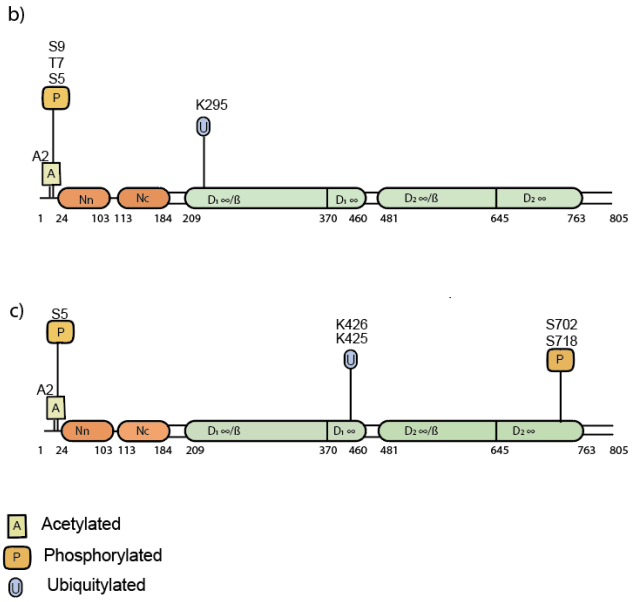

Figure 3. 29 Modifications identified on p97 in S-phase and mitosis. a) p97 was immnoprecipitated from chromatin in S-phase (chromatin treated with NMS-873), or mitosis (chromatin treated with caffeine, MLN4984, NMS-873, Cyclin 1AΔ) and analysed by mass spectrometry. Posttranslational modifications identified within p97 protein are indicated with the number of peptides that were identified with such a modification in brackets. * Percentage of confidence in identification of modified peptide as calculates by Scaffold programme. b) The model shows posttranslational modification is S-phase and c) in mitosis. The schematic structure of p97 in *Xenopus* shows that it consists of N domain (Nn: amino acids sequences from 1 to 103, Nc: amino acids sequences from 103 to 184), D1 and D2 domain and C terminal tail (amino acids sequences from 763 to 805). D1 and D2 domain consist of α-helix and B sheet rich region and fallowing by a small α-helix rich region.

Using this method, we were able to identify modifications in the N-terminal part of p97: phosphorylation at Serine 5 (S5), Threonine 7 (T7) and Serine 9 (S9) and acetylation at Alanine 2 (A2). We also found ubiquitylation at lysine295 (K295) in the D1 domain in S-phase (Figure 3.29.a and 3.29.b). We detected 8 unmodified p97 peptides in control and 539 unmodified peptides in total p97

S phase IP. Moreover 50 peptides were phosphorylated, 19 peptides were acetylated, and 16 peptides were ubiquitylated. Alanin 2 and lysine 295 are conserved in similar position in human. In mitosis however, we found phosphorylation at Serine 5 (S5), Serine 702 (S702), Serine 718 (S718) in the D2 domain, and acetylation at Alanine 2 in the N-terminal end and ubiquitylation at lysine425 (K425) and lysine426 (K426) in the D2 domain of p97 (Figure 3.29.a and 3.29.c). The number of unmodified peptides were 1 in control and 503 in total p97 mitosis IP. We detected 7 peptides that were phosphorylated, 23 peptides that were acetylated and 2 peptides that were ubiquitylated. Serine 702, serine 718, alanine2, lysine 425 and lysine 426 are conserved in similar position in human.

3.3.3. Discussion

3.3.3.1. Replisome disassembly during mitosis requires p97 ATPase activity

It has been shown that ubiquitylation of Mcm7 as part of the CMG terminated helicase is driven by $Cul2^{Lrr1}$ and in *Caenorhabditis elegans (Maric, Maculins et al. 2014, Sonneville, Moreno et al. 2017)*, *Xenopus laevis* egg extract (Dewar, Low et al. 2017, Gambus 2017, Sonneville, Moreno et al. 2017) and in mouse (Villa, Fujisawa et al. 2021). Ubiquitylated CMG, as well as replisome machinery attached to the CMG helicase, is extracted from chromatin by p97 (Moreno, Bailey et al. 2014). If the S-phase pathway of replisome disassembly is blocked or a problem with replication fork progression occurs e.g. treatment with aphidicolin and hydroxyurea (Hashimoto and Tanaka 2020), this prevents converging of forks and failure to disassemble the replisome in S phase. The replisomes are then alternatively unloaded in mitosis. This second disassembly pathway requires TRAIP E3 ligase and p97 segregase activity (Deng, Wu et al. 2019, Priego Moreno, Jones et al. 2019, Villa, Fujisawa et al. 2021). The replisome complexes in S-phase or in mitosis, post-termination or stalled, have diverse structures. Mcm7 is ubiquitylated by K48 and K6-linked ubiquitin chains during S-phase termination, but only K48-linked ubiquitin chains promote unloading, whereas K6 and K63-linked ubiquitin chains are able to drive disassembly of CMG helicase in mitosis. This shows that the unloading activity of p97 is strictly regulated by specific substrates and specific types of ubiquitin chains (Meyer and Rape 2014, Heidelberger, Voigt et al. 2018, Priego Moreno, Jones et al. 2019). It is well known that p97 cofactors recognise substrates ubiquitylated with K48-linked ubiquitin chains, however, which cofactors recognise other types of ubiquitin chains is still unknown. How does p97 extract ubiquitylated Mcm7 linked with different ubiquitin chains from chromatin? It might be the combinations of different p97 cofactors, which allow this role to be completed.

My results suggest that Ubxn7 interacting with Cul2 recruits p97 to chromatin rather than polyubiquitylated substrates at the termination of DNA replication in S phase. However, another E3 ligase, TRAIP, is responsible for ubiquitylation of Mcm7 in mitosis. Therefore, we wanted to explore the recruitment mechanism of p97 to the chromatin in this case. When replisome unloading in S-phase is blocked by inhibition of Cullin neddylation, which also inhibits Ubxn7 interaction with $Cul2^{Lrr1}$, and these replisomes are on chromatin in mitosis, they are removed from chromatin by p97, which is most likely recruited to chromatin by polyubiquitylated substrates, as inhibition of polyubiquitylation reduces that interaction (Figure 3.23). We cannot, however, exclude the role of Ubxn7 in this process as in our experiment Ubxn7 binding to Cul2 was blocked throughout the experiment.

3.3.3.2. Potential p97 cofactors in mitotic replisome disassembly pathway

We wanted then to determine possible distinct cofactors, which could identify different ubiquitin chains built on terminated helicase. In addition, we wanted to analyse proteins interacting with p97 in mitosis. For this purpose, we immunoprecipitated p97 from mitotic chromatin and then the sample was analysed by mass spectrometry.

I identified cofactors Ufd1-Npl4, Ubxn7, Aspscr1 and p47 interacting with chromatin bound p97 in mitosis. The contributions of the Ufd1-Npl4 heterodimeric major cofactors of p97 in extracting ubiquitylated proteins from chromatin in mitosis is well known. These are: Aurora B or spindle assembly factors XMAP215, TPX2 or Plx1 (Vaz, Halder et al. 2013). Franz et al (Franz, Orth et al. 2011) revealed that the p97/Ufd1-Npl4 core complex regulates CDT-1 degradation upon extraction of Cdc45 and GINS in in *C. elegans* embryos and in *X. laevis* egg extract during mitosis. Moreover, Ufd1 and Npl4 with p97 have already been shown to be essential for mitotic replisome disassembly in *C. elegans* (Gaggioli and Zegerman 2017, Sonneville, Moreno et al. 2017). Besides this, p97 with Ufd1/Npl4 is required for spindle disassembly to exit from mitosis in yeast and *Xenopus* egg extracts (Cao, Nakajima et al. 2003). However, many more Npl4 peptides than Ufd1 peptides have been identified in the p97 IP. Ye et al. (Ye, Meyer et al. 2003), Flierman et al. (Flierman, Ye et al. 2003) and Sato et al. (Sato, Tsuchiya et al. 2019) revealed that Npl4 *via* its NZF domain, which is important for ubiquitin binding, associates with K48-linked and K63-linked ubiquitin chains, Ufd1 through its UT3 domain only binds K48-linked ubiquitin chains in mammals. Mutational analysis revealed that C-terminal domain (CTD) of Npl4 have role in ubiquitin chain specificity and initial binding of the ubiquitin linkage (Bodnar, Kim et al. 2018). The Gambus group recently suggested that K63-linked ubiquitin chains on Mcm7 drives replisome disassembly in mitosis (Priego Moreno, Jones et al. 2019). This result could explain why we

see higher levels of Npl4 than Ufd1 in the mass spectrometry analysis of cofactors interacting with p97 in mitosis. Furthermore, Ufd1 and Npl4 may have separate functions in cells. For example, Heo et al. showed that Vms1 (VCP/Cdc48-associated Mitochondrial Stress-responsive), which has VCP Interaction Motif (VIM), interacts specifically with Cdc48-Npl4 in yeast and mammals. While Cdc48-Npl4-Vms1 complex drives mitochondrial protein degradation, Cdc48-Ufd1 complex promotes Endoplasmic Reticulum associated protein degradation. Likewise, p97-Npl4 complex may be mainly responsible for unloading of Mcm7 modified with K63-linked ubiquitin chains during mitosis

The minor p97 cofactor with the highest number of peptides identified in IP of p97 from mitotic chromatin with accumulated replisomes was Ubxn7, despite the fact that the neddylation inhibitor MLN4924 was present in the experimental setup and should restrict Ubxn7 binding to Cul2. In the previous chapter of my thesis, we suggested that Ubxn7 binding to Cul2 recruits p97 to chromatin for replisome unloading in S phase. However, mitotic replisome unloading does not require Cul2 activity and instead needs TRAIP E3 ligase for ubiquitylation (Deng, Wu et al. 2019, Priego Moreno, Jones et al. 2019, Villa, Fujisawa et al. 2021, Wu, Pellman et al. 2021) and there are no known indications of interactions between Ubxn7 and TRAIP. Surprisingly, even though Ubxn7 had the largest number of peptides identified in the mitotic p97 IP, it was very difficult to detect by western blotting. It is possible that maybe post-translational modifications of Ubxn7 in mitosis are affecting the ability of our antibodies to detect it. However, my mass spectrometry analysis did not identify any posttranslational modification on Ubxn7 in either S phase or mitosis.

The next p97 cofactor with the highest number of peptides identified in IP of p97 from mitotic chromatin with accumulated replisomes was ASPCR1. ASPCR1 (ASPL, TUG, UBXD9) facilitates degradation of misfolded proteins attached to endoplasmic reticulum during Endoplasmic reticulum association degradation (ERAD) (Alberts, Sonntag et al. 2009). Overexpression of ASPL leads to blocking of the ERAD pathway through negatively affecting p97 activity (Orme and Bogan 2012, Cloutier, Lavallee-Adam et al. 2013, Arumughan, Roske et al. 2016). Besides these, the putative yeast orthologue of Aspscr1 is Ubx4, which drives dislocation of ubiquitylated RNA Pol II subunit Rpb1 from chromatin by Cdc48-Ufd1/Npl4-Ubx5 (Ubxn7) in UV treated cells in budding yeast (Verma, Oania et al. 2011). Aspscr1 with Ubxn7 might modulate p97 activity in the degradation of RNA Pol II in human cells (Verma, Oania et al. 2011) . However, its role during mitotic CMG disassembly is not known.

p47 is another major cofactor of p97 that is known to work in membrane fusion Golgi formation (Dreveny, Kondo et al. 2004, Huang, Tang et al. 2016). In addition, Cdc48-Ubx3 (yeast ortholog of p47) in mitotic progression does not directly influence cell cycle but promotes proteasome regulation; this complex also controls degradation of mitotic regulators in *C.elegans* (Chien and Chen 2013). This, in

combination with the fact that only 2 peptides of p47 were identified in p97 IP and none in replisome IP in mitosis, suggests that replisome unloading is not a potential substrate of p97-p47 complex.

Finally, Faf1 was identified in the replisome IP on mitotic chromatin but not in the p97 IP. Surprisingly, while we did not detect any Faf1 peptides in the mitotic p97 IP using mass spectrometry, we could observe low levels of Faf1 co-immunoprecipitating with p97 through western blotting (Figure 3.28.). This suggests that maybe the higher salt concentrations (300mM, used for mass spectrometry of the p97 IP) break the interaction between p97 and Faf1, while low salt concentration (100mM, used for replisome IP) does not. It has been shown in *C.elegans* that Ubxn-3 (orthologue of FAF1) is responsible for CMG removal from chromatin, helping CDC-48 (p97)-Ufd1/Npl4 dependent replisome disassembly during mitosis (Sonneville, Moreno et al. 2017).

3.3.3.3. Potential p97 substrates on mitotic chromatin

Our mass spectrometry results reveal that p97 interacts with CMG helicase components, that are to be unloaded in mitosis from chromatin: Mcm2, Mcm3, Mcm4, Mcm5, Mcm7 and Cdc45. GINS subunits, however, could not be seen, most probably due to their small size contributing relatively few peptides in mass spectrometry analysis. We analysed also which parts of the replisome remained interacting with p97 on mitotic chromatin. While RPA2, RPA3, Spt16, Ssrp1 and Dnmt1-s were found to directly interact with the CMG helicase, RPA1 looks to be interacting with p97. RPA1 was found also as a substrate in S-phase. When replisomes are not unloaded it may still be targeted by p97.

Dnmt1 plays a critical role in DNA methylation in *Xenopus* egg extract. Mortusewicz et al. revealed that Dnmt1 recruitment at the DNA damage sites occurs by PCNA for DNA repair (Mortusewicz, Schermelleh et al. 2005), however, the interaction with p97 has not been shown before.

Heller et al. (Heller, Kang et al. 2011) showed that Topbp1-α, which is one of the important origin firing factors, aids binding of Cdc45 and GINS to Mcm2-7 (Heller, Kang et al. 2011, Gambus 2017) and drives replication initiation (Gambus 2017). In addition, Topbp1 is a major factor in ATR dependent replication stress in S phase (Bass and Cortez 2019). The presence of ongoing replication forks on chromatin can delay mitotic entry through checkpoint activation (Hashimoto and Tanaka 2020) and it is possible that retained replisomes on chromatin in mitosis may activate a form of checkpoint that involves Topbp1. However, p97 with Topb1 interaction has not been previously suggested.

We also identified a number of DNA damage and DNA replication related proteins interacting with p97 in mitosis. CkII α, CkII β, Aurora B, Wrn helicases and Smarcal1 were enriched in the p97 IP, while

ATR, H1foo, Smarca5, Fancd2 and Smc2 were enriched also in the replisome IP. Protein kinase CKII, identified in the p97 IP, associates with p97 through the CSN (COS9 signalosome) complex. CSN regulates de-neddylation and the activity of CRL E3 ubiquitin ligases (Schwechheimer, Serino et al. 2001, Cope, Suh et al. 2002, Zhou, Wee et al. 2003) and activity of ligases, which regulates the ubiquitin dependant degradation of the substrate (Harari-Steinberg and Chamovitz 2004). p97 directly interacts with the CSN complex through the CSN5 subunit. CSN5 binds the C terminal end of p97 *via* its MPN domain (Cayli, Klug et al. 2009). Uhle and colleagues revealed that CSN co-immunoprecipitates the protein kinase CKII which has two subunits: CKII α and CKII β (Uhle, Medalia et al. 2003). Cayli et al. (Cayli, Klug et al. 2009) suggest that CSN interaction with protein kinase CKII controls p97 interaction with p97 substrate processing cofactors through phosphorylation.

CKII is also recruited by CSN to regulate ubiquitin dependent degradation. Together they phosphorylate p53 at Thr155, thereby regulating p53 ubiquitylation by E6AP for proteasomal degradation (Bech-Otschir, Kraft et al. 2001, Uhle, Medalia et al. 2003). p97 directly controls ubiquitylated p53 degradation by the proteasome (Valle, Min et al. 2011). We also detected E6AP ubiquitin ligase in the p97 IP. There is the possibility therefore that E6AP, CK2 and CSN regulate p97 activity in mitosis and maybe even replisome disassembly.

The next DNA damage related protein found in the p97 IP was Smarcal1 which is an annealing helicase. It is recruited to DNA damage sites through interaction with RPA to enable DNA repair (Ciccia, Bredemeyer et al. 2009, Yusufzai, Kong et al. 2009, Ghosal and Chen 2013). It is phosphorylated by ATR to help complete DNA replication and avoid stalled forks (Couch, Bansbach et al. 2013).

WRN belongs to the RecQ DNA helicase family, which has 3'-5' exonuclease and helicase activities (Rossi, Ghosh et al. 2010). It has roles in DNA replication and DNA repair to protect genomic stability (Rossi, Ghosh et al. 2010). The latest data shows that p97 directly interacts with WRN *via* its RQC domain to release it from the nucleolus during DNA damage (Indig, Partridge et al. 2004). WRN might be recruited by p97 to stalled or collapsed replication forks (Ramadan, Halder et al. 2017).

Ramadan and colleagues found that p97 extracted ubiquitylated Aurora B from chromatin during exit from mitosis resulting in chromosome decondensation and nucleus formation by inactivation of Aurora B (Ramadan, Bruderer et al. 2007). However, it has not been shown whether neither E6AP or CKII or Aurora B could modify p97.

A variety of other proteins appeared in the screening. This suggests that p97 has many different cellular roles in the cells apart from DNA replication. For instance, p97 has a novel role in actin regulation (Khong, Lai et al. 2020). Flna, Coronin, Coro1-c and Cttn actin binding proteins might be

potential substrates of p97 in actin regulation. In addition, although p97 interaction with Trafd1, which is a negative feedback regulator for excessive innate immune system (Sanada, Takaesu et al. 2008), has not been reported, p97-Ufd1/Npl4 acts as a regulator for proteasomal degradation during innate immune responses (Hao, Jiao et al. 2015).

3.3.3.4. Posttranslational modifications may regulate p97 activity in the cell cycle

p97 is highly modified by posttranslational modifications (PTMs) including phosphorylation, acetylation (Mori-Konya, Kato et al. 2009, Ewens, Kloppsteck et al. 2010, Hanzelmann and Schindelin 2017), ubiquitylation (Hanzelmann and Schindelin 2017), sumoylation (Hendriks, Lyon et al. 2017), palmitoylation (S-Acylation) (Fang, Zhang et al. 2016), lysine and arginine N-methylation (Kernstock, Davydova et al. 2012), S-glutathionylation (Noguchi, Takata et al. 2005). These modifications control the function of p97 in diverse cellular processes and p97 interactions with its cofactors (Ewens, Kloppsteck et al. 2010, Hanzelmann and Schindelin 2017). Posttranslational modifications can cause structural changes to the protein, alter protein interactions with other proteins, alter protein localisation or can act as a phospho-degron resulting in protein degradation. PTMs are regulated by enzymes, which are able to add or remove these modifications. The N domain, C terminal tail and D1 domain of p97 are exposed to PTMs (Hanzelmann and Schindelin 2017). 66 phosphorylated sites, 38 ubiquitylation sites and 24 acetylation sites on p97 have been identified by proteomics analysis PhosphoSitePlus (PSP, http://www.phosphosite.org/). Phosphorylation and acetylation of p97 have been revealed to help a variety of p97 related processes such as misfolded protein degradation, membrane fusion and transcription factor activation through modifying cofactor binding and regulating subcellular localization (Ewens, Kloppsteck et al. 2010).

In our mass spectrometry analysis, p97 IP from S phase chromatin has identified phosphorylation at Ser5, Thr7, Ser9 and acetylation at Ala2 in the N terminal extension, and ubiquitylation at the Lys295 D1 domain. p97 IP from mitotic chromatin however found phosphorylation at Ser5, Ser702 and Ser718, which are located in the D2 domain, acetylation at Ala2 in the N terminal extension and ubiquitylation on Lys425 and Lys426 in the D1 domain. Ubiquitylation at K295, K425 and K426, and phosphorylation at Ser702 and Ser718 have all been identified before by proteomic analysis *PhosphoSitePlus (PSP, http://www.phosphosite.org/).*

The first 24 amino acids of the N domain are called the N terminal extension and it is important for ATPase activity (Hanzelmann and Schindelin 2017). In addition, phosphorylation at Ser5, Thr7 and Ser9 (S phase p97 IP) and acetylation at Ala5 (in both our S phase and mitotic p97 IP) might regulate

affinity and binding of different cofactors and ubiquitylated substrates. For example, the SHP motif of cofactors (Ufd1 and p47) interacts with hydrophobic residues on the p97 N terminus (Hanzelmann and Schindelin 2016, Le, Kang et al. 2016). Phosphorylation in the N domain of p97 at Thr168 was shown to affect the affinity of binding of cofactors containing the SHP domain (Hanzelmann and Schindelin 2017). This could explain why we identified fewer Ufd1 peptides than Npl4 in the S phase p97 IP.

Phosphorylation of p97 has been identified at several amino acids such as Ser7, Ser352, Ser746, Ser748, Ser784 and Tyr805 (Livingstone, Ruan et al. 2005, Rush, Moritz et al. 2005, Villen, Beausoleil et al. 2007, Mori-Konya, Kato et al. 2009). Phosphorylation at tyrosine or serine residues on p97 contribute to a variety of processes including DNA repair and the ERAD pathway. Li et al. and Schaeffer et al. revealed that Tyr805 phosphorylation of p97 diminished interaction of the PUB/PUL domain of p97 with its cofactors (Li, Zhao et al. 2008, Schaeffer, Akutsu et al. 2014). Phosphorylation by AKT serine threonine kinase at Ser352, Ser746, and Ser748 helps maintain cell survival (Klein, Barati et al. 2005). Yang et al showed that p97 activity was increased by phosphorylation on the C terminal tail at Ser770 (Yang, Lin et al. 2013). It is known that phosphorylation at the C terminal tail of p97 can result in conformational changes, but it does not alter the ATPase activity of p97 (Egerton and Samelson 1994, Niwa, Ewens et al. 2012). In addition, phosphorylation of p97 at the C terminal tail has been found to block the interaction with some proteins such as Ufd3 and PGNase (Zhao, Zhou et al. 2007).

Zhu et al and Shao et al showed that phosphorylation of VCP on Ser784 within the C-terminal tail by ATM, ATR and DNA-PK has critical importance for DNA damage response and cell survival. While DNA damage-induced pSer784 of p97 increases chromatin-associated protein degradation, it leads to decreased binding of p97 to Ufd1/Npl4 and K48-linked polyubiquitylated substrates. Moreover, p97 phosphorylation on Ser784 causes reduces p97 interaction with chromatin. Phosphorylation on Ser784 within the C terminal tail of p97 results therefore in long-range inter-domain conformational changes in order to decrease the interaction of Ufd1/Npl4 at the N domain of p97 (Shao 2020, Zhu, Rogers et al. 2020). Besides this, additional cofactors of p97 may facilitate p97 to access chromatin independently from Ufd1/Npl4 (Shao 2020). Phosphorylation of p97 at Ser784 turns it into a more effective protein segregase, allowing it to disassemble more chromatin-associated substrates (Zhu, Rogers et al. 2020).

Our mass spectrometry data clearly showed that the number of identified peptides of Ufd1/Npl4 interacting with p97 is significantly decreased in mitotic p97 IP compared to the S phase p97 IP. It may be due to phosphorylation within the C terminal tail of p97 or there are other PTMs that we have not found either due to low amount of numbers or due to lack of PTMs enrichment. Moreover, as shown

previously (Shao 2020) if K48-linked substrate binding of p97 decreases once it is phosphorylated at the C terminal tail, p97 unloading of Mcm7 modified with K63-linked ubiquitin chains in mitosis could be due to the phosphorylation of S702 and S718 within C terminal tail. It was also reported that not only phosphorylation of Ser784, but also other phosphorylations within the C terminal tail of p97, such as Ser746 and Ser748 lead to decreased p97 interaction with polyubiquitin chain (Klein, Barati et al. 2005). Therefore, phosphorylation of p97 may generally affect unloading of chromatin-associated substrates upon different stimuli.

Interestingly, although the C terminal tail is unstructured, it associates with the N terminal domain through wrapping around the outside of the D2 domain (Niwa, Ewens et al. 2012). Direct interaction of p97 with its cofactors is affected by phosphorylation of p97 at the N terminal domain. For instance at Thr37 and Ser56 in the hydrophobic interdomain cleft and Tyr110 and Tyr143, to which UBX/UBXL domains of cofactors bind (Hanzelmann and Schindelin 2017).

Acetylation is one of the frequent posttranslational modifications, which plays a role in many critical processes in cells including cell signalling (Verdin and Ott 2015), neurodegenerative diseases (Saha and Pahan 2006), tumorigenesis (Haberland, Johnson et al. 2009, Kalvik and Arnesen 2013) and the stress response (Jones and O'Connor 2011, Ma and Wood 2011), which is reversible. Acetylation, which is catalysed at lysine amino acids in the N terminus of the protein, leads to conformational changes of the protein and, therefore, it affects binding functions to other proteins or DNA. p97 roles in transcription, replication and DNA repair are all modified by acetylation. For example, p97 is translocated to the nucleus in neuronal cells through phosphorylation at Ser612 and Thr613 and acetylation of Lys614 when there are abnormally high levels of proteins such as polyglutamins. In addition, acetylation can affect ubiquitin dependant proteasomal degradation *via* affecting ubiquitylation at the same lysines (Caron, Boyault et al. 2005). Hornbeck et al. showed that all 24 acetylation sites at lysines identified by proteomics analyses overlap with ubiquitylation and sumoylation sites in p97 (Hornbeck, Zhang et al. 2015).

Several lysine residues on p97 are known to be ubiquitylated, while ubiquitin chain linkages are still unknown. A number of E3 ubiquitin ligases interact with p97 directly, such as HOIP E3 ligase (Schaeffer, Akutsu et al. 2014), RNF8 (Singh, Oehler et al. 2019), Ube4a (Baranes-Bachar, Levy-Barda et al. 2018) and indirectly, such as Cul2 E3 ligase, which interacts via the UBX domain of the p97 cofactor Ubxn7 (Alexandru, Graumann et al. 2008). In addition p97 interacts directly with deubiquitylating enzymes i.e. VCIP135 (Uchiyama, Jokitalo et al. 2002), ATAXIN-3 (Boeddrich, Gaumer et al. 2006) and YOD1 (Ernst, Mueller et al. 2009). These ubiquitin ligases and DUBs may interact with p97 to regulate p97 itself but also to regulate p97 substrates. For instance, RNF8 is a critical E3 Ubiquitin ligase during DNA

repair. Singh et al suggested that upon IR promoted genotoxic stress, RNF8 that accumulates at DNA lesion sites can be removed from chromatin by p97 segregase-Ataxin 3 (ATX3) deubiquitinating enzyme in order to balance DNA repair through regulating proteasome-dependent homeostasis of RNF8 (Singh, Oehler et al. 2019).

D1 and D2 domains consist of D1 and D2 ATPase subdomains (the region is rich from α-helix and β sheet) and small D1α and D2α subdomains. As indicated previously (Hanzelmann and Schindelin 2017), ubiquitylation at Lys295 in the D1 ATPase domain of p97 was shown to affect cofactor binding to this domain. Ubiquitylated p97 is then recognised by the cofactors that have at least one ubiquitin binding domain such as Npl4 through NZF or Ubxn7 *via* the UBX domain (Hanzelmann and Schindelin 2017). In addition Chia et al suggests that ATP binding at the D1 domain is necessary for Ufd1/Npl4 binding to the p97 N terminal domain (Chia, Chia et al. 2012). It might be that p97 ubiquitylation at Lys295 leads to increased ATP binding, resulting in more Ufd1/Npl4 recruitment and allowing Ubxn7 binding to p97.

How ubiquitylation of p97 regulates its cellular functions is still unclear, but ubiquitylation may cause conformational changes in the protein and alter its affinity for interaction with cofactors or substrates. The N domain, D1 and D2 domains are known to be target regions for ubiquitylation, but sites have not been identified in the C terminal tail (Hanzelmann and Schindelin 2017).

There is also a possibility that we have not identified all posttranslational modifications on p97 in both stages of the cell cycle. If the level of PTMs was too low for detection due to lack of specific PTM enrichment, we could have missed it.

We identified differential modifications of p97 in S-phase and in mitosis. The potential function of these post translational modifications in the DNA damage response and replication will be very interesting to unravel in the future.

Table 3. 7 Potential modifying enzymes identified in S-phase and in mitosis. p97 was immunoprecipitated from chromatin in S-phase (chromatin treated with NMS-873), or mitosis (chromatin treated with caffeine, MLN4984, NMS-873, Cyclin 1AΔ) and analysed by mass spectrometry. Ubiquitin ligases or kinases are identified for p97 protein in the S phase and mitosis chromatin is indicated, with the peptide numbers were identified with such a modification in brackets.

		IP from S-phase chromatin assembled in extract treated with NMS-873 (TSC)	IP from mitotic chromatin assembled in extract treated with MLN 4924, NMS-873 (TCS)
Ubiquitin ligases	Brca1 (176 kD)	90	0
	E6AP (105 kD)	11	4
	Cul1 (90 kD)	9	0
	WWP2 (85 kD)	6	0
	RNF31 (118 kD)	5	0
	Hectd1 (281 kD)	4	0
	Uhrf1 (87 kD)	3	0
Kinases	ATR (301 kD)	0	56
	WSTF (166 kD)	27	0
	CK II α (41 kD)	10	6
	CK II β (25 kD)	4	5
	Aurora B (41 kD)	0	5

Although it is known that p97 is a subject of post translational modifications, the enzymes responsible for these modifications are less known. Our mass spectrometry of p97 immunoprecipitation from chromatin in S-phase and in mitosis identified a number of protein kinases and ubiquitin ligases interacting with p97 (Figure 3.30). Many of them have been previously linked with p97, which was discussed previously (Section 3.3.1.3. and 3.3.3.3) as potential cofactors or substrates of p97. However, the enzymes identified as interactors can be potentially responsible for the phosphorylation and ubiquitylation of p97, which we identified in S-phase and in mitosis (Table 3.7). For example, WWP2 ubiquitylates the RNAPII subunit RPB1, which is a substrate of p97 for proteasomal degradation, with K48-linked ubiquitin chains (Caron, Pankotai et al. 2019). RNF31 makes a linear ubiquitin chain on its substrate (Schlicher, Wissler et al. 2016), whereas Hectd1 conjugates K63-linked polyubiquitin chains (Tran, Bustos et al. 2013) and Uhrf1 ubiquitylates histone H3 at Lys23 (Nishiyama, Yamaguchi et al. 2013). Furthermore, p97-Ufd1/Npl4 is known to regulate removal of Aurora B from chromatin to exit mitosis in *Xenopus* egg extract (Ramadan, Bruderer et al. 2007) and in human cells (Dobrynin, Popp et al. 2011). WSTF tyrosine protein kinase plays a role in the DNA damage response by phosphorylation of H2AX at Tyr142 (Xiao, Li et al. 2009). However, none of the above ubiquitin ligases or protein kinases have been found in relation to ubiquitylation or phosphorylation of p97 except ATR kinases. Mu et al showed that p97 could be phosphorylated by ATR (a replication stress

master regulator kinase) (Mu, Wang et al. 2007). Therefore, ATR kinase could be a potential modifier of p97

4. DISCUSSION

4.1. Ubxn7 is required for efficient replisome disassembly in S phase

p97 ATP-dependent molecular chaperone (also referred as VCP, Cdc48 and Ter94) is conserved from yeast to mammalian cells (Ye, Tang et al. 2017). p97 provides the segregase activity during replisome disassembly, which is a critical event in DNA replication termination (Dewar, Low et al. 2017, Sonneville, Moreno et al. 2017, Deegan, Mukherjee et al. 2020, Villa, Fujisawa et al. 2021)

We observed that Ubxn7 interacts with p97 and Cul2 and propose a model where $Cul2^{Lrr1}$ recognises terminated CMG helicase and once active interacts also with Ubxn7 during replisome disassembly at the end of DNA replication. Ubxn7, in turn, restricts $Cul2^{Lrr1}$ activity by restricting the length of ubiquitin chains formed on Mcm7 but at the same time bringing p97 to Mcm7 ubiquitylated with such shorter chains. In this way, substrate extraction is driven by p97 and is likely to be most efficient as p97 does not need to first unwind very long ubiquitin chains (Inano, Sato et al. 2020). Although there is a delay in unloading of replisomes in absence of Ubxn7, more $Cul2^{Lrr1}$ is accumulated, as its activity is unrestricted when Ubxn7 is depleted. In this way, more active Cul2 may build longer ubiquitin chains on Mcm7 resulting finally in binding of p97-Ufd1/Npl4 (UN) complex despite the lack of Ubxn7, and disassembly of CMG complex by p97/UN (Bochman 2014). The bridge between $Cul2^{Lrr1}$ and p97 made by Ubxn7 may explain why p97 efficiently unloads helicase ubiquitylated with K48-linked ubiquitin chains by $Cul2^{Lrr1}$ and why inhibition of polyubiquitylation of all substrates (Ubi-NOK addition) leads to accumulation of p97 on chromatin. The increased activity of $Cul2^{Lrr1}$ could compensate for not having Ubxn7. Because without hinderance of Ubxn7, Cul2 may be more active and make very long chain on Mcm7.

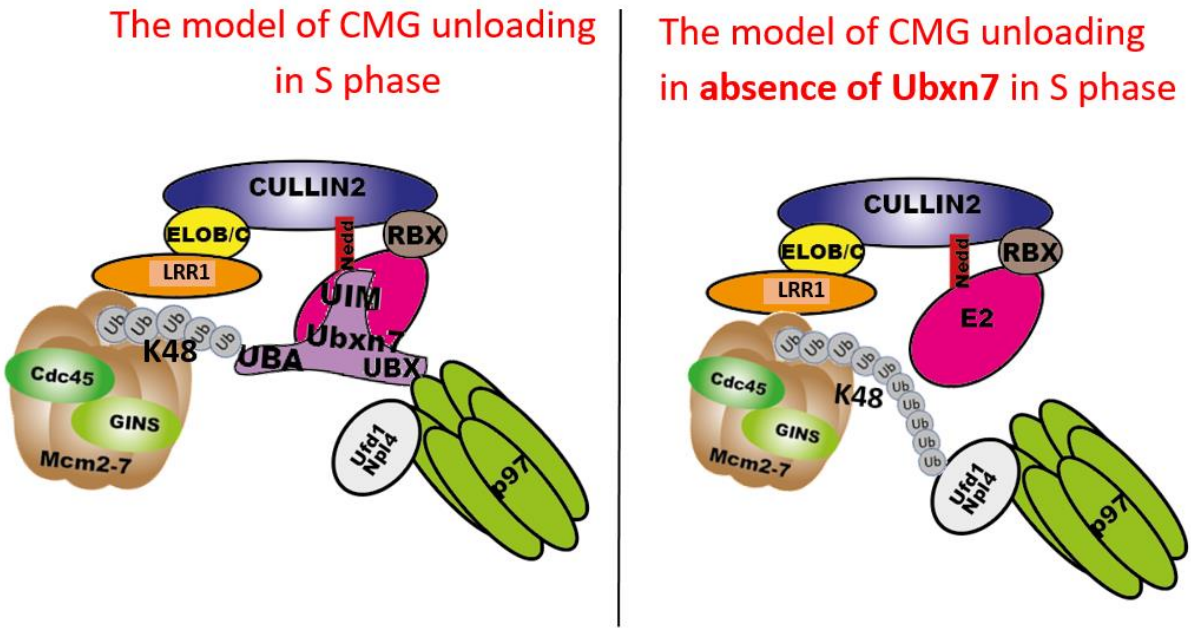

Figure 3.30. A model of terminated CMG unloading in the presence or in the absence of Ubxn7 at the termination of DNA replication in S phase. During termination, $Cul2^{Lrr1}$ recognizes MCM7 within terminated CMG and polyubiquitylates it, while Ubxn7 comes and binds neddylated Cul2. Presence of Ubxn7 restricts $Cul2^{Lrr1}$ activity as a negative regulator. Then this complex recruits p97 for unloading of replisome from chromatin. However, when there is no Ubxn7 during termination, $Cul2^{Lrr1}$ remains bound to terminated CMG keeps polyubiquitylating Mcm7, resulting in very long chains on Mcm7. These long chains can more efficiently recruit p97/Ufd1/Npl4 to extract CMG from chromatin.

Ubxn7 has been shown previously to play a role in a number of different cellular processes and Ubxn7 protein levels are also actively regulated. Ubxn7 protein levels are controlled by the Mul1 ubiquitin ligase to regulate the cellular response to oxidative stress and low oxygen. For example, in times of oxidative stress, Mul1 modifies Ubxn7 with K48-linked ubiquitin chains, resulting in low levels of Ubxn7. A decreased level of Ubxn7 (Di Gregorio, Cilenti et al. 2021) and p97-Ufd1/Npl4 (Ramadan, Bruderer et al. 2007) leads to inactivation of $CRL3^{KEAP1}$ and an increase in NRF2 protein level, which is a key player in the response to oxidative stress. A decreased level of Ubxn7 also causes Cul2 activation, resulting in decreased levels of Hif1α protein. During hypoxia, however, Ubxn7 is overexpressed due to inactive Mul1 and this leads to Cul2 inactivation and increased levels of Hif1α, but does not affect NRF2. Therefore, Hif1α, which cannot degraded by proteasome due to increased level of Ubxn7 and so unable polyubiquitylation functions of Cul2, resulted in glycolysis (Di Gregorio, Cilenti et al. 2021). The important cellular response of hypoxia in the cells activation of DNA damage signalling pathways which resulted in genomic instability and cancer. Prolonged hypoxia promotes impairment of DNA repair pathways such as DNA double-strand break repair, mismatch repair, and nucleotide excision repair (Scanlon and Glazer 2015). Therefore, increased level of Ubxn7 in hypoxic cell could related with tumorigenesis.

Furthermore, separate depletion of p97, Ufd1 or Ubxn7 prevented degradation of nucleotide excision repair Cockayne syndrome group A proteins (CBS), which are ubiquitylated and degraded in UV exposed cells. This suggests that Ubxn7 plays a role in regulation of levels of CBS upon UV irradiation. In support of this, authors also found an accumulation of Ubxn7 on damaged chromatin (Fei, Ma et al. 2017). It shows that CMG helicase could not be unloaded from chromatin upon UV irradiation. It might me this one of the reasons why Ubxn7 could accumulate on UV damaged chromatin. Finally, Ubxn7 downregulation was also shown to reduce p97 recruitment to the chromatin upon UV irradiation, while downregulation of CBS substrate protein did not affect it (He, Zhu et al. 2016). All these data reveal that Ubxn7 acts to stabilise p97-substrate complex, and p97 and Ubxn7 are independently recruited to the ubiquitylated substrates (He, Zhu et al. 2016). These studies support our experiments in that inhibition of p97 did not affect binding of Ubxn7 to the chromatin. On the contrary, inactive p97 led to accumulation of Ubxn7.

Faf1 is a critical cofactor which stabilizes replication forks in *C.elegans* and human cell lines (Franz, Ackermann et al. 2016) and it is required for efficient unloading of replisome with p97-Ufd1/Npl4 core complex in mitosis (Sonneville, Moreno et al. 2017). Our studies revealed that Faf1 interacts with p97 in both S phase and mitosis. Although Faf1 seems to bind to chromatin differently than Ubxn7, more experiments are needed to confirm that this is reproducible.

4.2. Ubxn7 in Cancer and Potential Cancer Therapy Target

Ubxn7 induces cell proliferation, migration and inhibits apoptosis in hepatocellular cancer (Yao, Zhang et al. 2020). Increased level of RNA expression of Ubxn7 was observed in liver cancer. In addition, different types of mutations for Ubxn7 have been observed in various cancer cell lines. For example, whereas missense mutations of Ubxn7 were observed in skin basal cell carcinoma (Sharpe, Pau et al. 2015), lung adenocarcinoma, colon carcinoma (Mouradov, Sloggett et al. 2014) and cerebellum glioma (Nomura, Mukasa et al. 2017), frameshift insertion of Ubxn7 was seen in endometrioid carcinoma (Wu, Veras et al. 2017) and frameshift deletion was observed in malignant melanoma (https://cancer.sanger.ac.uk/cosmic/gene/analysis?ln=UBXN7#overview).

Furthermore, increased level of Ubxn7 RNA expression has seen in lung cancer, breast cancer, head and neck cancer, endometrial cancer, urethral cancer, stomach cancer, colorectal cancer, liver cancer, prostate cancer, ovaria cancer, cervical and pancreatic cancer

(https://www.proteinatlas.org/ENSG00000163960-UBXN7/pathology). Faulty expression of Ubxn7 could lead to increase on cell proliferation and evasion of apoptosis, which can develop in cancer cells. However, even though increased level of Ubxn7 expression has not been targeted as therapeutic agent, understanding of its mechanism is important for cancer treatment.

4.3. Cancer therapy targeting for p97

DNA helicases unwind double stranded DNA in a number of DNA related processes such as DNA replication and repair to protect genome stability (Croteau, Popuri et al. 2014). Any faults in these processes cause genome instability and thereby promote proliferative diseases such as cancers and other life-threatening diseases (Bochman 2014). Discovery of novel drugs to kill cancer is of the upmost importance. Indeed, there are drugs now available, which block replisome activity, and which could develop into potential anticancer therapies. More specifically, these target the proteins interacting with MCMs to inhibit replication (Rizwani, Alexandrow et al. 2009) and block phosphorylation of MCMs to inhibit cell proliferation (Huang, Rong et al. 2005).

Apart from targeting the helicase itself, several research groups have now shown evidence that loss or overexpression of p97 or its adaptors is linked with a variety of cancers and diseases including breast, colorectal, lung and pancreatic cancers, cystic fibrosis and neurodegenerative disorders (Vij 2008, Haines 2010, Min, Bodas et al. 2011, Li, Huang et al. 2021). p97 with its cofactors interacts with different proteins associated with tumorigenesis, such as Hif1α (Bandau, Knebel et al. 2012) and Aurora B (overexpressed in cancer cells) (Ramadan, Halder et al. 2017) and plays an important role in maintaining cancer cells proliferation. Understanding the role of p97, its cofactors and its substrates in cell proliferation may help to discover or develop anticancer drugs. For example bortezomib (Velcade), which is a proteasome inhibitor, is used as a treatment for multiple myeloma, mantle, cell lymphoma (Shah and Orlowski 2009), whilst non-small cell lung carcinoma tumour growth was experimentally shown to be reduced (Valle, Min et al. 2011). A novel p97 ATPase inhibitor OSSL_325096 works to block cell proliferation and promote apoptosis in multiple myeloma cells (Nishimura, Radwan et al. 2019). Therefore, drugs targeting p97 and cofactors have therapeutic importance.

Altogether, we should determine the mechanism of p97 action and activation, and determine the endogenous factors affecting interactions between p97, Cul2, Ubxn7 and their substrate, the CMG

replicative helicase. This knowledge will help in designing new and better inhibitors that can be used against cancers in the future.

4.4. The potential p97 cofactors in mitosis

The Mcm7 subunit of the CMG complex is ubiquitylated with a K48-linked ubiquitin chain in S phase (Maric, Maculins et al. 2014, Moreno, Bailey et al. 2014). This ubiquitylation is performed by SCF^{Dia2} in yeast (Maric, Maculins et al. 2014) and $Cul2^{Lrr1}$ in *C. elegans* (Sonneville, Moreno et al. 2017), *Xenopus* (Moreno, Bailey et al. 2014, Dewar, Low et al. 2017, Sonneville, Moreno et al. 2017) and in mouse ES cells (Villa, Fujisawa et al. 2021). The ubiquitylated CMG is then recognised and disassembled from the chromatin by the p97 with its cofactors Ufd1-Npl4 in yeast (Maric, Mukherjee et al. 2017), worms and frog (Sonneville, Moreno et al. 2017) and mouse (Villa, Fujisawa et al. 2021).

Mcm7 is only unloaded when ubiquitylated with K48-linked ubiquitin chains by $Cul2^{Lrr1}$ in S-phase. When p97 function is inhibited in S phase however, Mcm7 can be modified with K6 and K63-linked ubiquitin chains by Traip E3 ligase, but they do not stimulate replisome unloading. The reason could be that the p97 cofactor complex cannot recognise K6-linked ubiquitin chains due to a lack of appropriate cofactor or appropriate posttranslational modification (Priego Moreno, Jones et al. 2019). This suggests that p97 segregase activity is strictly regulated by not only specific substrate but also specific ubiquitin chains (Morreale, Conforti et al. 2009) (Bruderer, Brasseur et al. 2004). There is a variety of cofactors binding p97 through different domains, which recognise specific ubiquitin linkages. It is likely that the combination of cofactors interacting with p97 allows it to distinguish between different ubiquitin chain types on substrates and we explored the process of replisome disassembly to dissect the mechanism of cofactors interaction and cooperation.

We identified p97 cofactors Ufd1/Npl4 and Ubxn7, which associate with chromatin-bound p97 in mitosis. The Ufd1/Npl4 heterodimer is known to work with p97 to unload CMG from chromatin during mitosis in *C.elegans* (Gaggioli and Zegerman 2017), therefore this heterodimeric cofactor complex could regulate mitotic replisome disassembly in *Xenopus* egg extract. Ubxn7 was found to immunoprecipitate with K63 linked chains in an *in vitro* experiment, but it has not been followed up and we do not yet know the lysine specificity *in vivo*. Ubxn7 has not previously been shown to interact with K6-linked chains, nor is it known to interact with Traip. Even though we did not initially identify the Faf1 cofactor in mass spectrometry analysis, Faf1 did co-immunoprecipitate with p97, when lower levels of salt concentration were used. Moreover, Faf1 recognises both K48 and K63-linked ubiquitin chains (Kloppsteck, Ewens et al. 2012, Stach and Freemont 2017). It might be a potential cofactor for

p97, working with Ufd1/Npl4 to regulate mitotic CMG disassembly, as in *C. elegans* (Gaggioli and Zegerman 2017, Sonneville, Moreno et al. 2017).

4.5. Posttranslational modification of p97 may regulate its interaction with complexes and cofactors

We wanted to explore how the modifications of p97 control the formation of complexes with cofactors in S phase and mitosis. p97 is known to be highly post-translationally modified in proteome wide screens (Hanzelmann and Schindelin 2017). Many PTMs have been found in the N-terminal extension of p97, which includes the first 24 amino acids (Hanzelmann and Schindelin 2017), allowing regulation of p97 functions (Schuller, Beck et al. 2016). The N-terminal extension has a regulating role in ATPase activity: it is flexible and is normally in the 'down' conformation when ADP is bound to p97. It converts to the "up" state upon ATP binding, allowing for the N domain to insert into the D2 domain like a swing (Schuller, Beck et al. 2016). The N terminal and D1 domains also contain identified PTMs (Hanzelmann and Schindelin 2017). Furthermore, interaction of p97 with cofactors and ubiquitylated substrates were shown to be affected by phosphorylation at the N terminal domain (Mori-Konya, Kato et al. 2009). For example phosphorylation of the hydrophobic residue in the N-terminal domain, which interacts with the SHP domains of Ufd1 and p47, affects the affinity of these interactions (Hanzelmann and Schindelin 2017). Even though we did not find any modification in the N domain, phosphorylation of p97 at Ser5, Thr7 and Ser9 on the N-terminal extension can affect cofactor and substrates binding and assembly with p97. Fewer Ufd1 peptides were identified in the S phase p97 IP than Npl4, which may support this. In addition, acetylation or/and phosphorylation of the N-terminal extension (Ser5, Thr7, Ser9, Ala5) may inhibit the N-terminus insertion into the D2 domain, which would result in a block to the substrate binding channel.

The D1 ATPase domain has a role in cofactor binding to this domain, resulting in recognition of ubiquitylated substrates by the cofactor. It is known that ATP binding to the D1 domain promotes the interaction between the Ufd1/Npl4 heterodimeric cofactor and the N domain of p97. Therefore, we suggest that ubiquitylation at sites lys295, lys425 and lys426, which are located in the D1 domain, could promote ATP binding and recruitment of Ufd1/Npl4 and potentially Ubxn7 to p97. Like the D1 domain, D2α also affects p97 ATPase activity (Mori-Konya, Kato et al. 2009). Therefore, it is possible that phosphorylation at Ser702 and Ser708 on mitotic p97 could affect p97 ATPase activity in mitosis.

Even though a number of p97 modifications have been identified in both S phase and mitosis, the enzymes which remove or add these modifications are less well known. Our mass spectrometry

analysis is therefore very useful as we identified some kinases and ligases, which are potential post translational regulators of p97. Among them, only the DNA damage response kinase ATR has been previously shown to interact with p97, potentially being responsible for phosphorylation of p97 at Ser784 (He, Zhu et al. 2016).

4.6. Potential substrates of p97 in S phase and mitosis

RPA1 was identified in our S-phase p97 IP when replisomes are not unloaded. It could therefore be a potential substrate of p97 in this process. Previously it has been shown that in response to DNA damage caused by mitomycin C (MMC), ATR and ATM kinases phosphorylate RFWD3 E3 ligase and induce its ubiquitin ligase activity (Inano, Sato et al. 2020), allowing ubiquitylation of RPA and disassembly by p97 and proteasomal degradation (Inano, Sato et al. 2020). Chromatin unloading of RPA from DNA damage sites was also shown to promote homologous recombination (HR) (Inano, Sato et al. 2020).

4.7. Conclusion and Future Direction

Given my results so far, I would speculate that Ubxn7 interacts with the neddylated, active form of $Cul2^{Lrr1}$ and that these two together are recruited to the terminating helicase whilst also recruiting the p97 core complex in S phase. This would mean, interestingly, that p97 is not recruited to the chromatin through just binding to ubiquitylated substrates. During DNA replication termination, Mcm7 is polyubiquitylated by Cul2 and extracted by p97. The interaction of Cul2 and p97 through Ubxn7 may allow p97 recognition and unloading of replisome once it has been modified with K48-linked ubiquitin chains by $Cul2^{Lrr1}$.

On the other hand, during mitosis, p97 is probably recruited to chromatin by polyubiquitylated substrates. In this case, CMG helicase is modified with K63-linked ubiquitin chains and removed from mitotic chromatin by p97-Ufd1/Npl4. Further experiments are needed to fully determine the roles of both Ubxn7 and Faf1 in replisome unloading in mitosis.

RPA1 has been shown to be ubiquitylated in the DNA damage response (Elia, Wang et al. 2015). However, it could be a potential substrate of p97 in unperturbed replication. Indeed, we identified it in our mass spectrometry results both from S phase and mitosis p97 IP. We also identified ATR kinase in our mass spectrometry of p97 IP in mitosis. We believe this suggests p97 to be a substrate of ATR,

rather than ATR being a substrate of p97, as p97 has previously been shown to be phosphorylated by ATR kinase in the DNA damage response (Mu, Wang et al. 2007). Further investigations are need to be done to understand the new interactors of p97.

It has been shown that the functions of p97 are regulated by posttranslational modifications (Hanzelmann and Schindelin 2017). We hypothesise that these modifications affect and change p97 interactions with specific cofactors in S phase and mitosis. IP of p97 in both S phase and mitosis should be enriched in terms of PTMs before a new Mass spectrometry analysis. These modifications should revaluate how affect regulation of p97 functions and cofactors interaction.

Overall, we propose that Ubxn7 regulates the activity of $Cul2^{Lrr1}$ and p97 and interplays with Faf1 to direct p97 specifically to terminated replisome modified with different types of ubiquitin chains in S-phase and mitosis. Furthermore, the specific combinations of cofactors in higher-order complex assemblies are regulated by its posttranslational modifications and provide chain type specificity.

Future experiments

During my project, I analysed the patterns of chromatin binding of p97, Ubxn7 and other proteins involved in replisome unloading process. I used these analyses to extrapolate the information of p97 and Ubxn7 interaction with post-termination replisome. However, there can be other substrates on chromatin that can direct p97 and Ubxn7 chromatin binding. It remains therefore to be confirmed whether p97 and Ubxn7 direct interaction with replisome is regulated in analogous way as the chromatin binding of these proteins. One way to do this would be to perform an immunoprecipitation of GINS as a CMG helicase member from S phase and mitotic chromatin, in the presence of different inhibitors.

Upon analysing the chromatin binding pattern of Ubxn7 I concluded that Ubxn7 interacts specifically with active neddylated Cul2. However, it will be important to see whether the direct interaction between Ubxn7 with Cul2 depends on neddylation of Cul2 in *Xenopus* egg extract with one clear IP experiment i.e., that of Cul2 from chromatin upon supplementation of extract with Nedd8 inhibitor MLN4924.

We propose that Ubxn7 bridges p97 with $Cul2^{Lrr1}$ on chromatin at the terminated replisome. This explains why inhibition of polyubiquitylation with Ubi-NOK stimulates chromatin binding of p97. It would be interesting to test this directly by analysing chromatin binding of p97 in mock and Ubxn7 depleted extract, upon addition of Ubi-NOK; accumulation of p97 should be reduced without Ubxn7 to confirm our hypothesis. Furthermore, how does Ubxn7 affect the activity of $Cul2^{Lrr1}$? Is the ubiquitin

chain length on Mcm7 increased upon Ubxn7 depletion? Are these long chains needed for recruitment of p97 to the chromatin?

If granted more time, I would like to utilise more the Ubxn7 mutants I have generated. It has been shown that Ubxn7 interacts with Cul2 through its UIM domain (Bandau, Knebel et al. 2012). Even though we have seen that the UIM mutant affects Cul2 interaction with chromatin, an important control experiment would be to find out whether Cul2 interacts with Ubxn7 through its UIM domain in *Xenopus* egg extract. Having confirmed this, it will be important to determine whether the delays in replisome unloading and increased Cul2 level in the Ubxn7 immunodepleted extract can be rescued by the recombinant mutants of Ubxn7.

Some further questions, which could also be explored in the future: whether Ubxn7 and Faf1 play roles together or independently in regulation of replisome disassembly. Therefore, we need to understand whether p97, Ufd1, Npl4, Faf1 and Ubxn7 co-immunoprecipitate together in the same complex or not and act as separate p97-substrate protein complexes. Analysis of the chromatin binding pattern of Faf1 in Ubxn7 depleted extract would also help us to understand whether Faf1 works with Ubxn7 in the same pathway or independently. Later, understanding the importance of Ubxn7 and Faf1 to replisome unloading in S-phase and mitosis is essential. UBXN-3 (worm ortholog of Faf1) with p97/Ufd1-Npl4 is responsible for replisome unloading in *C. elegans* during mitosis (Sonneville, Moreno et al. 2017). It will be important to determine whether Faf1 is required for CMG disassembly in S phase and mitosis.

Posttranslational modifications of p97 can affect its localization and interactions (Hanzelmann and Schindelin 2017). It is therefore critical to deeply understand the role of posttranslational modifications on p97 in S-phase and in mitosis and which are the determined enzymes important for particular modifications. More widely, the mechanism of replisome disassembly, with a substrate and chain type specific unloading by p97, allows us also to investigate how different types of ubiquitin chains that are built on Mcm7 are recognised by specific p97 cofactors and how they stimulate particular types of p97 complexes binding.

5. LIST OF REFERENCES

Abbas, T., M. A. Keaton and A. Dutta (2013). "Genomic instability in cancer." Cold Spring Harb Perspect Biol 5(3): a012914.

Acs, K., M. S. Luijsterburg, L. Ackermann, F. A. Salomons, T. Hoppe and N. P. Dantuma (2011). "The AAA-ATPase VCP/p97 promotes 53BP1 recruitment by removing L3MBTL1 from DNA double-strand breaks." Nat Struct Mol Biol 18(12): 1345-1350.

Aguiar, B. G., C. Dumas, H. Maaroufi, P. K. Padmanabhan and B. Papadopoulou (2020). "The AAA + ATPase valosin-containing protein (VCP)/p97/Cdc48 interaction network in Leishmania." Sci Rep 10(1): 13135.

Akopian, D. and M. Rape (2017). "Conducting the finale of DNA replication." Genes Dev 31(3): 226-227.

Alberts, S. M., C. Sonntag, A. Schafer and D. H. Wolf (2009). "Ubx4 modulates cdc48 activity and influences degradation of misfolded proteins of the endoplasmic reticulum." J Biol Chem 284(24): 16082-16089.

Alexandru, G., J. Graumann, G. T. Smith, N. J. Kolawa, R. Fang and R. J. Deshaies (2008). "UBXD7 binds multiple ubiquitin ligases and implicates p97 in HIF1alpha turnover." Cell 134(5): 804-816.

Aquila, L. and B. S. Atanassov (2020). "Regulation of Histone Ubiquitination in Response to DNA Double Strand Breaks." Cells 9(7).

Arias, E. E. and J. C. Walter (2007). "Strength in numbers: preventing rereplication via multiple mechanisms in eukaryotic cells." Genes Dev 21(5): 497-518.

Arumughan, A., Y. Roske, C. Barth, L. L. Forero, K. Bravo-Rodriguez, A. Redel, S. Kostova, E. McShane, R. Opitz, K. Faelber, K. Rau, T. Mielke, O. Daumke, M. Selbach, E. Sanchez-Garcia, O. Rocks, D. Panakova, U. Heinemann and E. E. Wanker (2016). "Quantitative interaction mapping reveals an extended UBX domain in ASPL that disrupts functional p97 hexamers." Nat Commun 7: 13047.

Arunkumar, A. I., M. E. Stauffer, E. Bochkareva, A. Bochkarev and W. J. Chazin (2003). "Independent and coordinated functions of replication protein A tandem high affinity single-stranded DNA binding domains." J Biol Chem 278(42): 41077-41082.

Asher, G., P. Tsvetkov, C. Kahana and Y. Shaul (2005). "A mechanism of ubiquitin-independent proteasomal degradation of the tumor suppressors p53 and p73." Genes Dev 19(3): 316-321.

Baek, K., D. C. Scott and B. A. Schulman (2020). "NEDD8 and ubiquitin ligation by cullin-RING E3 ligases." Curr Opin Struct Biol 67: 101-109.

Bailey, R., S. Priego Moreno and A. Gambus (2015). "Termination of DNA replication forks: "Breaking up is hard to do"." Nucleus 6(3): 187-196.

Bambara, R. A., R. S. Murante and L. A. Henricksen (1997). "Enzymes and reactions at the eukaryotic DNA replication fork." J Biol Chem 272(8): 4647-4650.

Banchenko, S., A. Arumughan, S. Petrovic, D. Schwefel, E. E. Wanker, Y. Roske and U. Heinemann (2019). "Common Mode of Remodeling AAA ATPases p97/CDC48 by Their Disassembling Cofactors ASPL/PUX1." Structure 27(12): 1830-1841 e1833.

Bandau, S., A. Knebel, Z. O. Gage, N. T. Wood and G. Alexandru (2012). "UBXN7 docks on neddylated cullin complexes using its UIM motif and causes HIF1alpha accumulation." BMC Biol 10: 36.

Baranes-Bachar, K., A. Levy-Barda, J. Oehler, D. A. Reid, I. Soria-Bretones, T. C. Voss, D. Chung, Y. Park, C. Liu, J. B. Yoon, W. Li, G. Dellaire, T. Misteli, P. Huertas, E. Rothenberg, K. Ramadan, Y. Ziv and Y. Shiloh (2018). "The Ubiquitin E3/E4 Ligase UBE4A Adjusts Protein Ubiquitylation and Accumulation at Sites of DNA Damage, Facilitating Double-Strand Break Repair." Molecular Cell 69(5): 866-+.

Bass, T. E. and D. Cortez (2019). "Quantitative phosphoproteomics reveals mitotic function of the ATR activator ETAA1." J Cell Biol 218(4): 1235-1249.

Bech-Otschir, D., R. Kraft, X. Huang, P. Henklein, B. Kapelari, C. Pollmann and W. Dubiel (2001). "COP9 signalosome-specific phosphorylation targets p53 to degradation by the ubiquitin system." EMBO J 20(7): 1630-1639.

Bell, S. P. and K. Labib (2016). "Chromosome Duplication in Saccharomyces cerevisiae." Genetics 203(3): 1027-1067.

Bennett, C. B., A. L. Lewis, K. K. Baldwin and M. A. Resnick (1993). "Lethality induced by a single site-specific double-strand break in a dispensable yeast plasmid." Proc Natl Acad Sci U S A 90(12): 5613-5617.

Berndsen, C. E. and C. Wolberger (2014). "New insights into ubiquitin E3 ligase mechanism." Nat Struct Mol Biol 21(4): 301-307.

Besche, H. C., W. Haas, S. P. Gygi and A. L. Goldberg (2009). "Isolation of mammalian 26S proteasomes and p97/VCP complexes using the ubiquitin-like domain from HHR23B reveals novel proteasome-associated proteins." Biochemistry 48(11): 2538-2549.

Beskow, A., K. B. Grimberg, L. C. Bott, F. A. Salomons, N. P. Dantuma and P. Young (2009). "A conserved unfoldase activity for the p97 AAA-ATPase in proteasomal degradation." J Mol Biol 394(4): 732-746.

Blackford, A. N. and S. P. Jackson (2017). "ATM, ATR, and DNA-PK: The Trinity at the Heart of the DNA Damage Response." Molecular Cell 66(6): 801-817.

Blow, J. J. and R. A. Laskey (1986). "Initiation of DNA replication in nuclei and purified DNA by a cell-free extract of Xenopus eggs." Cell 47(4): 577-587.

Bochkareva, E., S. Korolev, S. P. Lees-Miller and A. Bochkarev (2002). "Structure of the RPA trimerization core and its role in the multistep DNA-binding mechanism of RPA." EMBO J 21(7): 1855-1863.

Bochman, M. L. (2014). "Roles of DNA helicases in the maintenance of genome integrity." Mol Cell Oncol 1(3): e963429.

Bodnar, N. and T. Rapoport (2017). "Toward an understanding of the Cdc48/p97 ATPase." F1000Res 6: 1318.

Bodnar, N. O., K. H. Kim, Z. Ji, T. E. Wales, V. Svetlov, E. Nudler, J. R. Engen, T. Walz and T. A. Rapoport (2018). "Structure of the Cdc48 ATPase with its ubiquitin-binding cofactor Ufd1-Npl4." Nat Struct Mol Biol 25(7): 616-622.

Boeddrich, A., S. Gaumer, A. Haacke, N. Tzvetkov, M. Albrecht, B. O. Evert, E. C. Muller, R. Lurz, P. Breuer, N. Schugardt, S. Plassmann, K. Xu, J. M. Warrick, J. Suopanki, U. Wullner, R. Frank, U. F. Hartl, N. M. Bonini and E. E. Wanker (2006). "An arginine/lysine-rich motif is crucial for VCP/p97-mediated modulation of ataxin-3 fibrillogenesis." EMBO J 25(7): 1547-1558.

Bogan, J. S., N. Hendon, A. E. McKee, T. S. Tsao and H. F. Lodish (2003). "Functional cloning of TUG as a regulator of GLUT4 glucose transporter trafficking." Nature 425(6959): 727-733.

Botstein, D. and G. R. Fink (2011). "Yeast: an experimental organism for 21st Century biology." Genetics 189(3): 695-704.

Brownell, J. E., M. D. Sintchak, J. M. Gavin, H. Liao, F. J. Bruzzese, N. J. Bump, T. A. Soucy, M. A. Milhollen, X. Yang, A. L. Burkhardt, J. Ma, H. K. Loke, T. Lingaraj, D. Wu, K. B. Hamman, J. J. Spelman, C. A. Cullis, S. P. Langston, S. Vyskocil, T. B. Sells, W. D. Mallender, I. Visiers, P. Li, C. F. Claiborne, M. Rolfe, J. B. Bolen and L. R. Dick (2010). "Substrate-assisted inhibition of ubiquitin-like protein-activating enzymes: the NEDD8 E1 inhibitor MLN4924 forms a NEDD8-AMP mimetic in situ." Mol Cell 37(1): 102-111.

Bruderer, R. M., C. Brasseur and H. H. Meyer (2004). "The AAA ATPase p97/VCP interacts with its alternative co-factors, Ufd1-Npl4 and p47, through a common bipartite binding mechanism." Journal of Biological Chemistry 279(48): 49609-49616.

Buchberger, A., H. Schindelin and P. Hanzelmann (2015). "Control of p97 function by cofactor binding." FEBS Lett 589(19 Pt A): 2578-2589.

Buchberger, A., H. Schindelin and P. Hanzelmann (2015). "Control of p97 function by cofactor binding." Febs Letters 589(19): 2578-2589.

Bulatov, E. and A. Ciulli (2015). "Targeting Cullin-RING E3 ubiquitin ligases for drug discovery: structure, assembly and small-molecule modulation." Biochem J 467(3): 365-386.

Burgers, P. M. (2009). "Polymerase dynamics at the eukaryotic DNA replication fork." J Biol Chem 284(7): 4041-4045.

Callis, J. (2014). "The ubiquitination machinery of the ubiquitin system." Arabidopsis Book 12: e0174.
Cao, K., R. Nakajima, H. H. Meyer and Y. Zheng (2003). "The AAA-ATPase Cdc48/p97 regulates spindle disassembly at the end of mitosis." Cell 115(3): 355-367.

Cappadocia, L. and C. D. Lima (2018). "Ubiquitin-like Protein Conjugation: Structures, Chemistry, and Mechanism." Chem Rev 118(3): 889-918.

Caren, H., A. Holmstrand, R. M. Sjoberg and T. Martinsson (2006). "The two human homologues of yeast UFD2 ubiquitination factor, UBE4A and UBE4B, are located in common neuroblastoma deletion regions and are subject to mutations in tumours." European Journal of Cancer 42(3): 381-387.

Caron, C., C. Boyault and S. Khochbin (2005). "Regulatory cross-talk between lysine acetylation and ubiquitination: role in the control of protein stability." Bioessays 27(4): 408-415.

Caron, P., T. Pankotai, W. W. Wiegant, M. A. X. Tollenaere, A. Furst, C. Bonhomme, A. Helfricht, A. de Groot, A. Pastink, A. C. O. Vertegaal, M. S. Luijsterburg, E. Soutoglou and H. van Attikum (2019). "WWP2 ubiquitylates RNA polymerase II for DNA-PK-dependent transcription arrest and repair at DNA breaks." Genes Dev 33(11-12): 684-704.

Caruso, M. E., S. Jenna, M. Bouchecareilh, D. L. Baillie, D. Boismenu, D. Halawani, M. Latterich and E. Chevet (2008). "GTPase-mediated regulation of the unfolded protein response in Caenorhabditis elegans is dependent on the AAA+ ATPase CDC-48." Mol Cell Biol 28(13): 4261-4274.

Cayli, S., J. Klug, J. Chapiro, S. Frohlich, G. Krasteva, L. Orel and A. Meinhardt (2009). "COP9 signalosome interacts ATP-dependently with p97/valosin-containing protein (VCP) and controls the ubiquitination status of proteins bound to p97/VCP." J Biol Chem 284(50): 34944-34953.

Chang, S., R. H. Wang, K. Akagi, K. A. Kim, B. K. Martin, L. Cavallone, C. Kathleen Cuningham Foundation Consortium for Research into Familial Breast, D. C. Haines, M. Basik, P. Mai, E. Poggi, C. Isaacs, L. M. Looi, K. S. Mun, M. H. Greene, S. W. Byers, S. H. Teo, C. X. Deng and S. K. Sharan (2011). "Tumor suppressor BRCA1 epigenetically controls oncogenic microRNA-155." Nat Med 17(10): 1275-1282

Chia, W. S., D. X. Chia, F. Rao, S. Bar Nun and S. Geifman Shochat (2012). "ATP binding to p97/VCP D1 domain regulates selective recruitment of adaptors to its proximal N-domain." PLoS One 7(12): e50490.

Chien, C. Y. and R. H. Chen (2013). "Cdc48 chaperone and adaptor Ubx4 distribute the proteasome in the nucleus for anaphase proteolysis." J Biol Chem 288(52): 37180-37191.

Ciccia, A., A. L. Bredemeyer, M. E. Sowa, M. E. Terret, P. V. Jallepalli, J. W. Harper and S. J. Elledge (2009). "The SIOD disorder protein SMARCAL1 is an RPA-interacting protein involved in replication fork restart." Genes Dev 23(20): 2415-2425.

Cilenti, L., J. Di Gregorio, C. T. Ambivero, T. Andl, R. Liao and A. S. Zervos (2020). "Mitochondrial MUL1 E3 ubiquitin ligase regulates Hypoxia Inducible Factor (HIF-1alpha) and metabolic reprogramming by modulating the UBXN7 cofactor protein." Sci Rep 10(1): 1609.

Cloutier, P., M. Lavallee-Adam, D. Faubert, M. Blanchette and B. Coulombe (2013). "A newly uncovered group of distantly related lysine methyltransferases preferentially interact with molecular chaperones to regulate their activity." PLoS Genet 9(1): e1003210.

Collart, C., N. D. L. Owens, L. Bhaw-Rosun, B. Cooper, E. De Domenico, I. Patrushev, A. K. Sesay, J. N. Smith, J. C. Smith and M. J. Gilchrist (2014). "High-resolution analysis of gene activity during the Xenopus mid-blastula transition." Development 141(9): 1927-1939.

Contino, G., F. Amati, S. Pucci, E. Pontieri, F. Pichiorri, A. Novelli, A. Botta, R. Mango, A. M. Nardone, F. C. Sangiuolo, G. Citro, L. G. Spagnoli and G. Novelli (2004). "Expression analysis of the gene encoding for the U-box-type ubiquitin ligase UBE4A in human tissues." Gene 328: 69-74.

Cope, G. A. and R. J. Deshaies (2003). "COP9 signalosome: a multifunctional regulator of SCF and other cullin-based ubiquitin ligases." Cell 114(6): 663-671.

Cope, G. A., G. S. Suh, L. Aravind, S. E. Schwarz, S. L. Zipursky, E. V. Koonin and R. J. Deshaies (2002). "Role of predicted metalloprotease motif of Jab1/Csn5 in cleavage of Nedd8 from Cul1." Science 298(5593): 608-611.

Couch, F. B., C. E. Bansbach, R. Driscoll, J. W. Luzwick, G. G. Glick, R. Betous, C. M. Carroll, S. Y. Jung, J. Qin, K. A. Cimprich and D. Cortez (2013). "ATR phosphorylates SMARCAL1 to prevent replication fork collapse." Genes Dev 27(14): 1610-1623.

Croteau, D. L., V. Popuri, P. L. Opresko and V. A. Bohr (2014). "Human RecQ Helicases in DNA Repair, Recombination, and Replication." Annual Review of Biochemistry, Vol 83 83: 519-552.

Cvetic, C. and J. C. Walter (2005). "Eukaryotic origins of DNA replication: could you please be more specific?" Seminars in Cell & Developmental Biology 16(3): 343-353.

Da Costa, I. C. and C. K. Schmidt (2020). "Ubiquitin-like proteins in the DNA damage response: the next generation." Essays Biochem 64(5): 737-752.

Dantuma, N. P. and T. Hoppe (2012). "Growing sphere of influence: Cdc48/p97 orchestrates ubiquitin-dependent extraction from chromatin." Trends Cell Biol 22(9): 483-491.

Davis, E. J., C. Lachaud, P. Appleton, T. J. Macartney, I. Nathke and J. Rouse (2012). "DVC1 (C1orf124) recruits the p97 protein segregase to sites of DNA damage." Nat Struct Mol Biol 19(11): 1093-1100.
de Bie, P. and A. Ciechanover (2011). "Ubiquitination of E3 ligases: self-regulation of the ubiquitin system via proteolytic and non-proteolytic mechanisms." Cell Death Differ 18(9): 1393-1402.

Deegan, T. D. and J. F. X. Diffley (2016). "MCM: one ring to rule them all." Current Opinion in Structural Biology 37: 145-151.

Deegan, T. D., P. P. Mukherjee, R. Fujisawa, C. P. Rivera and K. Labib (2020). "CMG helicase disassembly is controlled by replication fork DNA, replisome components and a ubiquitin threshold." Elife 9.

DeLaBarre, B. and A. T. Brunger (2003). "Complete structure of p97/valosin-containing protein reveals communication between nucleotide domains." Nature Structural Biology 10(10): 856-863.

Delphin, C., T. Guan, F. Melchior and L. Gerace (1997). "RanGTP targets p97 to RanBP2, a filamentous protein localized at the cytoplasmic periphery of the nuclear pore complex." Mol Biol Cell 8(12): 2379-2390.

den Besten, W., R. Verma, G. Kleiger, R. S. Oania and R. J. Deshaies (2012). "NEDD8 links cullin-RING ubiquitin ligase function to the p97 pathway." Nat Struct Mol Biol 19(5): 511-516, S511.

Deng, L., R. A. Wu, R. Sonneville, O. V. Kochenova, K. Labib, D. Pellman and J. C. Walter (2019). "Mitotic CDK Promotes Replisome Disassembly, Fork Breakage, and Complex DNA Rearrangements." Mol Cell 73(5): 915-929 e916.

Deol, K. K., S. Lorenz and E. R. Strieter (2019). "Enzymatic Logic of Ubiquitin Chain Assembly." Frontiers in Physiology 10.

Deshaies, R. J. and C. A. Joazeiro (2009). "RING domain E3 ubiquitin ligases." Annu Rev Biochem 78: 399-434.

Dewar, J. M., M. Budzowska and J. C. Walter (2015). "The mechanism of DNA replication termination in vertebrates." Nature 525(7569): 345-350.

Dewar, J. M., E. Low, M. Mann, M. Raschle and J. C. Walter (2017). "CRL2(Lrr1) promotes unloading of the vertebrate replisome from chromatin during replication termination." Genes Dev 31(3): 275-290.
Dewar, J. M. and J. C. Walter (2017). "Mechanisms of DNA replication termination." Nat Rev Mol Cell Biol 18(8): 507-516.

Di Gregorio, J., L. Cilenti, C. T. Ambivero, T. Andl, R. Liao, A. S. Zervos and J. Di Gregorio (2021). "UBXN7 cofactor of CRL3(KEAP1) and CRL2(VHL) ubiquitin ligase complexes mediates reciprocal regulation of NRF2 and HIF-1 alpha proteins." Biochimica Et Biophysica Acta-Molecular Cell Research 1868(4).

Dianov, G. L., B. R. Jensen, M. K. Kenny and V. A. Bohr (1999). "Replication protein A stimulates proliferating cell nuclear antigen-dependent repair of abasic sites in DNA by human cell extracts." Biochemistry 38(34): 11021-11025.

Dickson, K. A., A. J. Cole, A. J. Gill, A. Clarkson, G. B. Gard, A. Chou, C. J. Kennedy, B. R. Henderson, S. Australian Ovarian Cancer, S. Fereday, N. Traficante, K. Alsop, D. D. Bowtell, A. deFazio, R. Clifton-Bligh and D. J. Marsh (2016). "The RING finger domain E3 ubiquitin ligases BRCA1 and the RNF20/RNF40 complex in global loss of the chromatin mark histone H2B monoubiquitination (H2Bub1) in cell line models and primary high-grade serous ovarian cancer." Hum Mol Genet 25(24): 5460-5471.

Dikic, I., S. Wakatsuki and K. J. Walters (2009). "Ubiquitin-binding domains - from structures to functions." Nat Rev Mol Cell Biol 10(10): 659-671.

Ding, R., T. Zhang, D. J. Wilson, J. Xie, J. Williams, Y. Xu, Y. Ye and L. Chen (2019). "Discovery of Irreversible p97 Inhibitors." J Med Chem 62(5): 2814-2829.

Dittmar, G. and K. F. Winklhofer (2019). "Linear Ubiquitin Chains: Cellular Functions and Strategies for Detection and Quantification." Front Chem 7: 915.

Dobrynin, G., O. Popp, T. Romer, S. Bremer, M. H. Schmitz, D. W. Gerlich and H. Meyer (2011). "Cdc48/p97-Ufd1-Npl4 antagonizes Aurora B during chromosome segregation in HeLa cells." J Cell Sci 124(Pt 9): 1571-1580.

Dreveny, I., H. Kondo, K. Uchiyama, A. Shaw, X. Zhang and P. S. Freemont (2004). "Structural basis of the interaction between the AAA ATPase p97/VCP and its adaptor protein p47." EMBO J 23(5): 1030-1039.

Egerton, M. and L. E. Samelson (1994). "Biochemical characterization of valosin-containing protein, a protein tyrosine kinase substrate in hematopoietic cells." J Biol Chem 269(15): 11435-11441.

Elia, A. E. H., D. C. Wang, N. A. Willis, A. P. Boardman, I. Hajdu, R. O. Adeyemi, E. Lowry, S. P. Gygi, R. Scully and S. J. Elledge (2015). "RFWD3-Dependent Ubiquitination of RPA Regulates Repair at Stalled Replication Forks." Molecular Cell 60(2): 280-293.

Emberley, E. D., R. Mosadeghi and R. J. Deshaies (2012). "Deconjugation of Nedd8 from Cul1 is directly regulated by Skp1-F-box and substrate, and the COP9 signalosome inhibits deneddylated SCF by a noncatalytic mechanism." J Biol Chem 287(35): 29679-29689.

Ernst, R., B. Mueller, H. L. Ploegh and C. Schlieker (2009). "The otubain YOD1 is a deubiquitinating enzyme that associates with p97 to facilitate protein dislocation from the ER." Mol Cell 36(1): 28-38.
Evans, P. C. (2005). "Regulation of pro-inflammatory signalling networks by ubiquitin: identification of novel targets for anti-inflammatory drugs." Expert Rev Mol Med 7(12): 1-19.

Evrin, C., P. Clarke, J. Zech, R. Lurz, J. Sun, S. Uhle, H. Li, B. Stillman and C. Speck (2009). "A double-hexameric MCM2-7 complex is loaded onto origin DNA during licensing of eukaryotic DNA replication." Proc Natl Acad Sci U S A 106(48): 20240-20245.

Ewens, C. A., P. Kloppsteck, A. Forster, X. Zhang and P. S. Freemont (2010). "Structural and functional implications of phosphorylation and acetylation in the regulation of the AAA+ protein p97." Biochem Cell Biol 88(1): 41-48.

Ewens, C. A., S. Panico, P. Kloppsteck, C. McKeown, I. O. Ebong, C. Robinson, X. Zhang and P. S. Freemont (2014). "The p97-FAF1 protein complex reveals a common mode of p97 adaptor binding." J Biol Chem 289(17): 12077-12084.

Fang, C., X. Zhang, L. Zhang, X. Gao, P. Yang and H. Lu (2016). "Identification of Palmitoylated Transitional Endoplasmic Reticulum ATPase by Proteomic Technique and Pan Antipalmitoylation Antibody." J Proteome Res 15(3): 956-962.

Fei, L., Y. Ma, M. Zhang, X. Liu, Y. Luo, C. Wang, H. Zhang, W. Zhang and Y. Han (2017). "RACK1 promotes lung cancer cell growth via an MCM7/RACK1/ Akt signaling complex." Oncotarget 8(25): 40501-40513.

Feng, L. and J. Chen (2012). "The E3 ligase RNF8 regulates KU80 removal and NHEJ repair." Nat Struct Mol Biol 19(2): 201-206.

Finley, D. (2009). "Recognition and processing of ubiquitin-protein conjugates by the proteasome." Annu Rev Biochem 78: 477-513.

Fisher, D. (2011). "Control of DNA Replication by Cyclin-Dependent Kinases in Development." Cell Cycle in Development 53: 201-217.

Fisher, R. D., B. Wang, S. L. Alam, D. S. Higginson, H. Robinson, W. I. Sundquist and C. P. Hill (2003). "Structure and ubiquitin binding of the ubiquitin-interacting motif." J Biol Chem 278(31): 28976-28984.

Flierman, D., Y. Ye, M. Dai, V. Chau and T. A. Rapoport (2003). "Polyubiquitin serves as a recognition signal, rather than a ratcheting molecule, during retrotranslocation of proteins across the endoplasmic reticulum membrane." J Biol Chem 278(37): 34774-34782.

Fouad, S., O. S. Wells, M. A. Hill and V. D'Angiolella (2019). "Cullin Ring Ubiquitin Ligases (CRLs) in Cancer: Responses to Ionizing Radiation (IR) Treatment." Front Physiol 10: 1144.

Fox, J. T., K. Y. Lee and K. Myung (2011). "Dynamic regulation of PCNA ubiquitylation/deubiquitylation." FEBS Lett 585(18): 2780-2785.

Fragkos, M., O. Ganier, P. Coulombe and M. Mechali (2015). "DNA replication origin activation in space and time." Nat Rev Mol Cell Biol 16(6): 360-374.

Franz, A., L. Ackermann and T. Hoppe (2016). "Ring of Change: CDC48/p97 Drives Protein Dynamics at Chromatin." Front Genet 7: 73.

Franz, A., M. Orth, P. A. Pirson, R. Sonneville, J. J. Blow, A. Gartner, O. Stemmann and T. Hoppe (2011). "CDC-48/p97 coordinates CDT-1 degradation with GINS chromatin dissociation to ensure faithful DNA replication." Mol Cell 44(1): 85-96.

Franz, A., P. A. Pirson, D. Pilger, S. Halder, D. Achuthankutty, H. Kashkar, K. Ramadan and T. Hoppe (2016). "Chromatin-associated degradation is defined by UBXN-3/FAF1 to safeguard DNA replication fork progression." Nat Commun 7: 10612.

Franz, A., P. Valledor, P. Ubieto-Capella, D. Pilger, A. Galarreta, V. Lafarga, A. Fernandez-Llorente, G. de la Vega-Barranco, F. den Brave, T. Hoppe, O. Fernandez-Capetillo and E. Lecona (2021). "USP7 and VCPFAF1 define the SUMO/Ubiquitin landscape at the DNA replication fork." Cell Reports 37(2).

Friedberg, E. C. (2006). "Reversible monoubiquitination of PCNA: A novel slant on regulating translesion DNA synthesis." Mol Cell 22(2): 150-152.

Fullbright, G., H. B. Rycenga, J. D. Gruber and D. T. Long (2016). "p97 Promotes a Conserved Mechanism of Helicase Unloading during DNA Cross-Link Repair." Mol Cell Biol 36(23): 2983-2994.

Gaggioli, V. and P. Zegerman (2017). "Terminating the replication helicase." Nat Cell Biol 19(5): 410-412.

Gambus, A. (2017). "Termination of Eukaryotic Replication Forks." Adv Exp Med Biol 1042: 163-187.
Gambus, A., G. A. Khoudoli, R. C. Jones and J. J. Blow (2011). "MCM2-7 form double hexamers at licensed origins in Xenopus egg extract." J Biol Chem 286(13): 11855-11864.

Garcia-Barcena, C., N. Osinalde, J. Ramirez and U. Mayor (2020). "How to Inactivate Human Ubiquitin E3 Ligases by Mutation." Front Cell Dev Biol 8: 39.

George, A. J., Y. C. Hoffiz, A. J. Charles, Y. Zhu and A. M. Mabb (2018). "A Comprehensive Atlas of E3 Ubiquitin Ligase Mutations in Neurological Disorders." Front Genet 9: 29.

Ghosal, G. and J. Chen (2013). "DNA damage tolerance: a double-edged sword guarding the genome." Transl Cancer Res 2(3): 107-129.

Ghosal, G., J. W. Leung, B. C. Nair, K. W. Fong and J. Chen (2012). "Proliferating cell nuclear antigen (PCNA)-binding protein C1orf124 is a regulator of translesion synthesis." J Biol Chem 287(41): 34225-34233.

Giglia-Mari, G., A. Zotter and W. Vermeulen (2011). "DNA damage response." Cold Spring Harb Perspect Biol 3(1): a000745.

Gillespie, P. J., A. Gambus and J. J. Blow (2012). "Preparation and use of Xenopus egg extracts to study DNA replication and chromatin associated proteins." Methods 57(2): 203-213.

Gillespie, P. J., G. A. Khoudoli, G. Stewart, J. R. Swedlow and J. J. Blow (2007). "ELYS/MEL-28 chromatin association coordinates nuclear pore complex assembly and replication licensing." Curr Biol 17(19): 1657-1662.

Gillespie, P. J., J. Neusiedler, K. Creavin, G. S. Chadha and J. J. Blow (2016). "Cell Cycle Synchronization in Xenopus Egg Extracts." Cell Cycle Oscillators: Methods and Protocols 1342: 101-147.

Gurdon, J. B. (2006). "From nuclear transfer to nuclear reprogramming: The reversal of cell differentiation." Annual Review of Cell and Developmental Biology 22: 1-22.

Haberland, M., A. Johnson, M. H. Mokalled, R. L. Montgomery and E. N. Olson (2009). "Genetic dissection of histone deacetylase requirement in tumor cells." Proc Natl Acad Sci U S A 106(19): 7751-7755.

Haines, D. S. (2010). "p97-containing complexes in proliferation control and cancer: emerging culprits or guilt by association?" Genes Cancer 1(7): 753-763.

Hanzelmann, P., A. Buchberger and H. Schindelin (2011). "Hierarchical binding of cofactors to the AAA ATPase p97." Structure 19(6): 833-843.

Hanzelmann, P. and H. Schindelin (2011). "The structural and functional basis of the p97/valosin-containing protein (VCP)-interacting motif (VIM): mutually exclusive binding of cofactors to the N-terminal domain of p97." J Biol Chem 286(44): 38679-38690.

Hanzelmann, P. and H. Schindelin (2016). "Characterization of an Additional Binding Surface on the p97 N-Terminal Domain Involved in Bipartite Cofactor Interactions." Structure 24(1): 140-147.

Hanzelmann, P. and H. Schindelin (2017). "The Interplay of Cofactor Interactions and Post-translational Modifications in the Regulation of the AAA+ ATPase p97." Front Mol Biosci 4: 21.

Hao, Q., S. Jiao, Z. Shi, C. Li, X. Meng, Z. Zhang, Y. Wang, X. Song, W. Wang, R. Zhang, Y. Zhao, C. C. Wong and Z. Zhou (2015). "A non-canonical role of the p97 complex in RIG-I antiviral signaling." EMBO J 34(23): 2903-2920.

Harari-Steinberg, O. and D. A. Chamovitz (2004). "The COP9 signalosome: mediating between kinase signaling and protein degradation." Curr Protein Pept Sci 5(3): 185-189.

Hashimoto, Y. and H. Tanaka (2020). "Ongoing replication forks delay nuclear envelope breakdown upon mitotic entry." J Biol Chem.

He, J., Q. Zhu, G. Wani, N. Sharma and A. A. Wani (2016). "Valosin-containing Protein (VCP)/p97 Segregase Mediates Proteolytic Processing of Cockayne Syndrome Group B (CSB) in Damaged Chromatin." J Biol Chem 291(14): 7396-7408.

Hedglin, M. and S. J. Benkovic (2017). "Replication Protein A Prohibits Diffusion of the PCNA Sliding Clamp along Single-Stranded DNA." Biochemistry 56(13): 1824-1835.

Heidelberger, J. B., A. Voigt, M. E. Borisova, G. Petrosino, S. Ruf, S. A. Wagner and P. Beli (2018). "Proteomic profiling of VCP substrates links VCP to K6-linked ubiquitylation and c-Myc function." EMBO Rep 19(4).

Heller, R. C., S. Kang, W. M. Lam, S. Chen, C. S. Chan and S. P. Bell (2011). "Eukaryotic origin-dependent DNA replication in vitro reveals sequential action of DDK and S-CDK kinases." Cell 146(1): 80-91.

Hendriks, I. A., D. Lyon, C. Young, L. J. Jensen, A. C. Vertegaal and M. L. Nielsen (2017). "Site-specific mapping of the human SUMO proteome reveals co-modification with phosphorylation." Nat Struct Mol Biol 24(3): 325-336.

Herrmann, J., L. O. Lerman and A. Lerman (2007). "Ubiquitin and ubiquitin-like proteins in protein regulation." Circ Res 100(9): 1276-1291.

Hershko, A., A. Ciechanover and A. Varshavsky (2000). "Basic Medical Research Award. The ubiquitin system." Nat Med 6(10): 1073-1081.

Heubes, S. and O. Stemmann (2007). "The AAA-ATPase p97-Ufd1-Npl4 is required for ERAD but not for spindle disassembly in Xenopus egg extracts." J Cell Sci 120(Pt 8): 1325-1329.

Hicke, L., H. L. Schubert and C. P. Hill (2005). "Ubiquitin-binding domains." Nat Rev Mol Cell Biol 6(8): 610-621.
Hofmann, K. and L. Falquet (2001). "A ubiquitin-interacting motif conserved in components of the proteasomal and lysosomal protein degradation systems." Trends Biochem Sci 26(6): 347-350.

Hoogenboom, W. S., D. Klein Douwel and P. Knipscheer (2017). "Xenopus egg extract: A powerful tool to study genome maintenance mechanisms." Dev Biol 428(2): 300-309.

Hoppe, T. and E. Cohen (2020). "Organismal Protein Homeostasis Mechanisms." Genetics 215(4): 889-901.

Horn-Ghetko, D., D. T. Krist, J. R. Prabu, K. Baek, M. P. C. Mulder, M. Klugel, D. C. Scott, H. Ovaa, G. Kleiger and B. A. Schulman (2021). "Ubiquitin ligation to F-box protein targets by SCF-RBR E3-E3 super-assembly." Nature.

Hornbeck, P. V., B. Zhang, B. Murray, J. M. Kornhauser, V. Latham and E. Skrzypek (2015). "PhosphoSitePlus, 2014: mutations, PTMs and recalibrations." Nucleic Acids Res 43(Database issue): D512-520.

Huang, D. T., O. Ayrault, H. W. Hunt, A. M. Taherbhoy, D. M. Duda, D. C. Scott, L. A. Borg, G. Neale, P. J. Murray, M. F. Roussel and B. A. Schulman (2009). "E2-RING expansion of the NEDD8 cascade confers specificity to cullin modification." Mol Cell 33(4): 483-495.

Huang, L., E. Kinnucan, G. Wang, S. Beaudenon, P. M. Howley, J. M. Huibregtse and N. P. Pavletich (1999). "Structure of an E6AP-UbcH7 complex: insights into ubiquitination by the E2-E3 enzyme cascade." Science 286(5443): 1321-1326.

Huang, S., D. Tang and Y. Wang (2016). "Monoubiquitination of Syntaxin 5 Regulates Golgi Membrane Dynamics during the Cell Cycle." Dev Cell 38(1): 73-85.

Huang, X. P., T. H. Rong, Q. L. Wu, J. H. Fu, H. Yang, J. M. Zhao and Y. Fang (2005). "MCM4 expression in esophageal cancer from southern China and its clinical significance." Journal of Cancer Research and Clinical Oncology 131(10): 677-682.

Hurley, J. H., S. Lee and G. Prag (2006). "Ubiquitin-binding domains." Biochem J 399(3): 361-372.
Hussain, S., Y. Zhang and P. J. Galardy (2009). "DUBs and cancer: the role of deubiquitinating enzymes as oncogenes, non-oncogenes and tumor suppressors." Cell Cycle 8(11): 1688-1697.

Huttner, D. and H. D. Ulrich (2008). "Cooperation of replication protein A with the ubiquitin ligase Rad18 in DNA damage bypass." Cell Cycle 7(23): 3629-3633.

Hyun, M., S. Park, E. Kim, D. H. Kim, S. J. Lee, H. S. Koo, Y. S. Seo and B. Ahn (2012). "Physical and functional interactions of Caenorhabditis elegans WRN-1 helicase with RPA-1." Biochemistry 51(7): 1336-1345.

Imami, K., N. Sugiyama, Y. Kyono, M. Tomita and Y. Ishirama (2008). "Automated phosphoproteome analysis for cultured cancer cells by two-dimensional nanoLC-MS using a calcined titania/C18 biphasic column." Analytical Sciences 24(1): 161-166.

Inano, S., K. Sato, Y. Katsuki, W. Kobayashi, H. Tanaka, K. Nakajima, S. Nakada, H. Miyoshi, K. Knies, A. Takaori-Kondo, D. Schindler, M. Ishiai, H. Kurumizaka and M. Takata (2020). "RFWD3-Mediated Ubiquitination Promotes Timely Removal of Both RPA and RAD51 from DNA Damage Sites to Facilitate Homologous Recombination." Mol Cell 78(1): 192.

Indig, F. E., J. J. Partridge, C. von Kobbe, M. I. Aladjem, M. Latterich and V. A. Bohr (2004). "Werner syndrome protein directly binds to the AAA ATPase p97/VCP in an ATP-dependent fashion." J Struct Biol 146(1-2): 251-259.

Isaacson, R. L., V. E. Pye, P. Simpson, H. H. Meyer, X. Zhang, P. S. Freemont and S. Matthews (2007). "Detailed structural insights into the p97-Npl4-Ufd1 interface." J Biol Chem 282(29): 21361-21369.

Jones, J. D. and C. D. O'Connor (2011). "Protein acetylation in prokaryotes." Proteomics 11(15): 3012-3022.

Jung, H., J. A. Lee, S. Choi, H. Lee and B. Ahn (2014). "Characterization of the Caenorhabditis elegans HIM-6/BLM helicase: unwinding recombination intermediates." PLoS One 9(7): e102402.

Kalvik, T. V. and T. Arnesen (2013). "Protein N-terminal acetyltransferases in cancer." Oncogene 32(3): 269-276.

Kamitani, T., K. Kito, H. P. Nguyen and E. T. Yeh (1997). "Characterization of NEDD8, a developmentally down-regulated ubiquitin-like protein." J Biol Chem 272(45): 28557-28562.

Kamura, T., K. Maenaka, S. Kotoshiba, M. Matsumoto, D. Kohda, R. C. Conaway, J. W. Conaway and K. I. Nakayama (2004). "VHL-box and SOCS-box domains determine binding specificity for Cul2-Rbx1 and Cul5-Rbx2 modules of ubiquitin ligases." Genes Dev 18(24): 3055-3065.

Kang, S., M. S. Kang, E. Ryu and K. Myung (2017). "Eukaryotic DNA replication: Orchestrated action of multi-subunit protein complexes." Mutat Res.

Kannouche, P. L. and A. R. Lehmann (2004). "Ubiquitination of PCNA and the polymerase switch in human cells." Cell Cycle 3(8): 1011-1013.

Kannouche, P. L., J. Wing and A. R. Lehmann (2004). "Interaction of human DNA polymerase eta with monoubiquitinated PCNA: a possible mechanism for the polymerase switch in response to DNA damage." Mol Cell 14(4): 491-500.

Kernstock, S., E. Davydova, M. Jakobsson, A. Moen, S. Pettersen, G. M. Maelandsmo, W. Egge-Jacobsen and P. O. Falnes (2012). "Lysine methylation of VCP by a member of a novel human protein methyltransferase family." Nat Commun 3: 1038.

Khong, Z. J., S. K. Lai, C. G. Koh, S. Geifman-Shochat and H. Y. Li (2020). "A novel function of AAA-ATPase p97/VCP in the regulation of cell motility." Oncotarget 11(1): 74-85.

Kilgas, S., A. N. Singh, S. Paillas, C. K. Then, I. Torrecilla, J. Nicholson, L. Browning, I. Vendrell, R. Konietzny, B. M. Kessler, A. E. Kiltie and K. Ramadan (2021). "p97/VCP inhibition causes excessive MRE11-dependent DNA end resection promoting cell killing after ionizing radiation." Cell Reports 35(8).

Kim, J. E., S. R. Tannenbaum and F. M. White (2005). "Global phosphoproteome of HT-29 human colon adenocarcinoma cells." Journal of Proteome Research 4(4): 1339-1346.

Klein, J. B., M. T. Barati, R. Wu, D. Gozal, L. R. Sachleben, Jr., H. Kausar, J. O. Trent, E. Gozal and M. J. Rane (2005). "Akt-mediated valosin-containing protein 97 phosphorylation regulates its association with ubiquitinated proteins." J Biol Chem 280(36): 31870-31881.

Kloppsteck, P., C. A. Ewens, A. Forster, X. D. Zhang and P. S. Freemont (2012). "Regulation of p97 in the ubiquitin-proteasome system by the UBX protein-family." Biochimica Et Biophysica Acta-Molecular Cell Research 1823(1): 125-129.

Komander, D. (2009). "The emerging complexity of protein ubiquitination." Biochem Soc Trans 37(Pt 5): 937-953.

Komander, D., M. J. Clague and S. Urbe (2009). "Breaking the chains: structure and function of the deubiquitinases." Nat Rev Mol Cell Biol 10(8): 550-563.

Komander, D. and M. Rape (2012). "The ubiquitin code." Annu Rev Biochem 81: 203-229.

Kopanic, J. L., M. Al-Mugotir, S. Zach, S. Das, R. Grosely and P. L. Sorgen (2013). "An Escherichia coli strain for expression of the connexin45 carboxyl terminus attached to the 4th transmembrane domain." Front Pharmacol 4: 106.

Kornbluth, S., J. Yang and M. Powers (2006). "Analysis of the cell cycle using Xenopus egg extracts." Curr Protoc Cell Biol Chapter 11: Unit 11 11.

Kovalchuk, I. and O. Kovalchuk (2016). "Genome Stability From Virus to Human Application Introduction." Genome Stability: From Virus to Human Application: Xix-Xxii.

Kung, W. W., S. Ramachandran, N. Makukhin, E. Bruno and A. Ciulli (2019). "Structural insights into substrate recognition by the SOCS2 E3 ubiquitin ligase." Nat Commun 10(1): 2534.

Kurz, T., Y. C. Chou, A. R. Willems, N. Meyer-Schaller, M. L. Hecht, M. Tyers, M. Peter and F. Sicheri (2008). "Dcn1 functions as a scaffold-type E3 ligase for cullin neddylation." Mol Cell 29(1): 23-35.

Labib, K., J. A. Tercero and J. F. Diffley (2000). "Uninterrupted MCM2-7 function required for DNA replication fork progression." Science 288(5471): 1643-1647.

Lata, S., R. Mishra and A. C. Banerjea (2018). "Proteasomal Degradation Machinery: Favorite Target of HIV-1 Proteins." Front Microbiol 9: 2738.

Le, L. T., W. Kang, J. Y. Kim, O. T. Le, S. Y. Lee and J. K. Yang (2016). "Structural Details of Ufd1 Binding to p97 and Their Functional Implications in ER-Associated Degradation." PLoS One 11(9): e0163394.

Lebofsky, R., T. Takahashi and J. C. Walter (2009). "DNA replication in nucleus-free Xenopus egg extracts." Methods Mol Biol 521: 229-252.

Lee, C. S. K., M. F. Cheung, J. Li, Y. Zhao, W. H. Lam, V. Ho, R. Rohs, Y. Zhai, D. Leung and B. K. Tye (2021). "Humanizing the yeast origin recognition complex." Nat Commun 12(1): 33.

Lehmann, A. R. (2011). "Ubiquitin-family modifications in the replication of DNA damage." FEBS Lett 585(18): 2772-2779.

Li, C., Y. S. Huang, Q. Q. Fan, H. Y. Quan, Y. Q. Dong, M. Nie, J. Q. Wang, F. C. Xie, J. Ji, L. Zhou, Z. Zheng and L. Wang (2021). "p97/VCP is highly expressed in the stem-like cells of breast cancer and controls cancer stemness partly through the unfolded protein response." Cell Death & Disease 12(4).

Li, G., G. Zhao, H. Schindelin and W. J. Lennarz (2008). "Tyrosine phosphorylation of ATPase p97 regulates its activity during ERAD." Biochem Biophys Res Commun 375(2): 247-251.

Li, N., J. Wang, S. S. Wallace, J. Chen, J. Zhou and A. D. D'Andrea (2020). "Cooperation of the NEIL3 and Fanconi anemia/BRCA pathways in interstrand crosslink repair." Nucleic Acids Res 48(6): 3014-3028.

Li, W., M. H. Bengtson, A. Ulbrich, A. Matsuda, V. A. Reddy, A. Orth, S. K. Chanda, S. Batalov and C. A. Joazeiro (2008). "Genome-wide and functional annotation of human E3 ubiquitin ligases identifies MULAN, a mitochondrial E3 that regulates the organelle's dynamics and signaling." PLoS One 3(1): e1487.

Li, Z. H., Y. Wang, M. Xu and T. Jiang (2017). "Crystal structures of the UBX domain of human UBXD7 and its complex with p97 ATPase." Biochem Biophys Res Commun 486(1): 94-100.

Liu, J., M. Furukawa, T. Matsumoto and Y. Xiong (2002). "NEDD8 modification of CUL1 dissociates p120(CAND1), an inhibitor of CUL1-SKP1 binding and SCF ligases." Mol Cell 10(6): 1511-1518.

Livingstone, M., H. Ruan, J. Weiner, K. R. Clauser, P. Strack, S. Jin, A. Williams, H. Greulich, J. Gardner, M. Venere, T. A. Mochan, R. A. DiTullio, Jr., K. Moravcevic, V. G. Gorgoulis, A. Burkhardt and T. D. Halazonetis (2005). "Valosin-containing protein phosphorylation at Ser784 in response to DNA damage." Cancer Res 65(17): 7533-7540.

Loor, G., S. J. Zhang, P. Zhang, N. L. Toomey and M. Y. Lee (1997). "Identification of DNA replication and cell cycle proteins that interact with PCNA." Nucleic Acids Res 25(24): 5041-5046.

Low, E., G. Chistol, M. S. Zaher, O. V. Kochenova and J. C. Walter (2020). "The DNA replication fork suppresses CMG unloading from chromatin before termination." Genes & Development 34(21-22): 1534-1545.

Ma, Q. and T. K. Wood (2011). "Protein acetylation in prokaryotes increases stress resistance." Biochem Biophys Res Commun 410(4): 846-851.

Machida, Y. J., J. L. Hamlin and A. Dutta (2005). "Right place, right time, and only once: replication initiation in metazoans." Cell 123(1): 13-24.

Maculins, T., N. Carter, T. Dorval, K. Hudson, J. W. Nissink, R. T. Hay and H. Alwan (2016). "A Generic Platform for Cellular Screening Against Ubiquitin Ligases." Sci Rep 6: 18940.

Maculins, T., P. J. Nkosi, H. Nishikawa and K. Labib (2015). "Tethering of SCF(Dia2) to the Replisome Promotes Efficient Ubiquitylation and Disassembly of the CMG Helicase." Curr Biol 25(17): 2254-2259.
Magnaghi, P., R. D'Alessio, B. Valsasina, N. Avanzi, S. Rizzi, D. Asa, F. Gasparri, L. Cozzi, U. Cucchi, C. Orrenius, P. Polucci, D. Ballinari, C. Perrera, A. Leone, G. Cervi, E. Casale, Y. Xiao, C. Wong, D. J. Anderson, A. Galvani, D. Donati, T. O'Brien, P. K. Jackson and A. Isacchi (2013). "Covalent and allosteric inhibitors of the ATPase VCP/p97 induce cancer cell death." Nat Chem Biol 9(9): 548-556.

Marheineke, K. and O. Hyrien (2004). "Control of replication origin density and firing time in Xenopus egg extracts - Role of a caffeine-sensitive, ATR-dependent checkpoint." Journal of Biological Chemistry 279(27): 28071-28081.

Maric, M., T. Maculins, G. De Piccoli and K. Labib (2014). "Cdc48 and a ubiquitin ligase drive disassembly of the CMG helicase at the end of DNA replication." Science 346(6208): 1253596.

Maric, M., P. Mukherjee, M. H. Tatham, R. Hay and K. Labib (2017). "Ufd1-Npl4 Recruit Cdc48 for Disassembly of Ubiquitylated CMG Helicase at the End of Chromosome Replication." Cell Rep 18(13): 3033-3042.

Masai, H., S. Matsumoto, Z. You, N. Yoshizawa-Sugata and M. Oda (2010). "Eukaryotic chromosome DNA replication: where, when, and how?" Annu Rev Biochem 79: 89-130.

Maskey, R. S., M. S. Kim, D. J. Baker, B. Childs, L. A. Malureanu, K. B. Jeganathan, Y. Machida, J. M. van Deursen and Y. J. Machida (2014). "Spartan deficiency causes genomic instability and progeroid phenotypes." Nature Communications 5.

Matsumoto, M. L., K. E. Wickliffe, K. C. Dong, C. Yu, I. Bosanac, D. Bustos, L. Phu, D. S. Kirkpatrick, S. G. Hymowitz, M. Rape, R. F. Kelley and V. M. Dixit (2010). "K11-linked polyubiquitination in cell cycle control revealed by a K11 linkage-specific antibody." Mol Cell 39(3): 477-484.

Mechali, M. (2010). "Eukaryotic DNA replication origins: many choices for appropriate answers." Nature Reviews Molecular Cell Biology 11(10): 728-738.

Meerang, M., D. Ritz, S. Paliwal, Z. Garajova, M. Bosshard, N. Mailand, P. Janscak, U. Hubscher, H. Meyer and K. Ramadan (2011). "The ubiquitin-selective segregase VCP/p97 orchestrates the response to DNA double-strand breaks." Nature Cell Biology 13(11): 1376-U1204.

Metzger, M. B., J. N. Pruneda, R. E. Klevit and A. M. Weissman (2014). "RING-type E3 ligases: master manipulators of E2 ubiquitin-conjugating enzymes and ubiquitination." Biochim Biophys Acta 1843(1): 47-60.

Meyer, H. (2012). "p97 complexes as signal integration hubs." BMC Biol 10: 48.

Meyer, H., M. Bug and S. Bremer (2012). "Emerging functions of the VCP/p97 AAA-ATPase in the ubiquitin system." Nat Cell Biol 14(2): 117-123.

Meyer, H. and C. C. Weihl (2014). "The VCP/p97 system at a glance: connecting cellular function to disease pathogenesis." J Cell Sci 127(Pt 18): 3877-3883.

Meyer, H. J. and M. Rape (2014). "Enhanced protein degradation by branched ubiquitin chains." Cell 157(4): 910-921.

Miki, Y., J. Swensen, D. Shattuck-Eidens, P. A. Futreal, K. Harshman, S. Tavtigian, Q. Liu, C. Cochran, L. M. Bennett, W. Ding and et al. (1994). "A strong candidate for the breast and ovarian cancer susceptibility gene BRCA1." Science 266(5182): 66-71.

Min, T., M. Bodas, S. Mazur and N. Vij (2011). "Critical role of proteostasis-imbalance in pathogenesis of COPD and severe emphysema." Journal of Molecular Medicine-Jmm 89(6): 577-593.

Mirsanaye, A. S., D. Typas and N. Mailand (2021). "Ubiquitylation at Stressed Replication Forks: Mechanisms and Functions." Trends Cell Biol.

Moreno, S. P., R. Bailey, N. Campion, S. Herron and A. Gambus (2014). "Polyubiquitylation drives replisome disassembly at the termination of DNA replication." Science 346(6208): 477-481.

Moreno, S. P. and A. Gambus (2015). "Regulation of Unperturbed DNA Replication by Ubiquitylation." Genes (Basel) 6(3): 451-468.

Moreno, S. P., R. M. Jones, D. Poovathumkadavil, S. Scaramuzza and A. Gambus (2019). "Mitotic replisome disassembly depends on TRAIP ubiquitin ligase activity." Life Science Alliance 2(2).

Mori-Konya, C., N. Kato, R. Maeda, K. Yasuda, N. Higashimae, M. Noguchi, M. Koike, Y. Kimura, H. Ohizumi, S. Hori and A. Kakizuka (2009). "p97/valosin-containing protein (VCP) is highly modulated by phosphorylation and acetylation." Genes Cells 14(4): 483-497.

Morreale, G., L. Conforti, J. Coadwell, A. L. Wilbrey and M. P. Coleman (2009). "Evolutionary divergence of valosin-containing protein/cell division cycle protein 48 binding interactions among endoplasmic reticulum-associated degradation proteins." Febs Journal 276(5): 1208-1220.

Mortusewicz, O., L. Schermelleh, J. Walter, M. C. Cardoso and H. Leonhardt (2005). "Recruitment of DNA methyltransferase I to DNA repair sites." Proceedings of the National Academy of Sciences of the United States of America 102(25): 8905-8909.

Mouradov, D., C. Sloggett, R. N. Jorissen, C. G. Love, S. Li, A. W. Burgess, D. Arango, R. L. Strausberg, D. Buchanan, S. Wormald, L. O'Connor, J. L. Wilding, D. Bicknell, I. P. M. Tomlinson, W. F. Bodmer, J. M. Mariadason and O. M. Sieber (2014). "Colorectal Cancer Cell Lines Are Representative Models of the Main Molecular Subtypes of Primary Cancer." Cancer Research 74(12): 3238-3247.

Mouysset, J., A. Deichsel, S. Moser, C. Hoege, A. A. Hyman, A. Gartner and T. Hoppe (2008). "Cell cycle progression requires the CDC-48UFD-1/NPL-4 complex for efficient DNA replication." Proc Natl Acad Sci U S A 105(35): 12879-12884.

Moyer, S. E., P. W. Lewis and M. R. Botchan (2006). "Isolation of the Cdc45/Mcm2-7/GINS (CMG) complex, a candidate for the eukaryotic DNA replication fork helicase." Proc Natl Acad Sci U S A 103(27): 10236-10241.

Mu, J. J., Y. Wang, H. Luo, M. Leng, J. L. Zhang, T. Yang, D. Besusso, S. Y. Jung and J. Qin (2007). "A proteomic analysis of ataxia telangiectasia-mutated (ATM)/ATM-Rad3-related (ATR) substrates identifies the ubiquitin-proteasome system as a regulator for DNA damage checkpoints." Journal of Biological Chemistry 282(24): 17330-17334.

Newport, J. and M. Kirschner (1982). "A Major Developmental Transition in Early Xenopus-Embryos .1. Characterization and Timing of Cellular-Changes at the Midblastula Stage." Cell 30(3): 675-686.
Nieminuszczy, J., R. Broderick, M. A. Bellani, E. Smethurst, R. A. Schwab, V. Cherdyntseva, T. Evmorfopoulou, Y. L. Lin, M. Minczuk, P. Pasero, S. Gagos, M. M. Seidman and W. Niedzwiedz (2019). "EXD2 Protects Stressed Replication Forks and Is Required for Cell Viability in the Absence of BRCA1/2." Molecular Cell 75(3): 605-+.

Nijman, S. M., M. P. Luna-Vargas, A. Velds, T. R. Brummelkamp, A. M. Dirac, T. K. Sixma and R. Bernards (2005). "A genomic and functional inventory of deubiquitinating enzymes." Cell 123(5): 773-786.

Nishimura, N., M. O. Radwan, M. Amano, S. Endo, E. Fujii, H. Hayashi, S. Ueno, N. Ueno, H. Tatetsu, H. Hata, Y. Okamoto, M. Otsuka, H. Mitsuya, M. Matsuoka and Y. Okuno (2019). "Novel p97/VCP inhibitor induces endoplasmic reticulum stress and apoptosis in both bortezomib-sensitive and -resistant multiple myeloma cells." Cancer Science 110(10): 3275-3287.

Nishiyama, A., L. Yamaguchi, J. Sharif, Y. Johmura, T. Kawamura, K. Nakanishi, S. Shimamura, K. Arita, T. Kodama, F. Ishikawa, H. Koseki and M. Nakanishi (2013). "Uhrf1-dependent H3K23 ubiquitylation couples maintenance DNA methylation and replication." Nature 502(7470): 249-253.

Niwa, H., C. A. Ewens, C. Tsang, H. O. Yeung, X. Zhang and P. S. Freemont (2012). "The role of the N-domain in the ATPase activity of the mammalian AAA ATPase p97/VCP." J Biol Chem 287(11): 8561-8570.

Noguchi, M., T. Takata, Y. Kimura, A. Manno, K. Murakami, M. Koike, H. Ohizumi, S. Hori and A. Kakizuka (2005). "ATPase activity of p97/valosin-containing protein is regulated by oxidative modification of the evolutionally conserved cysteine 522 residue in Walker A motif." J Biol Chem 280(50): 41332-41341.

Nomura, M., A. Mukasa, G. Nagae, S. Yamamoto, K. Tatsuno, H. Ueda, S. Fukuda, T. Umeda, T. Suzuki, R. Otani, K. Kobayashi, T. Maruyama, S. Tanaka, S. Takayanagi, T. Nejo, S. Takahashi, K. Ichimura, T. Nakamura, Y. Muragaki, Y. Narita, M. Nagane, K. Ueki, R. Nishikawa, J. Shibahara, H. Aburatani and N. Saito (2017). "Distinct molecular profile of diffuse cerebellar gliomas." Acta Neuropathologica 134(6): 941-956.

Oakley, G. G. and S. M. Patrick (2010). "Replication protein A: directing traffic at the intersection of replication and repair." Front Biosci (Landmark Ed) 15: 883-900.

Orme, C. M. and J. S. Bogan (2012). "The ubiquitin regulatory X (UBX) domain-containing protein TUG regulates the p97 ATPase and resides at the endoplasmic reticulum-golgi intermediate compartment." J Biol Chem 287(9): 6679-6692.

Osakabe, A., H. Tachiwana, W. Kagawa, N. Horikoshi, S. Matsumoto, M. Hasegawa, N. Matsumoto, T. Toga, J. Yamamoto, F. Hanaoka, N. H. Thoma, K. Sugasawa, S. Iwai and H. Kurumizaka (2015). "Structural basis of pyrimidine-pyrimidone (6-4) photoproduct recognition by UV-DDB in the nucleosome." Sci Rep 5: 16330.

Pacek, M. and J. C. Walter (2004). "A requirement for MCM7 and Cdc45 in chromosome unwinding during eukaryotic DNA replication." EMBO J 23(18): 3667-3676.

Partridge, J. J., J. O. Lopreiato, Jr., M. Latterich and F. E. Indig (2003). "DNA damage modulates nucleolar interaction of the Werner protein with the AAA ATPase p97/VCP." Mol Biol Cell 14(10): 4221-4229.

Passmore, L. A. and D. Barford (2004). "Getting into position: the catalytic mechanisms of protein ubiquitylation." Biochem J 379(Pt 3): 513-525.

Peters, J. M., M. J. Walsh and W. W. Franke (1990). "An abundant and ubiquitous homo-oligomeric ring-shaped ATPase particle related to the putative vesicle fusion proteins Sec18p and NSF." EMBO J 9(6): 1757-1767.

Pichler, A., A. Gast, J. S. Seeler, A. Dejean and F. Melchior (2002). "The nucleoporin RanBP2 has SUMO1 E3 ligase activity." Cell 108(1): 109-120.

Pickart, C. M. and M. J. Eddins (2004). "Ubiquitin: structures, functions, mechanisms." Biochim Biophys Acta 1695(1-3): 55-72.
Polo, S., S. Sigismund, M. Faretta, M. Guidi, M. R. Capua, G. Bossi, H. Chen, P. De Camilli and P. P. Di Fiore (2002). "A single motif responsible for ubiquitin recognition and monoubiquitination in endocytic proteins." Nature 416(6879): 451-455.

Postow, L., C. Ghenoiu, E. M. Woo, A. N. Krutchinsky, B. T. Chait and H. Funabiki (2008). "Ku80 removal from DNA through double strand break-induced ubiquitylation." J Cell Biol 182(3): 467-479.

Priego Moreno, S., R. M. Jones, D. Poovathumkadavil, S. Scaramuzza and A. Gambus (2019). "Mitotic replisome disassembly depends on TRAIP ubiquitin ligase activity." Life Sci Alliance 2(2).

Prioleau, M. N. and D. M. MacAlpine (2016). "DNA replication origins-where do we begin?" Genes & Development 30(15): 1683-1697.

Prokhorova, T. A. and J. J. Blow (2000). "Sequential MCM/P1 subcomplex assembly is required to form a heterohexamer with replication licensing activity." J Biol Chem 275(4): 2491-2498.

Puumalainen, M. R., D. Lessel, P. Ruthemann, N. Kaczmarek, K. Bachmann, K. Ramadan and H. Naegeli (2014). "Chromatin retention of DNA damage sensors DDB2 and XPC through loss of p97 segregase causes genotoxicity." Nature Communications 5.

Qian, H., Y. Zhang, B. Wu, S. Wu, S. You, N. Zhang and Y. Sun (2020). "Structure and Function of HECT E3 Ubiquitin Ligases and their Role in Oxidative Stress." J Transl Int Med 8(2): 71-79.

Rahighi, S. and I. Dikic (2012). "Selectivity of the ubiquitin-binding modules." FEBS Lett 586(17): 2705-2710.

Ramadan, K. (2012). "p97/VCP- and Lys48-linked polyubiquitination form a new signaling pathway in DNA damage response." Cell Cycle 11(6): 1062-1069.

Ramadan, K., R. Bruderer, F. M. Spiga, O. Popp, T. Baur, M. Gotta and H. H. Meyer (2007). "Cdc48/p97 promotes reformation of the nucleus by extracting the kinase Aurora B from chromatin." Nature 450(7173): 1258-1262.

Ramadan, K., S. Halder, K. Wiseman and B. Vaz (2017). "Strategic role of the ubiquitin-dependent segregase p97 (VCP or Cdc48) in DNA replication." Chromosoma 126(1): 17-32.

Raman, M., C. G. Havens, J. C. Walter and J. W. Harper (2011). "A genome-wide screen identifies p97 as an essential regulator of DNA damage-dependent CDT1 destruction." Mol Cell 44(1): 72-84.

Remus, D. and J. F. Diffley (2009). "Eukaryotic DNA replication control: lock and load, then fire." Curr Opin Cell Biol 21(6): 771-777.

Reyes-Turcu, F. E., K. H. Ventii and K. D. Wilkinson (2009). "Regulation and cellular roles of ubiquitin-specific deubiquitinating enzymes." Annu Rev Biochem 78: 363-397.

Rezvani, K. (2016). "UBXD Proteins: A Family of Proteins with Diverse Functions in Cancer." Int J Mol Sci 17(10).

Rieckher, M., A. Bujarrabal, M. A. Doll, N. Soltanmohammadi and B. Schumacher (2018). "A simple answer to complex questions: Caenorhabditis elegans as an experimental model for examining the DNA damage response and disease genes." Journal of Cellular Physiology 233(4): 2781-2790.

Rizwani, W., M. Alexandrow and S. Chellappan (2009). "Prohibitin physically interacts with MCM proteins and inhibits mammalian DNA replication." Cell Cycle 8(10): 1621-1629.

Ronau, J. A., J. F. Beckmann and M. Hochstrasser (2016). "Substrate specificity of the ubiquitin and Ubl proteases." Cell Res 26(4): 441-456.

Rossi, M. L., A. K. Ghosh and V. A. Bohr (2010). "Roles of Werner syndrome protein in protection of genome integrity." DNA Repair (Amst) 9(3): 331-344.

Rotin, D. and S. Kumar (2009). "Physiological functions of the HECT family of ubiquitin ligases." Nat Rev Mol Cell Biol 10(6): 398-409.

Rush, J., A. Moritz, K. A. Lee, A. Guo, V. L. Goss, E. J. Spek, H. Zhang, X. M. Zha, R. D. Polakiewicz and M. J. Comb (2005). "Immunoaffinity profiling of tyrosine phosphorylation in cancer cells." Nat Biotechnol 23(1): 94-101.

Ruthemann, P., C. B. Pogliano and H. Naegeli (2016). "Global-genome Nucleotide Excision Repair Controlled by Ubiquitin/Sumo Modifiers." Frontiers in Genetics 7.

Saha, R. N. and K. Pahan (2006). "HATs and HDACs in neurodegeneration: a tale of disconcerted acetylation homeostasis." Cell Death Differ 13(4): 539-550.

Sanada, T., G. Takaesu, R. Mashima, R. Yoshida, T. Kobayashi and A. Yoshimura (2008). "FLN29 deficiency reveals its negative regulatory role in the Toll-like receptor (TLR) and retinoic acid-inducible gene I (RIG-I)-like helicase signaling pathway." J Biol Chem 283(49): 33858-33864.

Sarikas, A., T. Hartmann and Z. Q. Pan (2011). "The cullin protein family." Genome Biol 12(4): 220.

Sato, Y., H. Tsuchiya, A. Yamagata, K. Okatsu, K. Tanaka, Y. Saeki and S. Fukai (2019). "Structural insights into ubiquitin recognition and Ufd1 interaction of Npl4." Nat Commun 10(1): 5708.

Scanlon, S. E. and P. M. Glazer (2015). "Multifaceted control of DNA repair pathways by the hypoxic tumor microenvironment." DNA Repair (Amst) 32: 180-189.

Schaeffer, V., M. Akutsu, M. H. Olma, L. C. Gomes, M. Kawasaki and I. Dikic (2014). "Binding of OTULIN to the PUB domain of HOIP controls NF-kappaB signaling." Mol Cell 54(3): 349-361.

Scharer, O. D. (2013). "Nucleotide excision repair in eukaryotes." Cold Spring Harb Perspect Biol 5(10): a012609.

Schlicher, L., M. Wissler, F. Preiss, P. Brauns-Schubert, C. Jakob, V. Dumit, C. Borner, J. Dengjel and U. Maurer (2016). "SPATA2 promotes CYLD activity and regulates TNF-induced NF-kappaB signaling and cell death." EMBO Rep 17(10): 1485-1497.

Schmidt, M. W., P. R. McQuary, S. Wee, K. Hofmann and D. A. Wolf (2009). "F-box-directed CRL complex assembly and regulation by the CSN and CAND1." Mol Cell 35(5): 586-597.

Schuberth, C. and A. Buchberger (2008). "UBX domain proteins: major regulators of the AAA ATPase Cdc48/p97." Cellular and Molecular Life Sciences 65(15): 2360-2371.

Schuller, J. M., F. Beck, P. Lossl, A. J. R. Heck and F. Forster (2016). "Nucleotide-dependent conformational changes of the AAA+ ATPase p97 revisited." Febs Letters 590(5): 595-604.

Schwechheimer, C., G. Serino, J. Callis, W. L. Crosby, S. Lyapina, R. J. Deshaies, W. M. Gray, M. Estelle and X. W. Deng (2001). "Interactions of the COP9 signalosome with the E3 ubiquitin ligase SCFTIRI in mediating auxin response." Science 292(5520): 1379-1382.

Shah, J. J. and R. Z. Orlowski (2009). "Proteasome inhibitors in the treatment of multiple myeloma." Leukemia 23(11): 1964-1979.

Shao, J. Y. (2020). "Ser(784) phosphorylation: a clinically relevant enhancer of VCP function in the DNA damage response." Molecular & Cellular Oncology 7(5).

Sharpe, H. J., G. Pau, G. J. Dijkgraaf, N. Basset-Seguin, Z. Modrusan, T. Januario, V. Tsui, A. B. Durham, A. A. Dlugosz, P. M. Haverty, R. Bourgon, J. Y. Tang, K. Y. Sarin, L. Dirix, D. C. Fisher, C. M. Rudin, H. Sofen, M. R. Migden, R. L. Yauch and F. J. de Sauvage (2015). "Genomic Analysis of Smoothened Inhibitor Resistance in Basal Cell Carcinoma." Cancer Cell 27(3): 327-341.

Sigismund, S., S. Polo and P. P. Di Fiore (2004). "Signaling through monoubiquitination." Curr Top Microbiol Immunol 286: 149-185.

Singh, A. N., J. Oehler, I. Torrecilla, S. Kilgas, S. D. Li, B. Vaz, C. Guerillon, J. Fielden, E. Hernandez-Carralero, E. Cabrera, I. D. C. Tullis, M. Meerang, P. R. Barber, R. Freire, J. Parsons, B. Vojnovic, A. E. Kiltie, N. Mailand and K. Ramadan (2019). "The p97-Ataxin 3 complex regulates homeostasis of the DNA damage response E3 ubiquitin ligase RNF8." Embo Journal 38(21).

Skaar, J. R., J. K. Pagan and M. Pagano (2014). "SCF ubiquitin ligase-targeted therapies." Nat Rev Drug Discov 13(12): 889-903.

Sonneville, R., R. Bhowmick, S. Hoffmann, N. Mailand, I. D. Hickson and K. Labib (2019). "TRAIP drives replisome disassembly and mitotic DNA repair synthesis at sites of incomplete DNA replication." Elife 8.

Sonneville, R., S. P. Moreno, A. Knebel, C. Johnson, C. J. Hastie, A. Gartner, A. Gambus and K. Labib (2017). "CUL-2(LRR-1) and UBXN-3 drive replisome disassembly during DNA replication termination and mitosis." Nat Cell Biol 19(5): 468-479.

Soucy, T. A., P. G. Smith, M. A. Milhollen, A. J. Berger, J. M. Gavin, S. Adhikari, J. E. Brownell, K. E. Burke, D. P. Cardin, S. Critchley, C. A. Cullis, A. Doucette, J. J. Garnsey, J. L. Gaulin, R. E. Gershman, A. R. Lublinsky, A. McDonald, H. Mizutani, U. Narayanan, E. J. Olhava, S. Peluso, M. Rezaei, M. D. Sintchak, T. Talreja, M. P. Thomas, T. Traore, S. Vyskocil, G. S. Weatherhead, J. Yu, J. Zhang, L. R. Dick, C. F. Claiborne, M. Rolfe, J. B. Bolen and S. P. Langston (2009). "An inhibitor of NEDD8-activating enzyme as a new approach to treat cancer." Nature 458(7239): 732-736.

Stach, L. and P. S. Freemont (2017). "The AAA+ ATPase p97, a cellular multitool." Biochem J 474(17): 2953-2976.

Stein, A., A. Ruggiano, P. Carvalho and T. A. Rapoport (2014). "Key Steps in ERAD of Luminal ER Proteins Reconstituted with Purified Components." Cell 158(6): 1375-1388.

Stolz, A., W. Hilt, A. Buchberger and D. H. Wolf (2011). "Cdc48: a power machine in protein degradation." Trends Biochem Sci 36(10): 515-523.

Strausfeld, U. P., M. Howell, P. Descombes, S. Chevalier, R. E. Rempel, J. Adamczewski, J. L. Maller, T. Hunt and J. J. Blow (1996). "Both cyclin A and cyclin E have S-phase promoting (SPF) activity in Xenopus egg extracts." J Cell Sci 109 (Pt 6): 1555-1563.

Swanson, K. A., R. S. Kang, S. D. Stamenova, L. Hicke and I. Radhakrishnan (2003). "Solution structure of Vps27 UIM-ubiquitin complex important for endosomal sorting and receptor downregulation." EMBO J 22(18): 4597-4606.

Takisawa, H., S. Mimura and Y. Kubota (2000). "Eukaryotic DNA replication: from pre-replication complex to initiation complex." Curr Opin Cell Biol 12(6): 690-696.

Tanaka, K. (2009). "The proteasome: overview of structure and functions." Proc Jpn Acad Ser B Phys Biol Sci 85(1): 12-36.

Thakar, T., W. Leung, C. M. Nicolae, K. E. Clements, B. Shen, A. K. Bielinsky and G. L. Moldovan (2020). "Ubiquitinated-PCNA protects replication forks from DNA2-mediated degradation by regulating Okazaki fragment maturation and chromatin assembly." Nat Commun 11(1): 2147.

Torrecilla, I., J. Oehler and K. Ramadan (2017). "The role of ubiquitin-dependent segregase p97 (VCP or Cdc48) in chromatin dynamics after DNA double strand breaks." Philos Trans R Soc Lond B Biol Sci 372(1731).

Totsukawa, G., A. Matsuo, A. Kubota, Y. Taguchi and H. Kondo (2013). "Mitotic phosphorylation of VCIP135 blocks p97ATPase-mediated Golgi membrane fusion." Biochem Biophys Res Commun 433(2): 237-242.

Tran, H., D. Bustos, R. Yeh, B. Rubinfeld, C. Lam, S. Shriver, I. Zilberleyb, M. W. Lee, L. Phu, A. A. Sarkar, I. E. Zohn, I. E. Wertz, D. S. Kirkpatrick and P. Polakis (2013). "HectD1 E3 ligase modifies adenomatous polyposis coli (APC) with polyubiquitin to promote the APC-axin interaction." J Biol Chem 288(6): 3753-3767.

Twomey, E. C., Z. Ji, T. E. Wales, N. O. Bodnar, S. B. Ficarro, J. A. Marto, J. R. Engen and T. A. Rapoport (2019). "Substrate processing by the Cdc48 ATPase complex is initiated by ubiquitin unfolding." Science 365(6452).

Uchiyama, K., E. Jokitalo, F. Kano, M. Murata, X. Zhang, B. Canas, R. Newman, C. Rabouille, D. Pappin, P. Freemont and H. Kondo (2002). "VCIP135, a novel essential factor for p97/p47-mediated membrane fusion, is required for Golgi and ER assembly in vivo." J Cell Biol 159(5): 855-866.

Uhle, S., O. Medalia, R. Waldron, R. Dumdey, P. Henklein, D. Bech-Otschir, X. Huang, M. Berse, J. Sperling, R. Schade and W. Dubiel (2003). "Protein kinase CK2 and protein kinase D are associated with the COP9 signalosome." EMBO J 22(6): 1302-1312.

Ulrich, H. D. (2012). "Ubiquitin and SUMO in DNA repair at a glance." J Cell Sci 125(Pt 2): 249-254.
Ulrich, H. D. and H. Walden (2010). "Ubiquitin signalling in DNA replication and repair." Nat Rev Mol Cell Biol 11(7): 479-489.

Valle, C. W., T. H. Min, M. Bodas, S. Mazur, S. Begum, D. N. Tang and N. Vij (2011). "Critical Role of VCP/p97 in the Pathogenesis and Progression of Non-Small Cell Lung Carcinoma." Plos One 6(12).

van den Boom, J., M. Wolf, L. Weimann, N. Schulze, F. Li, F. Kaschani, A. Riemer, C. Zierhut, M. Kaiser, G. Iliakis, H. Funabiki and H. Meyer (2016). "VCP/p97 Extracts Sterically Trapped Ku70/80 Rings from DNA in Double-Strand Break Repair." Mol Cell 64(1): 189-198.

van den Bosch, M., R. T. Bree and N. F. Lowndes (2003). "The MRN complex: coordinating and mediating the response to broken chromosomes." Embo Reports 4(9): 844-849.

van der Veen, A. G. and H. L. Ploegh (2012). "Ubiquitin-like proteins." Annu Rev Biochem 81: 323-357.
Vaz, B., S. Halder and K. Ramadan (2013). "Role of p97/VCP (Cdc48) in genome stability." Front Genet 4: 60.

Verdin, E. and M. Ott (2015). "50 years of protein acetylation: from gene regulation to epigenetics, metabolism and beyond." Nat Rev Mol Cell Biol 16(4): 258-264.

Verma, R., R. Oania, R. H. Fang, G. T. Smith and R. J. Deshaies (2011). "Cdc48/p97 Mediates UV-Dependent Turnover of RNA Pol II." Molecular Cell 41(1): 82-92.

Vetter, I. R., C. Nowak, T. Nishimoto, J. Kuhlmann and A. Wittinghofer (1999). "Structure of a Ran-binding domain complexed with Ran bound to a GTP analogue: implications for nuclear transport." Nature 398(6722): 39-46.

Vij, N. (2008). "AAA ATPase p97/VCP: cellular functions, disease and therapeutic potential." Journal of Cellular and Molecular Medicine 12(6a): 2511-2518.

Villa, F., R. Fujisawa, J. Ainsworth, K. Nishimura, A. L. M. Lie, G. Lacaud and K. P. Labib (2021). "CUL2(LRR1) , TRAIP and p97 control CMG helicase disassembly in the mammalian cell cycle." EMBO Rep 22(3): e52164.

Villen, J., S. A. Beausoleil, S. A. Gerber and S. P. Gygi (2007). "Large-scale phosphorylation analysis of mouse liver." Proc Natl Acad Sci U S A 104(5): 1488-1493.

Vitor, A. C., P. Huertas, G. Legube and S. F. de Almeida (2020). "Studying DNA Double-Strand Break Repair: An Ever-Growing Toolbox." Frontiers in Molecular Biosciences 7.

Walden, H. and K. Rittinger (2018). "RBR ligase-mediated ubiquitin transfer: a tale with many twists and turns." Nat Struct Mol Biol 25(6): 440-445.

Waters, L. S., B. K. Minesinger, M. E. Wiltrout, S. D'Souza, R. V. Woodruff and G. C. Walker (2009). "Eukaryotic Translesion Polymerases and Their Roles and Regulation in DNA Damage Tolerance." Microbiology and Molecular Biology Reviews 73(1): 134-+.

Watson, I. R., M. S. Irwin and M. Ohh (2011). "NEDD8 pathways in cancer, Sine Quibus Non." Cancer Cell 19(2): 168-176.

Webster, C. P., E. F. Smith, P. J. Shaw and K. J. De Vos (2017). "Protein Homeostasis in Amyotrophic Lateral Sclerosis: Therapeutic Opportunities?" Front Mol Neurosci 10: 123.

Weith, M., J. Seiler, J. van den Boom, M. Kracht, J. Hulsmann, I. Primorac, J. D. Garcia, F. Kaschani, M. Kaiser, A. Musacchio, M. Bollen and H. Meyer (2018). "Ubiquitin-Independent Disassembly by a p97 AAA-ATPase Complex Drives PP1 Holoenzyme Formation." Molecular Cell 72(4): 766-+.

Welchman, R. L., C. Gordon and R. J. Mayer (2005). "Ubiquitin and ubiquitin-like proteins as multifunctional signals." Nat Rev Mol Cell Biol 6(8): 599-609.

Wickliffe, K. E., A. Williamson, H. J. Meyer, A. Kelly and M. Rape (2011). "K11-linked ubiquitin chains as novel regulators of cell division." Trends Cell Biol 21(11): 656-663.

Wiggins, C. M., P. Tsvetkov, M. Johnson, C. L. Joyce, C. A. Lamb, N. J. Bryant, D. Komander, Y. Shaul and S. J. Cook (2011). "BIM(EL), an intrinsically disordered protein, is degraded by 20S proteasomes in the absence of poly-ubiquitylation." J Cell Sci 124(Pt 6): 969-977.

Wold, M. S. (1997). "Replication protein A: a heterotrimeric, single-stranded DNA-binding protein required for eukaryotic DNA metabolism." Annu Rev Biochem 66: 61-92.

Wu, J. T., H. C. Lin, Y. C. Hu and C. T. Chien (2005). "Neddylation and deneddylation regulate Cul1 and Cul3 protein accumulation." Nat Cell Biol 7(10): 1014-1020.

Wu, R. A., D. S. Pellman and J. C. Walter (2021). "The Ubiquitin Ligase TRAIP: Double-Edged Sword at the Replisome." Trends Cell Biol 31(2): 75-85.

Wu, R. A., D. R. Semlow, A. N. Kamimae-Lanning, O. V. Kochenova, G. Chistol, M. R. Hodskinson, R. Amunugama, J. L. Sparks, M. Wang, L. Deng, C. A. Mimoso, E. Low, K. J. Patel and J. C. Walter (2019). "TRAIP is a master regulator of DNA interstrand crosslink repair." Nature 567(7747): 267-272.

Wu, R. C., E. Veras, J. Lin, E. Gerry, A. Bahadirli-Talbott, A. Baras, A. Ayhan, I. M. Shih and T. L. Wang (2017). "Elucidating the pathogenesis of synchronous and metachronous tumors in a woman with endometrioid carcinomas using a whole-exome sequencing approach." Cold Spring Harbor Molecular Case Studies 3(6).

Xia, D., W. K. Tang and Y. Ye (2016). "Structure and function of the AAA+ ATPase p97/Cdc48p." Gene 583(1): 64-77.

Xia, Y., L. H. Yan, B. Huang, M. Liu, X. Liu and C. Huang (2014). "Pathogenic mutation of UBQLN2 impairs its interaction with UBXD8 and disrupts endoplasmic reticulum-associated protein degradation." J Neurochem 129(1): 99-106.

Xia, Y. S., R. Fujisawa, T. D. Deegan, R. Sonneville and K. P. M. Labib (2021). "TIMELESS-TIPIN and UBXN-3 promote replisome disassembly during DNA replication termination in Caenorhabditis elegans." Embo Journal 40(17).

Xiao, A., H. Li, D. Shechter, S. H. Ahn, L. A. Fabrizio, H. Erdjument-Bromage, S. Ishibe-Murakami, B. Wang, P. Tempst, K. Hofmann, D. J. Patel, S. J. Elledge and C. D. Allis (2009). "WSTF regulates the H2A.X DNA damage response via a novel tyrosine kinase activity." Nature 457(7225): 57-62.

Xirodimas, D. P. (2008). "Novel substrates and functions for the ubiquitin-like molecule NEDD8." Biochem Soc Trans 36(Pt 5): 802-806.

Xu, P., D. M. Duong, N. T. Seyfried, D. M. Cheng, Y. Xie, J. Robert, J. Rush, M. Hochstrasser, D. Finley and J. Peng (2009). "Quantitative Proteomics Reveals the Function of Unconventional Ubiquitin Chains in Proteasomal Degradation." Cell 137(1): 133-145.

Yang, F. C., Y. H. Lin, W. H. Chen, J. Y. Huang, H. Y. Chang, S. H. Su, H. T. Wang, C. Y. Chiang, P. H. Hsu, M. D. Tsai, B. C. Tan and S. C. Lee (2013). "Interaction between salt-inducible kinase 2 (SIK2) and p97/valosin-containing protein (VCP) regulates endoplasmic reticulum (ER)-associated protein degradation in mammalian cells." J Biol Chem 288(47): 33861-33872.

Yao, J. N., X. X. Zhang, Y. Z. Zhang, Y. L. Li, C. F. Wang and L. F. Zhang (2020). "[Circular RNA-UBXN7 promotes proliferation, migration and suppresses apoptosis in hepatocellular cancer]." Zhonghua Gan Zang Bing Za Zhi 28(5): 421-427.

Yao, Y. and W. Dai (2014). "Genomic Instability and Cancer." J Carcinog Mutagen 5.

Yardimci, H., X. Wang, A. B. Loveland, I. Tappin, D. Z. Rudner, J. Hurwitz, A. M. van Oijen and J. C. Walter (2012). "Bypass of a protein barrier by a replicative DNA helicase." Nature 492(7428): 205-209.
Ye, Y. (2006). "Diverse functions with a common regulator: ubiquitin takes command of an AAA ATPase." J Struct Biol 156(1): 29-40.

Ye, Y., H. H. Meyer and T. A. Rapoport (2003). "Function of the p97-Ufd1-Npl4 complex in retrotranslocation from the ER to the cytosol: dual recognition of nonubiquitinated polypeptide segments and polyubiquitin chains." J Cell Biol 162(1): 71-84.

Ye, Y. H., W. K. Tang, T. Zhang and D. Xia (2017). "A Mighty "Protein Extractor" of the Cell: Structure and Function of the p97/CDC48 ATPase." Frontiers in Molecular Biosciences 4.

Ying, C. Y. and J. Gautier (2005). "The ATPase activity of MCM2-7 is dispensable for pre-RC assembly but is required for DNA unwinding." EMBO J 24(24): 4334-4344.

Yu, C., J. Cresswell, M. G. Loffler and J. S. Bogan (2007). "The glucose transporter 4-regulating protein TUG is essential for highly insulin-responsive glucose uptake in 3T3-L1 adipocytes." J Biol Chem 282(10): 7710-7722.

Yusufzai, T., X. Kong, K. Yokomori and J. T. Kadonaga (2009). "The annealing helicase HARP is recruited to DNA repair sites via an interaction with RPA." Genes Dev 23(20): 2400-2404.

Zhao, G., X. Zhou, L. Wang, G. Li, H. Schindelin and W. J. Lennarz (2007). "Studies on peptide:N-glycanase-p97 interaction suggest that p97 phosphorylation modulates endoplasmic reticulum-associated degradation." Proc Natl Acad Sci U S A 104(21): 8785-8790.

Zhao, Y., M. A. Morgan and Y. Sun (2014). "Targeting Neddylation pathways to inactivate cullin-RING ligases for anticancer therapy." Antioxid Redox Signal 21(17): 2383-2400.

Zheng, J., X. Yang, J. M. Harrell, S. Ryzhikov, E. H. Shim, K. Lykke-Andersen, N. Wei, H. Sun, R. Kobayashi and H. Zhang (2002). "CAND1 binds to unneddylated CUL1 and regulates the formation of SCF ubiquitin E3 ligase complex." Mol Cell 10(6): 1519-1526.

Zheng, N. and N. Shabek (2017). "Ubiquitin Ligases: Structure, Function, and Regulation." Annu Rev Biochem 86: 129-157.

Zhou, C., S. Wee, E. Rhee, M. Naumann, W. Dubiel and D. A. Wolf (2003). "Fission yeast COP9/signalosome suppresses cullin activity through recruitment of the deubiquitylating enzyme Ubp12p." Mol Cell 11(4): 927-938.

Zhou, L., Y. Jiang, Q. Luo, L. Li and L. Jia (2019). "Neddylation: a novel modulator of the tumor microenvironment." Mol Cancer 18(1): 77.

Zhu, C. G., A. Rogers, K. Asleh, J. Won, D. X. Gao, S. Leung, S. Li, K. R. Vij, J. Zhu, J. M. Held, Z. S. You, T. O. Nielsen and J. Y. Shao (2020). "Phospho-Ser(784)-VCP Is Required for DNA Damage Response and Is Associated with Poor Prognosis of Chemotherapy-Treated Breast Cancer." Cell Reports 31(10).

Zou, Y., Y. Liu, X. Wu and S. M. Shell (2006). "Functions of human replication protein A (RPA): from DNA replication to DNA damage and stress responses." J Cell Physiol 208(2): 267-273.